



## Microcontainers for antibiotic delivery to biofilms

**Birk, Stine Egebro**

*Publication date:*  
2021

*Document Version*  
Publisher's PDF, also known as Version of record

[Link back to DTU Orbit](#)

*Citation (APA):*  
Birk, S. E. (2021). *Microcontainers for antibiotic delivery to biofilms*. DTU Health Technology.

---

### General rights

Copyright and moral rights for the publications made accessible in the public portal are retained by the authors and/or other copyright owners and it is a condition of accessing publications that users recognise and abide by the legal requirements associated with these rights.

- Users may download and print one copy of any publication from the public portal for the purpose of private study or research.
- You may not further distribute the material or use it for any profit-making activity or commercial gain
- You may freely distribute the URL identifying the publication in the public portal

If you believe that this document breaches copyright please contact us providing details, and we will remove access to the work immediately and investigate your claim.

PhD thesis

# MICROCONTAINERS FOR ANTIBIOTIC DELIVERY TO BIOFILMS

---

Stine Egebro Birk

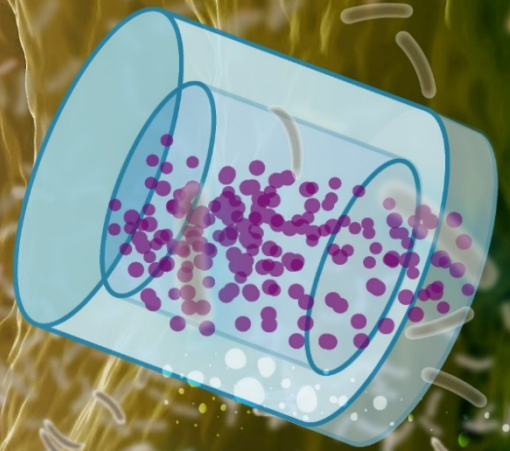
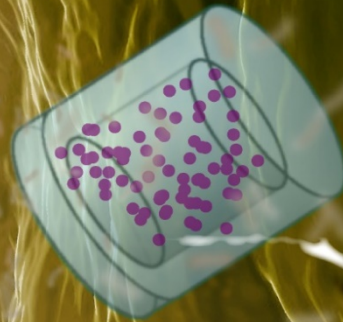
JANUARY 2021

---

Department of Health Technology  
Technical University of Denmark (DTU)

Supervisor: Anja Boisen

Co-supervisor: Line Hagner Nielsen





## PREFACE

---

The present thesis was submitted as a partial fulfillment of the requirements to obtain a PhD degree at the Technical University of Denmark (DTU). The research was carried out in the section “Intelligent Drug Delivery and Sensing Using Microcontainers and Nanomechanics” (IDUN), Department of Health Technology from 1<sup>st</sup> of February 2018 to 31<sup>st</sup> of January 2021. Additionally, some experiments were conducted in the Department of Biotechnology and Biomedicine (DTU Bioengineering), in the Novo Nordisk Foundation Center for Biosustainability (DTU Biosustain) and in the Biofilm group (Interdisciplinary Nanoscience Center, Aarhus University). The project was a part of the IDUN project funded by the Danish National Research Foundation (grant no. DNRF122) and by the Villum Fonden (grant no. 9301). The work was performed under the supervision of Professor Anja Boisen and Associate Professor Line Hagner Nielsen, Department of Health Technology, Technical University of Denmark.

*Stine Egebro Birk*

*Department of Health Technology, Technical University of Denmark*

*Kongens Lyngby, January 2021*



VILLUM FONDEN



## ACKNOWLEDGEMENTS

---

Foremost, I would like to acknowledge my principal supervisor, Professor Anja Boisen, who made this PhD possible. Thanks for many fruitful discussions and for guiding me to become an independent researcher. Despite being a busy professor, the door to Anja's office has always been open. When things got tough, Anja was always there, to which I am truly grateful. I would like to express my deepest gratitude to my supervisor Associate Professor Line Hagner Nielsen for guidance, inspiration and inestimable support throughout the project. Thank you for being a solid pillar during the ups and downs, both scientifically and personally. Line has been a great mentor, supportive yet also motivating me to perform even better.

I would like to thank my collaborators at Center for Biosustainability, DTU, Staff Scientist Janus Anders Juul Haagenen, Professor Helle Krogh Johansen and Professor Søren Molin. Thank you for introducing me to the fascinating world of microbiology. I would also like to thank Senior Researcher Claus Sternberg, Department of Biotechnology and Biomedicine, DTU, for his expert assistance and support regarding the confocal microscope. Thank you to my external collaborator Associate Professor Rikke Louise Meyer, Interdisciplinary Nanoscience Center (iNano), University of Aarhus, for inviting me into the biofilm group.

I would like to thank everyone in the IDUN group for support, great company and lots of fun. It has been a pleasure working with all of you. Thanks for creating a pleasant working environment with interesting discussions and a genuine interest in the well-being of others. Most people come from different backgrounds and I have truly learnt something from each of you. A special thanks to my colleagues and friends Chiara, Morten, Varadarajan, Juliane, Mette, and Laura for countless of fun times, scientific and less scientific discussions and for being there when everything got too much. I want to thank Morten for being the best office mate one could imagine. I enjoyed co-supervising master students together with Chiara and Laura. Laura, we faced the world of microbiology together and it has for sure not always been easy. Thanks for being a part of the ride with me. I would also like to thank Senior Researcher Kinga for being supportive and having a genuine interest in my success. Thanks to Juliane, Chiara, and Laura, for proofreading this thesis. I am truly grateful for your help. A big thanks to my students Jesper Højgaard, Valentina Cavallo, Madeeha Javed, and Beate Krongaard, whose dedicated work was crucial for this project. I have truly enjoyed supervising all of you. I learned a lot about myself, while teaching you.

Finally, I would like to thank my family and friends for their never ending support, encouragement, kindness and understanding during the course of this project. I wish to thank my parents, my sister and in-laws for being there throughout the successes and frustrations. To my husband, Martin Birk, I could not have completed this journey without your support and never ending love. Thanks for putting up with me and my craziness the last three years. I would never have made it without you.

When I graduated as a pharmacist I was eager to continue my research career. However, little did I know about how this journey would be. The last three years has taught me more than what I ever imagined. I am truly grateful for getting this opportunity.

# ABSTRACT

---

Chronic infections frequently involve formation of bacterial biofilm. The biofilm protects the embedded bacteria from antibiotic treatment and host immune responses, rendering many traditional antibiotic therapies ineffective. This, together with the lack of new antibiotics in the developmental pipeline, highlights the need for innovative treatment strategies optimizing the dosing of currently available drugs. Traditional drug delivery formulations often result in a suboptimal drug concentration at the desired site with the consequence of an insufficient treatment. Micro- and nanotechnology is looked at as an extremely promising way to create new carriers to improve antibiotic treatments. New carriers have the potential to I) deliver adequate amounts of antibiotics to the site of biofilm, and II) penetrate the biofilm and kill the tolerant biofilm-embedded strains. In this way, one can achieve the same therapeutic effect with the use of less drug, ultimately reducing the dose-related toxicity and minimizing the risks of resistance development.

Recently, microfabricated devices have been explored as oral drug delivery carriers controlling drug release and intestinal bioavailability. One type of microfabricated device is microcontainers. Microcontainers are cylindrical drug-reservoirs with a unidirectional opening. Interestingly, microcontainers have been shown to embed in the intestinal mucus.

In this work, we explore the effect of embedment and localized delivery when using microcontainers for improved biofilm therapy. Antibiotics with different physiochemical and antibiofilm properties (ciprofloxacin, colistin and nisin) are loaded separately or together into microcontainers. Subsequent functionalization of the cavity of the microcontainers is completed with the use of various polymers aimed at realizing a mucoadhesive, release-controlling and/or biofilm-degrading effect (polyethylene glycol, Eudragit S100, and chitosan with or without N-acetylcysteine). The microcontainer properties are evaluated *in vitro* regarding drug loading capacity, morphology of polymer-functionalization, drug release and mucoadhesion. Furthermore, we address the performance of antibiotic-loaded microcontainers against planktonic and biofilm-associated *Pseudomonas aeruginosa* along with multispecies oral biofilms. The proof-of-concept results show that functionalized microcontainers provide prolonged ciprofloxacin release with a 3-fold higher local killing of *P. aeruginosa* compared to treatment with a single bolus dose. Moreover, they give rise to a bacterial killing similar to after constant perfusion of a 2.75 times higher concentration of solubilized antibiotic. Nisin release from chitosan-functionalized microcontainers occurs in a burst manner, resulting in a faster killing of multispecies oral biofilms than from a solution-based antibiotic treatment.

Decreased biofilm susceptibility to antibiotics has been attributed to multiple factors, including difference in metabolic activity in the biofilm and obstruction of antibiotic penetration through the biofilm matrix. Therefore, we co-deliver antibiotics with different mechanism of action, targeting different subpopulations of a *P. aeruginosa* biofilm, using microcontainers. The co-delivery demonstrate synergistic activity superior to monotherapy, resulting in a complete eradication of planktonic bacterial populations. As a second approach, we functionalize the microcontainers with a mucoadhesive and mucolytic lid



consisting of chitosan and N-acetylcysteine, aimed to increase biofilm susceptibility to antibiotic therapy. To enable investigation of the functionalized microcontainers, we realize growth of mucin-embedded biofilm on a newly developed centrifugal microfluidic platform, mimicking part of the *in vivo* biofilm habitat. The results reveal large differences in the development of biofilms in the mucin-containing medium. The microcontainers functionalized with chitosan and N-acetylcysteine improve killing of mucin-embedded biofilm compared to chitosan-coated microcontainers or a bolus antibiotic injection. This effect we ascribe to the localized microcontainer-based delivery in combination with the proven mucoadhesive and biofilm-matrix degrading effects.

This thesis highlights the use of a microdevice-based drug delivery system as a strategy for delivering high local concentrations of antibiotics ultimately improving the efficacy against bacteria enclosed in biofilms. Benefits and drawbacks of the microcontainers including future optimization strategies are discussed. Overall, the results are encouraging for further design of microdevices for antibiotic delivery. Thus, solving the unmet clinical need in the treatment of biofilm-associated infections.

## RESUMÉ (DANISH)

---

Kroniske infektioner skyldes ofte bakterier der vokser i en biofilm. I biofilmen er bakterierne beskyttet mod antibiotika og kroppens eget immunforsvar hvilket medfører, at antibiotika behandling ofte kun har en minimal effekt på infektionerne. Dette, sammen med den manglende udvikling af nye virksomme antibiotika, tydeliggør behovet for udvikling af nye innovative behandlingsstrategier, der kan optimere brugen af de allerede eksisterende antibiotika. Traditionelle systemer til levering af lægemidler resulterer ofte i suboptimale koncentrationer der hvor lægemidlet skal virke, hvilket har den konsekvens at behandlingen ikke lykkes. Mikro- og nanoteknologi anses som et lovende forskningsområde, der kan bruges til at opfinde nye leveringssystemer til at optimere antibiotika behandlingen. De nye leveringssystemer kan bruges til at I) opnå en tilstrækkelig høj koncentration af antibiotika i biofilmen og II) penetrere biofilmen og dermed slå bakterierne indeni ihjel. Ved at opnå den samme terapeutiske effekt, men ved brugen af mindre antibiotika, kan den dosisrelaterede toksicitet reduceres og risikoen for udvikling af resistens minimeres.

Anvendelsen af mikrofabrikerede systemer til levering af antibiotika er i den seneste tid blevet undersøgt med den hensigt, at de kan kontrollere frigivelsen af lægemiddel og den intestinale biotilgængelighed. Et eksempel på et mikrofabrikeret system er mikrocontainere. Mikrocontainere er cylindriske beholdere med en åbning i den ene side til frigivelse af lægemiddel. Studier har vist at mikrocontainerne sætter sig fast i det slimlag af mucus som dækker tarmoverfladen.

I denne afhandling undersøges det om mikrocontainere kan forbedre behandlingen af biofilm ved at hæfte sig til biofilmen og øge koncentrationen af antibiotika i biofilmen. Antibiotika med forskellige fysisk-kemiske og antibiofilm egenskaber (ciprofloxacin, colistin og nisin) blev fyldt i mikrocontainerne separat eller sammen. Derefter blev åbningen af mikrocontainerne overtrukket med forskellige polymerer, med det formål at opnå en mucoadhesiv, frigivelses-kontrolleret og/eller biofilm-nedbrydende effekt (polyethylen glycol, Eudragit S100 samt chitosan med eller uden N-acetylcysteine). Mikrocontainerne blev evalueret *in vitro* i forhold til hvor meget antibiotika de kan indeholde, morfologien af polymer-overtrækket, lægemiddelfrigivelses-profilen samt deres adhæsion til mucus. Desuden blev effekten af antibiotika-påfyldte mikrocontainere på planktonisk og biofilm-indkapslet *Pseudomonas aeruginosa* samt orale biofilm indeholdende flere forskellige bakteriearter undersøgt.

Resultaterne fra det initiale proof-of-concept studie viste, at de polymer-overtrukne mikrocontainere resulterede i forlænget frigivelse af ciprofloxacin og et 3 gange højere drab af *P. aeruginosa* sammenlignet med en enkelt bolus dosis. Derudover målte et bakterielt drab svarende til en konstant perfusion af 2,75 gange højere koncentration af antibiotika i opløsning. Frigivelse af nisin fra chitosan-overtrukne mikrocontainere skete med det samme og resulterede i et hurtigt drab af de forskellige bakterier i en oral biofilm sammenlignet med antibiotika behandling i opløsning.

Biofilmens nedsatte følsomhed over for antibiotika er gennem tiden blevet tilskrevet forskellige årsager, blandt andet forskel i den metaboliske aktivitet i biofilmen samt hindring af antibiotika penetrering gennem biofilm-matriksen. Derfor blev mikrocontainerne fyldt med to typer af antibiotika, der hver især

påvirker de forskellige subpopulationer i en *P. aeruginosa* biofilm. Den samtidige levering viste sig at være bedre end behandling med antibiotika hver for sig, da det resulterede i et fuldt drab af planktonisk *P. aeruginosa*.

Som en anden strategi for at øge biofilmens modtagelighed overfor antibiotika, blev mikrocontainerne overtrukket med et mucoadhesivt og mucus-nedbrydende låg bestående af chitosan og N-acetylcysteine. En nyudviklet centrifugal mikrofluid platform blev anvendt til at gro biofilm sammen med mucin, der er hovedkomponenten i mucus. Ved at inkludere mucin kunne vi bedre efterligne det *in vivo* miljø som biofilmen vokser i og dermed opnå en mere korrekt evaluering af de overtrukne mikrocontainere. Resultaterne viste, at biofilmen udviklede sig forskelligt afhængig af koncentrationen af mucin. Mikrocontainerne, der var overtrukket med chitosan og N-acetylcysteine, forbedrede drabet af den mucin-indkapslede biofilm sammenlignet med mikrocontainere der kun var overtrukket med chitosan eller en bolus injektion af antibiotika i opløsning. Vi mener, at denne effekt skyldes den øget lokale levering af antibiotika opnået med mikrocontainerne samt den dokumenterede mucus og biofilm-nedbrydende effekt af overtrækket.

Denne PhD afhandling fremhæver brugen af et mikrofabrikeret system til at levere høje lokale koncentrationer af antibiotika og dermed forbedre effekten af antibiotika på bakterier i en biofilm. Fordele og ulemper ved mikrocontainerne bliver diskuteret sammen med flere optimeringsidéer. Samlet set er resultaterne i denne afhandling lovende og tilskynder yderligere design samt videreudvikling af mikrofabrikerede systemer til levering af antibiotika. Disse systemer kan potentielt set løse det kliniske behov der er for forbedring af biofilm-relaterede infektioner.



# TABLE OF CONTENTS

---

<b>PREFACE</b> .....	<b>I</b>
<b>ACKNOWLEDGEMENTS</b> .....	<b>II</b>
<b>ABSTRACT</b> .....	<b>III</b>
<b>RESUMÉ (DANISH)</b> .....	<b>V</b>
<b>TABLE OF CONTENTS</b> .....	<b>VII</b>
<b>LIST OF ABBREVIATIONS</b> .....	<b>VIII</b>
<b>LIST OF PUBLICATIONS AND OTHER CONTRIBUTIONS</b> .....	<b>IX</b>
<b>1 INTRODUCTION</b> .....	<b>1</b>
1.1 Hypothesis and aims .....	2
1.2 Outline of the thesis.....	2
<b>2 BACKGROUND</b> .....	<b>4</b>
2.1 Biofilms.....	4
2.1.1. Biofilm development and their composition .....	4
2.1.2. Biofilm-associated infections .....	6
2.2 Antibiotic therapy .....	9
2.2.1. Biofilm tolerance to antibiotics.....	12
2.2.2. Targeting microbial biofilms .....	14
2.3 Drug delivery systems for biofilm treatment.....	17
2.4 Microdevices as drug delivery system.....	20
2.4.1. Polymeric functionalization .....	24
<b>3 RESULTS AND DISCUSSION</b> .....	<b>26</b>
3.1 Antibiotic-loaded microcontainers against biofilms – Proof-of-concept.....	26
3.2 Co-delivery of synergistic antibiotics using microcontainers.....	32
3.3 Mucolytic functionalization of microcontainers to disrupt biofilms .....	37
3.4 Treatment of oral multispecies biofilms using microcontainers.....	44
<b>4 CONCLUSION</b> .....	<b>47</b>
<b>5 FUTURE PERSPECTIVES</b> .....	<b>49</b>
<b>6 REFERENCES</b> .....	<b>51</b>
<b>APPENDICES</b> .....	<b>68</b>

## LIST OF ABBREVIATIONS

---

<b>AFM</b>	Atomic force microscopy
<b>AMPs</b>	Antimicrobial peptides
<b>ASM</b>	Artificial sputum medium
<b>BCA</b>	Background corrected absorption
<b>BCoD</b>	Bacterial-Culture-on-Disc
<b>CIP</b>	Ciprofloxacin hydrochloride
<b>CLSM</b>	Confocal laser scanning microscopy
<b>COL</b>	Colistin sulfate
<b>DNA</b>	Deoxyribonucleic acid
<b>eDNA</b>	Extracellular deoxyribonucleic acid
<b>EPS</b>	Extracellular polymeric substances
<b>FAB</b>	Minimal medium with glucose as the only carbon source
<b>Fc</b>	Fluorocarbon
<b>GFP</b>	Green fluorescent protein
<b>LPS</b>	Lipopolysaccharides
<b>MCs</b>	Microcontainers
<b>MIC</b>	Minimal inhibitory concentration
<b>MSNs</b>	Mesoporous silica nanoparticles
<b>NAC</b>	N-acetylcysteine
<b>NEMs</b>	Nano-in-micro particles
<b>PCL</b>	Polycaprolactone
<b>PD</b>	Pharmacodynamic
<b>PDMS</b>	Polydimethylsiloxane
<b>PEG</b>	Polyethylene glycol
<b>PK</b>	Pharmacokinetic
<b>PLGA</b>	Poly (lactic-co-glycolic acid)
<b>PLLA</b>	Poly (L-lactic acid)
<b>PMMA</b>	Poly-methylmethacrylate
<b>QCM-D</b>	Quartz crystal microbalance with dissipation
<b>SEM</b>	Scanning electron microscopy
<b>SLNs</b>	Solid lipid nanoparticles
<b>TEM</b>	Transmission electron microscopy
<b>Ti/Au</b>	Titanium/gold
<b>μCT</b>	X-ray micro-computed tomography

# LIST OF PUBLICATIONS AND OTHER CONTRIBUTIONS

---

The findings in this PhD study have led to five papers and three conference contributions. Throughout the PhD thesis, the papers will be referred to as Paper I, Paper II, Paper III, Paper IV, and Paper V.

## PUBLICATIONS

- Paper I      *Polymeric nano- and microparticulate drug delivery systems for treatment of biofilms*  
S.E. Birk, A. Boisen, L.H. Nielsen. *Advanced Drug Delivery Reviews*, 2020  
(review submitted)
- Paper II      *Microcontainer delivery of antibiotic improves treatment of Pseudomonas aeruginosa biofilms*  
S.E. Birk, J.A.J. Haagensen, H.K. Johansen, S. Molin, L.H. Nielsen, A. Boisen. *Advanced Healthcare Materials*, 2020, 9 (10): 1901779
- Paper III      *Co-delivery of ciprofloxacin and colistin using microcontainers for bacterial biofilm treatment*  
S.E. Birk, C. Mazzoni, M.M. Javed, M.B. Hansen, H.K. Johansen, J.A.J. Haagensen, S. Molin, L.H. Nielsen, A. Boisen. *International Journal of Pharmaceutics*, 2021  
(submitted)
- Paper IV      *Enhanced eradication of mucin-embedded bacterial biofilm by locally delivered antibiotics in functionalized microcontainers*  
S.E. Birk\*, L. Seriola\*, V. Cavallo, J.A.J. Haagensen, S. Molin, L.H. Nielsen, K. Zór, A. Boisen. *Journal of Controlled Release*, 2020 (submitted, \*The authors contributed equally to the work)
- Paper V      *Management of oral biofilms by nisin delivery in adhesive microdevices*  
S.E. Birk, M.D. Mosgaard, R.B. Kjeldsen, A. Boisen, R.L. Meyer, L.H. Nielsen. 2021. (research note, ready for submission to *European Journal of Pharmaceutics and Biopharmaceutics*)

## OTHER CONTRIBUTIONS

- Poster I      *Microcontainers for improved treatment of Pseudomonas aeruginosa biofilm infections*  
S.E. Birk, J.A.J. Haagensen, H.K. Johansen, S. Molin, L.H. Nielsen, A. Boisen. *Controlled Release Society Annual Meeting & Exposition*, Valencia, July 2019
- Oral talk I      *Improving antibiotic treatment of Pseudomonas aeruginosa biofilms using N-acetylcysteine functionalized microcontainers*  
S.E. Birk, L. Seriola, V. Cavallo, J.A.J. Haagensen, S. Molin, K. Zór, L.H. Nielsen, A. Boisen. *Controlled Release Society Annual Meeting & Exposition*, Online, June 2020
- Oral talk II      *Development of N-acetylcysteine functionalized microcontainers for degradation of biofilm matrix*  
S.E. Birk, V. Cavallo, J.A.J. Haagensen, H.K. Johansen, S. Molin, L.H. Nielsen, A. Boisen. *Pharmaceutics, Biopharmaceutics and Pharmaceutical Technology*, Vienna, May 2021 (postponed twice)



# 1 INTRODUCTION

---

Bacterial infections represent one of the biggest human healthcare threats causing approximately 700,000 deaths per year worldwide – a number that is predicted to grow up to 10 million by 2050, killing more people than currently dying from cancer [1]. The introduction of antibiotics in the mid-twentieth century was one of the most impactful interventions for human health and antibiotics have long been saving innumerable amounts of valuable lives. However, new antibiotics are now sparsely being developed, and meanwhile the acquisition of antibiotic resistance and tolerance is increasing with an alarming rate [2]. For this reason, novel strategies to treat bacterial infections are direly needed.

Decades ago, it became clear that the predominant part of bacteria on earth do not grow as single cell cultures. Instead, they adhere to each other, or to surfaces, creating micro-communities known as biofilms [3]. These communities protect the bacteria with a self-produced matrix, house different species with different metabolic states, and possess a highly active cell-to-cell communication [4–6]. Biofilm formation is now recognized as a key virulence factor for chronic infections and, according to the US National Institutes of Health, they account for over 80 % of microbial infections in the body [7]. Biofilm-associated bacteria are less susceptible to most antibiotics, imposing great challenges for the use of traditional antibiotic delivery methods [8]. The decreased susceptibility has been attributed to multiple factors: I) the matrix can impede drug penetration or cause drug inactivation, II) tolerant or persister cells may develop, and III) the fact that many bacteria within the biofilm do not metabolize and replicate sufficiently for the antibiotics to function effectively [3,7,9–11].

Traditional drug delivery often results in suboptimal concentration of drugs at the desired site with the consequence of an insufficient treatment. However, increasing the antibiotic dose can cause side effects and worsen antibiotic resistance. Antibiotic delivery systems, providing high local drug concentrations at the site of biofilm infection, have been suggested to overcome the limits of traditional antibiotic-based antimicrobial strategies against bacterial biofilms [8]. Micro- and nanotechnology present extremely promising ways to create antibiotic delivery systems. The encapsulation of antibiotics into particles have been widely studied to deliver a sufficient amount of antibiotics to the biofilm, while at the same time overcoming the problem of antibiotic deactivation and allowing drug penetration through the dense biofilm/mucus mesh to reach the bacterial colonies [12]. Delivering the antibiotic to the site of infection can reduce the dose-related toxicity, and using less drug while achieving the same therapeutic efficacy may ultimately alleviate resistance development.

## 1.1 HYPOTHESIS AND AIMS

It is hypothesized that drug delivery devices, known as microcontainers (MCs), used for antibiotic encapsulation, will improve the treatment of *in vitro* biofilms by delivering high local drug concentrations to the biofilm.

To support this hypothesis, the overall aim of this work was to develop, characterize and evaluate antibiotic-loaded polymer-coated MCs for their effect on bacterial biofilms. The project was divided into four parts with the following study aims:

- I) To conduct a proof-of-concept study assessing the *in vitro* performance of MCs on planktonic bacteria and mature *Pseudomonas aeruginosa* biofilm
- II) To realize and test MC-based co-delivery of synergistic antibiotics to *P. aeruginosa* biofilm
- III) To design and study a combined mucoadhesive and mucolytic functionalization of MCs for improving the treatment of mucin-embedded *P. aeruginosa* biofilm
- IV) To assess and evaluate the potential of using MCs for treatment of oral multispecies biofilm

## 1.2 OUTLINE OF THE THESIS

The main results obtained during this PhD project are presented through four original research papers (**Paper II-V**) as illustrated in the overview (**Figure 1**). In addition, a review (**Paper I**) presents and discusses polymeric nano- and microparticulate drug delivery systems for treatment of biofilms. **Paper I** will not be discussed in the PhD thesis, but few selected topics are included in the background section.

The following background section, introduces the concept of biofilms, provides an overview of the causes of biofilm development and their related tolerance towards antibiotics, along with strategies in combatting biofilms. Furthermore, a short summary of available drug delivery systems for biofilm treatment is provided and the concept of microdevices is introduced.

In **Paper II**, antibiotic-loaded MCs are functionalized with various polymeric lids and the efficacy is assessed towards planktonic cultures and mature *P. aeruginosa* biofilms. In **Paper III**, MCs were co-loaded with two antibiotics with synergistic activity towards *P. aeruginosa* in order to address subpopulations not affected in Paper II. In **Paper IV**, the MCs were further modified with a mucolytic coating aimed to disrupt a mucus-embedded biofilm. Lastly, in **Paper V**, the potential of using MCs for treating oral biofilms was investigated through adhesion studies on buccal mucosa as well as treatment of oral multispecies biofilms isolated from patients.

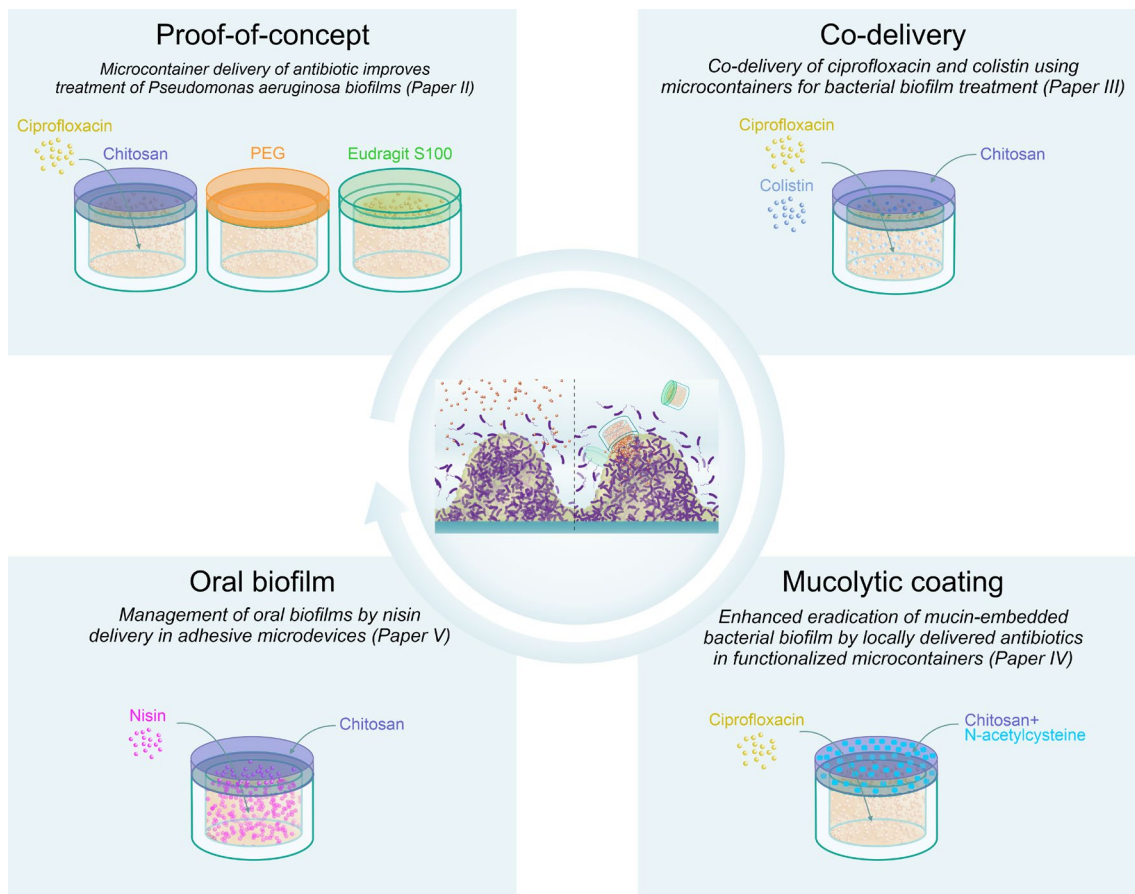


**Figure 1.** Schematic overview of the thesis outline. The potential of using microcontainers (MCs) for improving biofilm treatment was investigated in a proof-of-concept study on *P. aeruginosa* biofilm, focusing on different polymeric functionalizations of the MCs (**Paper II**). In **Paper III**, we studied the possibility and effect of co-loading MCs with two antibiotics working synergistically on *P. aeruginosa* biofilm. In **Paper IV**, a mucolytic agent was incorporated into the polymeric coating, and to allow investigation of the efficacy, a centrifugal microfluidic platform to grow *P. aeruginosa* within mucus was developed. Lastly, in **Paper V**, the activity of MCs on oral multispecies biofilm was assessed together with adhesion studies on oral buccal mucosa.



## 2 BACKGROUND

---

### 2.1 BIOFILMS

Bacterial growth is characterized by two forms of lifestyles, one being single planktonic cells and the other being sessile aggregates, commonly referred to as biofilm [13]. Until the late 1970s, microbiologists perceived bacteria as being purely free-flowing single cells and based their entire research on this perception. This may seem peculiar today, as it was later estimated that less than 0.1 % of the total microbial biomass lives as planktonic single cells [9,14]. The first medical observation of clumps or aggregates of bacteria were published by Høiby and co-authors in 1977, studying the sputum from the lungs of cystic fibrosis patients [15]. The term 'biofilm' was introduced by one of the biofilm-pioneers Costerton in 1978 [16], and in 1999, it was defined as 'a structured community of bacterial cells enclosed in a self-produced polymeric matrix, adherent to a surface' [4]. After decades of research, the scientific community became aware that bacteria, including the pathogenic ones, mostly grow in structured consortia, highly changing the way we perceive bacteria and their associated infections. The amount of publications on biofilms has drastically increased ever since. Many divergent definitions of bacterial biofilms have been published and the term is constantly being refined to accommodate new knowledge, yet, all agreeing that biofilms are aggregates of bacteria adhering to each other and/or to surfaces.

#### 2.1.1. BIOFILM DEVELOPMENT AND THEIR COMPOSITION

The switch from the solitary planktonic bacterial lifestyle to the communal biofilm way of life occurs in response to a variety of environmental stress signals. This includes changes in the availability of nutrients or oxygen, fluctuations in temperature, osmolarity, and pH, along with the presence of toxic components as for example antimicrobials [17]. The development process has been described as a complex and highly regulated process, involving five phenotypically distinct stages (**Figure 2**) [7,17,18]. It is initiated by a reversible attachment of single microbes to a surface or to other microbes (step 1), a process that implicates the use of their motility structures *i.e.* their flagella and pili [9,19]. After adhesion, the attachment becomes irreversible which coincides with the loss of their motility, and the production of biofilm matrix components is initiated (step 2). The clusters of cells develop, become thickened and highly embedded in the self-produced matrix (step 3). Biofilms then fully mature into large clusters reaching their maximum thickness (step 4). Thereafter, the biofilm life cycle continues as the biofilms disperse with cells evacuating from the interior of the cell clusters, spreading to colonize elsewhere (step 5).

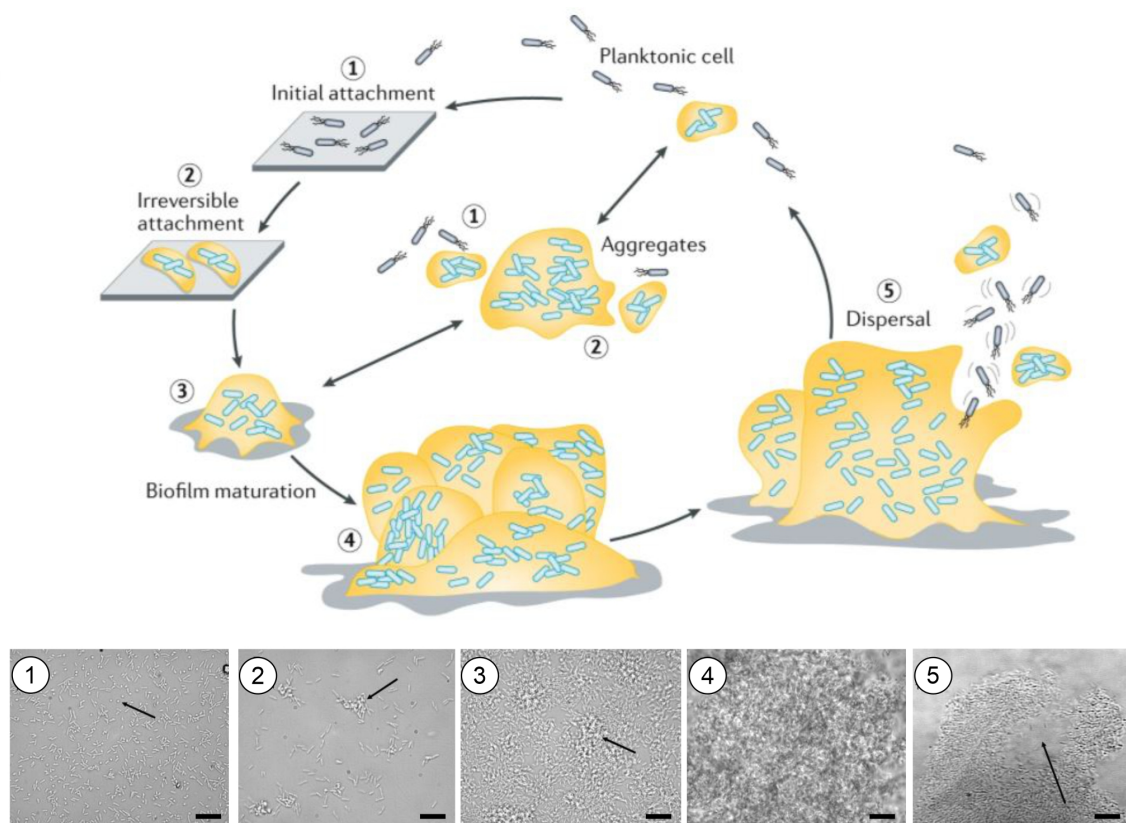


**Figure 2.** Stages of biofilm development. Planktonic bacteria adhere to a substratum, being either a surface or other cells (1). The attachment becomes irreversible and the production of biofilm matrix components is initiated (2). The clusters increase in size (3) until they reach their maximum thickness (4). The biofilm life cycle continues as the biofilm cells disperse and spread to form biofilms in new areas (5) [20]. The stages of biofilm formation are paired with a photomicrograph of a developing *P. aeruginosa* PAO1 biofilm. Scale bars: 10  $\mu\text{m}$  [21]. Reprinted/adapted with permission from Springer Nature [20] and American Society for Microbiology [21].

The biofilm matrix, in which the cells reside, consist of different biopolymers also known as extracellular polymeric substances (EPS). Its composition varies depending on the species in the biofilm, but the main components include gel-forming polysaccharides, proteins, and extracellular DNA (eDNA) (**Figure 3**) [22–24]. These constituents form the scaffold of the three-dimensional architecture of the biofilm and are responsible for the adhesion to a surface, the cohesion in the biofilm, and the associated mechanical stability [13,24]. Host-derived molecules such as mucus are also included in the EPS matrix [9]. In most biofilms, the microbes actually constitute less than 10 % of the dry mass, whereas the matrix components account for over 90 % [13,24].

Being a part of a biofilm is advantageous for the bacteria as the attachment to surfaces prevents removal by fluid flow [25]. Furthermore, the EPS shields the embedded bacteria from the external environment thereby, protecting against toxic agents such as the host immune defense and antibiotic therapy [26]. Bacteria within a biofilm cooperate closely and communicate using a phenomenon known as quorum sensing [27], in which intra- and extracellular signal molecules up-or downregulate biofilm formation and development [28]. When the number of biofilm layers increase, gradients of nutrients and oxygen

establish, providing different localized habitats (**Figure 3**). The bacteria in the inner core of the biofilm typically have a lowered metabolic activity as their access to nutrients and oxygen is limited [29,30]. The opposite accounts for the metabolically active bacteria residing on the outer edge of the biofilm, as oxygen and nutrient levels are high. Therefore, EPS formation favors an altered gene expression with phenotypic differentiations in order for the bacteria to survive in various microenvironments [3].

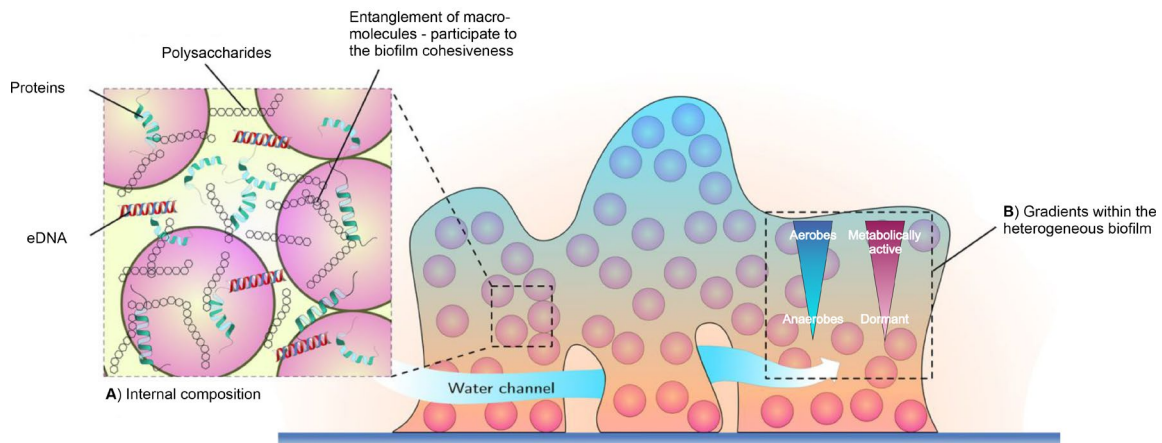


**Figure 3.** Biofilm composition and its heterogeneities. **A)** Biofilms are made of bacteria surrounded by a matrix (EPS) consisting of polysaccharides, proteins, extracellular DNA (eDNA), and other macromolecules that contributes to the structural stability of the biofilm. **B)** EPS formation leads to establishment of gradients that provide different localized habitats at a small scale. Bacteria, in the inner core of the biofilm, do not have access to nutrients and oxygen, and their proliferation is consequentially halted resulting in dormant cells. On the contrary, the environment of the outer edge-liquid interface is abundant in oxygen and nutrients translating into metabolically active cells. Proximity to a water channel may, however, provide oxygen and nutrients to certain areas within the biofilm. Reprinted/adapted with permission from Springer Nature [31].

### 2.1.2. BIOFILM-ASSOCIATED INFECTIONS

The ability of biofilm-embedded bacteria to withstand the host immune defense and the action of antibiotics presents a substantial challenge for clinicians trying to cure infections. Meanwhile, the number of diseases discovered to be implicated by biofilm is only growing every single year [9]. Most medical important microorganisms can grow in biofilms, including both Gram-positive or Gram-negative bacteria as well as the aerobic or anaerobic ones [9]. The sessile communities of bacteria attach to and establish on a variety of biological surfaces such as in cutaneous wounds [32,33], the oral cavity [34,35], the ears [36,37], the urinary tract [38] as well as the gastrointestinal tract [39], but also attach to each other forming bacterial clusters as for example in the airways of cystic fibrosis patients [26,40]. Moreover, biofilms can in principle form on any type of foreign object inserted into the human body such as on catheters, bone implants, and heart valves [9,41]. The host immune system might be capable of clearing the initial infection in a limited amount of cases, however, if not, persistent bacterial infections start to evolve [4]. Immunocompromised patients, *i.e.* individuals undergoing chemotherapy [42] or suffering from diseases like diabetes mellitus [43] or cystic fibrosis [44], are particularly prone to become infected.

Colonization of pathogenic bacteria in the oral cavity is responsible for the development of some of the most prevalent oral infections such as periodontal disease and dental carries [45]. Microbes of the genus *Streptococcus* and *Actinomyces* act as the earliest colonizers, and they are able to bind directly to components in the salivary pellicle initiating biofilm formation [35,45]. Afterwards a wide variety of strains establish, including *Porphyromonas gingivalis* and *Fusobacterium nucleatum*, allowing the formation of a dense multispecies oral biofilm [35].

Alterations of the gastrointestinal microbiota may also promote the outgrowth of a thick dense pathogenic biofilm [46,47]. The protective biofilm microenvironment promotes the escape from the host defense mechanisms. This may further aggravate into various gastrointestinal diseases including inflammatory bowel disease, colon cancer, gastric cancer, gastroenteritis, and irritable bowel syndrome [47,48]. For example, in inflammatory bowel disease the mean density of the mucosal biofilm was two powers higher than in healthy individuals [49]. In general, the strains *Fusobacterium nucleatum*, *Escherichia coli*, and *Helicobacter pylori* are known to cause gastrointestinal diseases in the form of invasive biofilms [46]. **Figure 4** shows selected human biofilm-associated infections together the major causal pathogenic species.

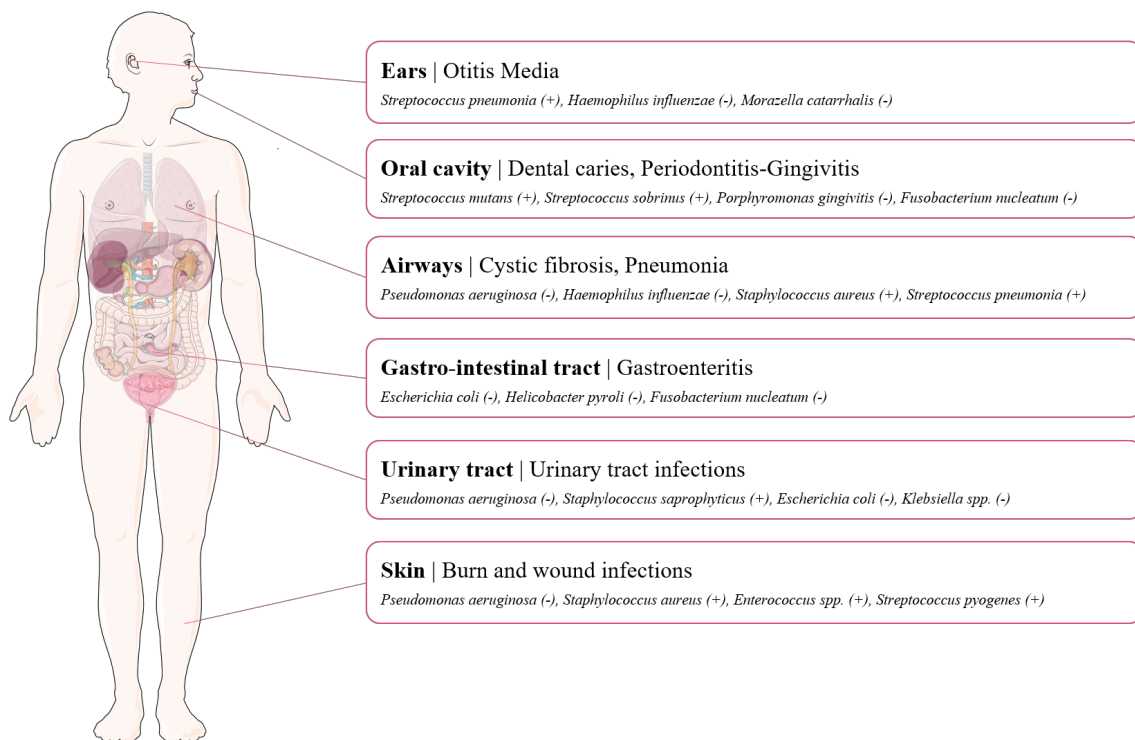


**Figure 4.** Representation of selected human biofilm-associated infections and the major causal pathogenic species. Medical device-associated biofilms are not included. Illustration was created based on [2,35,46–48,50] and with figures adapted from Servier Medical Art by Servier and licensed under a Creative Commons Attribution 3.0.

In this thesis, the primary focus has been on *P. aeruginosa* - an opportunistic pathogen considered as one of the most critical super bugs associated with high levels of morbidity and mortality [51]. *P. aeruginosa* is a Gram-negative rod-shaped bacillus measuring 0.5-0.8  $\mu\text{m}$  by 1.5-3.0  $\mu\text{m}$  [52]. It is motile by means of its flagella, and its pili aid bacterial attachment promoting colonization [52]. It is highly versatile and can thrive in a wide range of ecological niches including soil or marine habitats [53]. In the majority of *P. aeruginosa* infections, the biofilm lifestyle predominates [54]. *P. aeruginosa* is responsible for a wide range of clinical manifestations, including pneumonia, urinary tract infections, chronic wounds, and bacteremia [42,55]. The accumulation of thick, sticky mucus and the consequently impaired mucociliary clearance, seen in patients suffering from cystic fibrosis, promotes *P. aeruginosa* infections, among many other infections [40]. *P. aeruginosa* can also cause serious intestinal infections, where, for example, it has been isolated from patient suffering from inflammatory bowel disease or cancer [56,57]. Interestingly, some consider the gastrointestinal tract to be an important reservoir for *P. aeruginosa* as the presence in the intestines is responsible for increased mortality in gut-derived sepsis and bacteremia and facilitates hematogenous spread of infection to others organs such as the lungs [57]. The biofilm of *P. aeruginosa* is one of the most well-studied and is a commonly used model microorganisms for assessment of biofilm treatments. Moreover, *P. aeruginosa* is classified as one of six ESKAPE nosocomial pathogens that causes the majority of hospital-acquired infections exhibiting multidrug resistance and constituting a major healthcare problem [58]. Further, the World Health Organization included *P. aeruginosa* as one of three pathogens on their global priority list of antibiotic-resistant bacteria, promoting the need for novel treatment strategies [59].

## 2.2 ANTIBIOTIC THERAPY

Antibiotics have been used as the major weapon against bacterial infection since Alexander Flemming discovered penicillin in 1928 [60]. For several decades, they have saved numerous lives by controlling infectious diseases that have long been the leading cause of human morbidity and mortality [60]. Originally, antibiotics were produced by other microorganisms, yet, nowadays most are manufactured using synthetic techniques [61].

The cell wall composition varies whether the bacterium is Gram-positive or Gram-negative (**Figure 5**). The Gram-negative bacterium (e.g. *P. aeruginosa*) has an inner and an outer membrane, whereas the Gram-positive bacterium (e.g. *Staphylococcus aureus*) contains a thick peptidoglycan layer on the outside of the cell instead of the outer membrane. The structure of the cell membrane highly influences the efficacy of different antibiotics towards the two types of bacteria.

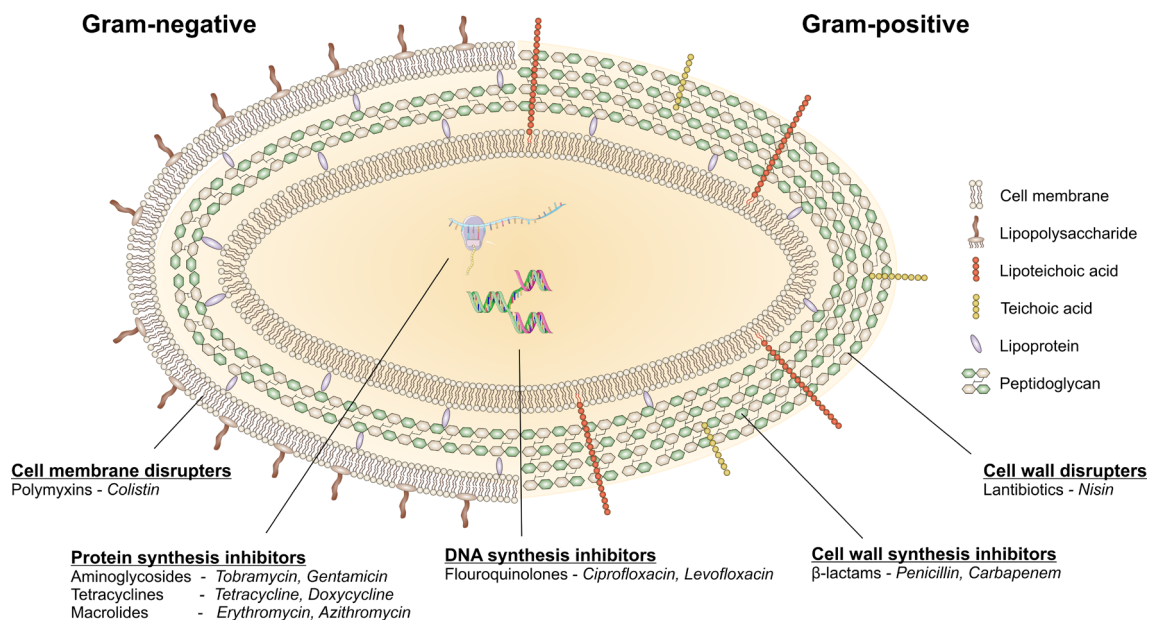


**Figure 5.** Cell wall structure of the Gram-negative and Gram-positive bacterium, together with an overview of the most common cellular targets for antibiotic therapy, their associated antibiotic classes, and examples of these. The Gram-negative bacterium consists of a thin peptidoglycan layer in the periplasmic space in between the inner and outer lipid membranes. The outer membrane contains lipopolysaccharides (LPS). The Gram-positive bacterium has a single lipid membrane surrounded by a thick peptidoglycan cell wall. Drawing is not to scale. Schematic was created with inspiration from [62], and using figures adapted from Servier Medical Art by Servier and licensed under a Creative Commons Attribution 3.0.

Antibiotics are classified according to their molecular structures, mode of action, and spectrum of activity [61]. Those that kill bacteria are termed bactericidal, while those that inhibit bacterial growth are bacteriostatic. They interfere with specific cellular targets responsible for bacterial proliferation and reproduction such as the cell wall synthesis, protein synthesis, synthesis of deoxyribonucleic acids (DNA), or the cell membrane/wall function (**Figure 5**). Some common antibiotics include the  $\beta$ -lactams,

macrolides, tetracyclines, quinolones, aminoglycosides, and polymyxins [61]. In the following section, the focus will be on the antibiotics applied in this PhD thesis: Ciprofloxacin (fluoroquinolone), colistin (polymyxin), and nisin (lantibiotic).

Fluoroquinolones are broad-spectrum antibacterial agents that are extensively used for treatment of infections [63]. Ciprofloxacin (**Figure 6**) is a fluoroquinolone with great activity against a wide range of Gram-negative and Gram-positive bacteria including *P. aeruginosa* and *S. aureus*, that are associated with debilitating infections of the lung [64,65], in wounds [66], in the eyes, and ears [67]. Ciprofloxacin has  $pK_a$  values of about 6.2 and 8.8 [68]. This means that ciprofloxacin is practically insoluble in water (0.080 mg/mL at 30 °C [69]) as neutral pH is around the isoelectric point, affecting drug release and uptake. Therefore, it is often used as the corresponding hydrochloride salt. Different solubilities have been reported in the literature ranging from 0.17-30 mg/mL depending on buffer and temperature [70–72]. Ciprofloxacin is primarily bacteriostatic, however, high doses can result in double-strand DNA breaks and thus, a bactericidal activity [67,73]. The bacteriostatic mode of action of ciprofloxacin involves interferences with DNA replication by noncovalent binding to the DNA gyrase and topoisomerase IV enzymes, thus inhibiting cellular division [63,67]. Therefore, the activity of ciprofloxacin is greater on actively dividing cells than on the non-growing dormant ones [3].

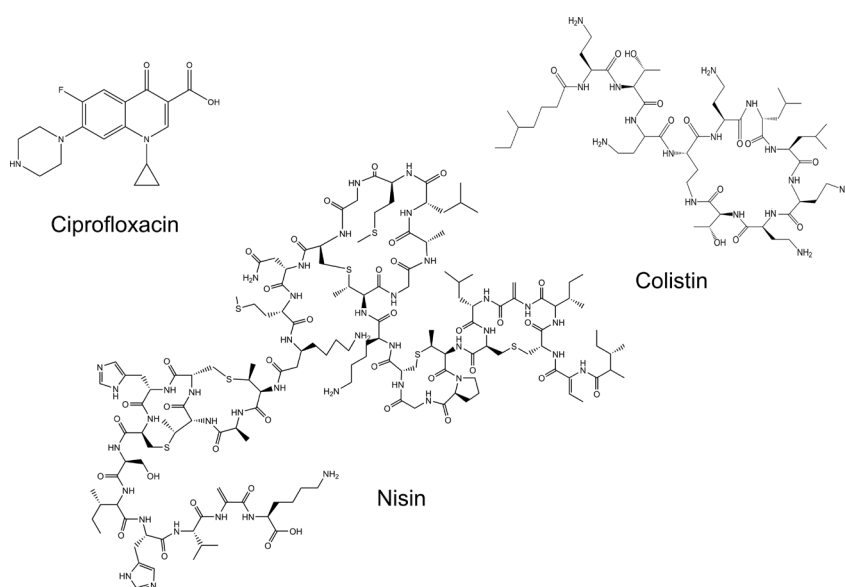


**Figure 6.** Molecular structures of antibiotics applied in this PhD thesis: Ciprofloxacin (fluoroquinolone), colistin (polymyxin), and nisin (lantibiotic).

With the progressive development of antibiotic resistance, much hope is focused on antimicrobial peptides (AMPs) due to their potency and lower stimulation of bacterial resistance. AMPs are an important component of our innate immune system and is, therefore, a natural alternative to the traditional antibiotics [74]. Generally, AMPs have a net positive charge and contain 10-50 amino acid residues of which approximately half are hydrophilic [75]. The amphipathic nature of the AMPs is believed

to facilitate electrostatic interactions with the negatively charged bacterial membranes, thus causing perturbation of the lipid bilayer [74].

Colistin (**Figure 6**) is a cyclic cationic decapeptide linked to a fatty acid side chain and belongs to the group of polymyxins [76]. Colistin is an old-class AMP, whose use was for long halted as it showed severe nephrotoxicity. Yet, the rapid increase in the prevalence of Gram-negative bacteria that are resistant to  $\beta$ -lactams, fluoroquinolones, and aminoglycosides has driven colistin's revival as a last line defense against severe Gram-negative infections [77–79]. For clinical use, colistin is available either as a sulfate salt (as applied in this thesis) delivered orally, or as the pro-drug colistimethate sodium, which is injected or inhaled [79]. Colistimethate sodium has a lower toxicity but no intrinsic antibacterial activity as it needs to be hydrolyzed *in vivo* into the active form [80]. The sulfate salt of colistin has a high aqueous solubility (50 mg/mL [81]) and is polycationic at physiological pH with a  $pK_a$  of 10 [82]. Lipopolysaccharides (LPS) found on the outer membrane of Gram-negative bacteria are responsible for cell membrane integrity and stability. Colistin binds to the lipid A component in the LPS by electrostatic interactions, mainly displacing  $Ca^{2+}$  and  $Mg^{2+}$  ions, and thereby drastically decreasing the stability of the outer membrane. The permeability of the cytoplasmic membrane is increased, leading to a loss of cellular components which culminates into bacterial cell death [79,83]. Colistin is therefore bactericidal in nature [79].

Nisin (**Figure 6**) is a member of the lantibiotic family of AMPs exhibiting high potency against many Gram-positive bacteria including staphylococci, bacilli and clostridia. In contrast, the antimicrobial activity against Gram-negative bacteria is limited as the outer lipid membrane shields the cytoplasmic peptidoglycan membrane [84]. Nisin is used world-wide as a food preservative [85–87]. The solubility at physiological pH in phosphate buffer is 10–20 mg/mL [88]. Nisin alters the structure of the cellular wall by formation of pores and prevention of peptidoglycan synthesis, ultimately leading to efflux of cellular components and cellular death [87,89]. Researchers have shown promising results for the use of nisin to treat bacterial infections, including *S. aureus* infections in atopic dermatitis [90], and respiratory tract infections [91] as well as saliva-derived multispecies biofilm [87].

In general, low metabolic cellular processes impair the efficacy of many antibiotics *i.e.* a low protein synthesis alters the effect of the aminoglycosides, a low DNA synthesis impairs the effect of the quinolones and low peptidoglycan production decreases the effect of  $\beta$ -lactams [11]. Studies have shown that spatially distinct subpopulations of metabolically active cells in the outer part of *P. aeruginosa* biofilms, classified as the cap-forming subpopulation, is able to develop phenotypic tolerance to colistin [76]. This is in contrast to the cells found in the core of the biofilm, that exhibit low metabolic activity and which are killed by colistin [76,92]. Other antibiotics, like ciprofloxacin and tetracycline, specifically kill the subpopulation of metabolically active biofilm cells, whereas the dormant subpopulation survives treatment [92]. Combining colistin treatment with tetracycline or ciprofloxacin, targeting the two distinct subpopulations has shown to almost completely eradicate all biofilm-associated cells (**Figure 7**) [92]. Colistin has also shown attractive synergistic antimicrobial activities against *P. aeruginosa* when combined with other antibiotics such as azithromycin [93] and rifampicin [94].



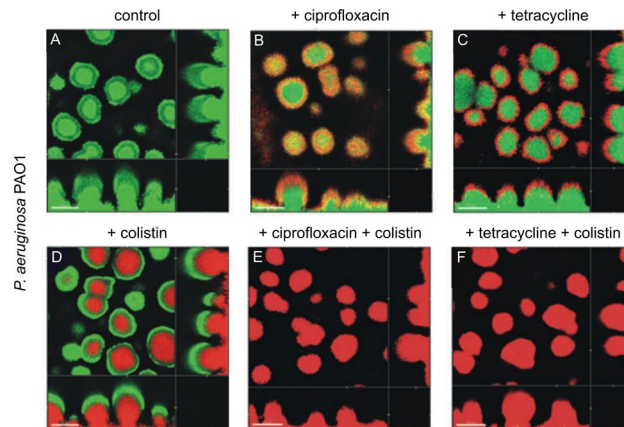


**Figure 7.** Targeting distinct subpopulation in a *P. aeruginosa* biofilm by single or combined antibiotic treatment. Biofilms were grown for 4 days and afterwards continuously exposed for 24 h to either **A)** propidium iodide as control, or **B-F)** 60 µg/ml ciprofloxacin, 200 µg/ml tetracycline, and/or 25 µg/ml colistin in different combinations together with propidium iodide. *P. aeruginosa* PAO1 was tagged with a green fluorescent protein (GFP) to allow visualization of live cells, and dead cells were visualized using propidium iodide. The confocal micrographs show a horizontal section with two images (to the right and at the bottom) representing the x-z and y-z planes. Scale bars: 50 µm. Reprinted/adapted with permission from John Wiley and Sons [92].

### 2.2.1. BIOFILM TOLERANCE TO ANTIBIOTICS

The problem of antibiotic resistance due to genetic mutated bacterial strains is not the only problem that hampers infection control. The second, still unsolved problem in the control of human bacterial infections is the poor activity of antibiotics on biofilm-associated infections. The definition ‘tolerance’ should not be mistaken with ‘resistance’. Resistance describes the inherited ability of bacteria to survive killing by antibiotics or the host immune system [95]. In contrast, tolerance is the ability of cells to survive without using genetic mutation mechanisms and it is therefore a phenotypical phenomenon [96,97]. Tolerant bacteria cease growing in the presence of antibiotics, however, they do survive and can initiate cellular division once the antibiotic therapy is removed [98]. Moreover, tolerant bacteria may survive antibiotic treatment in a biofilm, but if they disperse from the biofilm, and become single cells, their susceptibility to antibiotics is restored [95]. The development of tolerance takes time, but once established biofilm-associated bacteria present a 10-1,000 fold increased tolerance towards antibiotic treatment compared to their planktonic counterparts [7,99].

The tolerance of biofilm-associated bacteria to antibiotics is a multifactorial issue caused by both physical, physiological and adaptive matters [7,9]. Several factors have been suggested to account for this tolerance [3,7,9–11], including:

- I) The physical presence of the EPS matrix that limits the penetration of antibiotics and in which enzymatic inactivation may occur,
- II) The reduced metabolic growth rates in the biofilm due to oxygen and nutrient gradients inducing the dormancy state,
- III) The development of persister cells.

The biofilm mode of growth also promotes the occurrence of genetic mutations and cell-to-cell communication is increased [9,100]. Genes coding for resistance to antibiotics can pass horizontally from one bacterium to another due to their close proximity in the biofilm matrix, hence spreading resistance to other subpopulations [9]. The comprehensive signaling network, quorum sensing, allows coordination of the phenotypic expressions in response to changes in the population density [28].

The EPS matrix, in which the bacteria are deeply embedded, constitutes a physical barrier that the antibiotics need to diffuse through. Restricted antibiotic penetration may occur in cases where the antibiotic binds to components of the EPS matrix [10], such as alginate or eDNA [101,102]. Especially cationic antibiotics have shown restricted penetration in *P. aeruginosa* biofilms [103,104]. It is the general consensus that reduced diffusion through the biofilm primarily provides short-term protective effects against antibiotics and does not have a substantial role during long-term treatment [9]. However, it has been suggested that the slow diffusion of antibiotics permit plenty of time for the bacteria to evoke alternative protective responses adopting to a more tolerant state [99,105]. Additionally, biofilms most often reside in environments where the negatively charged mucus is also present. This is especially an issue in cystic fibrosis patients that have a genetic mutation causing an abnormal expression of chloride channels. This results in a thick viscous mucus covering their epithelial surfaces, such as the gastrointestinal tract and the lungs [106]. The mucus serves as an ideal environment for the colonization of bacteria with alterations of the normal microbiome and secondary development of chronic inflammation [106]. Mucus influences bacterial communication and motility, which play important roles in biofilm formation [107]. Moreover, the mucus layer adds an additional barrier limiting drug penetration by entrapping the molecules within and is therefore an important factor to account for in the design of *in vitro* biofilm models [103,108]. As for example, aminoglycosides have shown slow penetration through both mucus and biofilms due to electrostatic interactions [102,103]. Also, enzymes present in the biofilm matrix can inactivate or neutralize certain antibiotics. This has been shown for especially  $\beta$ -lactams, where induction of  $\beta$ -lactamase transcription in response to the presence of the antibiotic have been reported. The enzyme inactivates the antibiotic while penetrating through the biofilm layers [109]. This induction is an example of an antibiotic-specific adaptive tolerance mechanism.

Differential physiological activity of the bacteria in biofilms can also be an underlying cause of biofilm-associated antibiotic tolerance. As previously mentioned, biofilms are subject to oxygen and nutrient gradients creating subpopulations within the biofilm that are more or less susceptible to antibiotic therapy. Especially, the slow-growing or non-dividing populations found in the core of the biofilms display increased tolerance to most common antibiotics, as they often target cellular processes that occur in a growing bacteria such as replication or cell wall synthesis [92]. Therefore, the presence of metabolically inactive biofilm cells is a major factor contributing to the biofilm tolerance, and a combination of antibiotics targeting both the metabolically active and inactive subpopulations are needed for effective treatment [92].

Development of persister cells also contribute to the antibiotic tolerance of the biofilms [96]. The fraction of persister cells is usually low (typically less than 1 %) and they should be distinguished from the antibiotic-resistant mutants and the bulk subpopulation of metabolically inactive cells in the core of biofilms [95,96]. Persisters do not grow in the presence of antibiotics. Instead, they remain dormant during antibiotic exposure but retain the capacity to proliferate when antibiotic concentrations drops [110,111]. Therefore, persisters serve as a reservoir of surviving pathogens that are responsible for recurrent biofilm infections and therapeutic failures. The mechanism that underlies the formation of persisters remains to be solved [96]. However, it has been suggested that the persister cells form in response to the same stress factors that also promote biofilm formation, like starvation, changed temperatures along with exposure to low concentrations of antibiotics [95,96,112].

#### 2.2.2. TARGETING MICROBIAL BIOFILMS

Different strategies can be applied for biofilm treatment, targeting one or more of the above mentioned tolerance mechanisms. As shown in **Figure 8**, biofilm control can be achieved by:

- I) Preventing initial adhesion of bacteria to surfaces and reduce the planktonic population before biofilm establishment,
- II) Through removal of preformed biofilms by weakening, disruption or a direct killing.

In the early phase of biofilm development, the bacteria are more susceptible to antibiotic therapy, but as soon as a mature biofilm is established they become difficult to eradicate. Therefore, it is desirable to treat infections as early as possible to avoid bacterial aggregation and at a point where the host immune defense is capable of phagocytosing the remaining fraction of bacteria [9]. However, biofilms, at an initial stage, generate very little inflammation and are therefore most often impossible to detect. This is why preventive approaches have become popular with a prophylactic treatment of biofilm formation on implants or catheters [9]. These can be coated or impregnated with antimicrobials for prevention, thereby achieving higher localized antibiotic concentrations for longer periods of time compared to a systemic administration [8,113–115].

Eradication of already established biofilms can be achieved by a physical removal of the biofilm. This may be achieved by using mechanical, energy-based, or light-based disruption [8]. Moreover, biofilms can be eradicated by targeting vital structural and functional traits in the microbial biofilm including degradation of the EPS matrix, targeting the social communication within the biofilm or targeting the unique biofilm microenvironment, and elimination of the dormant cells [8].

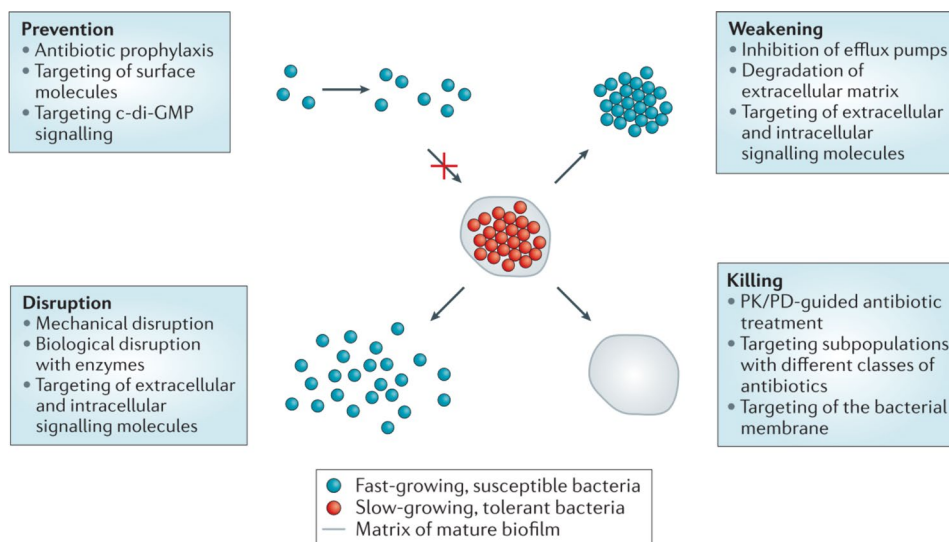


**Figure 8.** Anti-biofilm strategies. The blue circle represents susceptible bacteria and the red circle represent tolerant bacteria. The large light blue circle indicates the matrix of mature biofilms. Abbreviations: Cyclic diguanosine-5'-monophosphate (c-di-GMP); pharmacokinetics/pharmacodynamics (PK/PD). Reprinted/adapted with permission from Springer Nature [9].

Recent approaches include targeting of the EPS matrix, either by disrupting its synthesis, targeting the chemical components within or inducing EPS dispersal [8]. Although, one should consider the variability in the composition of the EPS matrix of biofilms of different bacterial species which provides an extra complexity to the development of EPS-targeting therapies [8]. Researchers have identified several signaling networks that promote EPS synthesis and constitute possible targets. An example is the second messenger cyclic-di-GMP, that governs the transition from the planktonic state to biofilm formation [116]. Molecules that bind or regulate free cyclic-di-GMP (such as diguanyl cyclase and phosphodiesterase) are potential EPS dispersing agents [8,116]. In general, quorum sensing also constitutes a possible target for biofilm treatment as this communication network is tightly linked to the stabilization of biofilms [117]. Researchers are still trying to understand the complex phenomenon of quorum sensing. Meanwhile, several studies have highlighted the beneficial effects of quorum sensing inhibitors, targeting the cell-to-cell communication instead of intracellular processes [117,118].

Matrix-degrading enzymes can help to disperse the bacteria within the biofilm by changing the viscoelastic properties of the EPS and ultimately lead to a more effective killing when combined with antibiotic treatment. Enzymes that degrade the polysaccharides in the EPS have gained interest, for example the glycoside hydrolase dispersin b that was found to induce biofilm disassembly in several bacterial species such as *Staphylococcus epidermidis* and *E. coli* [8,20,119]. The polysaccharide alginate also constitutes a major part of especially mucoid biofilms [44]. Degradation of alginate has been achieved by alginate lyase, thus rendering the biofilm-associated bacteria more susceptible to the antibiotic treatment. For example, co-administration of alginate lyase with gentamicin or ciprofloxacin increased the killing of mucoid *P. aeruginosa* [101,120,121]. Another main component of the EPS matrix is the eDNA that contributes to

the structural integrity of the biofilm [23]. Likewise, treating biofilms with the enzyme DNase has shown effective to release large amounts of biomass in various biofilm-forming species including *P. aeruginosa* [20,23]. However, the effectiveness of using DNase therapy seems to be limited to younger biofilms, owing to the fact that mature biofilms contain increasing amount of extracellular material other than eDNA affecting the recalcitrance [23].

The glycoprotein, mucin, constitutes another possible target for improving the treatment of biofilms. Mucins are the major structural and functional component of mucus and is responsible for the associated viscoelastic hydrogel properties [122]. The mucolytic agent, N-acetylcysteine (NAC), has been applied to decrease the viscosity of the highly cross-linked mucins [123]. NAC interacts with sulfhydryl groups, disrupting the disulfide bindings in the mucin proteins, thus reducing the viscosity of the mucus (**Figure 9**) [124,125]. Therefore, it is used to loosen the thick mucus *e.g.* in the lungs of cystic fibrosis patients [126]. Interestingly, NAC has also shown to possess antibacterial properties against both Gram-positive and Gram-negative bacteria [124,127,128], yet, the mechanism still remains to be fully clarified [129]. It has proven to be beneficial in inhibiting biofilm adherence and development as well as in disrupting preformed *P. aeruginosa* biofilms [123,124,127,129,130]. Combining antibiotics with NAC for efficient therapy has recently been done in spray dried powder for inhalation, finding that co-treatment with azithromycin, tobramycin or ciprofloxacin conserved or improved the inhibition of *P. aeruginosa* biofilms [131].

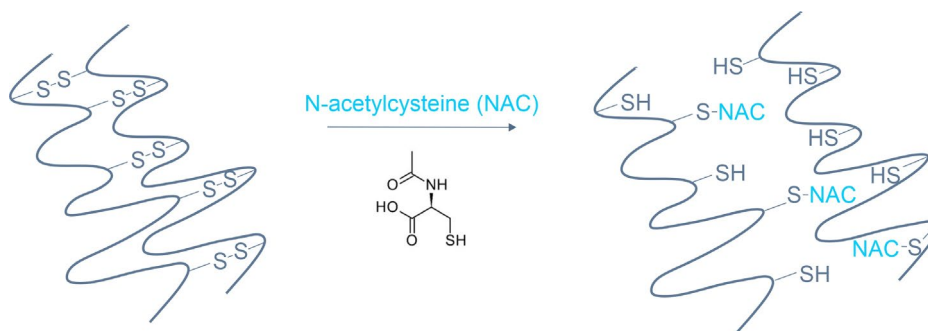


**Figure 9.** Mechanism of action of the mucolytic activity of N-acetylcysteine (NAC). Schematic was created with inspiration from [125].

A last strategy, aiming to kill all the bacteria in the biofilm, is to use synergistic antibiotics targeting the different subpopulations present in the biofilm [92]. Also, using AMPs represents an attractive approach in treatment of biofilms offering great advantages as an alternative to the traditional antibiotics. Their pore-forming activity can target metabolic active cells in addition to dormant cells, resulting in rapid bacterial killing, which might reduce the potential of the bacteria to develop resistance [8,132].

## 2.3 DRUG DELIVERY SYSTEMS FOR BIOFILM TREATMENT

A large therapeutic dose of antibiotic is usually needed to directly kill the bacteria, because of the high tolerance of biofilm towards these. This leads to an enlarged risk of systemic toxicity when using traditional drug delivery methods, such as tablets, powders or solutions to deliver the therapeutic compound for example orally, by inhalation or by injection [12,133]. By these means, many side effects have been reported such as allergic reactions, hepatotoxicity, and nephrotoxicity as well as damage of the otherwise healthy commensal microbiota [12]. One of the major challenges of these conventional formulations is that the antibiotic may be cleared away too quickly, as for example by the peristaltic movements of the intestines or mucociliary clearance in the lungs. This will limit the time in which the drug remains at a concentration above the effective minimal inhibitory concentration (MIC) at the site of infection. To increase the therapeutic efficacy, modern drug delivery systems, such as particulates encapsulating the antibiotics, play an important role providing a controlled antibiotic delivery to target sites of the body at an optimal rate and in a concentration within the therapeutic range [134].

Several drug delivery systems have been developed over the years (**Figure 10**). Inorganic carriers made of mesoporous silica have attracted attention as potential delivery systems of antibiotics as they can provide protection and prevent aggregation, control drug release, and reduce toxicity [134]. Mesoporous silica nanoparticles (MSNs) have well-defined pores capable of storing antibiotics. They display good chemical stability with a stable frame structure and a tunable surface chemistry [135]. Antibiotic loading efficiencies are high and mostly impacted by the electrostatic double-layer interaction between the antibiotics and the silica surface. Inadvertent release of drug from MSNs can be prevented by chemically conjugating the antibiotics to the MSNs, which can additionally increase the loading efficiency [2]. Nitric oxide-releasing MSNs showed more than 99 % killing of *P. aeruginosa*, with smaller particles sizes (50 nm) exhibiting superior eradication compared to larger ones (100-200 nm) [136]. In another study, a high therapeutic activity of lysozyme-loaded MSNs was observed towards *E. coli* biofilms compared to the bulk counterpart and, at the same time, a high lysozyme loading (350 mg/g particle) was achieved [135].

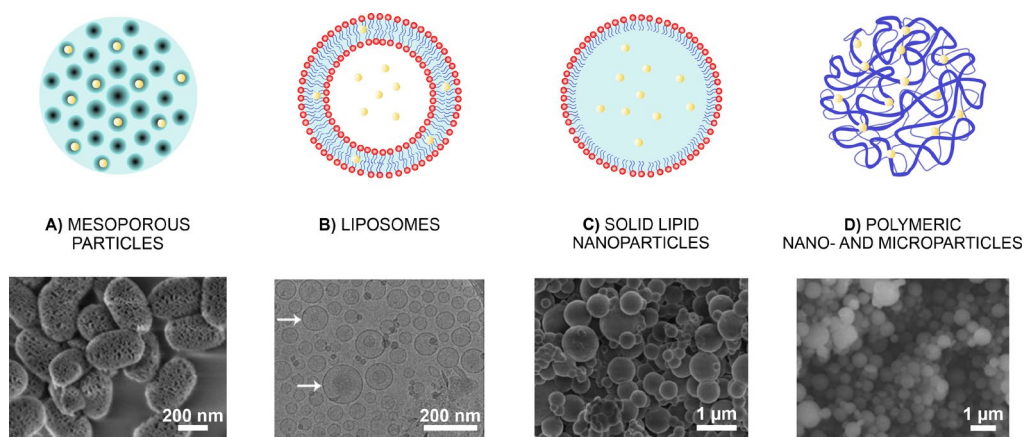


**Figure 10.** Selected particulates for drug delivery. **A)** Hollow mesoporous silica nanoparticles (MSNs) (imaged with TEM [135]). **B)** Liposomes (imaged with cryo-TEM [137]). **C)** Solid lipid nanoparticles (imaged with SEM [138]). **D)** Chitosan nanoparticles (imaged with SEM) [139]. Micrographs are reprinted/adapted with permission from Royal Society of Chemistry [135] and Springer Nature [137–139].

Lipid-based drug delivery carriers, *i.e.* liposomes, micelles, and solid lipid nanoparticles (SLNs), have been suggested as attractive antibiotic carriers due to their versatility and biocompatibility [134,140–143]. Liposomes are physiologically compatible vesicles composed of one or more phospholipid bilayers. Hydrophilic drugs can be encapsulated within the aqueous core, whereas lipophilic drugs can be incorporated into the phospholipid bilayer(s). They have the unique property of fusing with bacterial phospholipid bilayers, creating channels to release their antibiotic cargo directly into the intracellular space of the bacterium yielding superior killing of many Gram-positive and Gram-negative biofilm-embedded bacterial strains [134,144,145]. Based on an increasing number of studies on the interaction between liposomes and biofilms, the size, charge, and membrane fluidity of the liposome are considered important factors influencing penetration and thereby, the bactericidal activity [134]. For example, cationically modified liposomes were found to be more strongly attracted to the negatively charged bacterial cell wall leading to a better penetration into *S. aureus* and *P. aeruginosa* biofilms, improving bacterial killing compared to their uncharged and anionic counterpart [144,146]. Tobramycin-loaded liposomes were administered to the lungs of rats chronically infected with *P. aeruginosa*, and the results showed that by using a more fluidic phospholipid bilayer compared to a rigid one, a complete eradication of *P. aeruginosa* was obtained [147]. Liposomes can also shield their cargo from unintended binding with the biofilm matrix. Alipour *et al.* studied the incorporation of cationic antibiotics, tobramycin and polymyxin B, in liposomes [148]. Using the liposomes, they demonstrated an increase in antimicrobial activity against *P. aeruginosa* as the liposomes protected the antibiotics from binding to the polyanionic polymers commonly found in the cystic fibrosis sputum (eDNA, F-actin, lipopolysaccharides, and lipoteichoic acid) [148]. Utilizing liposomes for co-delivery of a quorum sensing inhibitor, farnesol, together with ciprofloxacin showed greater eradication of a *P. aeruginosa* biofilm. Further investigation with transmission electron microscopy (TEM) revealed partial disrupted cell walls, an effect believed to be caused by the liposomes [149]. When administering farnesol and ciprofloxacin together in liposomes, the ciprofloxacin concentration required to achieve similar biofilm inhibition was 125-fold or 10-fold lower compared to free ciprofloxacin or ciprofloxacin in liposomes, respectively [149]. However, the clinical effectiveness of the currently developed liposomal delivery systems is being debated. Their drug loading is often inadequate and the storage stability towards temperature fluctuations is poor. Moreover, under physiological conditions, the stability is also usually low, causing physical aggregation and premature drug release which influences the *in vivo* therapeutic efficacy [12,145,150].

In the last decades, a large amount of work has been directed towards the development of polymeric micro- and nanoparticles as drug carriers [151]. In **Paper I**, we present and discuss polymer-based particulate systems and their activity against biofilms. Particles containing poly (lactic-co-glycolic acid) (PLGA), chitosan and polycaprolactone (PCL) are in focus, but strategies involving combinations of these polymers are also reviewed. Compared to liposomes, polymeric particles are attractive as they are more stable, possessing a high structural integrity afforded by the rigidity of the polymer matrix [12,152]. They protect the antibiotic against environmental degradation, deactivation or clearing by which sustained

therapeutic concentrations are maintained. Drug release is controllable and occurs from the matrix by diffusion, swelling or polymer erosion, or a combination of these processes depending on the polymer of choice [153]. In general, achieving a slow and sustained drug release is a crucial aspect in drug delivery, as maintaining therapeutic concentrations for a longer time reduces the dosing frequency. It requires a combination of a fast and sustained antibiotic release (biphasic release) from the particulates to achieve an effective antimicrobial biofilm therapy [154–157]. An initial burst release will ensure a high antibiotic concentration for biofilm eradication and thereby, a lowered risk of promoting antibiotic resistance development [2,157]. Thereafter, the particles can serve as an antibiotic depot, providing a sustained release above the MIC, capable of minimizing any further biofilm growth [158,159].

Various polymers, both synthetic and natural ones, have been used for formulating biodegradable polymeric micro- and nanoparticles, with some of the most commonly used ones being PLGA, chitosan, and PCL [140,142,157,160]. They are appealing biopolymers for drug delivery as they have a great safety profile, good biocompatibility and adjustable biodegradability. They can be prepared with a controllable size distribution and surface charge [153] using a variety of techniques including nanoprecipitation [158,161], solvent displacement [162], emulsification [163–165], spray drying [165], electrospraying [166], ionic gelation [167], and hot-melt extrusion [168]. The difference in size between the micro- and nanoparticles has numerous effects and whether one is aiming for a micro- or nanometer sized carrier highly depends on the intended route of administration. The smaller the particle, the greater proportion of loaded drug will have access to the external environment, which can lead to quick loss of the payload [169]. On the other hand, nanoparticles may reach locations, such as the deep lung tissue, whereas the upper airways retain the larger particles. The biofilms are often embedded in thick mucus layers that can bind and inactivate antibiotics. The encapsulation of these antibiotics in nanoparticles can overcome the problem as it prevents interactions between the antibiotic and the EPS components, allowing drug penetration [126,170,171]. Also, using polyethylene glycol (PEG) coating (PEGylation) is a common approach to achieve neutral ‘mucus-inert’ particles [172] and has shown to increase the mobility of particles in *Burkholderia multivorans* and *P. aeruginosa* biofilms [173]. The advantages of microparticles, in contrast to nanometer-sized particles, are their larger drug loading capacity, longer time of particle degradation and thus, a greater potential of extended drug release [169]. Recently, the idea of embedding nanoparticles in microparticles (NEMs) has arisen, possessing benefits from both particular systems [165,170,174]. As for example, colistin-loaded PLGA nanoparticles were embedded in a carrier of lactose thus, producing NEMs suitable for inhalation therapy with optimal flow properties with subsequent biofilm penetration of the PLGA nanoparticles and a sustained release of colistin [170].



## 2.4 MICRODEVICES AS DRUG DELIVERY SYSTEM

With advances in material science, chemical engineering and manufacturing technology, numerous novel nano- or microparticulated delivery systems have appeared and had a paramount influence on improving drug therapeutics. However, particles are limited by their multidirectional release not only into the mucus but also into the lumen. Moreover, particles may differ considerably in size, and the drug-polymer ratio can vary between the particles, why it can be difficult to estimate the amount of loaded drug [175].

Microfabrication of drug delivery devices holds great potential for producing uniform devices of various sizes and with distinct morphologies. The general concept is that the drug is enclosed in a micro-reservoir protecting the drug from environmental degradation. Once the device reaches the intended site of drug delivery, it facilitates unidirectional drug release thus, limiting drug loss into the lumen [176,177]. Additionally, microdevices are also being developed for injection purposes, as for example to provide a controlled, pulsatile antigen delivery after subcutaneous injection [178]. Different sizes and shapes of microdevices have been suggested, ranging from patch-like structures, only few micrometers in height (**Figure 11A-B**) to squared, triangular or cylindrical ones having a height of up to 300  $\mu\text{m}$  (**Figure 11C-D**). The patch-like structures have shown improved mucoadhesion because of their high resistance to flow [179,180]. However, having a higher structure means that they can carry a larger amount of drug and have also been shown to embed in the intestinal mucus [181].

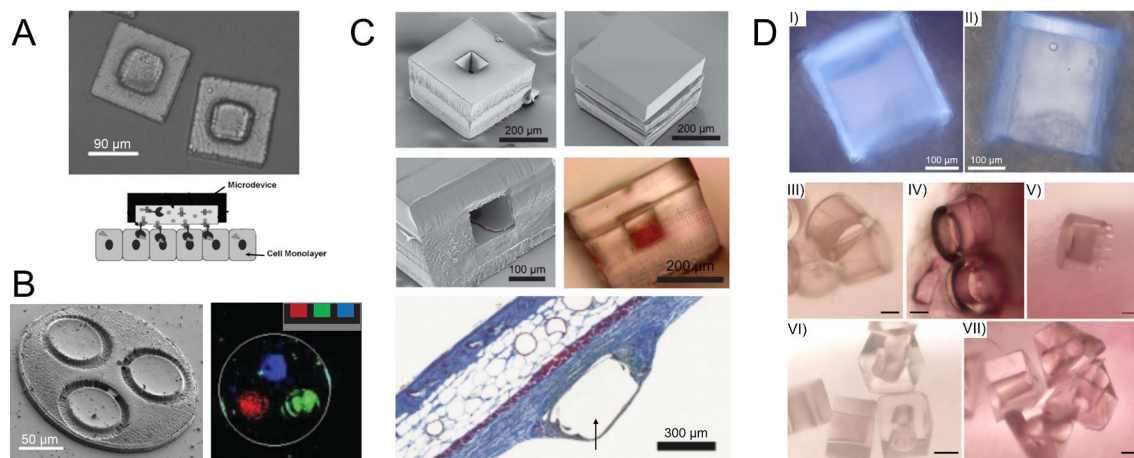


**Figure 11.** Microdevices for drug delivery. **A)** Poly-methylmethacrylate (PMMA) patches with a single reservoir [180], or **B)** SU-8 patches with three reservoirs loaded with multiple different drugs. The patches were designed for oral drug delivery, have a low resistance to flow and great mucoadhesive properties [179,182]. **C)** Microsquares fabricated in poly (lactic-co-glycolic acid) (PLGA) using the newly developed ‘stamped assembly of polymer layers’ (SEAL) technique. Particles were designed for timed pulsed delivery of antigens after subcutaneous injection (arrow in masson’s trichrome staining points at the injected device), but also showed suitable for pH-controlled intestinal drug delivery [178]. **D)** Microcontainers (MCs) embedded in intestinal mucus following *in situ* perfusion studies. MCs were cylindrical (I-IV), cylindrical with pillars (V), cubic (VI) or triangular (VII). Scale bars: 100  $\mu\text{m}$  [181,183]. Reprinted/adapted with permission from John Wiley and Sons [179,180,182], Elsevier [181], The American Association for the Advancement of Science and MDPI [183].

When intended for oral delivery, the smooth muscle contraction from peristalsis causes a convective flow, which can challenge the adherence of the microdevice to the epithelial lining [184]. To encounter this problem, researchers have chemically modified the surface of the microdevices with bioadhesive agents, such as lectin, aiding a stronger adhesion to the intestinal mucosa [182,185,186]. Moreover, microdevices have been designed to penetrate or adhere to the mucus layers by using approaches like nanostraw-patterning to allow topography-mediated adhesion (**Figure 12A**) [187]. Other types of larger devices have been designed with stimuli-responsive self-folding abilities such as the thermal-sensitive “grippers” attaching into the gastrointestinal mucosa with stiff tips and allowing extended drug release (**Figure 12B-C**) [188,189]. Traverso and co-authors also developed star-shaped ultra-long acting delivery devices enabling release of multiple different drugs purposed for HIV or malaria therapy. The devices stayed in the stomach for weeks providing a sustained drug delivery, whereafter it could pass through the gastrointestinal tract to be excreted (**Figure 12D**) [190,191]. Besides improving drug bioavailability, these devices offer an exciting strategy to treat various intestinal diseases locally. Further investigations of the effect of similar devices on gastric biofilms could be of great interest.

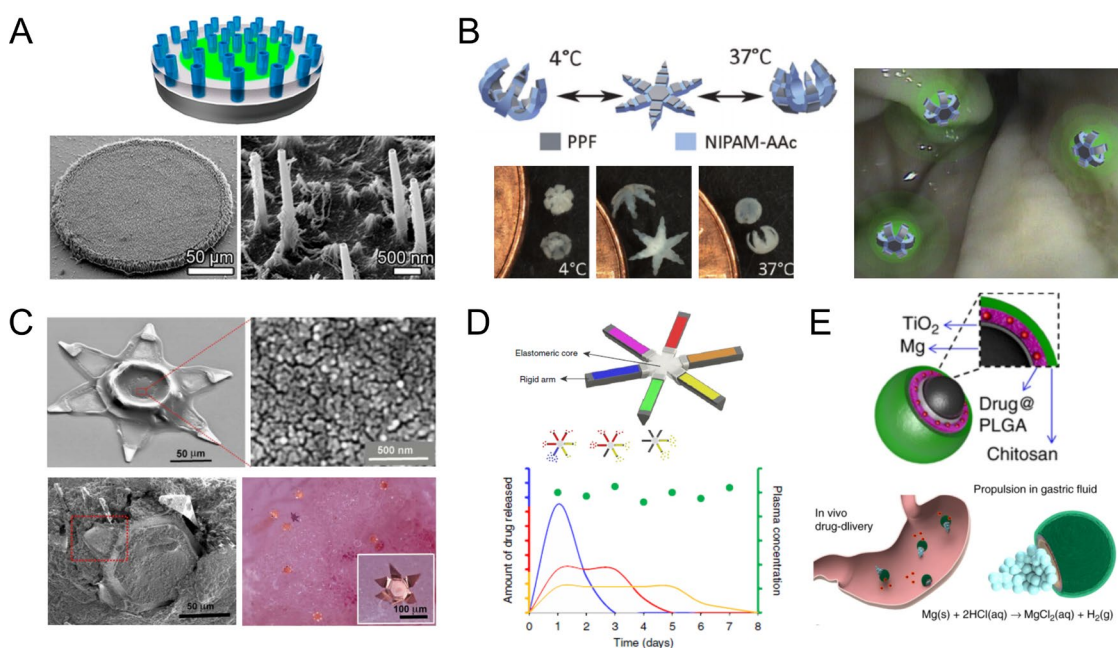


**Figure 12.** Advanced drug delivery devices. **A)** Sealed microdevice with nanostraw structures [187]. **B)** Microdevice (theragrippers) with stimuli-responsive self-folding abilities gripping into the tissue and releasing drug for up to 7 days in the stomach of a pig. Due to the thermal responsiveness of the material, the grippers reversible open and close around body temperature. Right: conceptual illustration of the theragrippers attached to the gastrointestinal mucosa [188]. **C)** Theragrippers for rectal administration apply sufficient force to penetrate the colonic mucosa. Scanning electron microscopy (SEM) and bright-field images show a single theragripper latching onto the colon mucosa *ex vivo* [189]. **D)** Gastric-resident star-shaped long-acting dosage forms for antiretroviral or malaria treatment. The dosage form consists of an elastomeric core and six drug-loaded arms that release at different rates. As shown from the graph, selection of appropriate polymers can result in sustained plasma drug concentrations over longer periods [191]. **E)** Micromotors (consisting of a Mg core, a TiO<sub>2</sub> shell coating, a clarithromycin-loaded poly (lactic-co-glycolic acid) (PLGA) layer, and a chitosan layer) provide *in vivo* propulsion for drug delivery against a *H. pylori* infection in a mouse stomach [192]. Reprinted/adapted with permission from American Chemical Society [187], John Wiley and Sons [188], Springer Nature [191,192], and American Association for the Advancement of Science [189].

Self-propelling microscale devices (*i.e.* micromotors) use gas-evolution reaction such as acid hydrolysis of a metal or hydrolysis of metal oxides, for self-propulsion towards the mucosal lining, resulting in mucoadhesion [184,193]. Micromotors have the unique ability to penetrate and be retained in the mucus layers without damaging the underlying epithelial. Micromotors have been applied to treat local infections in the stomach and dental biofilms [192,194,195]. De Ávila *et al.* loaded Mg/PLGA/chitosan-based micromotors with clarithromycin for treatment of *H. pylori* biofilm infections in a mouse model (**Figure 12E**). The micromotors retained in the stomach wall and performed *in vivo* bactericidal activity against *H. pylori* [192]. Recently, Villa *et al.* proposed self-propelled tubular micromotors against dental biofilms and demonstrated efficient dental biofilm disruption up to 95 % killing in only 5 min of treatment [194]. The killing effect was attributed to the combination of the antibacterial activity of the TiO<sub>2</sub>/Pt micromotors themselves with the simultaneous generation of hydroxyl radicals and microbubbles created on the surface of the biofilm [194]. Not long ago, Yuan *et al.* demonstrated micromotors modified with the antimicrobial peptide nisin for highly selective inactivation of Gram-positive bacteria and biofilms showing a 2-fold increase of the killing ability as compared to free peptide and the static counterparts [195]. Micromotors are still in their early-stage development, but it is envisioned that the concept in the future will be useful for eliminating hard-to-treat bacterial biofilms with the motor propulsion leading to biofilm penetration towards enhanced antibiotic delivery.

While being impressive in terms of the engineering creativity and possessing multiple benefits, these systems lack the simplicity needed for commercial upscaling. We propose the microcontainers (MCs) as one type of microdevices, due to their ease of fabrication, versatile functionalization possibilities as well as a high drug loading capacity. Previous works have shown that MCs enhance the oral bioavailability of small drugs such as furosemide and ketoprofen, most likely attributable to inherent mucoadhesive properties of MCs getting engulfed by the intestinal mucus [181,196]. We speculated that these properties could be exploited for biofilm treatment by I) delivering the antibiotic to the site of infection hence, avoiding unwanted side effects and limiting the use of antibiotic, and II) creating a high local antibiotic concentration, reaching therapeutic concentrations and thereby, an improved biofilm eradication.

MCs are polymeric containers consisting of walls and a bottom defining a reservoir in which drugs can be loaded. They are fabricated from SU-8 using photolithography as originally described by Tao *et al.* [197] and later modified by Nielsen *et al.* [198]. **Figure 13A** shows the principle of cross-linking SU-8 by exposure to UV-light, thereby shaping MCs by a two-step photolithography process. In previous works, it was shown that SU-8 MCs can be fabricated in many different sizes and shapes depending on the specific need. The mostly studied ones are cylindrical with inner diameters of 73-413  $\mu\text{m}$  and inner height of 210-270  $\mu\text{m}$  [181,183,198,199]. In this PhD thesis, cylindrical MCs with an inner diameter of about 230  $\mu\text{m}$  and a reservoir depth of about 220  $\mu\text{m}$  were applied (**Figure 13B-C**). Not long ago, also cubic and triangular MCs (**Figure 11D**) have been fabricated and showed to be more mucoadhesive than the cylindrical ones [183,200]. This suggests that the presence of corners or edges can influence the mucoadhesion properties of the MCs, however, the effect of such shapes on biofilms remains to be studied.

MCs or similar reservoir-based microdevices have been fabricated using a variety of materials and techniques. The choice of fabrication technique highly depends on the choice of material. The most common ones include photolithography [198], soft lithography [201], and hot embossing combined with mechanical punching [202] or hot punching [203]. Microdevices were initially fabricated in photoresists including poly-methylmethacrylate (PMMA) [186] and SU-8 [197]. SU-8 is an epoxy-based negative photoresist with great mechanical strength and chemical stability. Various micro/nanostructures for tissue engineering and drug delivery have been fabricated in SU-8, and it has been reported suitable as implant materials due to its biocompatibility [204,205]. However, SU-8 or similar resists are not biodegradable and therefore, several methods for the fabrication of microdevices in biodegradable polymers have been proposed including poly(lactic acid) (PLLA) [202,203,206], PCL [206,207], and PLGA [201,208]. Fabrication of biodegradable microdevices is paramount for the technology to reach the clinic. However, they are still in their development phase and incorporation of drugs and subsequent deposition of functional polymers still need to be optimized. Therefore, the MCs applied in this PhD thesis were fabricated in SU-8. This material is highly suitable for prototyping of microdevices and for proof-of-concept studies, as the fabrication process is well-established and easily controlled in terms of reproducibility [175].

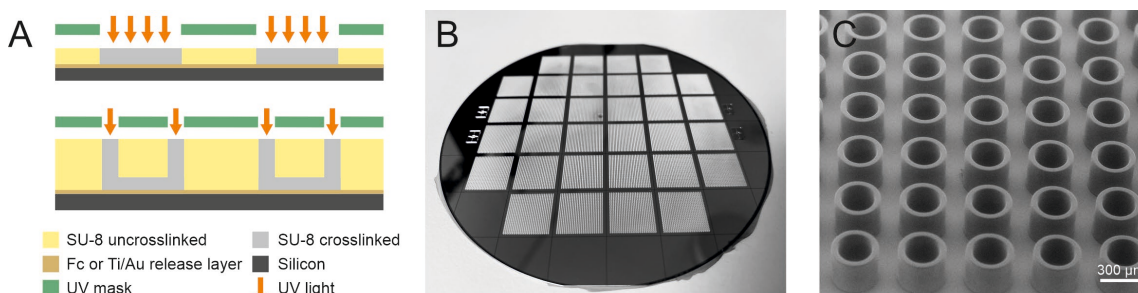


**Figure 13.** **A)** Microcontainers (MCs) are fabricated on top of silicon wafers using photolithography to first create the base and subsequently, the walls of the MCs. A release layer of fluorocarbon (Fc) or titanium/gold (Ti/Au) can be applied to allow release of single MCs. **B)** Image of a wafer containing 32 squares/chips, each holding 625 individual MCs. **C)** Zoom-in on MCs.

Various strategies have been developed for drug loading into MCs or similar microdevices, including inkjet printing [209,210], supercritical CO<sub>2</sub> impregnation [196,211], photolithography [176,182], and spin coating with subsequent hot punching [212]. Also, more manual techniques including powder embossing [213], centrifugal compaction [214], or manual powder filling using a spatula or brush [181,198] have been reported. By combining the latter methods with the use of a shadow mask that covers the gaps in-between the MCs, unintended drug loss can be avoided. The shadow mask has been prepared in aluminum by micro-milling [213] or in polydimethylsiloxane (PDMS) [215]. The first mentioned loading techniques are more time-consuming and complex than the manual ones, and the optimal choice of method should allow a homogenous and reproducible loading while providing a minimal drug waste. Which method to use is highly dictated by the physicochemical properties of the drug powder (*i.e.* particle size, stickiness, and solubility) and the need of any excipients along with the cost of the drug. In this thesis,

a combination of manual powder filling, centrifugal compaction, and powder embossing was applied. These techniques allow a simple drug loading, with no need of any excipients (solvents or polymers), meaning that the entire drug cavity could be loaded with drug (**Figure 14B**) [214].

#### 2.4.1. POLYMERIC FUNCTIONALIZATION

MCs can be coated with different functional polymers (**Figure 14**). Various polymer film depositing techniques exist, among which spray coating has shown to be useful in coating three-dimensional structures like MCs [196,216]. Ultrasonic spray coating includes the formation of a fine mist of a polymer solution by the use of high frequency sound vibrations [217]. The solution is deposited on a sample through a narrow orifice using air pressure and thereafter, coalesce to form a coating.

Mucoadhesive or mucopenetrating polymers, such as chitosan and PEG, have been widely used in the development of micro- and nanoparticulates [218,219]. By increasing the mucoadhesion and, thereby, the residence time of the drug formulation at the intended site of drug delivery, one can avoid unintended degradation or premature drug release in the lumen and achieve higher sustained local drug concentrations. As for example, colonization of *H. pylori* in the stomach requires administration of an anti-secretory agent together with one or more antibiotics, yet, the combination is limited due to side effects. Polymeric particles, such as chitosan microspheres, may serve as a great alternative by adhering to the gastric mucosa while releasing antibiotics in a sustained manner [220–222].

Chitosan is a cationic polysaccharide consisting of N-acetyl-D-glucosamine and D-glucosamine subunits linked together via 1-4-glycosidic bond (**Figure 14**) [223,224]. It is obtained by a partial deacetylation of the natural occurring chitin and is available in different molecular weights and degrees of deacetylation, which influences viscosity and solubility [218,223]. At low pH, the primary amine undergoes protonation ( $pK_a$  of 6.5), explaining the higher solubility in acidic solvents [223]. One of the key characteristics of chitosan is its gelation properties as it swells when in contact with water. The hydrogel formed can control drug release [225,226]. Furthermore, chitosan has gained much attention due to its non-toxic mucoadhesive properties [227]. Chitosan contains numerous polar functional groups enabling interaction with mucus through physical entanglements and secondary chemical bonds resulting in the formation of weakly cross-linked networks [226]. The cationic nature of chitosan provides strong electrostatic interactions with the negatively charged components of the mucus, such as mucins and nucleic acids, and the amino and hydroxyl groups of chitosan enables hydrogen bonding and covalent bonding [218]. Chitosan has also been shown to possess antimicrobial activity against a wide variety of microorganisms including *Streptococcus mutans* [228,229], *S. aureus* [230], and *P. aeruginosa* [231,232]. It was proposed that the interaction between the positively charged chitosan and the negatively charged LPS in the outer membrane of Gram-negative bacteria is the main mechanism of action of the antimicrobial activity, ultimately leading to leakage of intracellular constituents and cell death [223,233]. In general, low molecular weight chitosan has a higher antibacterial activity compared to the higher ones [229,234] and was therefore applied in this PhD thesis. *Ex vivo* retention studies on sections of porcine intestine showed that chitosan-coated MCs provided a three-fold increase in mucoadhesion compared to

uncoated MCs [216]. The same tendency accounted for PEG-coated MCs. PEG is an uncharged hydrophilic polymer (**Figure 14**) that has shown mucoadhesive or mucus penetrating properties, depending on the surface density and the molecular weight [171,235]. Wang *et al.* documented improved mucus penetration of polystyrene nanoparticles coated with low molecular weight PEG (2 kDa), whereas higher molecular weight PEG (10 kDa) improved mucoadhesion [219]. The low molecular weight PEG coatings possess hydrophilic and near neutrally-charged surfaces that minimize mucoadhesion by reducing hydrophobic or electrostatic interactions [236]. The increased mucoadhesion of higher molecular weight PEGs may be ascribed to the longer polymeric chains which entangle with the highly cross-linked mucin network and, moreover, a greater number of intermolecular interactions such as hydrogen bonding may be present [219]. In this PhD thesis, 11-15 kDa PEG was applied, which is believed to facilitate mucoadhesion. Other polymers have also been applied as functionalization of the MCs. This includes PLGA that has been used with the idea to enhance drug solubility by creating a more acidic local environment in close proximity to the MC [216]. Moreover, to protect the loaded cargo, the MCs can be sealed with a pH-sensitive polymer, such as the poly(meth)acrylate-based Eudragit (**Figure 14**), to trigger drug release at certain pH values such as in certain regions of the gastrointestinal tract [181,196].

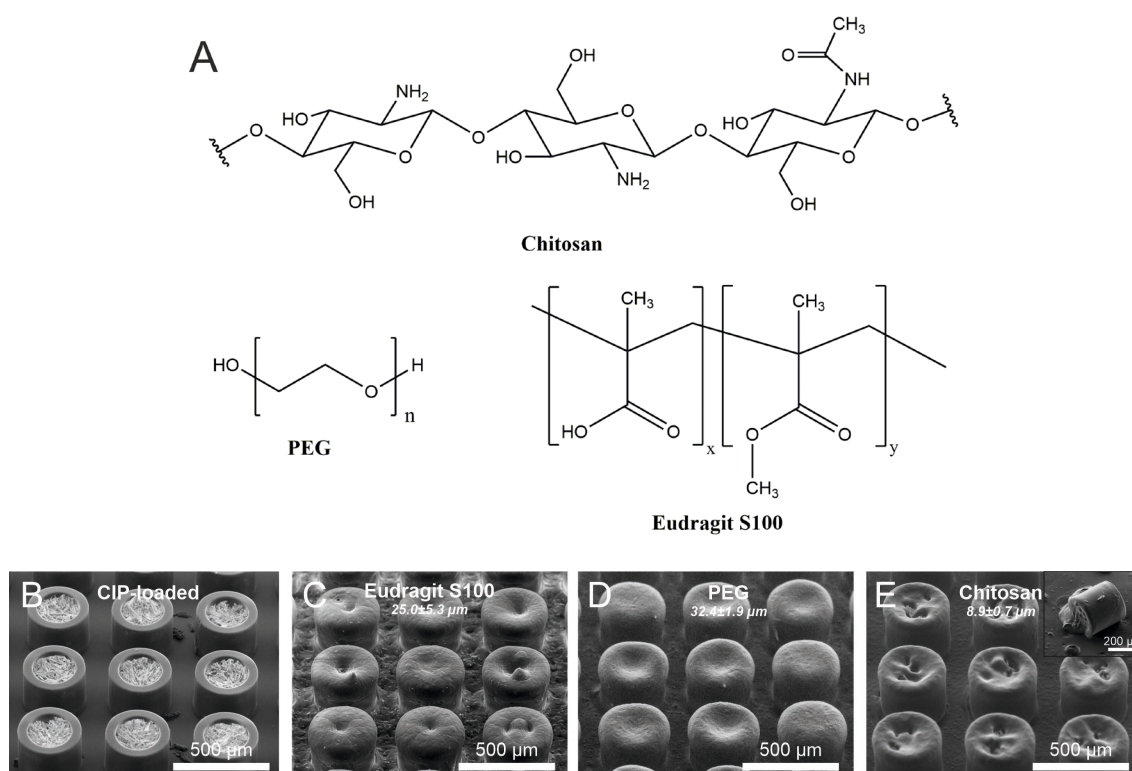


**Figure 14.** **A)** Chemical structures of the polymers applied in this PhD thesis. The backbone of chitosan consists of a linear polysaccharide composed of randomly distributed D-glucosamine (deacetylated part) and N-acetyl-D-glucosamine subunits. Polyethylene glycol (PEG) is a hydroxyl polyether chain. Eudragit S100 is made of methacrylic acid (x) and methyl methacrylate (y) subunits. **B-E)** Examples of coatings applied on microcontainers (MCs) in this PhD thesis. Uncoated MC loaded with ciprofloxacin hydrochloride (CIP) (**B**) and subsequently coated with Eudragit S100 (**C**), PEG (**D**), or chitosan before and after exposure to water (corner) (**E**). The coating thicknesses are reproduced from **Paper II**.



## 3 RESULTS AND DISCUSSION

---

The following section has been divided according to the papers (**Paper II-V**). Each subsection is composed of the overall purpose of the study, together with a comment section describing and discussing selected results along with methods, additional observations, and challenges related to the project.

### 3.1 ANTIBIOTIC-LOADED MICROCONTAINERS AGAINST BIOFILMS – PROOF-OF-CONCEPT

The following subsection is based on the results presented in **Paper II** “Microcontainer delivery of antibiotic improves treatment of *Pseudomonas aeruginosa* biofilms” (for full paper, see Appendix II) as well as selected additional findings not included in the paper.

#### PURPOSE

The aim of this study was to investigate the overall potential of MCs in the treatment of bacterial biofilms. The mucus-engulfment, tunable drug release and high drug loading capacity led us to think that MCs could overcome the challenge of delivering sufficient concentrations of antibiotics to biofilms. We believed that the bacterial killing would improve as the local drug concentration increase.

#### OUTCOMES

##### Drug loading capacity of MCs

There are several advantages with the use of MCs compared to other particulated delivery systems, such as liposomes, as the MCs can be loaded with any type of powdered drug, no matter size, charge or hydrophilicity. We chose ciprofloxacin hydrochloride (CIP) as a model drug, as this is a well-known fluoroquinolone antibiotic with clinical relevance in the treatment of a variety of bacterial infections including *P. aeruginosa* [237]. MCs also have a large drug loading capacity, exemplified in **Paper II**, where each MC was loaded with  $4.39 \pm 0.77$   $\mu\text{g}$  CIP corresponding to a loading capacity of 18.0-25.6 % w/w. This is considerable higher than what has been reported for other polymer-based drug delivery systems, where it is often much lower than 10 % w/w (see **Paper I**). In the future, an even higher drug loading capacity could be achieved by decreasing the wall thickness of the MCs to yield larger cores.

##### Flow chamber technology and efficacy of MCs on *P. aeruginosa*

*P. aeruginosa* was chosen as a model organism to test the overall potential of MCs in the treatment of bacterial biofilms. It was selected as it possesses good biofilm-forming properties, the biofilm is well-characterized, and it is involved in severe infections [238]. The properties of the biofilm differ significantly if grown in static conditions, where the medium is not replenished, from the ones exposed to flow, which is believed to enhance the physiological relevance of the biofilm [239,240]. Flow chambers offer a continuous supply of nutrients to the biofilm, aid in removal of waste and provide shear stress, which ultimately allow production of mature biofilms [241]. Therefore, microfluidic-based systems using flow

chambers combined with confocal laser scanning microscopy (CLSM) are considered the “golden standard” [242]. CLSM offers several advantages over conventional optical microscopes, including its high resolution with reduction of background noise away from the focal plane. Series of sections can be acquired through the depth of the specimen, making it extremely useful for studies on thick biofilms [243]. The combination of flow chamber systems with CLSM allows nondestructive observation of the three-dimensional biofilms in real time [240,244]. To enable this visualization, the strains have to be stained or tagged with a fluorescent probe. In **Paper II-IV**, *P. aeruginosa* (lab strain PAO1) was genetically modified to express green fluorescent protein (GFP) [245], while staining with propidium iodide allowed visualization of dead bacteria.

Previously designed flow chambers [242,246] could not be used to study MCs because of the dimensions of the MCs. Consequently, the flow chambers were redesigned and fabricated with an inlet channel to which a small piece of silicon tubing was glued, allowing for inoculation of MCs (**Figure 15**). Fabrication was performed by drilling in a 6 mm thick sheet of polycarbonate (for detailed protocol of standard flow chambers, see [246]). The chambers needed to be washed carefully multiple times with ethanol, water, and soap before leftover materials from the fabrication process did not influence cellular proliferation.

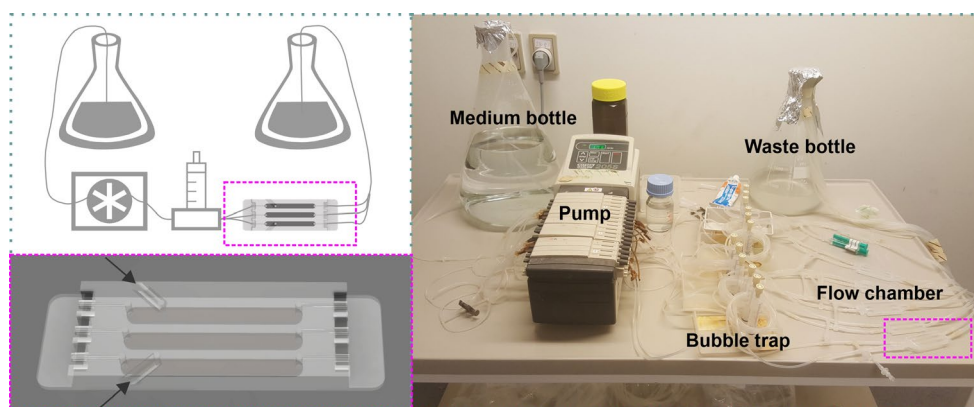


**Figure 15.** Schematic illustration of the flow chamber system together with an image of the system. Growth medium is pumped from the medium bottle through the bubble traps, to avoid destruction of developing biofilm structures in the flow chambers, and thereafter led into a waste bottle. The flow chamber (pink zoom-in) was designed in order to allow inoculation of microcontainers (MCs) through inlets (marked with arrows).

To ensure that the MCs did not possess any toxic effects, possibly causing microbial death, empty MCs were placed on an agar plate incubated with *P. aeruginosa*. No inhibition zones were observed after 24 h of incubation. Furthermore, adding empty MCs to a planktonic suspension of *P. aeruginosa* cells did not show any growth inhibition after monitoring the optical density and viable counts for 24 h. Lastly, incubation of empty MCs inoculated into a 96 h old biofilm did not show any growth inhibition as the biomass after 24 h treatment was  $11.2 \pm 0.6 \mu\text{m}^3/\mu\text{m}^2$ , compared to  $10.2 \pm 0.3 \mu\text{m}^3/\mu\text{m}^2$  before treatment. Therefore, we concluded that the MCs did not possess any toxic effects towards the *P. aeruginosa* cells. These observations correlate with the biocompatible nature of SU-8 previously evidenced by cell viability and *in vivo* histocompatibility studies [204].



Ultrasonic spray coating was used to coat the CIP-loaded MCs with PEG, chitosan, or Eudragit S100. PEG and chitosan were chosen based on their mucoadhesive properties [218,235], and since they provided a fast and sustained release of CIP, respectively. The pH-sensitive polymer, Eudragit S100, was included with the idea of activating the antibiotic release by changing the pH, but release profiles revealed sustained CIP release from MCs coated with Eudragit S100. In spite of that, Eudragit S100 was included in the antibacterial studies, since PMMA-Eudragit microparticles were previously reported to reduce adherent methicillin-resistant *S. aureus* compared to treatment with free antibiotics [247,248].

To assess the performance of polymer-coated CIP-loaded MCs against planktonic *P. aeruginosa*, standard viable counting and optical detection measurements were employed. The flow chamber system combined with CLSM allowed studying the effect of MCs on biofilm-associated *P. aeruginosa*. The mature biofilms were exposed to antibiotic treatment either as I) a single-dose bolus injection (CIP introduced directly in the tubing after the bubble trap and before the cell chamber), II) constant perfusion (CIP present in the growth medium), or III) CIP confined in coated MCs (**Figure 16**).

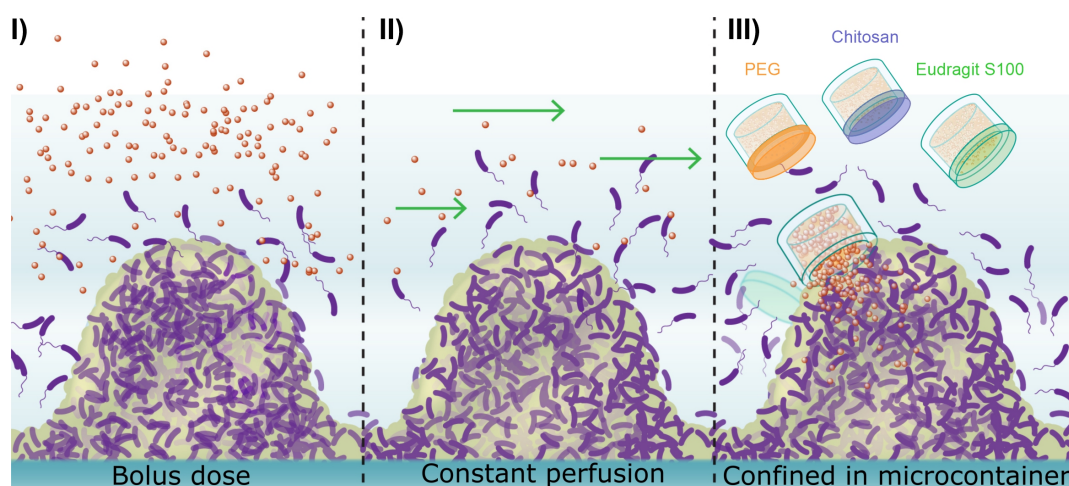


**Figure 16.** Schematic overview of the treatments, that *P. aeruginosa* biofilms were exposed to in flow chambers: I) Bolus dose of ciprofloxacin hydrochloride (CIP), II) constant perfusion of CIP, or III) CIP confined in polyethylene glycol (PEG), chitosan or Eudragit S100-coated microcontainers (MCs). Image modified from graphical abstract (**Paper II**).

All antibiotic-containing MCs inhibited planktonic growth of *P. aeruginosa* cells, but the degree of inhibition depended on the coating. PEG-coating (faster CIP release) provided the best and fastest killing of planktonic bacteria, whereas chitosan (sustained CIP release) performed best on biofilms (**Figure 17**). We believe that this may be due to a combination of the sustained drug release through the chitosan hydrogel lid as well as a local antibacterial activity of chitosan. However, when investigating the effect of empty chitosan-coated MCs on *P. aeruginosa* biofilm, no significant killing was observed. Increasing the concentration of chitosan could potential provide statistical significant killing.

In general, the MCs provided about three times more killing of biofilm-associated *P. aeruginosa* compared to a single bolus dose of CIP in the same concentration as delivered in the MCs (**Figure 17**). This clearly

demonstrates the importance of a sustained delivery of CIP to the biofilm. Moreover, the MCs provided killing equal to a constant flow of 2.75 higher concentration of solubilized CIP perfused over the course of 24 h (4  $\mu\text{g}/\text{mL}$ , corresponding to the minimal biofilm inhibitory concentration) (**Figure 17**), proving the benefit of delivering antibiotics locally in the MCs.

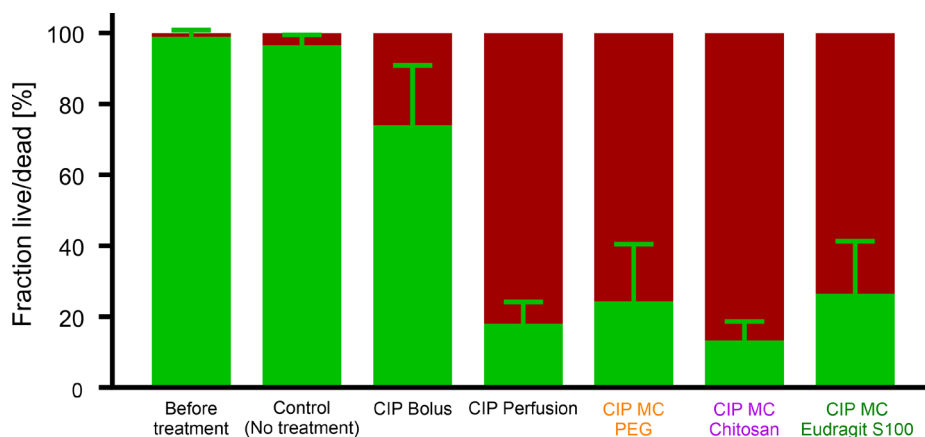


**Figure 17.** Comparison of the live/dead ratio (%) after 24 h treatment of a *P. aeruginosa* biofilm with ciprofloxacin hydrochloride (CIP) administered as: I) Bolus dose [120  $\mu\text{g}$ ], II) perfusion [330  $\mu\text{g}$  over the course of 24 h], or III) confined in microcontainers (MCs) [ $\sim 120 \mu\text{g}$ ] coated with either polyethylene glycol (PEG), chitosan, or Eudragit S100. Data is presented as mean+SD (n=4-24). Green represents live bacteria. Red represents dead bacteria.

MC-based antibiotic treatment did not completely eradicate the biofilm, and the remaining fraction might be an antibiotic-tolerant subpopulation of cells in a temporary dormant state with minimal cellular division and therefore, minimal susceptibility to CIP. Co-delivery of antibiotics targeting these different subpopulations could be useful to obtain full killing (as investigated in **Paper III**). Biofilm formation is regulated in response to nutrient levels in the environment [249]. Limitations in nutrients are known to favor biofilm development with transition of cells into dormancy. On the other hand, in extreme nutrient-rich conditions a greater number of cells are in the planktonic, metabolic active phase. In here, they rapidly regain their antibiotic susceptibility [250]. Thus an idea, yet to be tested, is using the MCs to deliver transient concentrations of a nutrient-rich compound, such as glucose or citrate, followed by intense antibiotic therapy. In this case, however, one should keep in mind the risk of possible spread of planktonic bacteria to establish biofilms in new niches.

#### Localized antimicrobial activity of MCs

It was of interest to investigate of the distance-dependent killing obtained from a single MC. In the results described above, multiple MCs were inoculated in order to have a detectable effect on the mature biofilm grown in flow chambers. Confocal images were acquired in close proximity to single MCs, however, the MCs only spread to some degree across the flow chamber making it difficult to obtain a distance-dependent killing profile. Therefore, *P. aeruginosa* was grown in a 24-well glass bottom plate allowing the development of a thin biofilm. After only 1 h of treating with a single CIP-loaded, uncoated MC, a local antibacterial activity in close proximity to the MC was evident (**Figure 18**). The killing decreased with

increasing distance from the opening of the MC and few colonies remained alive despite being in close proximity to the MC, which is believed to be tolerant subpopulations. Monitoring the distance-dependent killing for a prolonged period as well as the killing from MCs functionalized with different polymeric coatings would aid an even better understanding of the localized killing from the MCs. This was further addressed in **Paper IV**.

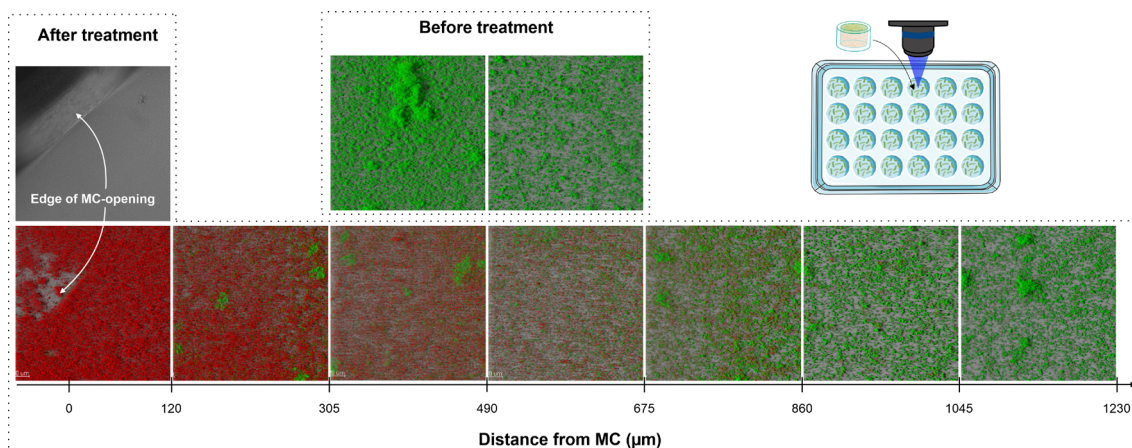


**Figure 18.** *P. aeruginosa* biofilm treated with an uncoated MC loaded with ciprofloxacin hydrochloride (CIP). The biofilm was grown for 24 h at 37 °C at 200 RPM in a 24-well glass bottom plate in FAB medium (see **Paper II** for preparation) with a final concentration of glucose of 30 mM (100x higher than used in the flow chamber due to the lack of flow of nutrients). Confocal images were acquired after 1 h of treatment and Imaris software was used to present live cells (green) and dead cells (red). The opening of the MC is located at the top left corner. Note: distances are approximations as no controlled stage was available.

To enable a fast and automated screening of functionalized MCs, an oCelloScope was employed. The oCelloScope is a novel optical system that allows real-time analysis of bacterial processes, by using digital time-lapse microscopy scanning to generate a series of images which can undergo subsequent algorithmic analysis to obtain growth kinetics [251]. The method has previously been applied for rapid and accurate real-time monitoring of bacterial proliferation and provided the MIC used to define the susceptibility breakpoints [251–253]. Thus, the majority of studies were conducted on cells in their exponential phase. Recently, it was suggested to include minimal bactericidal concentration determinations for more detailed understanding of the bacteria susceptibility to antibiotic drugs and, thus, more clinically relevant data [254]. Nevertheless, no studies have yet investigated the activity of antibiotics and their delivery system on already established biofilms using an oCelloScope. The feasibility of using the oCelloScope to study the local effect of a functionalized MC on biofilm was assessed. The MCs were loaded with CIP and functionalized with PLGA, PEG or chitosan. All MCs decreased the biomass over time (based on the incoming light intensity) compared to the growth control without addition of MCs (as exemplified with PLGA in **Figure 19**). Although, there was an evident effect of the treatment, we did not observe any significant changes in biomass between coated and uncoated MCs. Further optimization of the instrument and the use of it is needed for production of novel results concerning polymer-functionalized MCs.

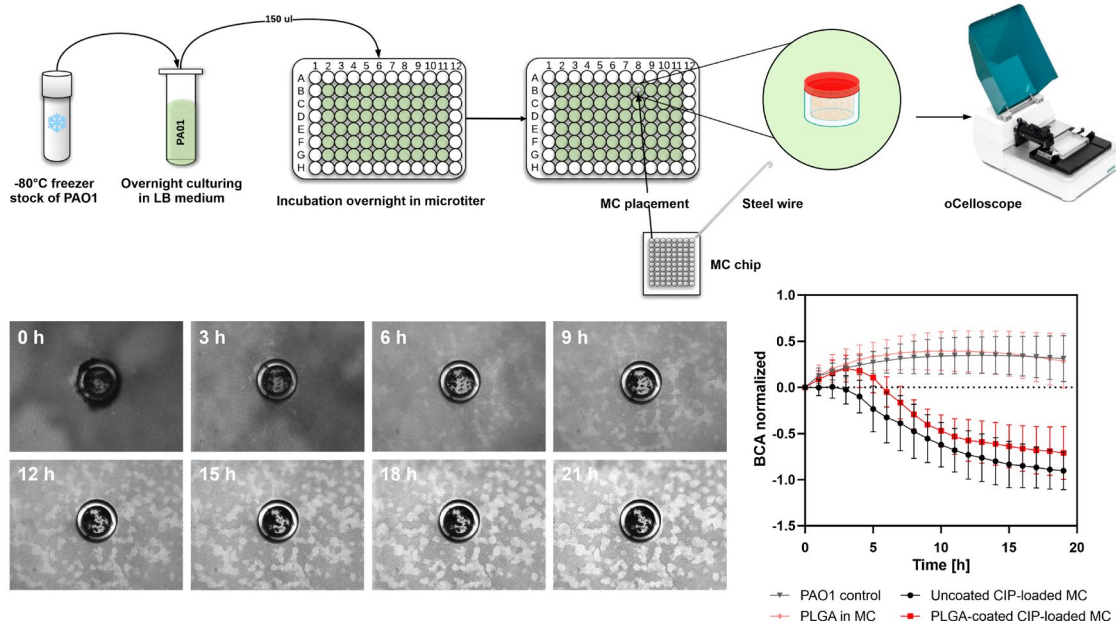


**Figure 19.** Eradication of *P. aeruginosa* biofilm assessed by the oCelloScope with subsequent image analysis using the built in background corrected absorption (BCA) algorithm. Biofilms were allowed to develop in 96-well plates for 24 h at 37 ° C. On the following day, they were exposed to either an uncoated microcontainer (MC) loaded with ciprofloxacin hydrochloride (CIP) or a CIP-loaded poly (lactic-co-glycolic acid) (PLGA)-coated MC. As controls, a MC loaded with pure PLGA and a growth control were included. Representative images show PLGA-coated CIP-loaded MC inhibition. Quantitative results are expressed as mean values±SD (n=5-17).

### 3.2 CO-DELIVERY OF SYNERGISTIC ANTIBIOTICS USING MICROCONTAINERS

The following subsection is based on the results presented in **Paper III** “Co-delivery of ciprofloxacin and colistin using microcontainers for bacterial biofilm treatment” (for full paper, see Appendix III) as well as selected additional findings not included in the paper.

#### PURPOSE

The aim of this study was to realize and test the co-loading of MCs with two antibiotics aimed at targeting metabolically active as well as dormant subpopulations of a *P. aeruginosa* biofilm.

#### OUTCOMES

In **Paper III**, we utilized MCs to co-deliver two synergistic antibiotics to *P. aeruginosa* biofilms. CIP is believed to be effective against metabolically active cells, and colistin sulfate (COL) thought to target and kill the metabolic inactive cells. The antibiotics were chosen based on their previously established activity against different subpopulations within a *P. aeruginosa* biofilm [92]. Previous studies have realized co-delivery of CIP:COL, however, only using lipid-based formulations [83,137,255]. For co-loading, the powders were mixed in a 1:8 w/w ratio based on the MIC values of the individual antibiotics towards *P. aeruginosa* PAO1 cells (0.125 µg/mL for CIP [256]; 1 µg/mL of COL [257]). The CIP:COL powder was successfully loaded into MCs by combining centrifugal compaction [214] with the powder embossing method [213] to ensure maximal powder loading. The co-loaded MCs were functionalized with chitosan based on the promising results presented in **Paper II**.

The effect of delivering the two antibiotics using the MCs was evaluated *in vitro* regarding the drug release. Moreover, the performance against planktonic and biofilm-associated *P. aeruginosa* was addressed by different techniques including time-kill studies with viable counting, scanning electron microscopy (SEM), atomic force microscopy (AFM) and monitoring with CLSM (**Figure 20**).

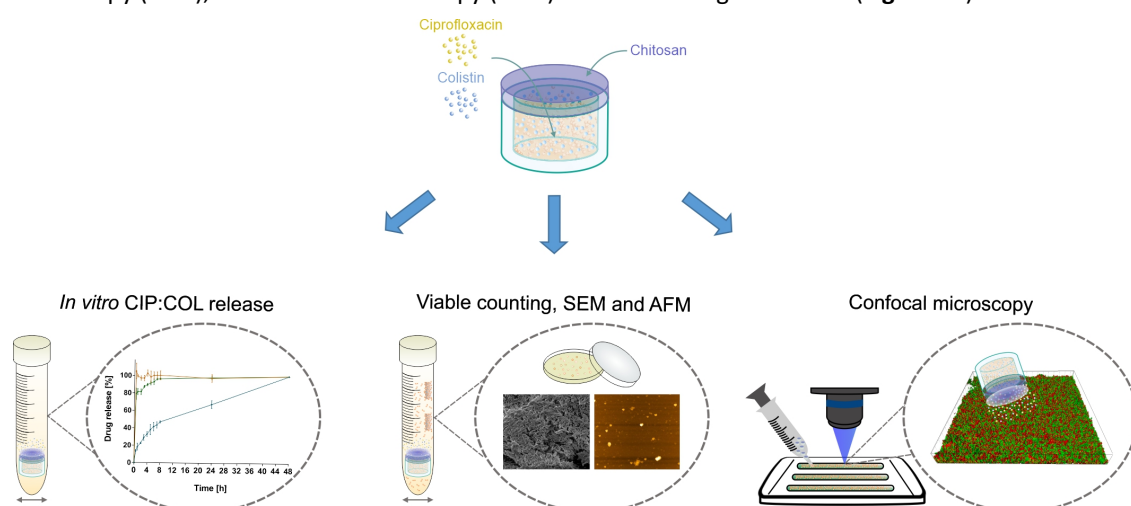


**Figure 20.** Schematic overview of the conducted experiments aimed to study the effect of co-delivering two antibiotics in MCs. Abbreviations: Ciprofloxacin hydrochloride (CIP), colistin sulfate (COL), scanning electron microscopy (SEM), and atomic force microscopy (AFM).



## Drug release and antimicrobial activity

This is the first time that two synergistic antibiotics have been delivered in MCs, and the results prove that the co-loaded MCs work significantly better than antibiotic monotherapy, providing a complete killing of the entire planktonic culture in a 24 h time-kill study. This did not account for biofilm consortia of *P. aeruginosa* grown in flow chambers, as they were not fully killed. However, the co-loaded MCs worked significantly faster than constant antibiotic perfusion ( $62.5 \pm 8.3$  % versus  $10.6 \pm 10.1$  % dead biomass after 5 h) (**Figure 21**). This is believed to be a consequence of the localized release from the MCs.

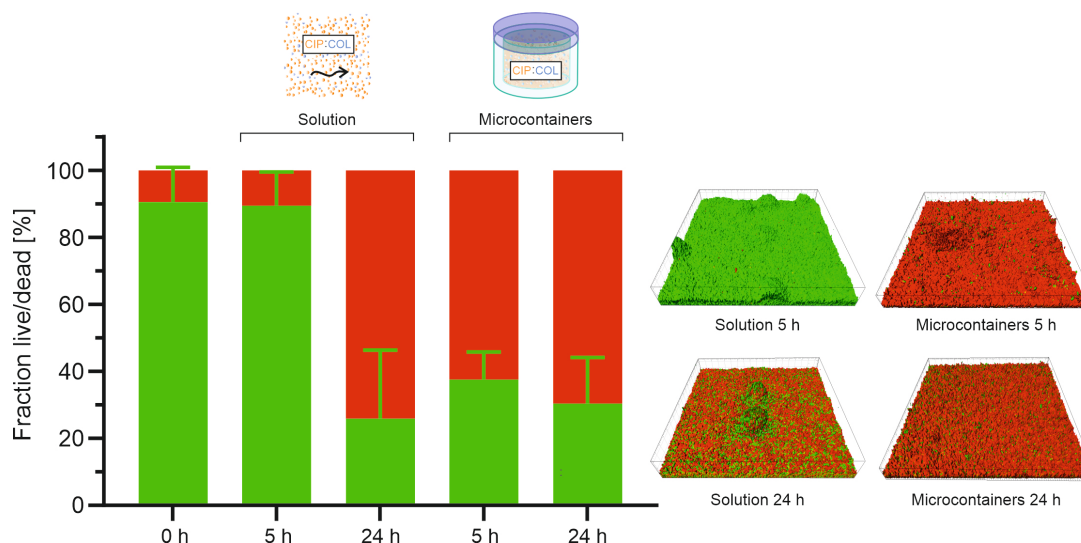


**Figure 21.** Comparison of the live/dead ratio (%) and representative confocal images after 5 and 24 h treatment of a *P. aeruginosa* biofilm with ciprofloxacin hydrochloride and colistin sulfate (CIP:COL) confined in MCs coated with chitosan or as a solution. Data is presented as mean+SD (n=12-20). Green represents live bacteria and red shows dead bacteria.

Co-loaded MCs coated with chitosan released  $98.7 \pm 5.7$  % COL and  $79.0 \pm 6.4$  % CIP through the chitosan hydrogel mesh within 30 min. SEM investigations confirmed intact lid morphology after 30 min, showing that the fast release was through the hydrogel and not caused by removal of the lid during the experiment. The release was significantly faster than what was observed for CIP single-loaded ( $13.8 \pm 1.2$  % CIP released within 30 min). Within the same timeframe, the entire cargo was released from COL single-loaded MCs, and it therefore appeared that the water-soluble and fast-releasing COL drove the release of the less soluble CIP. Incorporation of COL in liposomes have previously shown to accelerate the release of co-loaded CIP, an effect that was attributed to the amphiphilic nature of COL, acting as a surfactant affecting the liposomal bilayer [137]. It is well known, that the presence of surfactants influence the degree of hydrogel swelling and can provide micellar solubilization of poorly water-soluble drugs [258,259]. Therefore, the accelerated release may be attributed to COL serving as a surfactant affecting the degree of swelling of the chitosan-coating on the MCs and the associated release profile.

After 24 h, the co-loaded MCs and the solution showed similar killing ( $69.6 \pm 13.8$  % and  $74.1 \pm 20.4$  %, respectively) (**Figure 21**). As co-loaded and single COL-loaded MCs released their cargo quickly after

treatment initiation, one could suspect that the antibiotic concentrations would be diluted due to the flow. Surprisingly, we did not observe any regrowth after 24 h. By extending the timeframe of our experiment and monitoring the biofilm for 48-72 h after treatment using the CLSM, one could achieve valuable insight into the duration of the growth suppression.

Pamp *et al.* provided clear evidence that a combined CIP:COL-treatment kills almost all *P. aeruginosa* biofilm cells, as less than 10 cell/mL survived the combinational treatment compared to  $3.80 \times 10^5$ - $2.25 \times 10^7$  cells/mL in separately treated biofilm [92]. In **Paper III**, the biofilm was exposed to concentrations of CIP and COL based on the maximum number of MCs suitable for inoculation into the currently fabricated flow chambers. This corresponded to 4 µg/mL CIP, 2.5 µg/mL COL, or 0.34:2.85 µg/mL CIP:COL (equivalent to 32xMIC, 2.5xMIC and 2.72:2.83xMIC). These concentrations were significantly lower than the ones applied by Pamp *et al.* (60:25 µg/mL CIP:COL). For that reason, the absolute killing of mature biofilms could potentially be improved by significantly increasing the dose or varying the ratio between the co-delivered antibiotics. In **Paper III**, 82.6±9.8 % of the biomass was killed after exposing the biofilm to MCs only loaded with CIP. In **Paper II**, where the biofilm was exposed to about one-third of the total CIP dose as administered in **Paper III** (~120 µg versus ~336 µg), the amount of dead biomass was the same (88.2±5.3 %). This interesting comparison reveals that no further improvement in the bacterial killing was found despite increasing the concentration of CIP. Thus, CIP-loaded MCs are effective even with lower antibiotic concentrations.

There is generally a poor correlation between traditional antibiotic testing methods (such as MIC determination) and clinical outcomes in the treatment of biofilm infections [260]. Haagenen *et al.* developed a flow-based *in vitro* model aiming to resemble *in vivo* pharmacokinetics (PK) and pharmacodynamics (PD) with changing antibiotic concentrations, as seen with a clinical relevant intravenous bolus dose [260]. Using the PK/PD-model to treat *P. aeruginosa* with CIP (same concentration as applied in our study) led to an about 60 % reduction in biomass [261], which is lower than what we achieved with the MCs (83 %). If MC-based treatment can provide similar or even better therapeutic activities on the biofilm, one could avoid the side effects seen after systemic administration. PK/PD studies remain to be conducted with COL and the combination of CIP and COL.

#### Changes in bacterial morphology using SEM and AFM

CLSM provided valuable insight into the changes in bacterial population inactivation after treatment of *P. aeruginosa* biofilm with co-loaded MCs. However, the detailed bacterial morphology is difficult to image by optical light microscopes [262]. Therefore, SEM and AFM were applied. SEM is a well-established and widely used tool for surface imaging. A focused beam of electrons is scanned across the sample and the emitted secondary electrons or backscattered electrons are used to build up the image [262]. Electrons have a natural smaller wavelength than photons, why higher resolution images with a higher depth of focus can be obtained using SEM compared to standard optical microscopy. Unlike SEM, AFM can provide valuable quantitative height evaluation of biofilms. AFM is a highly sensitive and well-known imaging tool providing information about the morphology and topography of a given surface. The

technique is widely applied for imaging within nanofabrication and material sciences. Besides these, it is becoming more popular within the field of microbiology [263,264], and have previously been utilized for studying the effect of drug delivery systems on biofilm [83,265]. AFM uses a cantilever with a sharp flexible tip mounted to scan over a sample surface [263]. A laser beam detects the bending of the cantilever ultimately providing information about the topography of the sample [263]. When imaging a soft sample such as a bacterial cell surface or biofilms, the tapping mode is often applied [266]. Here, the tip oscillates just above the surface and a high-speed feedback loop ensures that the probe does not crash with the sample thereby, avoiding any damage of the sample [266].

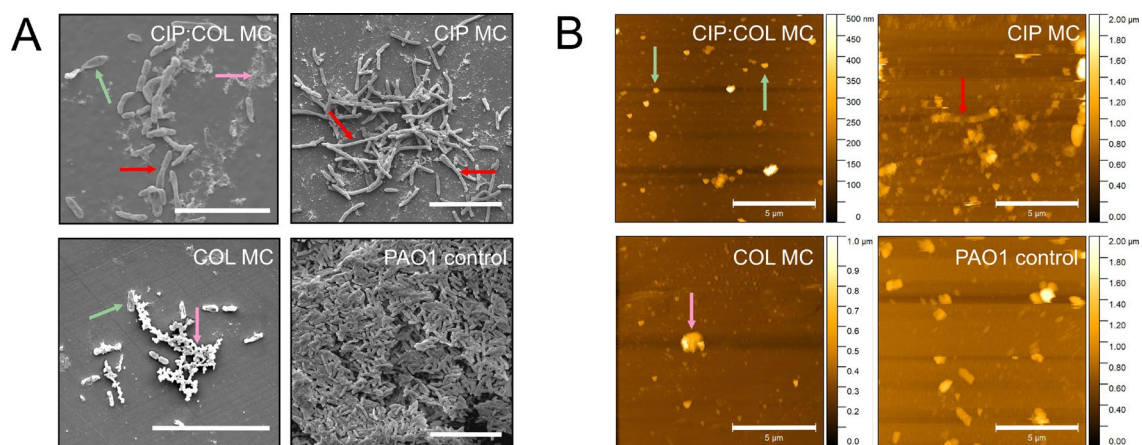


**Figure 22.** A) Scanning electron microscopy (SEM) and B) atomic force microscopy (AFM) micrographs. *P. aeruginosa* PAO1 biofilms were grown for 24 h and simultaneously treated with co-loaded ciprofloxacin hydrochloride (CIP) and colistin sulfate (COL) microcontainers (MCs), CIP MCs, or COL MCs. An untouched biofilm was included as control. Scale bars: 10 μm (SEM) and 5 μm (AFM). Arrows indicate examples of elongated bacteria (red), shrunken/collapsed bacteria (green), and extracellular debris/agglomerates (pink).

The antibiotic-loaded MCs clearly affected the morphology and population density of the bacteria (Figure 22). The morphological changes appeared to correlate with the mechanism of action of the individual antibiotics. CIP promoted cellular elongation, as it inhibits DNA replication and ultimately cellular division [63]. COL triggered cellular membrane disruption, resulting in a reduction of the number of cells as well as the emergence of extracellular debris together with shrunken and collapsed cells [79]. For the co-loaded CIP:COL MCs, the predominant effect on bacterial morphology appeared to originate from COL. Cellular debris and deformed/shrunken bacteria were observed, yet, few bacteria also appeared elongated on the SEM micrograph. This tendency is most likely a consequence of two factors. The co-loaded MCs contained significantly more COL than CIP, and secondly, COL quickly destabilizes the membrane thereby, evading the cellular elongation as otherwise observed after the treatment with only CIP. The PAO1 control SEM micrograph revealed a dense and intact biofilm. However, only few bacteria were observed on the control AFM scan, and some appeared deformed due to unknown reasons. More replicates of AFM scanning and method optimization is required in order to evaluate the effect of treatment. Therefore, the AFM scans were not included in Paper III. When growing the biofilms on the glass slide, they grew heterogeneously, which complicated AFM scanning as the scanning range was only



15 x 15  $\mu\text{m}$  on the available AFM. For further optimization, one could consider to coat the glass substrate with 0.01 % w/v poly-L-lysine hydrobromide to enhance bacterial cell adhesion and to prevent biofilm removal [83].

The SEM and AFM micrographs shown above represented inhibition of biofilm growth, as the biofilms were developed together with the respective treatments. SEM or AFM investigation of mature biofilms grown under flow could provide deeper insight into the efficacy of a MC-based treatment on clinically relevant biofilms. This could be done by isolating the glass pieces from the top of the flow chamber for subsequent SEM or AFM imaging [262]. Conventional SEM, as employed in this PhD thesis, requires fixation, dehydration and metal coating of the biofilm before observation. Since biofilms mainly consist of water, this sample preparation can influence the biofilm structure. Using Cryo-SEM or environmental-SEM techniques could be beneficial, as they have shown to leave the biofilm matrix unaffected. However, they suffer from a poorer resolution when compared to conventional SEM [262]. This is partly because of the lack of conductivity in the wet sample. To solve this, one could coat the biofilms with an ionic liquid, which is a salt that exist in the liquid state at room temperature, does not evaporate under vacuum and is electrically conductive [267]. Using ionic liquids to prepare biofilm samples for SEM observation have shown to cause less cracking of the biofilm, and does not require the extensive fixation and dehydration as conventional SEM [267].

### 3.3 MUCOLYTIC FUNCTIONALIZATION OF MICROCONTAINERS TO DISRUPT BIOFILMS

The following subsection is based on the results presented in **Paper IV** “Enhanced eradication of mucin-embedded bacterial biofilm by locally delivered antibiotics in functionalized microcontainers” (for full paper, see Appendix IV) as well as selected additional results not included in the paper.

#### PURPOSE

The aim of this study was to functionalize antibiotic-loaded MCs with a mucolytic and mucoadhesive coating. Additionally, to mimic the *in vivo* habitat of the bacteria, thus better predicting the true efficacy of the functionalized MCs, we aimed to realize biofilm growth with mucins on a perfusion microfluidic platform.

#### OUTCOMES

In **Paper IV**, we developed and tested the efficacy of chitosan/NAC-functionalized MCs, believed to possess mucoadhesive and mucolytic properties, thereby improving adhesion of the MC to the biofilm and disruption of the biofilm. Functionalization of MCs with pure NAC was not possible because of the lack of polymer properties and therefore, NAC was integrated within the chitosan coating. We found it important to test whether this incorporation compromised the activity of NAC. Therefore, the mucolytic activity of NAC was investigated in the presence of chitosan using a Quartz Crystal Microbalance with Dissipation (QCM-D) assay. Moreover, the *in vitro* drug release from MCs functionalized with chitosan/NAC was characterized (**Figure 23**).

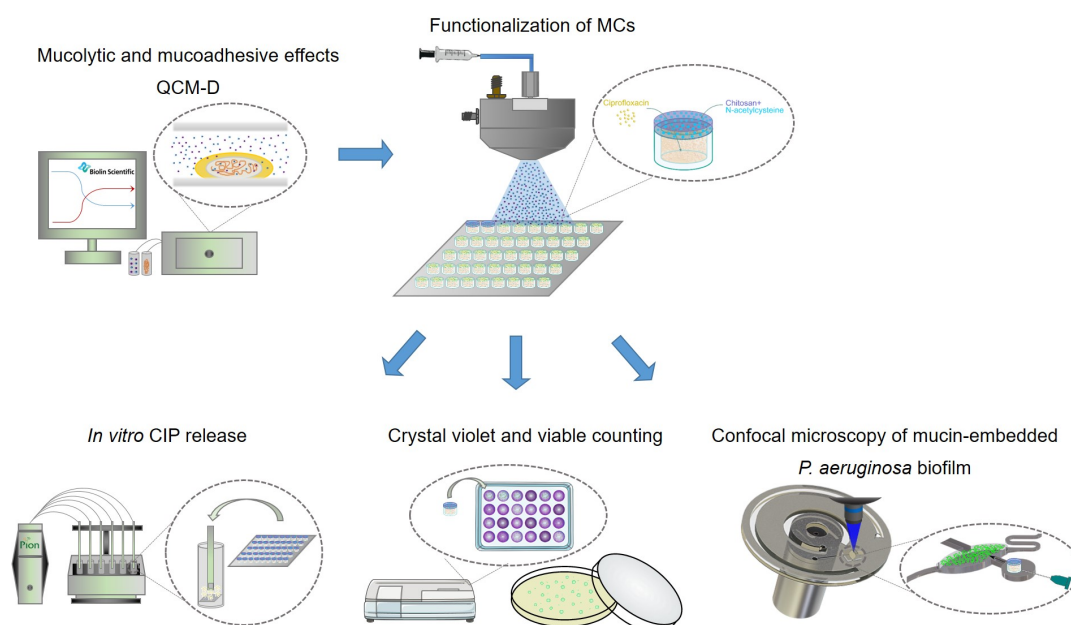


**Figure 23.** Schematic overview of conducted experiments aimed to study the effect of chitosan/N-acetylcysteine (NAC)-functionalized microcontainers (MCs). Abbreviations: Ciprofloxacin hydrochloride (CIP); Quartz Crystal Microbalance with Dissipation (QCM-D).

The complex microenvironment at the site of biofilm infections is rarely taken into account when investigating the efficacy of drug delivery systems on biofilms *in vitro*. It has previously been shown that *P. aeruginosa* biofilm development proceeds differently in the presence of mucins, as the bacteria are immobilized within the pores of the mucin structures [107,273]. Incorporation of mucins represents a model for the mucus layer, and will provide more correct *in vitro* results when testing drug delivery devices. Therefore, in **Paper IV**, we applied a mucin-containing growth medium, artificial sputum medium (ASM). Besides mucins, ASM contains DNA, and essential and non-essential amino acids, which are found in the sputum from cystic fibrosis patients [268]. The effect of chitosan/NAC MCs on *P. aeruginosa* was studied using crystal violet staining and viable counting. Moreover, we showed for the first time that it is possible to use the mucin-containing medium in a microfluidic perfusion platform. This platform was utilized to assess the efficacy of chitosan/NAC MCs on *P. aeruginosa* biofilms (**Figure 23**).

#### Investigation of mucolytic and mucoadhesive effects using QCM-D

QCM-D is able to record changes in mass and structural changes, *i.e.* viscoelastic properties due to simultaneous monitoring of changes in frequency ( $\Delta f$ ) and dissipation ( $\Delta d$ ) [269]. In brief, a quartz crystal between two electrodes is oscillating when voltage is applied. When a thin film attaches to the sensor, such as mucins, the frequency will decrease as the mass on the sensor is increasing. As the mucin layer is a soft layer, it will not be in the same oscillation phase as the crystal and dissipation will increase [270]. Afterwards, a drug formulation can be applied onto the mucin layer and changes in frequency and dissipation will reveal the interaction mechanisms [269]. In short, decrease in frequency indicates an increase in mass, and increase in dissipation implies a softer layer.

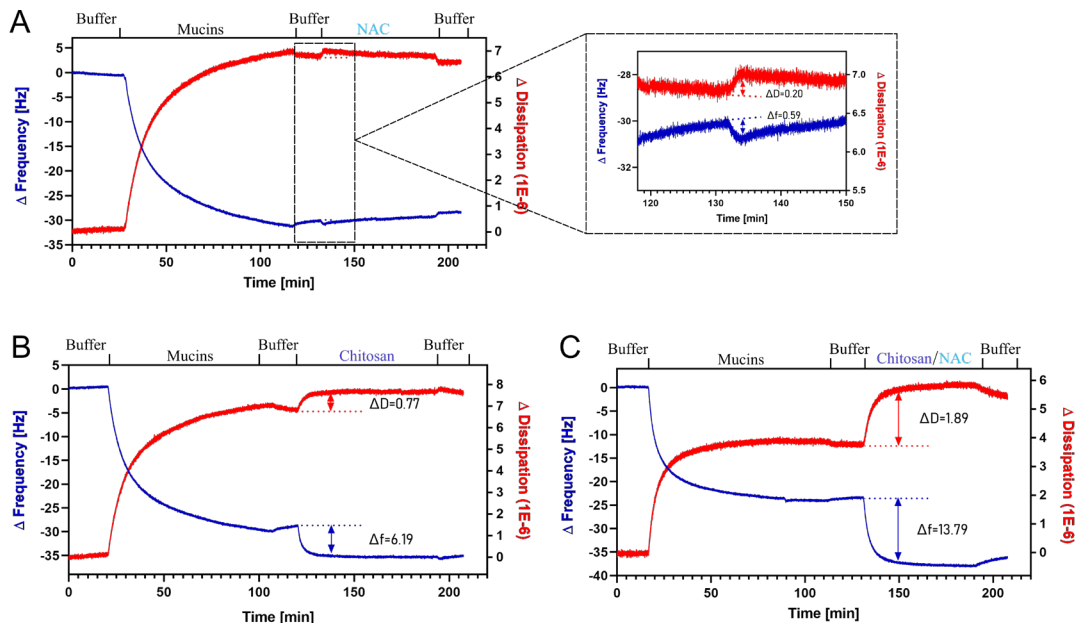


**Figure 24.** QCM-D real-time monitoring of changes in frequency (blue line) and dissipation (red line) of an established mucin layer on gold-coated sensor, in the presence of **A)** 0.4 mg/mL N-acetylcysteine (NAC), **B)** 100 mg/L chitosan, or **C)** 0.4 mg/mL NAC in 100 mg/mL chitosan. Results are representative of three independent assays in duplicates. Reprinted from **Paper IV**.

When applying the chitosan/NAC blend (as in the coating of the MCs) onto the mucin layer, we observed a decreased frequency ( $\Delta f=13.79$ ) and an increased dissipation ( $\Delta D=1.89$ ). Both of these values were higher than the ones measured after addition of only NAC or chitosan (**Figure 24**). NAC breaks the mucin chains by attaching covalently to the sulfide groups, and chitosan intermingles with the mucin network by electrostatic interactions. Ultimately, more water is taken up leading to a lowered viscosity of the mucin layer as also observed from the increased dissipation. The synergistic effect of chitosan and NAC can be explained by the fact that the adhesive chitosan may entrap NAC, bringing it in close contact with the mucins. In contrast, NAC by itself does not have ionic interaction mechanisms with the mucins and might therefore be easier to be carried away by the flow.

The QCM-D is an excellent and highly sensitive tool. Utilizing it to study the effect of the chitosan/NAC combination on a biofilm embedded in mucins is of great interest. This investigation would better mimic the *in vivo* scenario compared to the use of merely mucins. Only few have employed QCM-D for biofilm growth [239], so this would require an in-depth investigation and characterization of biofilm development on the QCM-D sensor before treatment evaluations. In the QCM-D measurements, it was assumed that the effect of chitosan/NAC would be similar to when applied on MCs, however, we did not investigate this. A direct and quantitative measurement of the adhesiveness of functionalized MCs would contribute to this statement.

#### Effect of chitosan/NAC MCs - Crystal violet staining and viable counting

Crystal violet staining remains one of the most frequently used microtiter-based biofilm quantification techniques to estimate the adherence of biomass to the wells of the plate [244]. Crystal violet does not only stain cells but essentially any material adhering to the surface of the plate. This includes the biofilm matrix components, and any biomass detachment, due to the activity of NAC, would be detected [271]. Despite this, staining of biofilms grown in ASM showed no difference between the adhered biomass after exposure to CIP-loaded, chitosan and/or NAC-functionalized MCs as well as for the corresponding solutions (**Figure 25A**). The method is sensitive to human errors as a slight difference in the well washing procedure can easily lead to a false conclusion, and it may not be sensitive enough to detect smaller differences in the effect (for example the presence of NAC or not). However, it is more useful when studying biofilm formation (for example from different genotypic strains) or for determination of the minimal biofilm inhibitory concentration. While *P. aeruginosa*, grown in minimal medium, usually forms a biofilm that covers the substratum with a homogenous distribution of the biovolume, ASM also promotes the growth of discrete free-floating aggregates [272]. As crystal violet only stains adhering biomass, we wanted to enumerate the bacteria in the suspension. To allow viable counting, the aggregates in suspension were homogenized using a 27G needle and subsequently plated on agar plates. Slight differences appeared between the different treatments with or without NAC. However, the differences were minor when taking the absolute bacterial numbers into account (no significance using an ordinary one-way ANOVA with multiple comparison) (**Figure 25B**).

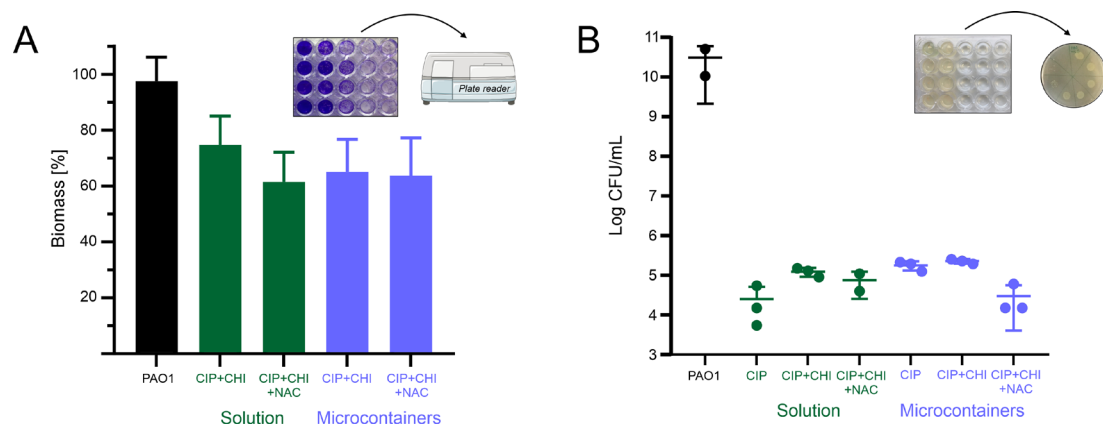


**Figure 25.** Test of microcontainers (MCs) on *P. aeruginosa* biofilms grown statically in artificial sputum medium (ASM). **A**) Crystal violet assay of biofilm adhering to the wells after treatment with ciprofloxacin hydrochloride (CIP)+chitosan (CHI) or CIP+CHI+N-acetylcysteine (NAC) either in solution or loaded in coated MCs. Data is presented as mean±SD (n=3-4). **B**) Viable counting of bacteria treated with CIP, CIP+CHI, CIP+CHI+NAC either in solution or loaded in coated MCs. Bacteria were homogenized using a 27G needle to allow correct viable counting on plates.

#### Growth of mucin-embedded biofilm

Microtiter-based biofilm assays are cheap with high-throughput, yet, biofilms formed under static conditions have different expression patterns than the biofilms formed under flow conditions, which has prompted the development of the flow chamber systems [273] (as applied in **Paper II** and **Paper III**). These laminar flow systems allow continuous supply of nutrients, removal of waste products along with providing shear for biofilm development. However, they are quite bulky and require the use of large quantities of growth medium. As an alternative, we employed the newly developed Bacterial-Culture-on-Disc (BCoD) platform [274] for growth of *P. aeruginosa* in the more *in vivo* like growth medium, ASM. Growing *P. aeruginosa* in ASM mimics growth during cystic fibrosis infections with formation of self-aggregating biofilm structures [268]. In pure ASM, *P. aeruginosa* initially adhered to the glass-surface. Hereafter, it detached and mostly clustered in the medium with only few, rather large, clusters remaining attached to the surface, which precluded CLSM monitoring [274]. Instead, a *P. aeruginosa* biofilm was grown in diluted ASM and compared to the growth in minimal growth medium FAB (as used in the flow chamber system in **Paper II** and **Paper III**). The ASM was diluted either I) x100 of all components (classified ‘mucin-poor ASM’), or II) x100 all components except the mucins which were only diluted x10 (classified ‘mucin-rich ASM’). We observed that the biofilm in diluted ASM grew faster and more homogeneously across the cell chamber with improved adhesion to the cover glass compared to FAB medium (**Figure 26**). When growing in mucin-rich ASM, the biomass reached the same density after 48 h as for 72 h growth in mucin-poor ASM. Additionally, we observed that the percentage of live biomass was higher with mucin-rich ASM than mucin-poor ASM (**Figure 27**). Thus, it appears that the higher mucin concentration facilitated bacterial adhesion to the surface, immobilized them and lowered the detachment due to flow velocity. The increased adhesion may be attributed to the mucin-specific adhesion proteins of *P. aeruginosa* mediating bacterium–mucin interactions [275].

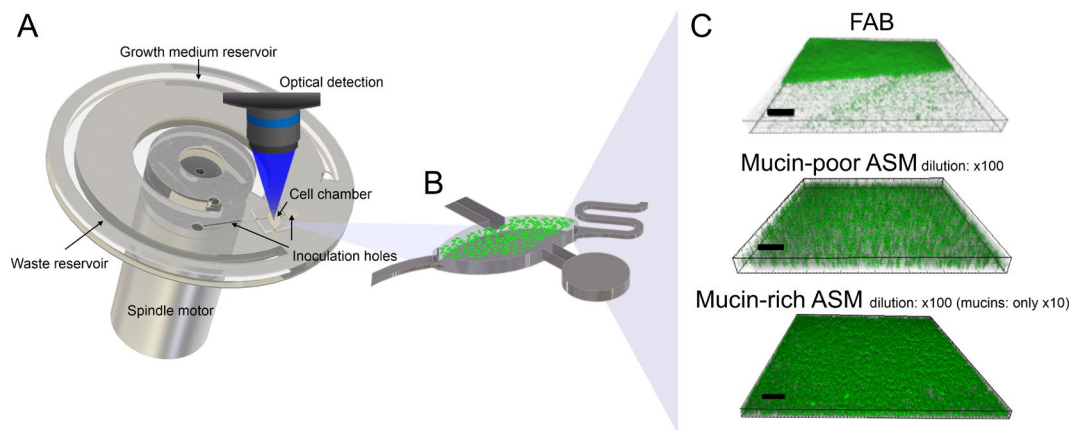


**Figure 26.** **A)** Bacterial-Culture-on-Disc (BCoD) platform for growth of *P. aeruginosa* designed with a growth medium reservoir, a cell chamber, inoculation holes, and a waste reservoir. **B)** Zoom-in on the cell chamber. **C)** *P. aeruginosa* biofilm grown for 24 h on the disc in a minimal medium with glucose as the only carbon source (FAB medium), artificial sputum medium (ASM) diluted x100 ('Mucin-poor ASM') or ASM where the mucin concentration was diluted x10 and the nutrient fraction diluted x100 from the standard preparation of ASM ('Mucin-rich ASM'). Scale bars: 40  $\mu\text{m}$ . See **Paper IV** and [274] for details on fabrication of disc, preparation of media, and growth of biofilm.

#### Effect of chitosan/NAC MCs on mucin-embedded biofilm

*P. aeruginosa* biofilms grown in mucin-poor or mucin-rich ASM were challenged with CIP as I) a bolus dose, II) in chitosan-coated MCs, or III) in chitosan/NAC-coated MCs (**Figure 27**). Chitosan/NAC MCs caused  $70.1 \pm 5.1\%$  dead biomass after 24 h treatment of the biofilm grown with a low mucin concentration, whereas  $88.5 \pm 4.1\%$  was dead when the concentration of mucins were higher. This is particularly interesting because it implies that NAC had a greater effect on the mucin-embedded biofilm. Chitosan-coated MCs killed  $74.6 \pm 9.3\%$  (mucin-poor ASM) and  $72.7 \pm 3.7\%$  (mucin-rich ASM) of the total biomass. Therefore, chitosan/NAC MCs performed better than chitosan MCs, but only when testing against biofilm grown with a higher mucin concentration. This demonstrates the importance of having mucins present in *in vitro* models. The amount of mucins did not influence the efficacy of the bolus dose.

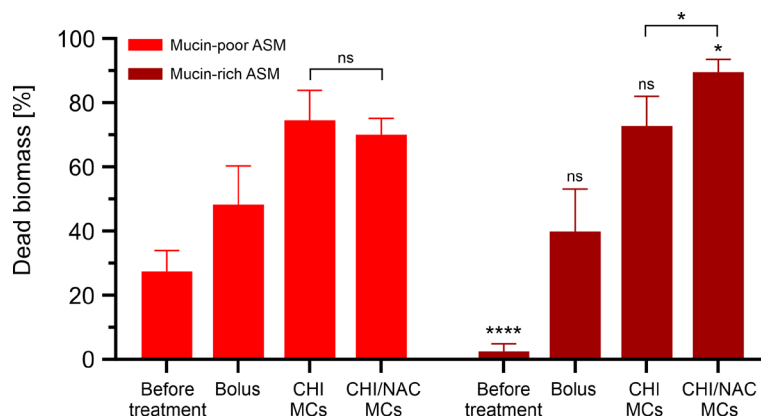


**Figure 27.** Comparison of the dead biomass (%) after 24 h treatment of *P. aeruginosa* biofilm with ciprofloxacin hydrochloride (CIP) administered as: I) bolus, II) in chitosan (CHI)-coated microcontainers (MCs), and III) in CHI/N-acetylcysteine (CHI/NAC)-coated MCs. Biofilms were grown in mucin-poor artificial sputum medium (ASM) or mucin-rich ASM. Data is presented as mean±SD (n=18). Significance between mucin-poor and mucin-rich ASM is given at columns of mucin-rich ASM. Significant difference: \*\*\*\*, p-value < 0.0001; \*, p-value < 0.05; ns, not significant.

In this paper, the CLSM images were acquired both closer to and further from the MCs to better understand the effect on the entire biofilm. Comparing the BCoD to the flow chamber system, as applied in **Paper II** and **Paper III**, the BCoD allowed a more controlled inoculation of MCs. The length of the cell culture chamber in the BCoD is 10 mm [274], whereas it is 40 mm in the flow chamber system [246]. The design allowed us to inoculate two MCs on the BCoD, and thereby it was possible to study the effect close and far from the MC.

After 5 h treatment with chitosan-coated MCs,  $72.8 \pm 1.5$  % biomass was dead in close proximity to the MC, whereas only  $39.1 \pm 3.4$  % was killed on average in the entire cell culture chamber (**Figure 28**). Having more biomass killed in close vicinity to the MC may be ascribed to the fact that MCs coated with chitosan have a slow release of CIP and, thus, only a small quantity of antibiotic was released after 5 h ( $23.3 \pm 8.2$  %), affecting only bacteria close to the MC. After 24 h, when most of the CIP was released from the MC in the cell chamber, the average dead biomass was  $72.7 \pm 3.7$  % with no significant difference based on the distance to the MC (**Figure 27**). The chitosan/NAC MCs provided immediate killing all over the cell chamber. This is possibly an effect due to the fast release of CIP from the MCs ( $83.7 \pm 2.6$  % within 30 min) and the biofilm-degrading activity of NAC, resulting in  $86.2 \pm 8.5$  % dead biomass close to the MC and  $79.6 \pm 8.3$  % far from the MC after 5 h treatment (**Figure 28**) (not significantly different). The larger amount of dead biomass was maintained for 24 h (**Figure 27**). It would be of interest to investigate the duration of the inhibition and determine when a possible regrowth would occur. Furthermore, the disruption of the biofilm, facilitated by NAC, might have promoted phenotypical changes, restoring the susceptibility of the certain subpopulations towards CIP. Investigations of the phenotypes within the treated biofilm, using for example flow cytometry, could reveal whether this hypothesis is true.

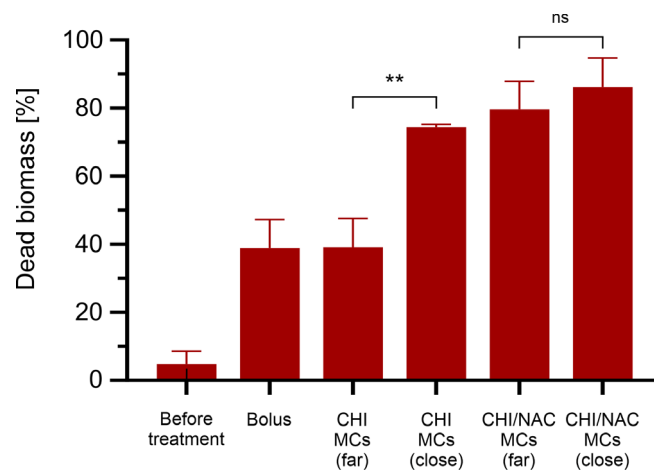


**Figure 28.** Comparison of the dead biomass (%) after 5 h treatment of a *P. aeruginosa* biofilm with ciprofloxacin hydrochloride (CIP) administered as: I) bolus, II) in chitosan (CHI)-coated microcontainers (MCs), and III) in CHI/N-acetylcysteine (CHI/NAC)-coated MCs. Biofilms were grown in mucin-rich artificial sputum medium (ASM). Confocal images were acquired closer to or further away from the MCs. Data is presented as mean+SD (n=18). Significant difference: \*\*, p-value < 0.01; ns, not significant.

In conclusion, chitosan/NAC-functionalized MCs performed significantly better than both the bolus and the chitosan-coated MCs presumably because of the fast release kinetic combined with the mucolytic activity of NAC as confirmed by QCM-D (**Figure 24**). Moreover, NAC has shown antibacterial properties against *P. aeruginosa* with MIC values ranging from 10-40 mg/mL [127,276]. MIC values are nonetheless determined on planktonic cultures, and the minimal eradication concentration of NAC towards biofilm grown on the BCoD will consequently be substantially higher. We applied 40 mg/mL NAC in the spray coating solution, however, this is not necessarily the final concentration obtained in the flow chamber. Utilizing a higher concentration of NAC could potentially improve the antibacterial contribution from NAC.

As next steps, one could exploit the chitosan/NAC MCs for delivery of antibiotics with other physiochemical properties. Studies have shown that CIP penetration is impeded through mucus, and using particulates to deliver CIP improved its diffusion [277,278]. However, CIP have also shown to penetrate biofilms more easily than other antibiotics like the aminoglycoside tobramycin, whose penetration is highly restricted through both biofilm and mucus [103,104]. Divergent opinions exist to whether the penetration of COL (as used in **Paper III**) is restricted through mucus. Some report that COL diffusion was not limited through mucus, despite its many positive charges [107], whereas others showed that COL loses its activity as it binds to the mucins [279]. Therefore, delivering cationic antibiotics, like tobramycin or colistin, to mucin-embedded biofilms using chitosan/NAC MCs could further elucidate the potential of the mucolytic functionalization.

Selective disruption of other EPS components to improve efficacy of antibiotics also constitutes an exciting approach. This includes enzymatic degradation of abundant EPS polymers and could be achieved by incorporation of alginate lyase, dispersin B, or DNase [9,20,119]. These could either be incorporated in the coating or loaded within the MCs. Incorporation in the coating would require ensurance of enzyme stability during the coating process.

The BCoD is a novel and convenient tool for studying biofilms. The presence of ASM makes the platform more physiologically relevant, and it could for example be useful when studying surface-attached biofilms such as the ones occurring in the oral cavity or the gastrointestinal tract. However, it does have certain limitations. First, it does not fully mimic the complexity of an *in vivo* biofilm infection and future aims could include incorporation of mucus from diseased patients, or even epithelial and host immune cells. The group of T. Bjarnsholt took an interesting approach to mimic the biofilm-mucus plugs. They inoculated alginate beads with a fluorescently tagged *P. aeruginosa*, and then isolated and cut the beads in half to visualize the edge and interior of the bead with confocal microscopy [280]. These beads could potentially also be applied in a mucin-containing environment. Investigating the chitosan/NAC-functionalized MCs on such a setup would yield more information on the impact on *in vivo*-like biofilms.



### 3.4 TREATMENT OF ORAL MULTISPECIES BIOFILMS USING MICROCONTAINERS

The following subsection is based on the results presented in **Paper V** “Management of oral biofilms by nisin delivery in adhesive microdevices” (for full paper, see Appendix V).

#### PURPOSE

The aim of this study was to investigate the adhesion of MCs in the oral cavity and assess the antimicrobial activity of MCs encapsulating an AMP towards oral multispecies biofilms isolated from patients.

#### OUTCOMES

In the previous papers (**Paper II-IV**), MCs with encapsulated antibiotics showed antimicrobial and antibiofilm activity against monomicrobial cultures of *P. aeruginosa*. In **Paper V**, we wanted to address their effect on polymicrobial biofilms. The oral cavity is colonized by numerous beneficial microbes that form biofilms on dental and mucosal surfaces to get access to nutrients and to avoid being carried away with the saliva [45,281]. However, oral biofilms are recognized as a key virulence factor to many oral infectious diseases as it serves as a reservoir for pathogenic bacteria [281]. Examples include periodontitis and dental caries with preceding tooth decay. Therefore, maintaining a low biofilm density in the oral cavity is paramount. Oral hygiene relies on mechanical removal of biofilms, but many products also contain antimicrobials. For effective eradication of biofilms with antimicrobials a high concentration and a long exposure time is required [282]. This is challenged by the rapid clearance of saliva in the oral cavity, and we suggest that MCs can serve as an alternative adhesive drug delivery carrier providing a prolonged exposure of antimicrobials to the oral microbiome. Therefore, in **Paper V**, the bioadhesion of MCs, the release of an AMP from MCs and the resulting antimicrobial activity were studied (**Figure 29**).

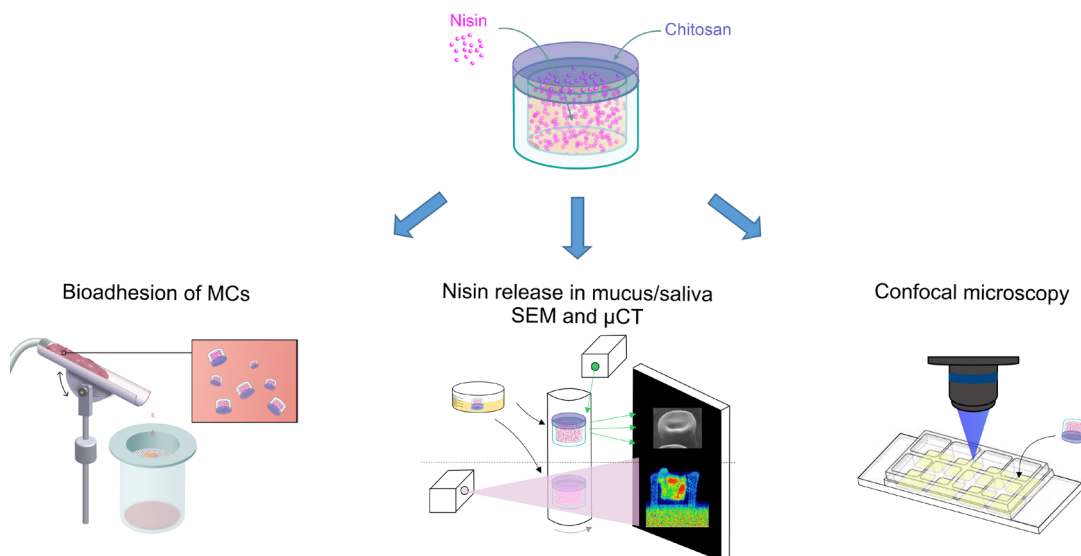


**Figure 29.** Schematic overview of conducted experiments aimed to study the effect of microcontainers (MCs) loaded with nisin and functionalized with chitosan. Abbreviations: Scanning electron microscopy (SEM); X-ray micro-computed tomography ( $\mu$ CT).

### Bioadhesion of MCs

The bioadhesion of MCs to tissue from the oral cavity was studied in a custom-made retention measurement setup [283]. The setup allowed control of humidity and temperature ( $89.0 \pm 2.3$  % and  $32.6 \pm 0.5$  °C) during the whole experiment mimicking the physiological environment and avoiding that the tissue dried out. Among the mucoadhesive polymers, chitosan is one of the most widely applied ones [218]. Madsen *et al.* exemplified the adhesiveness of chitosan microparticles on porcine buccal mucosa, showing a pronounced influence from the choice of irrigation medium used. A concentration of 2.50 % w/v gastric porcine mucins closely resembled the retention profile of the microparticles in stimulated human whole saliva and was therefore also applied in **Paper V** [284]. Functionalization of the MCs with a chitosan coating increased their adhesiveness to the buccal tissue two-fold from  $33.8 \pm 5.2$  % to  $68.6 \pm 14.3$  % (**Figure 30A**). In comparison, metformin microparticles spray dried with chitosan, to a size of 5-22  $\mu\text{m}$ , previously showed improved adhesion up until 20 min. Thereafter, no significant difference was observed compared to the microparticles without chitosan [284]. That the chitosan-coated MCs possessed better bioadhesion than the chitosan microparticles may be attributed to the magnitude of the chitosan hydrogel. MCs have a considerable larger chitosan-coated surface area than the smaller microparticles and thus a larger area for gel formation and the associated electrostatic interactions with the mucosal surface.

### Release of nisin from MCs

As the MCs showed suitable as an adhesive drug delivery system, our next step was to load the MCs with nisin. Nisin belongs to the group of AMPs, which stands out from traditional antibiotics because of their mode of action. They disrupt the bacterial membranes and thus, provide rapid bacterial killing, allowing minimal time for resistance development [87]. Functionalization of MCs with chitosan allowed encapsulation of nisin within the MC. Integrity of the chitosan coating was monitored using SEM (see **Paper V** for images). Release of nisin through the chitosan hydrogel was estimated using X-ray micro-computed tomography ( $\mu\text{CT}$ ). X-rays are used in  $\mu\text{CT}$  to obtain cross-sections of a sample without having to cut and destroy the sample [285]. As evident from **Figure 30B**, nisin released fully after 15 min in a physiological relevant mucus/saliva blend despite the use of a higher concentration chitosan than previously applied (1 % w/v versus 0.5 % w/v in **Paper II-IV**). The loaded powder did not only contain nisin, but also skim milk among other ingredients from the production process. As the aqueous solubility of skim milk is usually more than 99 %, this component may have driven the release [286]. To obtain an optimal formulation for oral care a high drug concentration and long exposure time are required. Therefore, one would need to ensure a sustained release of nisin by modifying the coating components. Biopolymers like zein [287], cellulose [288], and alginate [289] have been explored for making microparticles and films for controlled release of nisin. By firstly functionalizing the MCs with a layer of one of the abovementioned polymers followed by a coating of chitosan, a controlled-release and mucoadhesive properties could be obtained simultaneously.

## Antimicrobial activity against oral multispecies biofilm

Multispecies biofilms were developed in IBIDI-plates from saliva isolated from patients. Previous studies have shown that nisin inhibits planktonic growth of oral bacteria at low concentrations (2.5-50  $\mu\text{g/ml}$ ) [87], and in **Paper V** an approximated concentration of 16  $\mu\text{g/ml}$  of pure nisin was used. Confocal monitoring of the saliva-derived multispecies biofilms revealed antibacterial activity of nisin-loaded chitosan-coated MCs with a faster onset (after 3 h) compared to solution-based delivery (after 9 h) (**Figure 30C**). The improved effect can imply that the MCs may deliver initial high local drug concentrations in the biofilm, and in that way resulting in a faster and better killing, as many of them are in direct contact with the biofilm.

In the present study, we developed *in vitro* biofilms based on saliva samples isolated from patients, which were suspended in bulk amounts in order to exclude for patient-to-patient variations in biofilm composition. However, this involves a disruption of the biofilm and *in situ* investigations of intact biofilms developed in the oral cavity would provide insight into the true *in vivo* activity of the MCs. Furthermore, one needs to develop a suitable strategy to deliver the MCs in the oral cavity, which could potentially include incorporation into a gel. We believe that the results presented are encouraging for future design of sustained drug delivery microdevices to maintain a healthy oral microbiome.

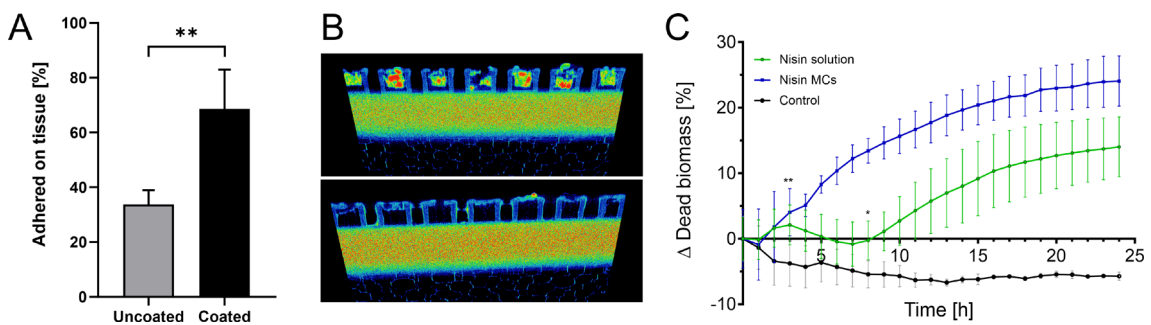


**Figure 30.** Selected data from **Paper V**. **A**) Percentage of uncoated or chitosan-coated microcontainers (MCs) adhering to porcine buccal mucosa after exposure to flow for 20 min. Data is presented as mean $\pm$ SD (n=4). Significant difference: \*\*, p=0.0038. **B**) X-ray micro-computed tomography ( $\mu\text{CT}$ ) images of MCs loaded with nisin and coated with 1% w/v chitosan, and  $\mu\text{CT}$  images of the same MCs after 15 min release in a 50:50% w/w mucus/saliva blend. **C**) Confocal microscopy time-lapse on oral multispecies biofilm after treatment with nisin in chitosan-coated MCs or nisin in solution. Percentage of dead biomass was calculated in relation to the total biomass at the specified time-point and normalized at t=0 in order to compare the changes in dead biomass. Data is presented as mean $\pm$ SD. Significant difference: \*, p=0.017; \*\*, p=0.0091.

## 4 CONCLUSION

---

The development of novel strategies to combat pathogenic biofilms poses an immense scientific challenge. Utilizing delivery systems to provide high local concentrations of antibiotics at the site of infection can improve the treatment and overcome many of the challenges associated with traditional drug delivery – minimizing side effects, avoiding deactivation and improving drug penetration into the biofilm. By using less drug while achieving the same therapeutic activity, resistance development may be alleviated.

The findings in this PhD thesis illustrate that MCs show great potential as antibiotic carriers. Antibiotics with different physiochemical and antibiofilm properties (CIP, COL, or nisin) were loaded separately or in combination into MCs. Functionalization of MCs was completed with different polymers aimed at realizing a mucoadhesive, release-controlling and/or biofilm-degrading effect (PEG, Eudragit S100, as well as chitosan and/or NAC). Fast or sustained release profiles were obtained depending on the choice and combination of polymer and drug. Moreover, functionalization of the MCs with a chitosan coating provided a two-fold increase in bioadhesion to buccal mucosa.

The loaded and functionalized MCs were examined in terms of their antibacterial and antibiofilm performance against planktonic bacteria as well as single species and multispecies biofilms. Growth of planktonic *P. aeruginosa* cells was partly inhibited with the CIP-loaded MCs and the degree of inhibition depended on the choice of coating (**Paper II**). In contrast, co-delivering CIP:COL demonstrated synergistic effects superior to monotherapy, resulting in a complete eradication of the entire bacterial population (**Paper III**).

Overall, the use of MCs as delivery system appeared to be a promising approach for improving antibiotic delivery to biofilms, by increasing the local concentration of antibiotics to therapeutic levels. In this work, we showed that MC-based treatment with CIP of biofilm-associated *P. aeruginosa* provided a 3-fold higher local killing compared to treatment with a bolus dose, and chitosan coating appeared to be the most promising. Moreover, MCs loaded with CIP provided a bacterial killing similar to after constant perfusion of a 2.75 times higher concentration of solubilized antibiotic (**Paper II**). Interestingly, the effect of burst antibiotic release from MCs was reflected in the killing of biomass, as a significantly faster killing was observed compared to simple perfusion of antibiotic. This effect was observed for both single-species *P. aeruginosa* biofilm (**Paper III-IV**) and oral polymicrobial biofilms (**Paper V**).

The complex microenvironments at the site of biofilm infections need to be taken into account when investigating the effect of drug delivery systems on *in vitro* biofilms and research should be directed towards development of models that better mimic the *in vivo* biofilm habitat. We realized biofilm growth on a newly developed microfluidic centrifugal BCoD platform, suitable for perfusion of a mucin-containing medium (**Paper IV**). The results demonstrated that the choice of growth medium highly influenced the bacterial proliferation and the efficacy of the antibiotic-loaded MCs. Treating biofilm infections requires combination therapies targeting more than one component of the complex biofilm microenvironment.

This, we demonstrated with chitosan/NAC-functionalized MCs that improved the biofilm killing compared to chitosan-coated MCs or a bolus antibiotic injection, an effect which we ascribed to the local delivery in MCs combined with the proven mucoadhesive and mucolytic activity of chitosan/NAC (**Paper IV**).

In conclusion, this work confirms, for the first time, the benefits of using MCs for treatment of biofilms, reducing the use of antibiotics while achieving improved antibiofilm effects by allowing a higher amount of antibiotic to reach the biofilm. We believe that the results are encouraging for further design of drug delivery devices to treat biofilm-associated infections, ultimately improving the life-quality for numerous of patients.

## 5 FUTURE PERSPECTIVES

---

An important aspect when developing commercial therapies is the possibility of scaling up the production, where inexpensive large-scale manufacturing methods are required. Although, SU-8 is a suitable material for proof-of-concept testing, the main drawback is that it is non-biodegradable and requires cleanroom-facilities not suitable for upscaling. High-throughput fabrication of MCs in biocompatible materials still constitute a major challenge, and recent efforts in our group have focused on the use of polymers like PLLA, PCL and PLGA for non-lithography based processing. When addressing the issue of biocompatibility, new continuous large-scale fabrication routes of MCs develops such as roll-to-roll and embossing, which needs to be further explored in the future.

Fabrication of MCs is time-consuming and will be less cost-efficient than other already developed delivery systems such as particulates. Therefore, the advantages obtained with MCs needs to be considerable, and thorough *in vitro* and *in vivo* investigations are important for them to be competitive. To realize a good correlation between *in vitro* and *in vivo* studies, the *in vitro* studies should mimic the *in vivo* situation as much as possible, which can be achieved by using constituents simulating the pathogenic biofilm microenvironment. As for example, considerable differences exist between mucus from healthy and diseased humans, as the viscosity is highly increased. Further investigation of the efficacy of MC-based co-delivery and chitsan/NAC-functionalization against mucus-biofilm complexes isolated from diseased patients could be of great interest. Moreover, testing MCs on clinical strains of mucoid nature as well as other biofilm-forming strains would further elucidate their potential. *In vivo* experiments would reflect the full interplay between the MCs, the host and the pathogens, which is not obtained in *in vitro* studies. This would provide insight into the suitability of MCs for commercial use against polymicrobial biofilms that are most often treated with systemic antibiotics rather than local treatments.

The optimal release profile of an antibiotic is believed to be an initial burst release, ensuring a high antimicrobial concentration for biofilm eradication, followed by a sustained release capable of minimizing any further biofilm growth. This could be achieved by a multi-layer loading technique of antibiotics embedded in a release-controlling polymer or by using multi-compartment MCs. The MCs are advantageous due to their large size and thereby, large drug loading capacity, but this also restricts their biofilm-penetrating effects. By encapsulating nanoparticles within MCs, one could achieve the benefits from both drug delivery systems: The large loading capacity and mucoadhesiveness of the MC together with the biofilm-penetrating properties of the nanoparticles.

Excitingly, many more functionalizations and modifications are yet to be explored to fully understand the behavior and benefits of the MCs as drug delivery system. Their versatility emphasize their prospect within personalized medicine. Although, the initial results presented in this PhD thesis are promising, realizing *in situ* drug delivery from MCs locally at the site of biofilm still constitutes a major, nevertheless, essential task. By increasing the targeting specificity or obtaining a stimuli-triggered release from the MCs, delivery to the pathogenic cells within the biofilm microenvironments will be improved, while protecting the host

tissue and the commensal microbiota. Using 'smart-surfaces' represents the most widely applied technique for various particulates under development. An example is the hybrid particles with a polymeric core and a lipid coat. They possess the benefits from both delivery systems, and bacterial toxins in the biofilm damage the liposomal coating, triggering the release of antibiotic from the polymeric core. Likewise, the weakly acidic environment within the biofilm has been exploited to trigger release from particulates. By using surface-charge switching polymers, a triggered release can be obtained within the biofilm. In the future, polymers like these could be applied onto the MCs.

## 6 REFERENCES

---

- [1] O'Neill J. Tackling drug-resistant infections globally. 2016.
- [2] Liu Y, Shi L, Su L, van der Mei HC, Jutte PC, Ren Y, et al. Nanotechnology-based antimicrobials and delivery systems for biofilm-infection control. *Chem Soc Rev* 2019;48:428–46.
- [3] Høiby N, Bjarnsholt T, Givskov M, Molin S, Ciofu O. Antibiotic resistance of bacterial biofilms. *Int J Antimicrob Agents* 2010;35:322–32.
- [4] Costerton JW, Stewart PS, Greenberg EP. Bacterial Biofilms: A Common Cause of Persistent Infections. *Science* 1999;284:1318–22.
- [5] Hall-Stoodley L, Costerton JW, Stoodley P. Bacterial biofilms: from the Natural environment to infectious diseases. *Nat Rev Microbiol* 2004;2:95–108.
- [6] Costerton JW. Introduction to biofilm. *Int J Antimicrob Agents* 1999;11:217–21.
- [7] Davies D. Understanding biofilm resistance to antibacterial agents. *Nat Rev Drug Discovery* 2003;2:114–22.
- [8] Koo H, Allan RN, Howlin RP, Stoodley P, Hall-Stoodley L. Targeting microbial biofilms: Current and prospective therapeutic strategies. *Nat Rev Microbiol* 2017;15:740–55.
- [9] Bjarnsholt T, Ciofu O, Molin S, Givskov M, Høiby N. Applying insights from biofilm biology to drug development — can a new approach be developed? *Nat Rev Drug Discovery* 2013;12:791–808.
- [10] Ciofu O, Rojo-Molinero E, Macià MD, Oliver A. Antibiotic treatment of biofilm infections. *Apmis* 2017;125:304–19.
- [11] Ciofu O, Tolker-Nielsen T. Tolerance and Resistance of *Pseudomonas aeruginosa* Biofilms to Antimicrobial Agents—How *P. aeruginosa* Can Escape Antibiotics. *Front Microbiol* 2019;10:1–15.
- [12] Xiong MH, Bao Y, Yang XZ, Zhu YH, Wang J. Delivery of antibiotics with polymeric particles. *Adv Drug Delivery Rev* 2014;78:63–76.
- [13] Flemming HC, Wingender J, Szewzyk U, Steinberg P, Rice SA, Kjelleberg S. Biofilms: An emergent form of bacterial life. *Nat Rev Microbiol* 2016;14:563–75.
- [14] Costerton JW, Lewandowski Z, Caldwell DE, Korber DR, Lappin-Scott HM. Microbial biofilms. *Annu Rev Microbiol* 1995;49:711–45.
- [15] Høiby N, Flensburg EW, Beck B, Friis B, Jacobsen VS, Jacobsen L. *Pseudomonas aeruginosa* infection in cystic fibrosis. Diagnostic and prognostic significance of *Pseudomonas aeruginosa* precipitins determined by means of crossed immunoelectrophoresis. *Scand J Respir Dis* 1977;58:65–79.
- [16] Costerton JW, Geesey GG, Cheng KJ. How bacteria stick. *Sci Am* 1978;238:86–95.
- [17] O'Toole GA, Kaplan HB, Kolter R. Biofilm Formation as Microbial Development. *Annu Rev Microbiol* 2000;54:49–79.
- [18] Stoodley P, Sauer K, Davies DG, Costerton JW. Biofilms as Complex Differentiated Communities. *Annu Rev Microbiol* 2002;56:187–209.
- [19] Harmsen M, Yang L, Pamp SJ, Tolker-Nielsen T. An update on *Pseudomonas aeruginosa* biofilm formation, tolerance, and dispersal. *FEMS Immunol Med Microbiol* 2010;59:253–68.
- [20] Rumbaugh KP, Sauer K. Biofilm dispersion. *Nat Rev Microbiol* 2020;18:571–86.



- [21] Sauer K, Camper AK, Ehrlich GD, Costerton JW, Davies DG. *Pseudomonas aeruginosa* Displays Multiple Phenotypes during Development as a Biofilm. *J Bacteriol* 2002;184:1140–54.
- [22] Wingender J, Strathmann M, Rode A, Leis A, Flemming H-C. Isolation and biochemical characterization of extracellular polymeric substances from *Pseudomonas aeruginosa*. *Methods Enzymol.*, Academic press; 2001, p. 302–14.
- [23] Whitchurch CB, Tolker-Nielsen T, Ragas PC, Mattick JS. Extracellular DNA Required for Bacterial Biofilm Formation. *Science* 2002;295:1487–1487.
- [24] Flemming HC, Wingender J. The biofilm matrix. *Nat Rev Microbiol* 2010;8:623–33.
- [25] Jefferson KK. What drives bacteria to produce a biofilm? *FEMS Microbiol Lett* 2004;236:163–73.
- [26] Ciofu O, Høiby N, Wang H, Jensen PØ, Tolker-Nielsen T. Antimicrobial resistance, respiratory tract infections and role of biofilms in lung infections in cystic fibrosis patients. *Adv Drug Delivery Rev* 2014;85:7–23.
- [27] LaSarre B, Federle MJ. Exploiting Quorum Sensing To Confuse Bacterial Pathogens. *Microbiol Mol Biol Rev* 2013;77:73–111.
- [28] Kim S-K, Lee J-H. Biofilm dispersion in *Pseudomonas aeruginosa*. *J Microbiol* 2016;54:71–85.
- [29] Sternberg C, Christensen BB, Johansen T, Toftgaard Nielsen A, Andersen JB, Givskov M, et al. Distribution of Bacterial Growth Activity in Flow-Chamber Biofilms. *Appl Environ Microbiol* 1999;65:4108–17.
- [30] Stewart PS, Franklin MJ. Physiological heterogeneity in biofilms. *Nat Rev Microbiol* 2008;6:199–210.
- [31] Boudarel H, Mathias J-D, Blaysat B, Grédiac M. Towards standardized mechanical characterization of microbial biofilms: analysis and critical review. *Npj Biofilms Microbiomes* 2018;4:17.
- [32] Malone M, Bjarnsholt T, McBain AJ, James GA, Stoodley P, Leaper D, et al. The prevalence of biofilms in chronic wounds: a systematic review and meta-analysis of published data. *J Wound Care* 2017;26:20–5.
- [33] James GA, Swogger E, Wolcott R, Pulcini E deLancey, Secor P, Sestrich J, et al. Biofilms in chronic wounds. *Wound Repair Regen* 2008;16:37–44.
- [34] Foster JS, Kolenbrander PE. Development of a Multispecies Oral Bacterial Community in a Saliva-Conditioned Flow Cell. *Appl Environ Microbiol* 2004;70:4340–8.
- [35] Diaz PI, Valm AM. Microbial Interactions in Oral Communities Mediate Emergent Biofilm Properties. *J Dent Res* 2020;99:18–25.
- [36] Hall-Stoodley L, Hu FZ, Gieseke A, Nistico L, Nguyen D, Hayes J, et al. Direct Detection of Bacterial Biofilms on the Middle-Ear Mucosa of Children With Chronic Otitis Media. *JAMA* 2006;296:202–11.
- [37] Bakaletz LO. Bacterial Biofilms in Otitis Media. *Pediatr Infect Dis J* 2007;26:S17–9.
- [38] Anderson GG. Intracellular Bacterial Biofilm-Like Pods in Urinary Tract Infections. *Science* 2003;301:105–7.
- [39] Probert H, Gibson G. Bacterial biofilms in the human gastrointestinal tract. *Curr Issues Intest Microbiol* 2002;3:23–7.
- [40] Burmølle M, Thomsen TR, Fazli M, Dige I, Christensen L, Homøe P, et al. Biofilms in chronic infections - A matter of opportunity - Monospecies biofilms in multispecies infections. *FEMS Immunol Med Microbiol* 2010;59:324–36.

- [41] Natan M, Banin E. From Nano to Micro: Using nanotechnology to combat microorganisms and their multidrug resistance. *FEMS Microbiol Rev* 2017;41:302–22.
- [42] Caselli D, Cesaro S, Ziino O, Zanazzo G, Manicone R, Livadiotti S, et al. Multidrug resistant *Pseudomonas aeruginosa* infection in children undergoing chemotherapy and hematopoietic stem cell transplantation. *Haematologica* 2010;95:1612–5.
- [43] Raya S, Belbase A, Dhakal L, Govinda Prajapati K, Baidya R, kishor Bimali N. In-Vitro Biofilm Formation and Antimicrobial Resistance of *Escherichia coli* in Diabetic and Nondiabetic Patients. *Biomed Res Int* 2019;2019:1–8.
- [44] Bjarnsholt T, Jensen PØ, Fiandaca MJ, Pedersen J, Hansen CR, Andersen CB, et al. *Pseudomonas aeruginosa* biofilms in the respiratory tract of cystic fibrosis patients. *Pediatr Pulmonol* 2009;44:547–58.
- [45] Silva BR Da, Freitas VAA De, Nascimento-Neto LG, Carneiro VA, Arruda FVS, Aguiar ASW De, et al. Antimicrobial peptide control of pathogenic microorganisms of the oral cavity: A review of the literature. *Peptides* 2012;36:315–21.
- [46] Deng Z, Luo XM, Liu J, Wang H. Quorum Sensing, Biofilm, and Intestinal Mucosal Barrier: Involvement the Role of Probiotic. *Front Cell Infect Microbiol* 2020;10:1–10.
- [47] Chandra N, Srivastava A, Kumar S. Bacterial biofilms in human gastrointestinal tract: An intricate balance between health and inflammatory bowel diseases. *World J Pharmacol* 2019;8:26–40.
- [48] von Rosenvinge EC, O'May GA, Macfarlane S, Macfarlane GT, Shirliff ME. Microbial biofilms and gastrointestinal diseases. *Pathog Dis* 2013;67:25–38.
- [49] Swidsinski A, Weber J, Loening-Baucke V, Hale LP, Lochs H. Spatial Organization and Composition of the Mucosal Flora in Patients with Inflammatory Bowel Disease. *J Clin Microbiol* 2005;43:3380–9.
- [50] Lynch AS, Abbanat D. New antibiotic agents and approaches to treat biofilm-associated infections. *Expert Opin Ther Pat* 2010;20:1373–87.
- [51] Lyczak JB, Cannon CL, Pier GB. Lung Infections Associated with Cystic Fibrosis. *Clin Microbiol Rev* 2002;15:194–222.
- [52] Iglewski B. *Pseudomonas*. In: Baron S, editor. *Med. Microbiol*. 4th ed., Galveston (TX): University of Texas Medical Branch at Galveston: 1996.
- [53] Tashiro Y, Yawata Y, Toyofuku M, Uchiyama H, Nomura N. Interspecies Interaction between *Pseudomonas aeruginosa* and Other Microorganisms. *Microbes Environ* 2013;28:13–24.
- [54] Taylor PK, Yeung ATY, Hancock REW. Antibiotic resistance in *Pseudomonas aeruginosa* biofilms: Towards the development of novel anti-biofilm therapies. *J Biotechnol* 2014;191:121–30.
- [55] Pachori P, Gothalwal R, Gandhi P. Emergence of antibiotic resistance *Pseudomonas aeruginosa* in intensive care unit; a critical review. *Genes Dis* 2019;6:109–19.
- [56] Markou P, Apidianakis Y. Pathogenesis of intestinal *Pseudomonas aeruginosa* infection in patients with cancer. *Front Cell Infect Microbiol* 2014;3:1–5.
- [57] Hwang IY, Koh E, Wong A, March JC, Bentley WE, Lee YS, et al. Engineered probiotic *Escherichia coli* can eliminate and prevent *Pseudomonas aeruginosa* gut infection in animal models. *Nat Commun* 2017;8:1–11.
- [58] Mulani MS, Kamble EE, Kumkar SN, Tawre MS, Pardesi KR. Emerging Strategies to Combat ESKAPE Pathogens in the Era of Antimicrobial Resistance: A Review. *Front Microbiol* 2019;10:1–24.

- [59] World Health Organization. Global priority list of antibiotic-resistant bacteria to guide research, discovery, and development of new antibiotics 2017:1–7. [https://www.who.int/medicines/publications/WHO-PPL-Short\\_Summary\\_25Feb-ET\\_NM\\_WHO.pdf](https://www.who.int/medicines/publications/WHO-PPL-Short_Summary_25Feb-ET_NM_WHO.pdf).
- [60] Aminov RI. A Brief History of the Antibiotic Era: Lessons Learned and Challenges for the Future. *Front Microbiol* 2010;1:1–7.
- [61] Etebu E, Ariekpar I. Antibiotics: Classification and mechanisms of action with emphasis on molecular perspectives. *Int J Appl Microbiol Biotechnol Res* 2016;4:90–9.
- [62] Brown L, Wolf JM, Prados-Rosales R, Casadevall A. Through the wall: extracellular vesicles in Gram-positive bacteria, mycobacteria and fungi. *Nat Rev Microbiol* 2015;13:620–30.
- [63] Aldred KJ, Kerns RJ, Osheroff N. Mechanism of quinolone action and resistance. *Biochemistry* 2014;53:1565–74.
- [64] Bjarnsholt T. *Pseudomonas aeruginosa* Biofilms in the Lungs of Cystic Fibrosis Patients. In: Moser C, Jensen PØ, Høiby N, editors. *Biofilm Infect.*, Springer; 2011, p. 167–85.
- [65] Schwerdt M, Neumann C, Schwartbeck B, Kampmeier S, Herzog S, Görlich D, et al. *Staphylococcus aureus* in the airways of cystic fibrosis patients - A retrospective long-term study. *Int J Med Microbiol* 2018;308:631–9.
- [66] Pastar I, Nusbaum AG, Gil J, Patel SB, Chen J, Valdes J, et al. Interactions of Methicillin Resistant *Staphylococcus aureus* USA300 and *Pseudomonas aeruginosa* in Polymicrobial Wound Infection. *PLoS One* 2013;8:e56846.
- [67] Rehman A, Patrick WM, Lamont IL. Mechanisms of ciprofloxacin resistance in *pseudomonas aeruginosa*: New approaches to an old problem. *J Med Microbiol* 2019;68:1–10.
- [68] Chen H, Gao B, Li H, Ma LQ. Effects of pH and ionic strength on sulfamethoxazole and ciprofloxacin transport in saturated porous media. *J Contam Hydrol* 2011;126:29–36.
- [69] Caço AI, Varanda F, De Melo MJP, Dias AMA, Dohrn R, Marrucho IM. Solubility of antibiotics in different solvents. Part II. non-hydrochloride forms of tetracycline and ciprofloxacin. *Ind Eng Chem Res* 2008;47:8083–9.
- [70] Olivera ME, Manzo RH, Junginger HE, Midha KK, Shah VP, Stavchansky S, et al. Biowaiver monographs for immediate release solid oral dosage forms: Ciprofloxacin hydrochloride. *J Pharm Sci* 2011;100:22–33.
- [71] Varanda F, Pratas De Melo MJ, Caço AI, Dohrn R, Makrydaki FA, Voutsas E, et al. Solubility of antibiotics in different solvents. 1. Hydrochloride forms of tetracycline, moxifloxacin, and ciprofloxacin. *Ind Eng Chem Res* 2006;45:6368–74.
- [72] Ross DL, Riley CM. Dissociation and complexation of the fluoroquinolone antimicrobials - an update. *J Pharm Biomed Anal* 1994;12:1325–31.
- [73] Silva F, Lourenço O, Queiroz JA, Domingues FC. Bacteriostatic versus bactericidal activity of ciprofloxacin in *Escherichia coli* assessed by flow cytometry using a novel far-red dye. *J Antibiot (Tokyo)* 2011;64:321–5.
- [74] Molchanova N, Hansen PR, Franzyk H. Advances in Development of Antimicrobial Peptidomimetics as Potential Drugs. *Molecules* 2017;22:1430.
- [75] Yeaman MR, Yount NY. Mechanisms of Antimicrobial Peptide Action and Resistance. *Pharmacol Rev* 2003;55:27–55.
- [76] Haagenen JAJ, Klausen M, Ernst RK, Miller SI, Folkesson A, Tolker-Nielsen T, et al. Differentiation

- and distribution of colistin- and sodium dodecyl sulfate-tolerant cells in *Pseudomonas aeruginosa* biofilms. *J Bacteriol* 2007;189:28–37.
- [77] Li J, Nation R, Turnidge J, Milne R, Coulthard K, Rayner C, et al. Colistin: the re-emerging antibiotic for multidrug-resistant Gram-negative bacterial infections. *Lancet Infect Dis* 2006;6:589–601.
- [78] Nation RL, Li J, Cars O, Couet W, Dudley MN, Kaye KS, et al. Framework for optimisation of the clinical use of colistin and polymyxin B: the Prato polymyxin consensus. *Lancet Infect Dis* 2015;15:225–34.
- [79] Bialvaei AZ, Samadi Kafil H. Colistin, mechanisms and prevalence of resistance. *Curr Med Res Opin* 2015;31:707–21.
- [80] Poirel L, Jayol A, Nordmann P. Polymyxins: Antibacterial Activity, Susceptibility Testing, and Resistance Mechanisms Encoded by Plasmids or Chromosomes. *Clin Microbiol Rev* 2017;30:557–96.
- [81] Wang W, Zhou QT, Sun SP, Denman JA, Gengenbach TR, Barraud N, et al. Effects of Surface Composition on the Aerosolisation and Dissolution of Inhaled Antibiotic Combination Powders Consisting of Colistin and Rifampicin. *AAPS J* 2016;18:372–84.
- [82] Ma Z, Wang J, Nation RL, Li J, Turnidge JD, Coulthard K, et al. Renal disposition of colistin in the isolated perfused rat kidney. *Antimicrob Agents Chemother* 2009;53:2857–64.
- [83] Sans-Serramitjana E, Fusté E, Martínez-Garriga B, Merlos A, Pastor M, Pedraz JL, et al. Killing effect of nanoencapsulated colistin sulfate on *Pseudomonas aeruginosa* from cystic fibrosis patients. *J Cyst Fibros* 2016;15:611–8.
- [84] Vukomanović M, Žunič V, Kunej Š, Jančar B, Jeverica S, Podlipec R, et al. Nano-engineering the Antimicrobial Spectrum of Lantibiotics: Activity of Nisin against Gram Negative Bacteria. *Sci Rep* 2017;7:4324.
- [85] Field D, O'Connor R, Cotter PD, Ross RP, Hill C. In vitro activities of nisin and nisin derivatives alone and in combination with antibiotics against *Staphylococcus* biofilms. *Front Microbiol* 2016;7:1–11.
- [86] Dreyer L, Smith C, Deane SM, Dicks LMT, van Staden AD. Migration of Bacteriocins Across Gastrointestinal Epithelial and Vascular Endothelial Cells, as Determined Using In Vitro Simulations. *Sci Rep* 2019;9:1–11.
- [87] Shin JM, Ateia I, Paulus JR, Liu H, Fenno JC, Rickard AH, et al. Antimicrobial nisin acts against saliva derived multi-species biofilms without cytotoxicity to human oral cells. *Front Microbiol* 2015;6:1–14.
- [88] Salmaso S, Elvassore N, Bertuccio A, Lante A, Caliceti P. Nisin-loaded poly-L-lactide nano-particles produced by CO<sub>2</sub> anti-solvent precipitation for sustained antimicrobial activity. *Int J Pharm* 2004;287:163–73.
- [89] Okuda KI, Zendo T, Sugimoto S, Iwase T, Tajima A, Yamada S, et al. Effects of bacteriocins on methicillin-resistant *Staphylococcus aureus* biofilm. *Antimicrob Agents Chemother* 2013;57:5572–9.
- [90] Valenta C, Bernkop-Schnürch A, Rigler HP. The Antistaphylococcal Effect of Nisin in a Suitable Vehicle: A Potential Therapy for Atopic Dermatitis in Man. *J Pharm Pharmacol* 1996;48:988–91.
- [91] De Kwaadsteniet M, Doeschate KT, Dicks LMT. Nisin F in the treatment of respiratory tract infections caused by *Staphylococcus aureus*. *Lett Appl Microbiol* 2009;48:65–70.
- [92] Pamp SJ, Gjermansen M, Johansen HK, Tolker-Nielsen T. Tolerance to the antimicrobial peptide colistin in *Pseudomonas aeruginosa* biofilms is linked to metabolically active cells, and depends

- on the *pmr* and *mexAB-*oprM** genes. *Mol Microbiol* 2008;68:223–40.
- [93] Lin L, Nonejuie P, Munguia J, Hollands A, Olson J, Dam Q, et al. Azithromycin Synergizes with Cationic Antimicrobial Peptides to Exert Bactericidal and Therapeutic Activity Against Highly Multidrug-Resistant Gram-Negative Bacterial Pathogens. *EBioMedicine* 2015;2:690–8.
- [94] Giamarellos-Bourboulis EJ, Sambatakou H, Galani I, Giamarellou H. In Vitro Interaction of Colistin and Rifampin on Multidrug-Resistant *Pseudomonas aeruginosa*. *J Chemother* 2003;15:235–8.
- [95] Brauner A, Fridman O, Gefen O, Balaban NQ. Distinguishing between resistance, tolerance and persistence to antibiotic treatment. *Nat Rev Microbiol* 2016;14:320–30.
- [96] Lewis K. Persister cells, dormancy and infectious disease. *Nat Rev Microbiol* 2007;5:48–56.
- [97] Bjarnsholt T. Introduction to Biofilms. In: Bjarnsholt T, Moser C, Jensen PØ, Høiby N, editors. *Biofilm Infect.* 1st ed., London: Springer; 2011, p. 1–11.
- [98] Levin BR, Rozen DE. Non-inherited antibiotic resistance. *Nat Rev Microbiol* 2006;4:556–62.
- [99] Mah TFC, O’Toole GA. Mechanisms of biofilm resistance to antimicrobial agents. *Trends Microbiol* 2001;9:34–9.
- [100] Cao B, Christophersen L, Thomsen K, Sonderholm M, Bjarnsholt T, Jensen PO, et al. Antibiotic penetration and bacterial killing in a *Pseudomonas aeruginosa* biofilm model. *J Antimicrob Chemother* 2015;70:2057–2063.
- [101] Alipour M, Suntres ZE, Omri A. Importance of DNase and alginate lyase for enhancing free and liposome encapsulated aminoglycoside activity against *Pseudomonas aeruginosa*. *J Antimicrob Chemother* 2009;64:317–25.
- [102] Chiang W-C, Nilsson M, Jensen PØ, Høiby N, Nielsen TE, Givskov M, et al. Extracellular DNA Shields against Aminoglycosides in *Pseudomonas aeruginosa* Biofilms. *Antimicrob Agents Chemother* 2013;57:2352–61.
- [103] Bahamondez-Canas TF, Zhang H, Tewes F, Leal J, Smyth HDC. PEGylation of Tobramycin Improves Mucus Penetration and Antimicrobial Activity against *Pseudomonas aeruginosa* Biofilms in Vitro. *Mol Pharmaceutics* 2018;15:1643–52.
- [104] Tseng BS, Zhang W, Harrison JJ, Quach TP, Song JL, Penterman J, et al. The extracellular matrix protects *Pseudomonas aeruginosa* biofilms by limiting the penetration of tobramycin. *Environ Microbiol* 2013;15:2865–78.
- [105] Szomolay B, Klapper I, Dockery J, Stewart PS. Adaptive responses to antimicrobial agents in biofilms. *Environ Microbiol* 2005;7:1186–91.
- [106] Dorsey J, Gonska T. Bacterial overgrowth, dysbiosis, inflammation, and dysmotility in the Cystic Fibrosis intestine. *J Cyst Fibros* 2017;16:S14–23.
- [107] Müller L, Murgia X, Siebenbürger L, Börger C, Schwarzkopf K, Sewald K, et al. Human airway mucus alters susceptibility of *Pseudomonas aeruginosa* biofilms to tobramycin, but not colistin. *J Antimicrob Chemother* 2018;73:2762–9.
- [108] Suk JS, Lai SK, Wang Y-Y, Ensign LM, Zeitlin PL, Boyle MP, et al. The penetration of fresh undiluted sputum expectorated by cystic fibrosis patients by non-adhesive polymer nanoparticles. *Biomaterials* 2009;30:2591–7.
- [109] Bagge N, Hentzer M, Andersen JB, Ciofu O, Givskov M, Høiby N. Dynamics and Spatial Distribution of  $\beta$ -Lactamase Expression in *Pseudomonas aeruginosa* Biofilms. *Antimicrob Agents Chemother* 2004;48:1168–74.

- [110] Lewis K. Persister Cells. *Annu Rev Microbiol* 2010;64:357–72.
- [111] Wood TK, Knabel SJ, Kwan BW. Bacterial Persister Cell Formation and Dormancy. *Appl Environ Microbiol* 2013;79:7116–21.
- [112] Helaine S, Kugelberg E. Bacterial persisters: formation, eradication, and experimental systems. *Trends Microbiol* 2014;22:417–24.
- [113] Lemire JA, Harrison JJ, Turner RJ. Antimicrobial activity of metals: mechanisms, molecular targets and applications. *Nat Rev Microbiol* 2013;11:371–84.
- [114] Siddiq DM, Darouiche RO. New strategies to prevent catheter-associated urinary tract infections. *Nat Rev Urol* 2012;9:305–14.
- [115] Johnson JR, Kuskowski MA, Wilt TJ. Systematic Review: Antimicrobial Urinary Catheters To Prevent Catheter-Associated Urinary Tract Infection in Hospitalized Patients. *Ann Intern Med* 2006;144:116–26.
- [116] McDougald D, Rice SA, Barraud N, Steinberg PD, Kjelleberg S. Should we stay or should we go: mechanisms and ecological consequences for biofilm dispersal. *Nat Rev Microbiol* 2012;10:39–50.
- [117] Rasmussen TB, Givskov M. Quorum-sensing inhibitors as anti-pathogenic drugs. *Int J Med Microbiol* 2006;296:149–61.
- [118] Carradori S, Di Giacomo N, Lobefalo M, Luisi G, Campestre C, Sisto F. Biofilm and Quorum Sensing inhibitors: the road so far. *Expert Opin Ther Pat* 2020;30:917–30.
- [119] Kaplan JB. Therapeutic Potential of Biofilm-Dispersing Enzymes. *Int J Artif Organs* 2009;32:545–54.
- [120] Alkawash M, Soothill J, Schiller N. Alginate lyase enhances antibiotic killing of mucoid *Pseudomonas aeruginosa* in biofilms. *APMIS* 2006;2:131–8.
- [121] Islan GA, Bosio VE, Castro GR. Alginate lyase and ciprofloxacin co-immobilization on biopolymeric microspheres for cystic fibrosis treatment. *Macromol Biosci* 2013;13:1238–48.
- [122] Boegh M, Nielsen HM. Mucus as a Barrier to Drug Delivery - Understanding and Mimicking the Barrier Properties. *Basic Clin Pharmacol Toxicol* 2015;116:179–86.
- [123] Dinicola S, De Grazia S, Carlomagno G, Pintucci JP. N-acetylcysteine as powerful molecule to destroy bacterial biofilms. A systematic review. *Eur Rev Med Pharmacol Sci* 2014;18:2942–8.
- [124] Marchese A, Bozzolasco M, Gualco L, Debbia EA, Schito GC, Schito AM. Effect of fosfomycin alone and in combination with N-acetylcysteine on *E. coli* biofilms. *Int J Antimicrob Agents* 2003;22:95–100.
- [125] Aldini G, Altomare A, Baron G, Vistoli G, Carini M, Borsani L, et al. N-Acetylcysteine as an antioxidant and disulphide breaking agent: the reasons why. *Free Radic Res* 2018;52:751–62.
- [126] Suk JS, Lai SK, Boylan NJ, Dawson MR, Boyle MP, Hanes J. Rapid transport of muco-inert nanoparticles in cystic fibrosis sputum treated with N-acetyl cysteine. *Nanomedicine* 2011;6:365–75.
- [127] Zhao T, Liu Y. N-acetylcysteine inhibit biofilms produced by *Pseudomonas aeruginosa*. *BMC Microbiol* 2010;10:1–8.
- [128] Pérez-Giraldo C, Rodríguez-Benito A, Morán FJ, Hurtado C, Blanco MT, Gómez-García AC. Influence of N-acetylcysteine on the formation of biofilm by *Staphylococcus epidermis*. *J Antimicrob Chemother* 1997;39:643–6.
- [129] Costa F, Sousa DM, Parreira P, Lamghari M, Gomes P, Martins MCL. N-acetylcysteine-

- functionalized coating avoids bacterial adhesion and biofilm formation. *Sci Rep* 2017;7:1–13.
- [130] Porsio B, Cusimano MG, Schillaci D, Craparo EF, Giammona G, Cavallaro G. Nano into Micro Formulations of Tobramycin for the Treatment of *Pseudomonas aeruginosa* Infections in Cystic Fibrosis. *Biomacromolecules* 2017;18:3924–35.
- [131] Lababidi N, Ofosu Kissi E, Elgaher WAM, Sigal V, Hauptenthal J, Schwarz BC, et al. Spray-drying of inhalable, multifunctional formulations for the treatment of biofilms formed in cystic fibrosis. *J Controlled Release* 2019;314:62–71.
- [132] Jorge P, Lourenço A, Pereira MO. New trends in peptide-based anti-biofilm strategies: a review of recent achievements and bioinformatic approaches. *Biofouling* 2012;28:1033–61.
- [133] Sanjay ST, Dou M, Fu G, Xu F, Li X. Controlled Drug Delivery Using Microdevices. *Curr Pharm Biotechnol* 2016;17:772–87.
- [134] Forier K, Raemdonck K, De Smedt SC, Demeester J, Coenye T, Braeckmans K. Lipid and polymer nanoparticles for drug delivery to bacterial biofilms. *J Controlled Release* 2014;190:607–23.
- [135] Xu C, He Y, Li Z, Ahmad Nor Y, Ye Q. Nanoengineered hollow mesoporous silica nanoparticles for the delivery of antimicrobial proteins into biofilms. *J Mater Chem B* 2018;6:1899–902.
- [136] Carpenter AW, Slomberg DL, Rao KS, Schoenfisch MH. Influence of scaffold size on bactericidal activity of nitric oxide-releasing silica nanoparticles. *ACS Nano* 2011;5:7235–44.
- [137] Wang S, Yu S, Lin Y, Zou P, Chai G, Yu HH, et al. Co-Delivery of Ciprofloxacin and Colistin in Liposomal Formulations with Enhanced In Vitro Antimicrobial Activities against Multidrug Resistant *Pseudomonas aeruginosa*. *Pharm Res* 2018;35:187.
- [138] Gathirwa JW, Omwoyo W, Ogutu B, Oloo F, Swai H, Kalombo L, et al. Preparation, characterization, and optimization of primaquine-loaded solid lipid nanoparticles. *Int J Nanomedicine* 2014;9:3865–74.
- [139] Ngan LTK, Wang S-L, Hiep ĐM, Luong PM, Vui NT, Đinh TM, et al. Preparation of chitosan nanoparticles by spray drying, and their antibacterial activity. *Res Chem Intermed* 2014;40:2165–75.
- [140] Tamilvanan S, Venkateshan N, Ludwig A. The potential of lipid- and polymer-based drug delivery carriers for eradicating biofilm consortia on device-related nosocomial infections. *J Controlled Release* 2008;128:2–22.
- [141] Martin C, Low W, Gupta A, Amin M, Radecka I, Britland S, et al. Strategies for Antimicrobial Drug Delivery to Biofilm. *Curr Pharm Des* 2014;21:43–66.
- [142] Ramos MADS, Da Silva PB, Spósito L, De Toledo LG, Bonifácio B, Vidal, Rodero CF, et al. Nanotechnology-based drug delivery systems for control of microbial biofilms: A review. *Int J Nanomedicine* 2018;13:1179–213.
- [143] Wang D-Y, van der Mei HC, Ren Y, Busscher HJ, Shi L. Lipid-Based Antimicrobial Delivery-Systems for the Treatment of Bacterial Infections. *Front Chem* 2020;7:1–15.
- [144] Dong D, Thomas N, Thierry B, Vreugde S, Prestidge CA, Wormald P-J. Distribution and Inhibition of Liposomes on *Staphylococcus aureus* and *Pseudomonas aeruginosa* Biofilm. *PLoS One* 2015;10:e0131806.
- [145] Rukavina Z, Vanić Ž. Current Trends in Development of Liposomes for Targeting Bacterial Biofilms. *Pharmaceutics* 2016;8:18.
- [146] Alhajlan M, Alhariri M, Omri A. Efficacy and Safety of Liposomal Clarithromycin and Its Effect on *Pseudomonas aeruginosa* Virulence Factors. *Antimicrob Agents Chemother* 2013;57:2694–704.

- [147] Beaulac C, Clément-Major S, Hawari J, Lagacé J. Eradication of mucoid *Pseudomonas aeruginosa* with fluid liposome-encapsulated tobramycin in an animal model of chronic pulmonary infection. *Antimicrob Agents Chemother* 1996;40:665–9.
- [148] Alipour M, Suntres ZE, Halwani M, Azghani AO, Omri A. Activity and Interactions of Liposomal Antibiotics in Presence of Polyanions and Sputum of Patients with Cystic Fibrosis. *PLoS One* 2009;4:e5724.
- [149] Bandara HMHN, Herpin MJ, Kolacny D, Harb A, Romanovicz D, Smyth HDC. Incorporation of Farnesol Significantly Increases the Efficacy of Liposomal Ciprofloxacin against *Pseudomonas aeruginosa* Biofilms in Vitro. *Mol Pharmaceutics* 2016;13:2760–70.
- [150] Drulis-Kawa Z, Dorotkiewicz-Jach A. Liposomes as delivery systems for antibiotics. *Int J Pharm* 2010;387:187–98.
- [151] Batycky RP, Hanes J, Langer R, Edwards DA. A theoretical model of erosion and macromolecular drug release from biodegrading microspheres. *J Pharm Sci* 1997;86:1464–77.
- [152] Pinto-Alphandary H, Andremont A, Couvreur P. Targeted delivery of antibiotics using liposomes and nanoparticles: Research and applications. *Int J Antimicrob Agents* 2000;13:155–68.
- [153] Misra R, Acharya S, Dilnawaz F, Sahoo SK. Sustained antibacterial activity of doxycycline-loaded poly(D,L-lactide-co-glycolide) and poly( $\epsilon$ -caprolactone) nanoparticles. *Nanomedicine* 2009;4:519–30.
- [154] Chronopoulou L, Di Domenico EG, Ascenzioni F, Palocci C. Positively charged biopolymeric nanoparticles for the inhibition of *Pseudomonas aeruginosa* biofilms. *J Nanoparticle Res* 2016;18:1–10.
- [155] Patel KK, Agrawal AK, Anjum MM, Tripathi M, Pandey N, Bhattacharya S, et al. DNase-I functionalization of ciprofloxacin-loaded chitosan nanoparticles overcomes the biofilm-mediated resistance of *Pseudomonas aeruginosa*. *Appl Nanosci* 2020;10:563–75.
- [156] Patel KK, Tripathi M, Pandey N, Agrawal AK, Gade S, Anjum MM, et al. Alginate lyase immobilized chitosan nanoparticles of ciprofloxacin for the improved antimicrobial activity against the biofilm associated mucoid *P. aeruginosa* infection in cystic fibrosis. *Int J Pharm* 2019;563:30–42.
- [157] Deacon J, Abdelghany SM, Quinn DJ, Schmid D, Megaw J, Donnelly RF, et al. Antimicrobial efficacy of tobramycin polymeric nanoparticles for *Pseudomonas aeruginosa* infections in cystic fibrosis: Formulation, characterisation and functionalisation with dornase alfa (DNase). *J Controlled Release* 2015;198:55–61.
- [158] Baelo A, Levato R, Julián E, Crespo A, Astola J, Gavaldà J, et al. Disassembling bacterial extracellular matrix with DNase-coated nanoparticles to enhance antibiotic delivery in biofilm infections. *J Controlled Release* 2015;209:150–8.
- [159] Jeong Y II, Na HS, Seo DH, Kim DG, Lee HC, Jang MK, et al. Ciprofloxacin-encapsulated poly(DL-lactide-co-glycolide) nanoparticles and its antibacterial activity. *Int J Pharm* 2008;352:317–23.
- [160] Thomas N, Thorn C, Richter K, Thierry B, Prestidge C. Efficacy of Poly-Lactic-Co-Glycolic Acid Micro- and Nanoparticles of Ciprofloxacin Against Bacterial Biofilms. *J Pharm Sci* 2016;105:3115–22.
- [161] Türeli NG, Torge A, Juntke J, Schwarz BC, Schneider-Daum N, Türeli AE, et al. Ciprofloxacin-loaded PLGA nanoparticles against cystic fibrosis *P. aeruginosa* lung infections. *Eur J Pharm Biopharm* 2017;117:363–71.
- [162] Iannitelli A, Grande R, di Stefano A, di Giulio M, Sozio P, Bessa LJ, et al. Potential antibacterial activity of carvacrol-loaded poly(DL-lactide-co-glycolide) (PLGA) nanoparticles against microbial biofilm. *Int J Mol Sci* 2011;12:5039–51.



- [163] Kumari A, Yadav SK, Yadav SC. Biodegradable polymeric nanoparticles based drug delivery systems. *Colloids Surfaces B Biointerfaces* 2010;75:1–18.
- [164] Hasan S, Thomas N, Thierry B, Prestidge CA. Biodegradable nitric oxide precursor-loaded micro- and nanoparticles for the treatment of *Staphylococcus aureus* biofilms. *J Mater Chem B* 2017;5:1005–14.
- [165] Ungaro F, D'Angelo I, Coletta C, d'Emmanuele di Villa Bianca R, Sorrentino R, Perfetto B, et al. Dry powders based on PLGA nanoparticles for pulmonary delivery of antibiotics: Modulation of encapsulation efficiency, release rate and lung deposition pattern by hydrophilic polymers. *J Controlled Release* 2012;157:149–59.
- [166] Li Y, Na R, Wang X, Liu H, Zhao L, Sun X, et al. Fabrication of Antimicrobial Peptide-Loaded PLGA/Chitosan Composite Microspheres for Long-Acting Bacterial Resistance. *Molecules* 2017;22:1637.
- [167] Jamil B, Habib H, Abbasi S, Nasir H, Rahman A, Rehman A, et al. Cefazolin loaded chitosan nanoparticles to cure multi drug resistant Gram-negative pathogens. *Carbohydr Polym* 2015;136:682–91.
- [168] Dash TK, Konkimalla VB. Poly-ε-caprolactone based formulations for drug delivery and tissue engineering: A review. *J Controlled Release* 2012;158:15–33.
- [169] Kohane DS. Microparticles and nanoparticles for drug delivery. *Biotechnol Bioeng* 2007;96:203–9.
- [170] D'Angelo I, Casciaro B, Miro A, Quaglia F, Mangoni ML, Ungaro F. Overcoming barriers in *Pseudomonas aeruginosa* lung infections: Engineered nanoparticles for local delivery of a cationic antimicrobial peptide. *Colloids Surfaces B Biointerfaces* 2015;135:717–25.
- [171] Lai SK, Wang Y-Y, Hanes J. Mucus-penetrating nanoparticles for drug and gene delivery to mucosal tissues. *Adv Drug Delivery Rev* 2009;61:158–71.
- [172] Ernst J, Klinger-Strobel M, Arnold K, Thamm J, Hartung A, Pletz MW, et al. Polyester-based particles to overcome the obstacles of mucus and biofilms in the lung for tobramycin application under static and dynamic fluidic conditions. *Eur J Pharm Biopharm* 2018;131:120–9.
- [173] Forier K, Messiaen AS, Raemdonck K, Deschout H, Rejman J, De Baets F, et al. Transport of nanoparticles in cystic fibrosis sputum and bacterial biofilms by single-particle tracking microscopy. *Nanomedicine* 2013;8:935–49.
- [174] Lababidi N, Montefusco-Pereira CV, Carvalho-Wodarz C de S, Lehr CM, Schneider M. Spray-dried multidrug particles for pulmonary co-delivery of antibiotics with N-acetylcysteine and curcumin-loaded PLGA-nanoparticles. *Eur J Pharm Biopharm* 2020;157:200–10.
- [175] Nielsen LH, Keller SS, Boisen A. Microfabricated devices for oral drug delivery. *Lab Chip* 2018;18:2348–58.
- [176] Ainslie KM, Kraning CM, Desai TA. Microfabrication of an asymmetric, multi-layered microdevice for controlled release of orally delivered therapeutics. *Lab Chip* 2008;8:1042–7.
- [177] Sant S, Tao SL, Fisher OZ, Xu Q, Peppas NA, Khademhosseini A. Microfabrication technologies for oral drug delivery. *Adv Drug Delivery Rev* 2012;64:496–507.
- [178] McHugh KJ, Nguyen TD, Linehan AR, Yang D, Behrens AM, Rose S, et al. Fabrication of fillable microparticles and other complex 3D microstructures. *Science* 2017;357:1138–42.
- [179] Chirra HD, Desai TA. Multi-Reservoir Bioadhesive Microdevices for Independent Rate-Controlled Delivery of Multiple Drugs. *Small* 2012;8:3839–46.

- [180] Ainslie KM, Lowe RD, Beaudette TT, Petty L, Bachelder EM, Desai TA. Microfabricated Devices for Enhanced Bioadhesive Drug Delivery: Attachment to and Small-Molecule Release Through a Cell Monolayer Under Flow. *Small* 2009;5:2857–63.
- [181] Nielsen LH, Melero A, Keller SS, Jacobsen J, Garrigues T, Rades T, et al. Polymeric microcontainers improve oral bioavailability of furosemide. *Int J Pharm* 2016;504:98–109.
- [182] Chirra HD, Shao L, Ciaccio N, Fox CB, Wade JM, Ma A, et al. Planar Microdevices for Enhanced In Vivo Retention and Oral Bioavailability of Poorly Permeable Drugs. *Adv Healthcare Mater* 2014;3:1648–54.
- [183] Christfort JF, Guillot AJ, Melero A, Thamdrup LHE, Garrigues TM, Boisen A, et al. Cubic Microcontainers Improve In Situ Colonic Mucoadhesion and Absorption of Amoxicillin in Rats. *Pharmaceutics* 2020;12:355.
- [184] Mandsberg NK, Christfort JF, Kamguyan K, Boisen A, Srivastava SK. Orally ingestible medical devices for gut engineering. *Adv Drug Delivery Rev* 2020;165–166:142–54.
- [185] Ahmed A, Bonner C, Desai TA. Bioadhesive microdevices with multiple reservoirs: A new platform for oral drug delivery. *J Controlled Release* 2002;81:291–306.
- [186] Tao SL, Lubeley MW, Desai TA. Bioadhesive poly(methyl methacrylate) microdevices for controlled drug delivery. *J Controlled Release* 2003;88:215–28.
- [187] Fox CB, Cao Y, Nemeth CL, Chirra HD, Chevalier RW, Xu AM, et al. Fabrication of Sealed Nanostraw Microdevices for Oral Drug Delivery. *ACS Nano* 2016;10:5873–81.
- [188] Malachowski K, Breger J, Kwag HR, Wang MO, Fisher JP, Selaru FM, et al. Stimuli-Responsive Theragrippers for Chemomechanical Controlled Release. *Angew Chemie Int Ed* 2014;53:8045–9.
- [189] Ghosh A, Li L, Xu L, Dash RP, Gupta N, Lam J, et al. Gastrointestinal-resident, shape-changing microdevices extend drug release in vivo. *Sci Adv* 2020;6:eabb4133.
- [190] Bellinger AM, Jafari M, Grant TM, Zhang S, Slater HC, Wenger EA, et al. Oral, ultra-long-lasting drug delivery: Application toward malaria elimination goals. *Sci Transl Med* 2016;8:365ra157–365ra157.
- [191] Kirtane AR, Abouzid O, Minahan D, Bense T, Hill AL, Selinger C, et al. Development of an oral once-weekly drug delivery system for HIV antiretroviral therapy. *Nat Commun* 2018;9:2.
- [192] de Ávila BE-F, Angsantikul P, Li J, Angel Lopez-Ramirez M, Ramírez-Herrera DE, Thamphiwatana S, et al. Author correction: Micromotor-enabled active drug delivery for in vivo treatment of stomach infection. *Nat Commun* 2017;8:1299.
- [193] Gao W, Dong R, Thamphiwatana S, Li J, Gao W, Zhang L, et al. Artificial Micromotors in the Mouse's Stomach: A Step toward in Vivo Use of Synthetic Motors. *ACS Nano* 2015;9:117–23.
- [194] Villa K, Viktorova J, Plutnar J, Ruml T, Hoang L, Pumera M. Chemical Microrobots as Self-Propelled Microbrushes against Dental Biofilm. *Cell Reports Phys Sci* 2020;1:100181.
- [195] Yuan K, Jurado-Sánchez B, Escarpa A. Dual-Propelled Lanibiotic Based Janus Micromotors for Selective Inactivation of Bacterial Biofilms. *Angew Chemie Int Ed* 2021;60:2–12.
- [196] Mazzoni C, Tentor F, Strindberg SA, Nielsen LH, Keller SS, Alstrøm TS, et al. From concept to in vivo testing: Microcontainers for oral drug delivery. *J Controlled Release* 2017;268:343–51.
- [197] Tao SL, Popat K, Desai TA. Off-wafer fabrication and surface modification of asymmetric 3D SU-8 microparticles. *Nat Protoc* 2007;1:3153–8.
- [198] Nielsen LH, Keller SS, Gordon KC, Boisen A, Rades T, Müllertz A. Spatial confinement can lead to

- increased stability of amorphous indomethacin. *Eur J Pharm Biopharm* 2012;81:418–25.
- [199] Mazzoni C, Tentor F, Antalaki A, Jacobsen RD, Mortensen J, Slipets R, et al. Where Is the Drug? Quantitative 3D Distribution Analyses of Confined Drug-Loaded Polymer Matrices. *ACS Biomater Sci Eng* 2019;5:2935–41.
- [200] Dalskov Mosgaard M, Strindberg S, Abid Z, Singh Petersen R, Højlund Eklund Thamdrup L, Joukainen Andersen A, et al. Ex vivo intestinal perfusion model for investigating mucoadhesion of microcontainers. *Int J Pharm* 2019;570:118658.
- [201] Tao SL, Desai TA. Microfabrication of Multilayer, Asymmetric, Polymeric Devices for Drug Delivery. *Adv Mater* 2005;17:1625–30.
- [202] Petersen RS, Mahshid R, Andersen NK, Keller SS, Hansen HN, Boisen A. Hot embossing and mechanical punching of biodegradable microcontainers for oral drug delivery. *Microelectron Eng* 2015;133:104–9.
- [203] Petersen RS, Keller SS, Boisen A. Hot punching of high-aspect-ratio 3D polymeric microstructures for drug delivery. *Lab Chip* 2015;15:2576–9.
- [204] Nemani K V., Moodie KL, Brennick JB, Su A, Gimi B. In vitro and in vivo evaluation of SU-8 biocompatibility. *Mater Sci Eng C* 2013;33:4453–9.
- [205] Voskerician G, Shive MS, Shawgo RS, Recum H von, Anderson JM, Cima MJ, et al. Biocompatibility and biofouling of MEMS drug delivery devices. *Biomaterials* 2003;24:1959–67.
- [206] Nagstrup J, Keller S, Almdal K, Boisen A. 3D microstructuring of biodegradable polymers. *Microelectron Eng* 2011;88:2342–4.
- [207] Abid Z, Strindberg S, Javed MM, Mazzoni C, Vaut L, Nielsen LH, et al. Biodegradable microcontainers – towards real life applications of microfabricated systems for oral drug delivery. *Lab Chip* 2019;19:2905–14.
- [208] Abid Z, Mosgaard MD, Manfroni G, Petersen RS, Nielsen LH, Müllertz A, et al. Investigation of mucoadhesion and degradation of PCL and PLGA microcontainers for oral drug delivery. *Polymer* 2019;11:1–10.
- [209] Marizza P, Keller SS, Boisen A. Inkjet printing as a technique for filling of micro-wells with biocompatible polymers. *Microelectron Eng* 2013;111:391–5.
- [210] Fox CB, Nemeth CL, Chevalier RW, Cantlon J, Bogdanoff DB, Hsiao JC, et al. Picoliter-volume inkjet printing into planar microdevice reservoirs for low-waste, high-capacity drug loading. *Bioeng Transl Med* 2017;2:9–16.
- [211] Marizza P, Pontoni L, Rindzevicius T, Alopaeus JF, Su K, Zeitler JA, et al. Supercritical impregnation of polymer matrices spatially confined in microcontainers for oral drug delivery: Effect of temperature, pressure and time. *J Supercrit Fluids* 2016;107:145–52.
- [212] Petersen RS, Keller SS, Boisen A. Loading of Drug-Polymer Matrices in Microreservoirs for Oral Drug Delivery. *Macromol Mater Eng* 2017;302:1–6.
- [213] Abid Z, Gundlach C, Durucan O, von Halling Laier C, Nielsen LH, Boisen A, et al. Powder embossing method for selective loading of polymeric microcontainers with drug formulation. *Microelectron Eng* 2017;171:20–4.
- [214] Jørgensen JR, Jepsen ML, Nielsen LH, Dufva M, Nielsen HM, Rades T, et al. Microcontainers for oral insulin delivery – In vitro studies of permeation enhancement. *Eur J Pharm Biopharm* 2019;143:98–105.
- [215] Kamguyan K, Thamdrup LHE, Vaut L, Nielsen LH, Zor K, Boisen A. Development and

- characterization of a PDMS-based masking method for microfabricated Oral drug delivery devices. *Biomed Microdevices* 2020;22:35.
- [216] Mazzone C, Jacobsen RD, Mortensen J, Jørgensen JR, Vaut L, Jacobsen J, et al. Polymeric Lids for Microcontainers for Oral Protein Delivery. *Macromol Biosci* 2019;19:1900004.
- [217] Bose S, Keller SS, Alstrøm TS, Boisen A, Almdal K. Process Optimization of Ultrasonic Spray Coating of Polymer Films. *Langmuir* 2013;29:6911–9.
- [218] Ways TM, Lau W, Khutoryanskiy V. Chitosan and Its Derivatives for Application in Mucoadhesive Drug Delivery Systems. *Polymer* 2018;10:267.
- [219] Wang YY, Lai SK, Suk JS, Pace A, Cone R, Hanes J. Addressing the PEG mucoadhesivity paradox to engineer nanoparticles that “slip” through the human mucus barrier. *Angew Chem, Int Ed* 2008;47:9726–9.
- [220] Hejazi R, Amiji M. Stomach-specific anti-H. pylori therapy. I: Preparation and characterization of tetracycline-loaded chitosan microspheres. *Int J Pharm* 2002;235:87–94.
- [221] Hejazi R, Amiji M. Stomach-specific anti-H. pylori Therapy. II. Gastric residence studies of tetracycline-loaded chitosan microspheres in gerbils. *Pharm Dev Technol* 2003;8:253–62.
- [222] Hejazi R, Amiji M. Stomach-specific anti-H. pylori therapy. Part III: Effect of chitosan microspheres crosslinking on the gastric residence and local tetracycline concentrations in fasted gerbils. *Int J Pharm* 2004;272:99–108.
- [223] Mohammed M, Syeda J, Wasan K, Wasan E. An Overview of Chitosan Nanoparticles and Its Application in Non-Parenteral Drug Delivery. *Pharmaceutics* 2017;9:53.
- [224] Rinaudo M. Chitin and chitosan: Properties and applications. *Prog Polym Sci* 2006;31:603–32.
- [225] Ahmadi F, Oveisi Z, Samani SM, Amoozgar Z. Chitosan based hydrogels: characteristics and pharmaceutical applications. *Res Pharm Sci* 2015;10:1–16.
- [226] Boateng J, Ayensu I, Pawar H. Chitosan. In: Khutoryanskiy V V, editor. *Mucoadhesive Mater. Drug Deliv. Syst.* 1st ed., 2014, p. 233–54.
- [227] Moreno JAS, Mendes AC, Stephansen K, Engwer C, Goycoolea FM, Boisen A, et al. Development of electrosprayed mucoadhesive chitosan microparticles. *Carbohydr Polym* 2018;190:240–7.
- [228] Costa EM, Silva S, Tavora FK, Pintado MM. Study of the effects of chitosan upon *Streptococcus mutans* adherence and biofilm formation. *Anaerobe* 2013;20:27–31.
- [229] de Paz LEC, Resin A, Howard KA, Sutherland DS, Wejse PL. Antimicrobial effect of chitosan nanoparticles on *Streptococcus mutans* biofilms. *Appl Environ Microbiol* 2011;77:3892–5.
- [230] Costa EM, Silva S, Tavora FK, Pintado MM. Insights into chitosan antibiofilm activity against methicillin-resistant *Staphylococcus aureus*. *J Appl Microbiol* 2017;122:1547–57.
- [231] Wu Y, Ying Y, Liu Y, Zhang H, Huang J. Preparation of chitosan/poly vinyl alcohol films and their inhibition of biofilm formation against *Pseudomonas aeruginosa* PAO1. *Int J Biol Macromol* 2018;118:2131–7.
- [232] Kucukoglu V, Uzuner H, Kenar H, Karadenizli A. In vitro antibacterial activity of ciprofloxacin loaded chitosan microparticles and their effects on human lung epithelial cells. *Int J Pharm* 2019;569:118578.
- [233] Rabea EI, Badawy ME-T, Stevens C V., Smagghe G, Steurbaut W. Chitosan as Antimicrobial Agent: Applications and Mode of Action. *Biomacromolecules* 2003;4:1457–65.
- [234] Liu N, Chen XG, Park HJ, Liu CG, Liu CS, Meng XH, et al. Effect of MW and concentration of chitosan

- on antibacterial activity of *Escherichia coli*. *Carbohydr Polym* 2006;64:60–5.
- [235] Liu M, Zhang J, Shan W, Huang Y. Developments of mucus penetrating nanoparticles. *Asian J Pharm Sci* 2014;10:275–82.
- [236] Lai SK, O’Hanlon DE, Harrold S, Man ST, Wang Y-Y, Cone R, et al. Rapid transport of large polymeric nanoparticles in fresh undiluted human mucus. *Proc Natl Acad Sci* 2007;104:1482–7.
- [237] Doring G, Conway S, Heijerman H, Hodson M, Hoiby N, Smyth A, et al. Antibiotic therapy against *Pseudomonas aeruginosa* in cystic fibrosis: a European consensus. *Eur Respir J* 2000;16:749–67.
- [238] Moradali MF, Ghods S, Rehm BHA. *Pseudomonas aeruginosa* Lifestyle: A Paradigm for Adaptation, Survival, and Persistence. *Front Cell Infect Microbiol* 2017;7:1–29.
- [239] Subramanian S, Huiszoon RC, Chu S, Bentley WE, Ghodssi R. Microsystems for biofilm characterization and sensing – A review. *Biofilm* 2020;2:100015.
- [240] Magana M, Sereti C, Ioannidis A, Mitchell CA, Ball AR, Magiorkinis E, et al. Options and limitations in clinical investigation of bacterial biofilms. *Clin Microbiol Rev* 2018;31:1–49.
- [241] Merritt JH, Kadouri DE, O’Toole GA. Growing and Analyzing Static Biofilms. *Curr. Protoc. Microbiol.*, vol. Chapter 1, Hoboken, NJ, USA: John Wiley & Sons, Inc.; 2005, p. 1–29.
- [242] Crusz SA, Papat R, Rybtke MT, Cámara M, Givskov M, Tolker-Nielsen T, et al. Bursting the bubble on bacterial biofilms: a flow cell methodology. *Biofouling* 2012;28:835–42.
- [243] Claxton NS, Fellers TJ, Davidson MW. Laser scanning confocal microscopy. In: Webster JG, editor. *Encycl. Med. Devices Instrum.*, Hoboken, NJ, USA: John Wiley & Sons, Inc.; 2006.
- [244] Azeredo J, Azevedo NF, Briandet R, Cerca N, Coenye T, Costa AR, et al. Critical review on biofilm methods. *Crit Rev Microbiol* 2017;43:313–51.
- [245] Klausen M, Heydorn A, Ragas P, Lambertsen L, Aaes-Jørgensen A, Molin S, et al. Biofilm formation by *Pseudomonas aeruginosa* wild type, flagella and type IV pili mutants. *Mol Microbiol* 2003;48:1511–24.
- [246] Tolker-Nielsen T, Sternberg C. Growing and analyzing biofilms in flow chambers. *Curr Protoc Microbiol* 2011;21:1B.2.1-1B.2.17.
- [247] Woischnig AK, Gonçalves LM, Ferreira M, Kuehl R, Kikhney J, Moter A, et al. Acrylic microparticles increase daptomycin intracellular and in vivo anti-biofilm activity against *Staphylococcus aureus*. *Int J Pharm* 2018;550:372–9.
- [248] Ferreira IS, Bettencourt A, Bétrisey B, Gonçalves LMD, Trampuz A, Almeida AJ. Improvement of the antibacterial activity of daptomycin-loaded polymeric microparticles by Eudragit RL 100: An assessment by isothermal microcalorimetry. *Int J Pharm* 2015;485:171–82.
- [249] Stanley NR, Lazazzera BA. Environmental signals and regulatory pathways that influence biofilm formation. *Mol Microbiol* 2004;52:917–24.
- [250] Fux CA, Costerton JW, Stewart PS, Stoodley P. Survival strategies of infectious biofilms. *Trends Microbiol* 2005;13:34–40.
- [251] Fredborg M, Andersen KR, Jørgensen E, Droce A, Olesen T, Jensen BB, et al. Real-time optical antimicrobial susceptibility testing. *J Clin Microbiol* 2013;51:2047–53.
- [252] Ungphakorn W, Lagerbäck P, Nielsen EI, Tängdén T. Automated time-lapse microscopy a novel method for screening of antibiotic combination effects against multidrug-resistant Gram-negative bacteria. *Clin Microbiol Infect* 2018;24:778.e7-778.e14.
- [253] McLaughlin HP, Sue D. Rapid antimicrobial susceptibility testing and  $\beta$ -lactam-induced cell

- morphology changes of Gram-negative biological threat pathogens by optical screening. *BMC Microbiol* 2018;18:1–15.
- [254] Kłodzińska SN, Priemel PA, Rades T, Nielsen HM. Combining diagnostic methods for antimicrobial susceptibility testing – A comparative approach. *J Microbiol Methods* 2018;144:177–85.
- [255] Yu S, Wang S, Zou P, Chai G, Lin YW, Velkov T, et al. Inhalable liposomal powder formulations for co-delivery of synergistic ciprofloxacin and colistin against multi-drug resistant gram-negative lung infections. *Int J Pharm* 2020;575:118915.
- [256] Soares A, Alexandre K, Lamoureux F, Lemée L, Caron F, Pestel-Caron M, et al. Efficacy of a ciprofloxacin/amikacin combination against planktonic and biofilm cultures of susceptible and low-level resistant *Pseudomonas aeruginosa*. *J Antimicrob Chemother* 2019;74:3252–9.
- [257] Bergen PJ, Bulitta JB, Forrest A, Tsuji BT, Li J, Nation RL. Pharmacokinetic/Pharmacodynamic Investigation of Colistin against *Pseudomonas aeruginosa* Using an In Vitro Model. *Antimicrob Agents Chemother* 2010;54:3783–9.
- [258] Gunathilake TMSU, Ching YC, Chuah CH, Illias HA, Ching KY, Singh R, et al. Influence of a nonionic surfactant on curcumin delivery of nanocellulose reinforced chitosan hydrogel. *Int J Biol Macromol* 2018;118:1055–64.
- [259] Wallace SJ, Li J, Nation RL, Prankerd RJ, Velkov T, Boyd BJ. Self-Assembly Behavior of Colistin and Its Prodrug Colistin Methanesulfonate: Implications for Solution Stability and Solubilization. *J Phys Chem B* 2010;114:4836–40.
- [260] Haagenen JAJ, Verotta D, Huang L, Spormann A, Yang K. New *In Vitro* Model To Study the Effect of Human Simulated Antibiotic Concentrations on Bacterial Biofilms. *Antimicrob Agents Chemother* 2015;59:4074–81.
- [261] Frimodt-Møller J, Rossi E, Haagenen JAJ, Falcone M, Molin S, Johansen HK. Mutations causing low level antibiotic resistance ensure bacterial survival in antibiotic-treated hosts. *Sci Rep* 2018;8:1–13.
- [262] Alhede M, Qvortrup K, Liebrechts R, Høiby N, Givskov M, Bjarnsholt T. Combination of microscopic techniques reveals a comprehensive visual impression of biofilm structure and composition. *FEMS Immunol Med Microbiol* 2012;65:335–42.
- [263] Liu S, Wang Y. Application of AFM in microbiology: a review. *Scanning* 2010;32:61–73.
- [264] Dorobantu LS, Gray MR. Application of atomic force microscopy in bacterial research. *Scanning* 2010;32:74–96.
- [265] Weldrick PJ, Hardman MJ, Paunov VN. Enhanced Clearing of Wound-Related Pathogenic Bacterial Biofilms Using Protease-Functionalized Antibiotic Nanocarriers. *ACS Appl Mater Interfaces* 2019;11:43902–19.
- [266] James SA, Powell LC, Wright CJ. Atomic Force Microscopy of Biofilms—Imaging, Interactions, and Mechanics. In: Dhanasekaran D, Thajuddin N, editors. *Microb. Biofilms - Importance Appl.*, InTech; 2016.
- [267] Asahi Y, Miura J, Tsuda T, Kuwabata S, Tsunashima K, Noiri Y, et al. Simple observation of *Streptococcus mutans* biofilm by scanning electron microscopy using ionic liquids. *AMB Express* 2015;5:0–8.
- [268] Kirchner S, Fothergill JL, Wright EA, James CE, Mowat E, Winstanley C. Use of Artificial Sputum Medium to Test Antibiotic Efficacy Against *Pseudomonas aeruginosa* in Conditions More Relevant to the Cystic Fibrosis Lung. *J Vis Exp* 2012;64:e3857.
- [269] Griebinger J, Dünnhaupt S, Cattoz B, Griffiths P, Oh S, Gómez SBI, et al. Methods to determine the

- interactions of micro- and nanoparticles with mucus. *Eur J Pharm Biopharm* 2015;96:464–76.
- [270] Oh S, Borrós S. Mucoadhesion vs mucus permeability of thiolated chitosan polymers and their resulting nanoparticles using a quartz crystal microbalance with dissipation (QCM-D). *Colloids Surfaces B Biointerfaces* 2016;147:434–41.
- [271] Coenye T, Nelis HJ. In vitro and in vivo model systems to study microbial biofilm formation. *J Microbiol Methods* 2010;83:89–105.
- [272] Haley CL, Colmer-Hamood JA, Hamood AN. Characterization of biofilm-like structures formed by *Pseudomonas aeruginosa* in a synthetic mucus medium. *BMC Microbiol* 2012;12:181.
- [273] Shi D, Mi G, Wang M, Webster TJ. In vitro and ex vivo systems at the forefront of infection modeling and drug discovery. *Biomaterials* 2019;198:228–49.
- [274] Seriola L, Laksafoss TZ, Haagensen JAJ, Sternberg C, Soerensen MP, Molin S, et al. Bacterial Cell Cultures in a Lab-on-a-Disc: A Simple and Versatile Tool for Quantification of Antibiotic Treatment Efficacy. *Anal Chem* 2020;92:13871–9.
- [275] Landry RM, An D, Hupp JT, Singh PK, Parsek MR. Mucin-*Pseudomonas aeruginosa* interactions promote biofilm formation and antibiotic resistance. *Mol Microbiol* 2006;59:142–51.
- [276] Olofsson AC, Hermansson M, Elwing H. N-acetyl-L-cysteine affects growth, extracellular polysaccharide production, and bacterial biofilm formation on solid surfaces. *Appl Environ Microbiol* 2003;69:4814–22.
- [277] Torge A, Wagner S, Chaves PS, Oliveira EG, Guterres SS, Pohlmann AR, et al. Ciprofloxacin-loaded lipid-core nanocapsules as mucus penetrating drug delivery system intended for the treatment of bacterial infections in cystic fibrosis. *Int J Pharm* 2017;527:92–102.
- [278] Zaichik S, Steinbring C, Menzel C, Knabl L, Orth-Höller D, Ellemunter H, et al. Development of self-emulsifying drug delivery systems (SEDDS) for ciprofloxacin with improved mucus permeating properties. *Int J Pharm* 2018;547:282–90.
- [279] Huang JX, Blaskovich MAT, Pelington R, Ramu S, Kavanagh A, Elliott AG, et al. Mucin binding reduces colistin antimicrobial activity. *Antimicrob Agents Chemother* 2015;59:5925–31.
- [280] Sønnerholm M, Kragh KN, Koren K, Jakobsen TH, Darch SE, Alhede M, et al. *Pseudomonas aeruginosa* Aggregate Formation in an Alginate Bead Model System Exhibits In Vivo-Like Characteristics. *Appl Environ Microbiol* 2017;83:e00113-17.
- [281] Biradar B, Biradar S, Malhan B, Ms A, Arora M. Oral Biofilm-A Review. *Int J Oral Heal Dent* 2017;3:142–8.
- [282] Kuang X, Chen V, Xu X. Novel Approaches to the Control of Oral Microbial Biofilms. *Biomed Res Int* 2018;2018:1–13.
- [283] Vaut L, Scarano E, Tosello G, Boisen A. Fully replicable and automated retention measurement setup for characterization of bio-adhesion. *HardwareX* 2019;6:e00071.
- [284] Madsen KD, Sander C, Baldursdottir S, Pedersen AML, Jacobsen J. Development of an ex vivo retention model simulating bioadhesion in the oral cavity using human saliva and physiologically relevant irrigation media. *Int J Pharm* 2013;448:373–81.
- [285] Kerckhofs G, Schrooten J, Van Cleynenbreugel T, Lomov S V., Wevers M. Validation of x-ray microfocus computed tomography as an imaging tool for porous structures. *Rev Sci Instrum* 2008;79:013711.
- [286] Pugliese A, Cabassi G, Chiavaro E, Paciulli M, Carini E, Mucchetti G. Physical characterization of whole and skim dried milk powders. *J Food Sci Technol* 2017;54:3433–42.

- [287] Xiao D, Davidson PM, Zhong Q. Release and antilisterial properties of nisin from zein capsules spray-dried at different temperatures. *LWT - Food Sci Technol* 2011;44:1977–85.
- [288] Guiga W, Swesi Y, Galland S, Peyrol E, Degraeve P, Sebti I. Innovative multilayer antimicrobial films made with Nisaplin® or nisin and cellulosic ethers: Physico-chemical characterization, bioactivity and nisin desorption kinetics. *Innov Food Sci Emerg Technol* 2010;11:352–60.
- [289] Hosseini SM, Hosseini H, Mohammadifar MA, German JB, Mortazavian AM, Mohammadi A, et al. Preparation and characterization of alginate and alginate-resistant starch microparticles containing nisin. *Carbohydr Polym* 2014;103:573–80.



# APPENDIX I

PAPER I

**Polymeric nano- and microparticulate drug delivery systems for treatment of biofilms**

S.E. Birk, A. Boisen, L.H. Nielsen

*Advanced Drug Delivery Reviews, 2020 (review submitted)*

# Polymeric nano- and microparticulate drug delivery systems for treatment of biofilms

*Stine Egebro Birk<sup>a\*</sup>, Anja Boisen<sup>a</sup>, Line Hagner Nielsen<sup>a\*</sup>*

<sup>a</sup>The Danish National Research Foundation and Villum Foundation's Center for Intelligent Drug Delivery and Sensing Using Microcontainers and Nanomechanics (IDUN), Department of Health Technology, Technical University of Denmark, Ørsteds Plads 345C, 2800 Kongens Lyngby, Denmark

\*Corresponding authors: Stine Egebro Birk, e-mail: stegha@dtu.dk; Line Hagner Nielsen, e-mail: lihan@dtu.dk

## ABSTRACT

Now-a-days healthcare systems face great challenges with antibiotic resistance and low efficacy of antibiotics when combating pathogenic bacteria and bacterial biofilms. Administration of an antibiotic in its free form is often ineffective due to lack of selectivity to the infectious site and breakdown of the antibiotic before it exerts its effect. Therefore, polymeric delivery systems, where the antibiotic is encapsulated into a formulation, has shown great promise, facilitating a high local drug concentration at the site of infection, a controlled drug release and less drug degradation. All this leads to improved therapeutic effects and fewer systemic side effects together with a lower risk of developing antibiotic resistance. Here, we review and provide a comprehensive overview of polymer-based nano- and microparticles as carriers for antimicrobial agents and their effect on eradicating bacterial biofilms. We have a main focus on polymeric particulates containing poly(lactic-co-glycolic acid), chitosan and polycaprolactone, but also strategies involving combinations of these polymers are included. In addition, we discuss promising future strategies for eradicating bacterial biofilms using polymeric nano- and microparticles.

## KEYWORDS

Antibiotics; Antimicrobials; Drug resistance; Bacterial biofilm infections, Poly(lactide-co-glycolide); Chitosan; Polycaprolactone; Nanoparticles; Microparticles

## TABLE OF CONTENTS

<b>1. INTRODUCTION .....</b>	<b>3</b>
<b>2. POLY (LACTIC-CO-GLYCOLIC ACID) (PLGA)-BASED DRUG DELIVERY SYSTEMS.....</b>	<b>5</b>
2.1. Production and characterization of PLGA formulations.....	5
2.2. Antimicrobial activity on bacteria and biofilm .....	7
2.3. Combinational strategies .....	8
<b>3. CHITOSAN (CS)-BASED DRUG DELIVERY SYSTEMS.....</b>	<b>12</b>
3.1. Production and characterization of CS formulations.....	12
3.2. Molecular weight and degree of deacetylation.....	13
3.3. Antimicrobial activity on bacteria and biofilm .....	14
3.4. Combinational strategies .....	15
<b>4. POLYCAPROLACTONE (PCL)-BASED DRUG DELIVERY SYSTEMS.....</b>	<b>19</b>
4.1. Production and characterization of PCL formulations .....	19
4.2. Antimicrobial activity on bacteria and biofilm .....	19
<b>5. DISCUSSION AND FUTURE OUTLOOK.....</b>	<b>28</b>
5.1. Antimicrobial delivery by the use of device-like structures .....	28
5.2. Advanced particulated systems for antimicrobial delivery .....	29
5.3. Targeted and/or triggered antimicrobial delivery .....	30
5.4. <i>In vitro</i> and <i>in vivo</i> models for improved correlation to the clinic.....	32
<b>6. CONCLUSION .....</b>	<b>34</b>

## 1. INTRODUCTION

Decades ago, it was found that most bacterial infections are caused by the ability of the microbes to organize themselves into dense micro-communities, also known as biofilms [1–3]. The extracellular biofilm matrix, consisting of various polysaccharides, proteins and extracellular DNA (eDNA), provides a protective barrier against harsh environmental changes due to *e.g.* a host immune response or antimicrobials. This renders the biofilm-associated cells 10-1,000 times less susceptible to antibiotics than their planktonic counterpart [4,5]. Biofilms are medically important as over 80 % of microbial infections in the body are due to biofilms [4], for example in cutaneous wounds [6,7], in the airways [8], in the ears [9] and in the gastro-intestinal tract [10].

The lack in development of new antibiotics together with the problem of low response of biofilms to conventional delivery of antibiotics is highlighting the need for innovative methods to optimize the drug delivery. Administration of the drug in its free form presents some disadvantages such as lack of selectivity to the location of the biofilms and breakdown or clearance of the antibiotic prior to reaching the target (Figure 1) [11,12]. Moreover, because of the high tolerance of biofilms towards antibiotics, a large therapeutic dose is usually needed, leading to an enlarged risk of systemic toxicity with many side effects such as allergic reactions, hepatotoxicity and nephrotoxicity as well as damage of the otherwise healthy microbiota of the gastro-intestinal tract [13].

For improving the therapeutic efficacy of antibiotics, advanced drug delivery systems play an important role providing a controlled delivery to target sites of the body at an optimal rate and in a concentration within the therapeutic range. A vast amount of research has focused on how to improve the effectiveness of already existing agents against biofilms by encapsulating them into nanoparticles (NPs) or microparticles (MPs). Using particulated drug delivery systems have several advantages including the possibility of a targeted and/or triggered release of the antibiotic, the possibility of incorporation both lipophilic as well as hydrophilic agents, protection of the encapsulated antibiotic as well as reducing the side effects [14,15].

Polymer-based NPs and MPs possess several unique characteristics for antibiotic delivery and have previously been highlighted by many as a great tool in the battle against biofilm tolerance [13,14,16]. The advantages of particles are manifold: <sup>1)</sup>They are structurally stable and provide protection of the antibiotic against environmental degradation, deactivation and clearance, thus maintaining appropriate therapeutic drug concentrations [13,17]; <sup>2)</sup>They can be prepared with a controllable size distribution as well as surface charge; <sup>3)</sup>Drug release kinetics is controllable and occurs from the matrix by diffusion, swelling or polymer erosion, or a combination of these processes depending on the polymer of choice [18].

Administration of free antibiotics results in a quick and fast effect with requirement of several doses per day and no local treatment at the site of infection which can limit the efficacy. The concept of sustained release from the particles is a crucial aspect in delivery of antibiotics, as maintaining a proper drug

concentration for a longer time reduces the dosing frequency. A successful antimicrobial therapy against biofilm infections is believed to require a combination of a fast and sustained antibiotic release (biphasic release) from the particulates [19–22]. The burst drug release in early stage of treatment is then ensuring a high antimicrobial concentration for biofilm eradication and thus, a lowered risk of development of resistance, followed by a sustained release capable of minimizing any further biofilm growth [23–25]. For this, it is also advantageous to use particles as they can act as a depot for part of the antibiotic dose, providing a sustained release above the minimal inhibitory concentration (MIC) [22]. Polymeric particles also have the ability to solve the technical issues associated with delivery of poorly water soluble drugs, an attractive feature, since almost one half of potential drug candidates are excluded in the drug screening phase due to poor solubility in water. For all of these reasons, by using polymeric particles for delivery of antibiotics, suitable therapeutic concentrations can be achieved at the site of infection, leading to an improved biofilm eradication.

Various polymers, both synthetic and natural, have been used for formulating biodegradable polymeric NPs and MPs. The most utilized polymers include poly (lactic-co-glycolic acid) (PLGA), chitosan (CS), polycaprolactone (PCL), all of which are widely used due to their biodegradability and/or mucoadhesive capacity [22,26–29]. Also, the amphipathic polymer polyethylene glycol (PEG), has been incorporated into other polymers to improve antibiotic encapsulation [30], as for example in preparation of MPs consisting of poly(ester-amide) and PEG [31].

This review provides a comprehensive overview of polymer-based NPs and MPs for antibiotic delivery with focus on the polymers: PLGA, CS, PCL, and their investigations on eradicating bacterial biofilms. Furthermore, other promising future strategies for combating biofilms are discussed. We do not report on prevention of biofilm formation by the use of surface modified implants or incorporations of antimicrobials to ultimately reduce bacterial attachment and subsequent biofilm development as this has been reviewed elsewhere [29,32,33].

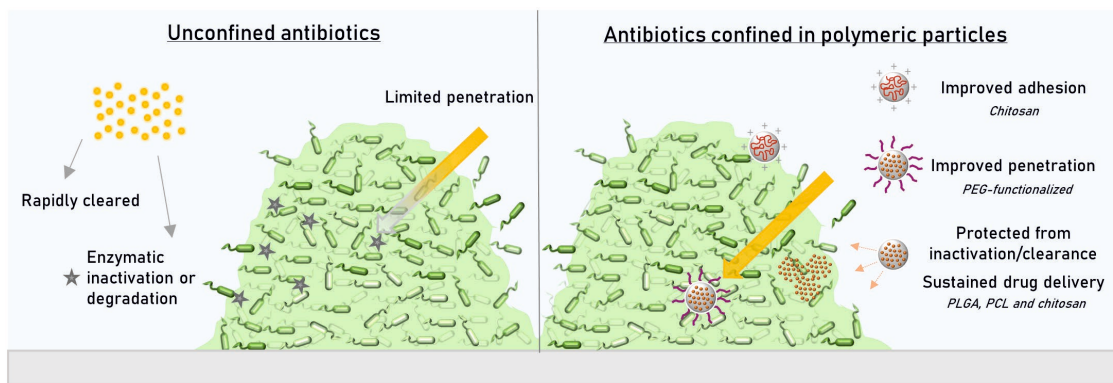


**Figure 1.** Schematic representation depicting the advantages of delivering antibiotics using polymer-based nano- or microparticles. Treatment with unconfined antibiotics is usually characterized by a rapid clearance of the antibiotic from the site of infection, enzymatic inactivation or degradation, and a limited penetration. Particle-based drug delivery systems serve as an alternative, providing protection of the antibiotic against clearance, inactivation or degradation as well as facilitate improved penetration and/or adhesion of the drug-loaded particulate. Thereby, they can deliver the antibiotics to the site of infection more effectively and for a prolonged period of time. Note: drawing not to scale.

## 2. POLY (LACTIC-CO-GLYCOLIC ACID) (PLGA)-BASED DRUG DELIVERY SYSTEMS

PLGA has received much attention as polymeric carrier due to attractive properties including a great safety profile, good biocompatibility and adjustable biodegradability [34–36]. It is approved by the European Medicine Agency and the Food and Drug Administration (FDA) for various drug delivery systems in humans. PLGA undergoes hydrolysis in the human body forming the biologically compatible moieties lactic acid and glycolic acid and therefore, a minimal toxicity is associated with the usage of PLGA-based drug delivery systems [17,37–41]. Assessment of blank PLGA particles, containing no antibiotics, have shown no inherent antimicrobial activity against *Escherichia coli*, *Staphylococcus aureus*, *Burkholderia cepacia* and *Pseudomonas aeruginosa* biofilms [27,28,38]. Information on previously reported use of PLGA particles for encapsulating antibiotics to eradicate biofilms can be found in Table 1.

### 2.1. Production and characterization of PLGA formulations

Several methods have been applied to prepare PLGA particulates of varying sizes including nanoprecipitation [23,39], solvent displacement [42], emulsification [37,43,44], spray drying [44] and electrospraying [34]. Depending on the method of preparation, the structural organization may differ as the drug is either entrapped inside the core of the particle, dispersed in the entire particle or adsorbed on the surface of the particle [17,37].

The appeal of PLGA lies in the fact that its properties can be manipulated to increase drug loading efficiencies and to tune drug release kinetics to suit a desired application. The degradation profile of PLGA is modified by altering the ratio of the monomers (lactic acid and glycolic acid), allowing control of drug release kinetics [17,45,46]. As glycolic acid is more hydrophilic than lactic acid, a high amount of glycolic acid units will decrease the hydrophobicity, resulting in higher absorption of water and thus, a faster

degradation [47]. Other particle parameters, *i.e.* particle diameter, polydispersity index (PDI) and zeta potential, were shown not to be affected when comparing different PLGA-ratios [44].

Investigation of antibiotic release from PLGA NPs revealed kinetic profiles that highly depends on the aqueous solubility of the encapsulated drug, as approximately 80 % of the water-soluble levofloxacin was released within 24 h, in contrast to the low-soluble ciprofloxacin in which only approximately 20 % was released within the same time frame [27].

For creating an attractive particulate system, it is important to have a high encapsulation efficiency (*i.e.* percentage of loaded drug in relation to the total amount of drug used during formulation) and a high drug loading (*i.e.* percentage of loaded drug in relation to the total weight of the particle). Indeed, PLGA-based NPs often present a high encapsulation efficiency. However, the drug loading is generally low, often reported to be <1 % w/w, meaning that the majority of the particle is the carrier material [17,47], and that large quantities needs to be dosed to reach the therapeutic dose. Therefore, the loading capacity is a key factor to solve in order for the particulates to reach the clinics. The amount of drug entrapped in a PLGA particle has been enhanced by modifying the pH of the formulation, thus, the hydrophilicity of certain drugs [18,48]. For example, gentamycin entrapment was improved from 6.4 to 22.4 µg/mg by changing the pH from 5 to 7.4 [48]. Furthermore, the solubility of antibiotics can be improved by encapsulating them in cyclodextrin (CD)-complexes, which can subsequently be loaded into PLGA NP. The solubility of roxithromycin (ROX) was drastically increased in a CD-complex achieving a higher drug encapsulation of 76 % compared to 57 % in PLGA particulates [49]. However in the same study, release of ROX was hindered due to electrostatic interactions among the individual components of a CD-ROX-PLGA, thus limiting the effect on *E.coli* and *S. aureus* compared to NP of ROX-PLGA [49].

MPs offer, in contrast to the nanometer-sized particles, a larger drug loading capacity. In general, the size of carrier will depend on the route of administration, and larger porous MPs have demonstrated effective lung deposition and enhanced lung residence time as a result of their large diameter and reduced clearance by macrophages in comparison to NPs, which are generally exhaled upon inhalation [44,50]. To address this issue, as well as the concern of a low drug loading capacity of NPs, the use of NPs embedded in MPs, also known as NEMs has gained a great interest. NEMs suitable for drug delivery have been obtained by spray drying PLGA particles with lactose, leucine or mannitol [44,51,52] or using a combined crosslinking-emulsion method with CS [34]. An antimicrobial peptide, KSL-W, was formulated into PLGA and PLGA/CS microspheres by electro spraying the emulsion and a crosslinking emulsification method, respectively [34]. The PLGA MPs had a size of approximately 7 µm, whereas for the PLGA/CS MPs, the PLGA MP was embedded in the external CS shell, resulting in a particle size of 61-80 µm depending on the polymer concentration. The PLGA/CS MP, that were suggested to be useful against dental biofilms, showed long-term sustained release of KSL-W for up to 80 days [34]. Recently, also PLGA NPs containing an anti-inflammatory agent (curcumin) was incorporated in MPs with a mucolytic agent (N-acetylcysteine) and antibiotics of tobramycin, ciprofloxacin or azithromycin, to potentially deliver higher local drug concentration compared to systemic applications [52].

## 2.2. Antimicrobial activity on bacteria and biofilm

PLGA particles have been used to entrap several antimicrobial agents, demonstrating a sustained delivery and efficacy in eradication of biofilms [23,53]. Gentamycin-loaded PLGA NPs were explored to clear an *in vivo* systemic 96 h old *P. aeruginosa* infection in mice. A dose of free gentamycin was able to reduce infection after 24 h, but bacterial levels returned to levels comparable to the saline-controls by 96 h. In contrast, when the animals were treated with the same concentration of PLGA-entrapped drug, this protective effect was still observed after 96 h presumably due to the sustained release of sufficient amount of gentamycin, maintaining concentrations within the therapeutic range [48].

In a time-dependent *E. coli* biofilm susceptibility test with levofloxacin- and ciprofloxacin-loaded PLGA NPs, conducted over 5 days, a subpopulation of bacteria survived despite treating with levofloxacin-PLGA NPs in a concentration above the minimal biofilm inhibitory concentration (MBIC) and regrowth took place. In comparison, ciprofloxacin-PLGA NPs suppressed regrowth for 5 days even at concentrations as low as 1/16 of the MBIC. It was then concluded that the ciprofloxacin-PLGA NPs, having 20 % burst release followed by sustained, were most promising in the treatment of *E. coli* biofilms [24]. However, it should be noted that this study did not take into consideration the possible effect of biofilm-NP interaction as NPs were not added directly to the site of biofilm, but instead samples collected from the *in vitro* release study were applied to the biofilms [24]. The effect of ciprofloxacin-PLGA NPs was also analyzed in an urinary tract infection animal model utilizing dialysis bags to create a localized *E. coli* infection [25]. Application of ciprofloxacin-PLGA NPs significantly reduced the bacterial counts (7 log<sub>10</sub> reduction) compared to free ciprofloxacin in which no reduction was observed, an effect suggested to be due to free ciprofloxacin being rapidly washed away, whereas ciprofloxacin-PLGA NPs provided a sustained and constant exposure [25]. However, few *in vitro* studies do report on reduced antimicrobial effects of the PLGA-encapsulated antibiotics. As for example, Sabaeifard *et al.* observed that PLGA-encapsulation caused higher minimal biofilm eradication concentration (MBEC) values of encapsulated amikacin compared to the free drug (512 µg/mL versus 128 µg/mL), despite having a burst release of 40 % in 1 h followed by sustained release for 10 h [54].

The efficacy of PLGA NPs (size of 300 nm) and MPs (size of 12 µm) containing ciprofloxacin was tested against *S. aureus* and *P. aeruginosa* biofilms and drug loading capacity was significantly higher for the MPs (7.5 % w/w) compared to the NPs (4.3 % w/w) [28]. Release of ciprofloxacin from the two particle sizes was comparable, releasing about half the cargo as burst followed by a sustained release over the course of 5 days. Both the NPs and MPs demonstrated a similar *in vitro* anti-biofilm performance against *P. aeruginosa* and *S. aureus*, but with a significant difference between the two strains (Figure 2A). The sustained release of ciprofloxacin from both the NPs and MPs was equally effective in eradication of *S. aureus* as the continuous treatment with ciprofloxacin solution, all of which provided a full eradication within 6 days. In contrast, *P. aeruginosa* was not fully eradicated, but a 4-5 log<sub>10</sub> reduction occurred with no significant differences in the number of surviving bacteria between ciprofloxacin NPs and MPs, suggesting that particle size was not a critical parameter for the anti-biofilm performance, when ciprofloxacin concentration was maintained constant [28]. Hasan *et al.* compared PLGA MPs and NPs



loaded with the nitric oxide precursor, isosorbide mononitrate (ISMN). Drug release was the same, but interestingly, the PLGA MPs, but not NPs, were able to deliver sufficient levels of ISMN to planktonic and biofilm-associated *S. aureus* to cause significant antibacterial effects simply due to the low drug loads of the NPs [43].

### 2.3. Combinational strategies

New approaches have been proposed aiming at increasing the mobility of administered particles through the tight mesh of mucus-embedded biofilms. Previous evaluation of the PLGA NP-mucus interaction using turbidity and zeta potential measurements has fostered the conclusion that PLGA NPs might show some mobility in mucus, and thereby, an improved penetration and accessibility of the antibiotic [39]. Having said that, much literature also present aggregation of PLGA NPs in the outer layer of the mucus, with limited mucus penetrative effects [55]. Instead, it has been shown that functionalization of the negatively charged PLGA NPs with the neutrally charged and “mucus-inert” PEG can reduce the adhesive ionic interaction of the PLGA NPs with mucus, facilitating enhanced diffusion in mucus and bacterial biofilms [38,55,56].

Tobramycin was encapsulated in PEG-PLGA with particle sizes of either 225–231 nm or 896–902 nm and the ability to overcome the biofilm barrier was compared [38]. 7-amino-4-methyl-3-coumarinylacetic acid (AMCA)-labelled PEG-PLGA particles were tracked through artificial sputum medium. The extent of permeation depended on the particle size and the presence of tobramycin, as permeation were 52 % vs. 35 % for unloaded AMCA-PEG-PLGA NPs vs. MPs, and 91 % vs. 56 % for loaded AMCA-PEG-PLGA NPs vs. MPs. The tobramycin-encapsulated NPs (zeta potential of  $-13.2 \pm 3.6$  mV) showed almost complete penetration through mucus within less than 10 h, whereas for the drug-free NPs (zeta potential of  $-27.9 \pm 2.0$  mV) only 40 % permeated mucus within the same time, indicating that a less negatively charged surface was beneficial [38]. In the same study, tobramycin-PEG-PLGA NPs were tested against the pulmonary biofilm-associated infectious strains *P. aeruginosa* and *B. cepacia*. Here, colony-forming unit (CFU) counting was applied after culturing in Müller-Hinton broth (MHB) or monitoring of live/dead-ratios with confocal laser scanning microscopy (CLSM) of biofilm grown in artificial sputum medium in static conditions or MHB in fluidic conditions (Figure 2B). Encapsulation of tobramycin in NPs and MPs strongly enhanced its effectiveness in eradication of biofilms grown under static or fluidic conditions [38]. Tobramycin-PEG-PLGA NPs and MPs, loaded with less than 0.77 mg/L antibiotic, were able to significantly reduce the CFUs of statically grown *P. aeruginosa* biofilms by a 1–1.5  $\log_{10}$  magnitude and *B. cepacia* biofilms with more than a 2  $\log_{10}$  magnitude. This effect was also supported by CLSM observations of biofilms grown in artificial sputum or MHB [38]. Considering a release efficiency of 30 % tobramycin after 24 h, the effective concentration, to which the biofilms were exposed to, was most likely even lower than 0.77 mg/L (*i.e.*  $\sim 0.25$  mg/L). This is 1.024-fold less than the MBEC of tobramycin against *P. aeruginosa* and 512-fold less than the MBEC for tobramycin against *B. cepacia* [38], proving the superior effect of using PLGA-PEG encapsulation.

Recently in another study, the impact of azithromycin-loaded D- $\alpha$ -tocopherol PEG 1000 succinate

(TPGS)-functionalized PLGA NPs were comprehensively investigated by quartz crystal microbalance with dissipation monitoring, total internal reflection fluorescence microscopy-based particle tracking and in an *in vitro* biofilm model cultured in a flow-chamber system with subsequent quantitative imaging analysis [57,58]. It was found that the mucus-inert, enzymatically cleavable TPGS shell, enabled PLGA NP penetration through mucus with accumulation in the deeper layers of the biofilms and the sustained release improved the killing efficacy of the azithromycin against *P. aeruginosa* [57]. As an alternative to the rigid PLGA NPs, nanogels based on the biodegradable hyaluronic acid (HA) have shown antiadhesive and anti-biofilm properties towards multiple bacteria [59]. Modification of HA with octenyl succinic anhydride (OSA) allows the production of an amphiphilic polymer capable of self-assembly into soft nanogels composed of hydrophilic and hydrophobic zones suitable for delivery of partially hydrophobic compounds [58]. In a comparison between TPGS-PLGA NPs and OSA-HA nanogels, the TPGS-PLGA NPs showed superior mucin interaction and longer retention time in the biofilm. Both delivery systems improved the antimicrobial and anti-virulence activity of azithromycin as well as allowed prevention and removal of preformed biofilms at substantially lower doses than non-encapsulated azithromycin [58]. Also, engineering of PLGA NPs with CS or polyvinyl alcohol (PVA) was studied for improved transport through artificial cystic fibrosis (CF) mucus (Figure 2C) [51]. Colistin-loaded PLGA NPs were subsequently embedded in an inert carrier of lactose thus, producing NEMs suitable for inhalation therapy with optimal flow properties. Free colistin showed a potent anti-biofilm activity, treating a 24 h statically grown *P.aeruginosa* biofilm for 24, 48 and 72 h [51]. After 24 h treatment with 7.5 or 15 µg/ml free colistin, up to 90 % of the biofilm biomass was eradicated, however, this effect was diminished after 48 h and completely lost after 72 h due to full regrowth of the biofilm. When colistin was incorporated in PVA or CS lactose-based NEMs, a weaker initial anti-biofilm activity was observed (approximately 50 % biomass reduction after 24 h). However in contrast, the long-term anti-biofilm activity was preserved especially with PVA NEMs (40 % for PVA and 25 % biomass reduction for CS after 72 h) [51], proving a prolonged efficacy when using NEMs compared to free colistin. This effect was ascribed to NP penetration with accompanying sustained release of colistin in the biofilm [51].

Lipid-polymer hybrid NPs have gained a great interest since they possess benefits from both delivery strategies. Levofloxacin-loaded phosphatidylcholine-coated PLGA NPs were prepared and examined against a *P. aeruginosa* biofilm. Compared to PLGA NPs, the hybrid NPs were more stable and resulted in a slower antibiotic release rate. They did not improve the biofilm affinity nor the antibacterial efficacy against planktonic bacterial cells, but on the other hand they did improve antibacterial efficacy against the biofilm-associated ones (0.1 % vs. 5 % survival rate). Since an effect was only observed on the biofilm, it was suggested, that the lipid-component may have enhanced the antibiotic diffusion into the biofilm matrix [60].

In contrast to the bacteria itself, the matrix of extracellular polymeric substances (EPS) is highly exposed to the surrounding environment. Co-targeting the bacteria and the compounds of the EPS simultaneously, could potentially increase the penetration of antibiotics into the deeper layers of the biofilm (where tolerant dormant cells reside) [61]. This was exemplified by Baelo *et al.*, who chemically functionalized

ciprofloxacin-loaded PLGA NPs with poly(lysine) to allow further functionalization with DNase I. The antimicrobial effect was assessed towards mature *P. aeruginosa* biofilms grown in flow chamber cells. Besides, providing the controlled release of ciprofloxacin, the incorporation of DNase I enabled targeting and disassembling of the biofilm by degradation of the eDNA that stabilized the biofilm matrix [23]. Compared to free ciprofloxacin, PLGA NPs loaded with ciprofloxacin decreased the planktonic bacterial population when applied in concentrations above 0.125 µg/ml. Chemical modification of PLGA with poly(lysine) resulted in the same effect against planktonic and biofilm-associated cells as compared to free ciprofloxacin. However, incorporation of DNase I significantly improved the efficacy of ciprofloxacin both in static and flow cell conditions. Therefore, DNase I modifications appear to be a promising approach. Moreover, repeated administration over three days of DNase I coated ciprofloxacin-encapsulated PLGA NPs was able to eradicate more than 99.8 % of the established biofilm, outperforming all the other NP formulations and the free drug tested in this study [23].

Another approach is to revert the biofilm bacteria back to their planktonic mode of growth, which was achieved through enzymatic depletion of available pyruvate using pyruvate dehydrogenase. This induced biofilm bacteria to disperse from the biofilm-associated mode of growth into the surrounding environment. However, a clinical use of enzymes is often not practical as the enzyme is susceptible to denaturation under storage, but encapsulation of pyruvate dehydrogenase in PLGA NPs was shown to disperse biofilms and maintain the enzymatic activity after being stored at 37 °C for 6 days [62].

Lastly, lytic bacteriophages (viruses that specifically kill bacteria) have received much attention as alternative to antibiotics in the treatment of pneumonia, however, their clinical use has been hindered by difficulties in delivering active phages to the deep lung. Interestingly, it was shown that phage-loaded polymeric PLGA MPs deposit throughout the lung via dry powder inhalation and that active phages were delivered and effectively reduced *P. aeruginosa* infections and the associated inflammation in mice [63].

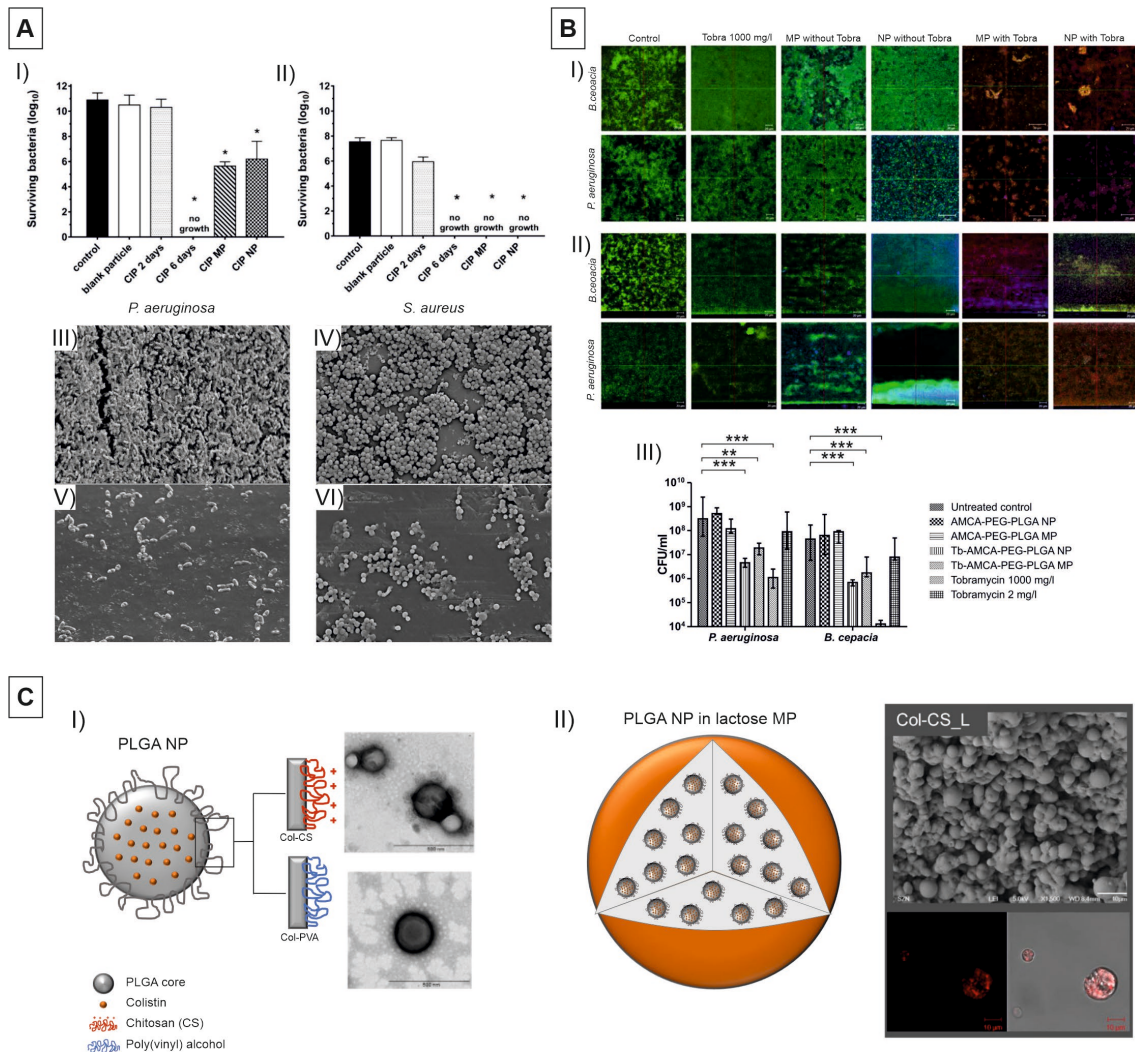


**Figure 2.** (A) Anti-biofilm performance of ciprofloxacin-loaded PLGA NPs and PLGA MPs for 2 and 6 days treatment of *P. aeruginosa* and *S. aureus* grown on Calgary devices. Viable counts were monitored (I, II) and representative SEM were taken prior to treatment (III, IV) after 6 days of treatment with ciprofloxacin-loaded MPs (V,VI). Reprinted and adapted from [28] with permission from Elsevier (Copyright© 2016). (B) *B. cepacia* and *P. aeruginosa* biofilms grown under static conditions in artificial sputum medium (ASM) (I), under flow in Müller-Hinton broth (MHB) (II) and in static conditions in MHB (III). The biofilms were treated with pure tobramycin, drug free PEG-PLGA NP or MP or tobramycin-loaded PEG-PLGA NP/MP. Effect of treatment on the viability of *B. cepacia* and *P. aeruginosa* was monitored using confocal laser scanning microscopy (CLSM) (I, II) or CFU/mL counting (III). AMCA: fluorescent tag making NPs/MPs visible in blue. Viable (green) and dead (red) cells were visualized using the live/dead staining. Reprinted and adapted from [38] with permission from Elsevier (Copyright© 2018). (C) Colistin-loaded PLGA NP coated with PVA or CS observed with TEM (I), and subsequently embedded in a lactose carrier forming a nano-embedded MP as seen from the representative SEM and CLSM image (II). Colistin-loaded NPs labelled with PLGA-Rhod (red) were embedded for CLSM studies. Reprinted and adapted from [51] with permission from Elsevier (Copyright© 2015).

### 3. CHITOSAN (CS)-BASED DRUG DELIVERY SYSTEMS

CS is a hydrophilic linear polysaccharide of randomly distributed  $\beta$ -1,4-linked D-glucosamine and N-acetyl-D-glucosamine. It is biocompatible and biodegradable, thus an appealing biopolymer for many pharmaceutical applications [64–66]. CS is well known to hold antimicrobial properties [65,67]. For this, several modes of action have been proposed in the literature, but the mechanism is still not fully known. The first hypothesis (and the most accepted) describes electrostatic interactions as the positive charged chains in CS interact with the negatively charged bacterial cell surfaces resulting in cell membrane damaging and thereby, leakage of intracellular components [68–71]. In addition, it has also been suggested that CS chelates metal ions leading to production of toxins and thus, inhibiting enzyme activity resulting in bacterial death [14,69]. At last, a possible explanation can also be that CS can change the cell permeability by binding to the bacterial DNA thereby, exhibiting an antibacterial effect [14]. Moreover, CS has strong mucoadhesive properties therefore, it can bind to the mucins in the biofilm making it an attractive material for particulates against bacteria and biofilms [65,70,72]. One of the disadvantages of CS is that it can be degraded by lysozymes and this enzyme is heavily found in the body *e.g.* in the lungs [67]. Therefore, the stability of these particulates is also important to investigate. Information on the CS particulates and their effect on bacteria and biofilm can be found in Table 2.

#### 3.1. Production and characterization of CS formulations

CS NPs can be produced in several ways, but the most standard method is ionic gelation [73–75]. This method is mainly suited for hydrophilic drug molecules, whereas if a hydrophobic drug is needed for encapsulation into the CS particles a co-solvent and a surfactant can be utilized to improve the apparent solubility of the drug [76]. CS particles have also been produced by spray drying [67,77] and this can be useful when a powder is needed as for example in pulmonary delivery. In addition, CS particles can also be prepared by emulsification often resulting in very small particle sizes [78].

It has been suggested that the penetration abilities of CS NPs into biofilms, for then to release their antimicrobial load, mainly depend on NP dimensions and surface charge. In particular, it has been reported that small cationic particles can penetrate biofilms more efficiently [19]. Chronopoulou *et al.* chose a molar ratio between the particle and antibiotic components which resulted in a size of 170 nm and a positive zeta potential of 12.2 mV. This was the optimal properties for achieving the best effect on eradicating a biofilm [19]. Ngan *et al.* also found that the smaller the size and the higher the zeta potential, the greater antibacterial activity was found for the CS particles when investigating for the bacteria, *S. aureus* [77]. The zeta potential of the particles is of course dependent on which drug is encapsulated. In the case of CS MP with an average size 721 nm, the zeta potential dropped when adding ciprofloxacin as the antibiotic. This meant that the particles without ciprofloxacin were more stable and did not have the same tendency to aggregate as the particles with the antibiotic [75].

The encapsulation efficiency of drug into CS particles seems to increase with drug concentration up to a certain point and is highly dependent on the drug of choice and on the preparation method. By spray drying, it was reported that more than 80 % of a drug was encapsulated into the CS particles, and other studies have shown encapsulation efficiency of approximately 100 % depending on the acid and excipients used [67,73,77]. The drug loading efficiency was also found to be highly variable depending on the solvents and settings of the spray drier and was, in one study, varying from 7 and up to 40 % w/w with ciprofloxacin as the chosen antibiotic [67]. Unfortunately, most studies of CS particulates for biofilm treatment do not report their antimicrobial loading efficiency (see Table 2), an essential factor when wanting to evaluate the usability of the particles in a clinical setting.

Release from CS particles was shown to be biphasic, when tobramycin was released from dextran sulfate NPs coated with CS. 15 % tobramycin was released within the first h, followed by a sustained release of 25 % in 60 h [19]. Similarly, ciprofloxacin from CS-DNase I was released in a biphasic fashion with first a burst release of 44 % within 3 h, followed by a sustained release for the next 21 h with a total release of 92 % [20]. In some cases, the drug release from CS particles was limited and very slow as an example from Kucukoglu *et al.* where an average release of 0.50 % of ciprofloxacin was observed within 24 h and the release was 0.54 % within the measurement period of 72 h [75]. In other reports, *in vitro* release of ciprofloxacin from CS particles was found to be improved compared to the dissolution of the pure drug. This can be explained by the poor solubility of the drug, and it was also found that ciprofloxacin was partly in its amorphous form, when encapsulated into CS particles, contributing to a better dissolution [67].

### **3.2. Molecular weight and degree of deacetylation**

Previously, it has been found that the molecular weight of CS has a great impact on the antibacterial effect of the polymer. For molecular weights between  $5.5 \times 10^4$  to  $15.5 \times 10^4$  Da, it was shown that the low molecular weight had a significant higher antibacterial activity compared to the higher ones against *E. coli* [79]. Liu *et al.* describe that the antibacterial activity of CS is dependent on the concentration of the  $-NH_2$  groups on CS until the molecular weight of  $9.2 \times 10^4$  Da. Above this molecular weight, it seems that the amino groups are too many and instead it provides a cross-linked structure through intramolecular hydrogen bonds and then the antibacterial activity decrease [80]. The antimicrobial efficacy of CS is generally stronger against Gram-positive bacteria than against Gram-negative ones [81]. NPs prepared from high molecular weight CS (500-550 kDa) showed a lower antimicrobial effect (20 to 25% killing) towards biofilms of *Streptococcus mutans* biofilms (Figure 3A), but with low molecular weight (20-150 kDa), the CS particles had a very high effect with almost all the bacterial cells damaged [82].

Besides the molecular weight, degree of deacetylation (DD) and degree of substitution (DS) on the amino groups are important factors for the antimicrobial activity as they are contributing to the positive charge density of CS and thereby, the degree of electrostatic interactions [64]. In a study by Kong *et al.*, they observed that when changing the DD from 83.7 to 63.6 %, the antibacterial effect of the CS formulation increased. This is due to the fact that with a low DD there are more acetyl groups presented in CS thereby,

resulting in a stronger hydrophobic effect between the polymer and the surface of the bacterial cell. Therefore, it was concluded that hydrophobic effects play an essential role in antibacterial activity of CS particulates [83].

### 3.3. Antimicrobial activity on bacteria and biofilm

There are many studies in the literature concerning CS particles encapsulating antimicrobials for destroying and eradicating bacterial biofilms [14]. CS particles with or without encapsulated drug are effective against a variety of bacterial strains such as *E. coli*, *P. aeruginosa* and *S. aureus* [75].

Kawakita *et al.* compared a CS dispersion with CS MPs [84]. On planktonic *S. mutans* bacteria, the dispersion performed more efficiently. On mature biofilms, the MPs improved diffusion through the biofilm due to its size, high zeta potential and spherical shape and could then distribute all the way through the biofilm. The dispersion interacted with the cell wall but did not have the possibility to reach all the way through the biofilm. The MPs also had better availability of the protonated amino groups and therefore, had a high antibacterial activity [84].

In a study, investigating the antibacterial activity on six strains of *P. aeruginosa*, it was found that on planktonic bacteria and on mature biofilm, the CS solution was very efficient and there was a large or complete reduction on all six strains [69]. The particles (in a size from 249-342 nm) were not as effective as the solution on planktonic bacteria and on the biofilm. This can be explained by the fact that the particles are partially neutralized by the cross-linker (tripolyphosphate) used for when preparing the particles. Thereby, the activity is not as strong as the CS in solution which still has many positively charged functional groups [69]. Another plausible reason is that the solution easier permeates the EPS matrix of the biofilm resulting in a better antimicrobial effect, compared to the particles which diffuse slowly [69]. Even though, it was concluded that the CS solution was much more efficient than the particles, it is important also to notice that the effect was not the same on all six strains and some strains were more resistant than others. The authors speculate that this can be due to that some clinically important strains of *P. aeruginosa* enzymatically break down CS and thus, the activity will not be as strong on those strains [69].

Blank CS particles have an antibacterial activity and the effect get more pronounced when having an addition of an antibiotic and the effect is similar on various types of bacteria [67]. This was very pronounced in a study presented by Andrade *et al.*, where an analog to nifuroxazide, N'-((5-nitrofuranyl)methylene)-2-benzhydrazide was developed. When encapsulated in CS particles, the drug had an increased effect (up to 3 times) compared to the pure drug or empty CS particles against three strains of *S. aureus* when measured the MIC values [76]. In a study by Ngan *et al.*, amoxicillin was loaded into CS NPs and the antibiotic and CS solutions, in various concentrations, were used as controls. Here, it was found that CS NPs without amoxicillin had a strong effect on inhibiting growth of the bacteria, *S. aureus*. As expected, this effect was stronger when having a complex of amoxicillin and CS NPs and the MIC value decreased to 10 µg/mL compared to 60 µg/mL for the antibiotic solution. This effect is explained by that

the complexes can enter the cells and here release amoxicillin, thereby inhibiting the bacteria [77].

For achieving an antimicrobial effect that can last for a long time to be as efficient as possible and to potentially reduce the needed amount of doses in a clinical setting, Patel *et al.* found that the antimicrobial activity was up to 48 h for CS NPs encapsulated with ciprofloxacin. There was no sign of growth in a *P. aeruginosa* biofilm within this time frame, whereas for ciprofloxacin in solution considerable growth was observed after 48 h [20]. This can be explained by the fact that the NPs could easily penetrate into the biofilm and have a higher adhesion to the bacterial cells compared to an antibiotic solution. Furthermore, the controlled and sustained drug release also had a high impact on the longer duration of the effect [20].

Many previous studies also report on the effect of the particles in various different setups for bacterial or biofilm growth. Jamil *et al.* saw that in a broth assay, the effect of CS NPs, with cefazolin encapsulated, was highest at the lowest drug concentration (200 µg/mL). This was not found in agar well diffusion studies, where the zone of inhibition was enlarged with increasing cefazolin concentration (up to 2000 µg/mL). This difference, in the two assays, was most likely observed because the drug permeation was inhibited in the agar gel network [73]. Chronopoulou *et al.* took a different approach compared to standard CS particles and produced particles of dextran sulfate containing the antibiotic tobramycin and then coated with CS to utilize the cationic properties of CS in this way. It was found that the development of *P. aeruginosa* biofilms were not affected with the complexes of dextran sulfate and CS without the antibiotic. When using the complexes with tobramycin and in the same concentration as the effective dose of free tobramycin, a 90 % reduction in biomass of the biofilm was observed. Thus, the effect was much better than for the free tobramycin [19].

It can be essential to evaluate how the interaction is between the particles and bacteria. By a Transmission electron microscopy (TEM) evaluation performed by Kucukoglu *et al.*, it was found that ciprofloxacin-loaded CS NPs were internalized by the bacteria. The average size of these particles were 721 nm, but only the fraction of the particles being smaller than 200 nm were internalized by the bacteria. For most of the *E. coli* cells, the cell wall and membrane were ribbed and for *S. aureus* most of the cells were lysed or fragmented [75].

### **3.4. Combinational strategies**

There has been much research on chemical modification of CS or combining CS with other molecules for improved antibacterial effects. Alginate has frequently been combined with CS through crosslinking using the crosslinking agent, CaCl<sub>2</sub>.

Combining CS together with alginate in particulates resulted in an effective antibacterial effect, where in a simple agar diffusion assay, 20 µg of the MP inhibited the growth of the bacteria of *S. aureus*, *Enterococcus faecalis*, *P. aeruginosa*, and *Proteus vulgaris* with inhibition zones of 12, 9, 6, 3 mm, respectively [85]. The particles were evaluated for their ability to reduce biofilm formation. Light microscopy revealed that the biofilm was disrupted after 24 h with the use of 40 µg particles. The same



trend in reduction was observed for four different biofilms consisting of clinical strains of *S. aureus*, *E. faecalis*, *P. aeruginosa*, and *P. vulgaris* [85]. Therefore, it was concluded by the authors that the combination of alginate and CS are effective against biofilm formation and could be a good choice of polymer materials for particles against biofilm.

The effect of CS/alginate NPs encapsulated with tobramycin was also studied *in vivo* utilizing a *Galleria mellonella* model (a step towards a PA01, *P. aeruginosa* infection). The percentage of survival showed that there was a similar therapeutic effect of the free tobramycin and when encapsulated in the particles. When pre-treating with tobramycin, 96 h before inoculation of *P. aeruginosa*, survival rates increased to 80 % for the NPs and 40 % for the free tobramycin, showing that the NPs were much more effective when used as prophylactic [22]. The CS/alginate particulates were further engineered with DNase I, with the aim of overcoming the mucus barrier in the lungs, by reducing mucus viscoelasticity by DNA cleavage [86], thus being able to deliver tobramycin, in a more deficient way [22]. With the addition of DNase I, it was possible to degrade DNA in the clinical isolates in CF sputum. Furthermore, it was found that the NPs were easier transported across the sputum layer when DNase I was conjugated to the particles [22]. Also, they assessed the antimicrobial efficacy of the particulates against *P. aeruginosa* using viable counting and found that the DNase I conjugated tobramycin NPs were either equally effective or superior to the free tobramycin (Figure 3B). Simple CS NPs loaded with ciprofloxacin were also functionalized with DNase I in a study by Patel *et al.* [20]. The functionalized particulates killed the *P. aeruginosa* biofilm-associated cells more efficiently than ciprofloxacin in solution. The particles without DNase I were as effective on the biofilm, but when functionalized with DNase I, ciprofloxacin was delivered deeper inside the biofilm [20]. This will be a great advantage for a thick biofilm which can often be found in the clinic. Therefore, the authors concluded that the functionalization with DNase I on CS NPs can be a safe and efficient approach to treat a *P. aeruginosa* biofilm infection in CF [20].

Alginate plays a major role in mucoid *P. aeruginosa* biofilm as it for example has great impact on cell adhesion, cell to biofilm connectivity and biofilm progression. Furthermore, it forms a three-dimensional structure making it difficult for antibiotic to penetrate and thereby, eradicate the biofilm. Therefore, it has been shown to be effective to functionalize CS NPs with alginate lyase as this enzyme can break down some of the structures within the biofilm [21]. For example, alginate lyase was bound covalently on the surface of CS particles and these particles reduced the biomass four times compared to an untreated biofilm. For the particles without the enzyme, the biomass was 1.5 times lower than the untreated biofilm [21]. This improved effect was explained by the authors to be due to the ability of alginate lyase to disrupt the EPS matrix of the biofilm. This is an effective approach for particles to penetrate into biofilm-associated infections with *P. aeruginosa*.

CS particulates have also been combined with other well-known polymers such as PLGA. Functionalization of clarithromycin (CAM)- or tobramycin-loaded PLGA NPs with CS was evaluated against *Staphylococcus epidermidis* or *P. aeruginosa*, respectively [53,87]. The presence of CS increased the NP size and resulted in a positive surface charge, in contrast to the negative surface charge of the PLGA NP. Live/dead staining of the biofilm revealed 38 % viable bacteria after treatment with CS-CAM-PLGA-NPs, in contrast to CAM-

PLGA-NPs, PLGA NPs and free CAM, where 47 %, 69.8 % and 63.4 % of the bacteria survived, respectively, proving the beneficial effect of combining PLGA and CS in NPs [53].

For improving the antimicrobial efficacy of CS, it has been suggested to combine it with silver, zinc oxide or both of these metals. Silver has shown to have a very broad spectrum of activity against microorganisms [88], and zinc oxide has been studied for its antibacterial properties [89]. Thaya *et al.* produced complexes of CS, silver and zinc oxide and observed that with zinc oxide the particles went from a rough surface to rod-shaped particles [90]. The particulate complexes of CS, silver and zinc oxide provided an antibacterial effect in terms of MIC values against a variety of bacteria such as Gram-positive bacteria (*Bacillus licheniformis* and *B. cereus*) and Gram-negative bacteria (*Vibrio parahaemolyticus* and *P. vulgaris*) [90]. In addition, when investigating the effect of these complexes on biofilm, the EPS production was significantly reduced to 40-86 % compared to the control group with the effect being largest for the Gram-positive bacteria [90].

Liposomes have often been reported in the literature as vehicles for antibiotics and with good effect, but stability can often be an issue [91]. Therefore, Qiu *et al.* decided to investigate the effect of a phosphatidylcholine-CS liposome NP loaded with gentamycin. Here, CS was the core of the particle, and then the lipid layer was surrounding this, followed by adsorption of gentamycin to the lipid surface [92]. Biofilms were formed by *Listeria monocytogenes* (Gram-positive) and *P. aeruginosa* (Gram-negative). Phosphatidylcholine-CS liposome NPs with adsorbed gentamycin reduced and inhibited the biofilms substantially compared to the antibiotic itself with or without chitosan (Figure 3C). The effect was the same even with the biofilms matured at different time points up to 48 h and was observed to be almost as effective on both Gram-positive and Gram-negative biofilms [92].

As can be seen above, CS particles have a strong effect on biofilms of various bacterial strains. There are still challenges with inter-laboratory reproducibility and also obstacles in completely understanding the physicochemical principles explaining the formation of the particles. This has delayed the introduction of CS particles to the market in their function as antimicrobials [93].

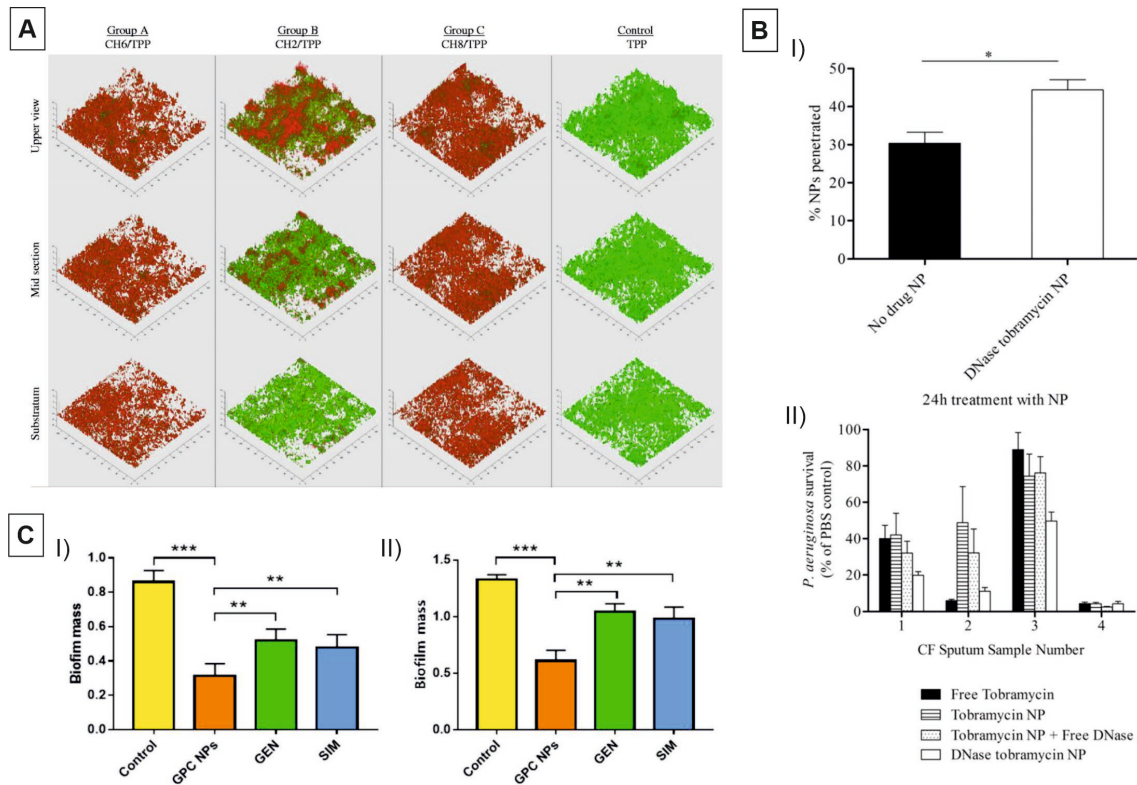


**Figure 3.** (A) Antimicrobial effect of different chitosan-tripolyphosphate complexes in *S. mutans* biofilms. 3D biofilm reconstructions show results with the live/dead stain (green: viable cells, and red: damaged cells) at different depths of the biofilms. Group A: High degree of deacetylation (DD), low molecular weight (Mw), Group B: High DD, High Mw, Group C: Low DD, low Mw. Reprinted and adapted from [82] with permission from American Society for Microbiology (Copyright© 2011). (B) Tobramycin-loaded alginate/CS NPs functionalized with DNase for DNA degradation improve NP penetrations through CF sputum. Tagging the NPs with rhodamine enabled tracking of the penetration, which revealed that DNase-functionalized NPs had improved penetration properties (I). The antimicrobial efficacy against *P. aeruginosa* in sputum samples was assessed using viable counting and the DNase I conjugated tobramycin NPs were either equally effective or superior to the free tobramycin (II). Reprinted and adapted from [22] with permission from Elsevier (Copyright© 2015). (C) *L. monocytogenes* (I) and *P. aeruginosa* (II) biofilms were exposed to gentamycin-loaded phosphatidylcholine-CS NPs (GPC NPs) loaded with gentamycin, equal amount of gentamycin (GEN), or the simple mixture of gentamycin and CS (SIM) for 24 h. Biofilm mass was determined using crystal violet assay. Scale bars: 50  $\mu$ m. Reprinted and adapted from [92] with permission from Elsevier (Copyright© 2020).

## 4. POLYCAPROLACTONE (PCL)-BASED DRUG DELIVERY SYSTEMS

PCL is a hydrophobic aliphatic polyester-based polymer, and is mostly used in combination with other polymers to create a particulated system. Furthermore, PCL is biodegradable, biocompatible and a FDA-approved polymer [24,65,94]. The degradation of PCL is slower than for example PLGA which means that PCL is suitable for formulations intended for long-term drug delivery. Moreover, it also has the ability to provide a sustained drug release [65,94]. PCL particles are negatively charged and the interaction between these particles and bacteria are due to hydrogen binding [15]. An overview of reported use of PCL particles for encapsulating antibiotics to eradicate biofilms can be found in Table 3.

### 4.1. Production and characterization of PCL formulations

The preparation of PCL particles has been done using multiple techniques such as emulsion solvent evaporation, diffusion solvent evaporation, spray drying and hot-melting [15,95,96]. Also more straightforward methods such as simple suspension has been applied [94].

Drug release from PCL particulates occur by erosion from the matrix and by diffusion of drug through the polymer matrix. It can be a challenge to encapsulate hydrophilic drugs inside the hydrophobic NP shell as there is a low affinity between the drug and the polymer [97]. It has been exemplified by Kho *et al.*, where the encapsulation efficiency of levofloxacin, was only 5–10 % resulting in a drug loading of 0.4 % w/w [94]. The release of levofloxacin from the PCL particles was 90 % within 3 h. This shows, that most likely, the drug was adsorbed to the surface of the particles instead of being encapsulated [94]. On the other hand, Ferreira *et al.* observed a drug loading of 13-19 % of either the antibiotics daptomycin or vancomycin, where the encapsulation efficiencies were found to be up 83 % [15]. Here, the release was much lower than observed by Kho *et al.* as the release was a maximum of 10 % over 72 h.

PCL particles can further be modified to obtain a better antimicrobial effect. A complex particulate system, presented in the literature, is linear polymer-dendrimer hybrids which have been made of for example poly ester amine dendrimer (PEA) as the dendrimer core and methoxypoly(ethylene glycol)-b-poly ( $\epsilon$ -caprolactone) (mPEG-b-PCL) linear block polymer as the shell. Here, PCL has the properties of being hydrophobic and thereby, providing higher stability, increased mechanical strength of the vesicle membrane and improved drug loading capacity compared to if PEG was the only compound in the shell [98].

### 4.2. Antimicrobial activity on bacteria and biofilm

PCL NPs encapsulated with a combination of imipenem/cilastatin were shown to have better antibacterial effect compared to PLGA encapsulated with the same compounds or to the free drugs. This effect could be due to the smaller size (132 nm) of the PCL particles compared to the PLGA NPs with a size of 348 nm [95]. In contrast, in a comparative study with PLGA and PCL either encapsulating levofloxacin or ciprofloxacin, it was found that the PLGA encapsulating ciprofloxacin was the most promising compared to the PCL. The main difference was the amount of drug which could be encapsulated into the particles.

Moreover, the drug release was also faster from the PLGA matrix compared to the PCL which resulted in a better antibacterial effect as it gave a higher local drug concentration [27].

For PCL MPs encapsulating either daptomycin or vancomycin, a large difference was observed between the use of the two antibiotics (Figure 4A). For the formulation with vancomycin, no or very little effect was observed both in the antibacterial effect and with the interaction with the biofilm. For the daptomycin formulation in a Methicillin-resistant *S. aureus* (MRSA) biofilm, it was observed that the biofilm after incubation with the particles was reduced to single bacteria. For an *S. epidermidis* biofilm, then it seemed more tolerant and it was not possible to eradicate the biofilm, but some disruption was visualized [15].

Also, PLGA and PCL have previously been combined to deliver doxycycline to *E. coli* biofilms. It was found that the doxycycline-loaded PLGA:PCL NPs decreased MIC and the minimal bactericidal concentration (MBC) as compared to free doxycycline. Furthermore, the NP-encapsulated doxycycline prevented growth of *E. coli* for five days, whereas the same concentration of free doxycycline regrowth occurred already after the second day, an effect probably caused by the protective effect and controlled release from the PLGA:PCL NPs [99].

Linear polymer-dendrimer hybrids with PEA and mPEG-b-PCL were shown to have a 7- and 16-fold decrease in MIC compared to the controls against the two bacteria *S. aureus* and MRSA and the effect was shown to last for up to 120 h compared to the controls, where there was no effect after 24 h [98]. The size of the particles was only approximately 50 nm and the authors emphasize that the smaller the particle, the higher surface area to volume ratio is obtained resulting in a better distribution and adsorption to the surface of the bacteria [98]. The hybrids were further tested on MRSA biofilms and by fluorescence microscopy, and it was observed that the hybrids caused a great reduction in biofilm biomass compared to the controls due to a destruction of the biofilm and the cell membranes of MRSA (Figure 4B). In addition, vancomycin was encapsulated into the hybrids and were then investigated *in vivo* on a mouse skin infection model, and here, the hybrids had a 103-fold reduction of bacteria compared to the untreated mouse group [98]. Lipid-core nanocapsules (LCN), which are composed of a lipid core, covered by a polymeric shell of PCL, have been proposed to overcome the biological barrier of mucus [100]. Ciprofloxacin-loaded LCN (approximately a size of 180 nm) showed a 50 % increase in drug permeation through mucus. Interestingly, formation of biofilm-like aggregates of *S. aureus* were observed when treating with free ciprofloxacin, and these were avoided when treating with LCN (Figure 4C) [100].

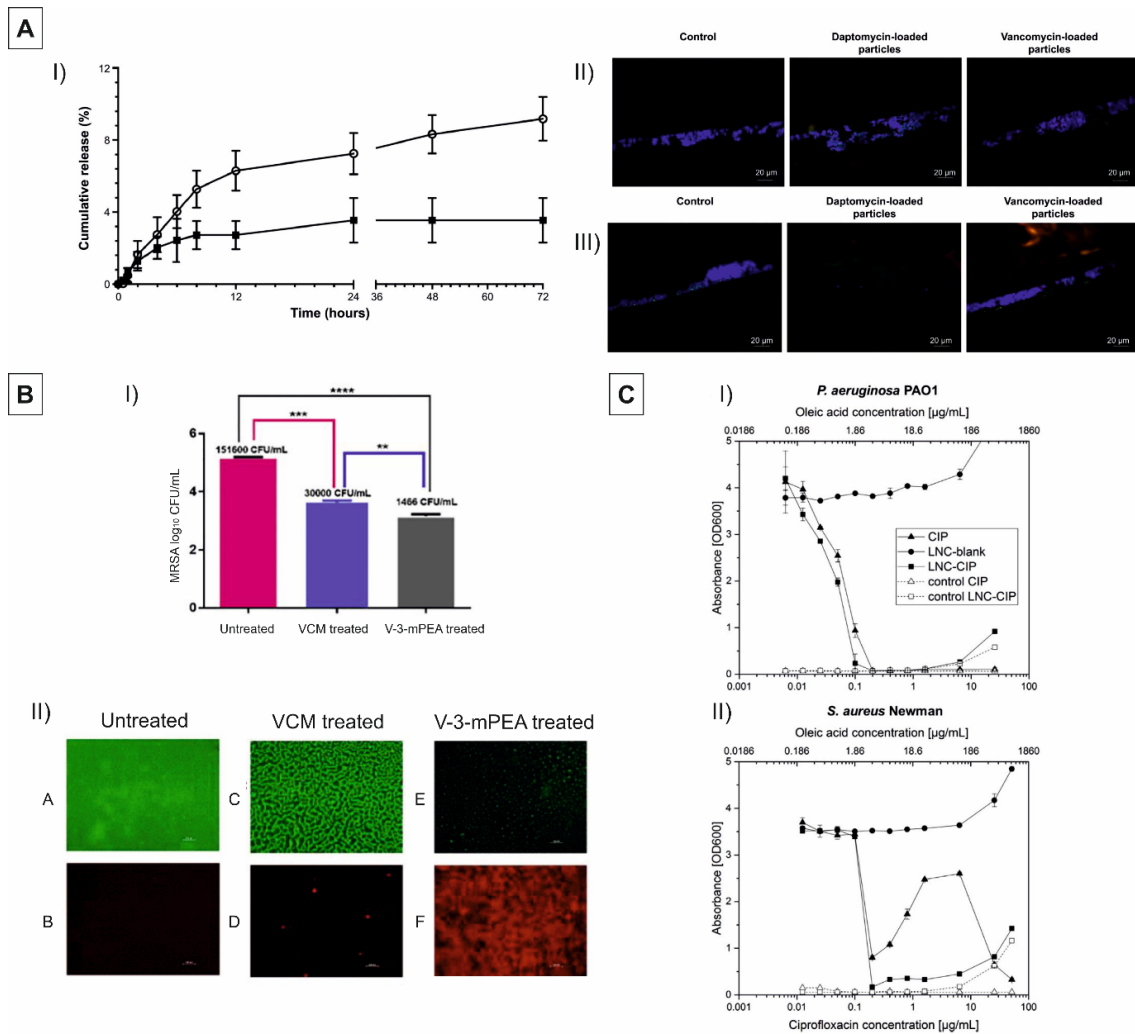


**Figure 4.** (A) Cumulative release (%) of daptomycin (circle) and vancomycin (square) from PCL MPs. Results are presented as mean±SD (n=3) (I). Fluorescence *in situ* hybridization (FISH) of *S. epidermidis* (II) and methicillin-resistant *S. aureus* (MRSA) (III) biofilms after 24 h incubation with daptomycin- and vancomycin-loaded PCL MPs. Magnification: 400x. Reprinted and adapted from [101] with permission from Dove Medical Press (Copyright© 2015). (B) Evaluation of the antibacterial effect of bare vancomycin (VCM), blank and vancomycin loaded 3-mPEA NPs (V-3-mPEA) against MRSA. mPEA= a linear polymer dendrimer hybrid star polymer comprising of a generation one poly (ester-amine) dendrimer (G1-PEA) and a diblock copolymer of methoxy poly (ethylene glycol)-b-poly(ε-caprolactone) (mPEG-b-PCL). Numbers are presented as mean±SD, n=3 (I). Fluorescence microscopy micrographs of the untreated, vancomycin treated and vancomycin-3-mPEA treated MRSA biofilms stained with Syto9 and propidium iodide. Scale bar: 100 μm (II). Reprinted and adapted from [98] with permission from Elsevier (Copyright© 2018). (C) Lipid-core nanocapsules (LCN) loaded with ciprofloxacin showed antimicrobial activity against the Gram-negative *Pseudomonas aeruginosa* (I) and Gram-positive *S. aureus* Newman (II). Values are expressed as mean±SD. Reprinted and adapted from [100] with permission from Elsevier (Copyright© 2017).

**Table 1.** Overview of poly(lactide-co-glycolic) acid (PLGA) nanoparticles (NPs) and microparticles (MPs) tested for drug delivery to biofilms.

Additional functionalization	Antimicrobial agents	Size	Charge (mV)	Antimicrobial load (% w/w)*	Preparation method	Biofilm	Antibacterial study type	Ref.
Poly-lysine (PL) DNase I	Ciprofloxacin	214 – 273 nm	Without PL/DNase: -12.9±11.2 With PL/DNase: 28.9 – 33.5	0.2-0.3	Nanoprecipitation	<i>P. aeruginosa</i> <i>S. aureus</i>	MIC CFU of biofilms (PEG lids) Confocal monitoring in flow chambers	[23]
-	Ciprofloxacin or levofloxacin	170 – 240 nm	N/A	0.5-2.3	Emulsion solvent evaporation	<i>E. coli</i>	MIC MBIC Dose-kill monitoring 5-day time-kill study	[24]
-	Levofloxacin	80 – 190 nm	N/A	0.7-1.1	Nanoprecipitation and emulsion solvent evaporation	<i>E. coli</i>	MIC MBIC Dose-kill monitoring 5-day time-kill study	[27]
-	Ciprofloxacin	0.3 µm 12 µm	NP: -4.1 MP: -4.5	NP: 4.3 MP: 7.5	Emulsion solvent evaporation	<i>P. aeruginosa</i> <i>S. aureus</i>	MIC MBEC 6-day time-kill study	[28]
Chitosan	Antimicrobial decapeptide (KSL-W)	6.8 – 80 µm	N/A	1.8-7.2	Electrospraying and combined crosslinking-emulsion method	<i>F. nucleatum</i>	Disc diffusion assay	[34]
PEG	Tobramycin	225 – 902 nm	-36.3 – (-9.6)	0.1-0.2	Emulsion solvent diffusion	<i>P. aeruginosa</i> <i>B. cepacia complex</i> (Bcc)	MIC MBEC Confocal monitoring in static and flow chambers	[38]
-	Ciprofloxacin	237 nm	-21.0±4.3	13.3	Nanoprecipitation	<i>P. aeruginosa</i>	Agar well diffusion	[39]
Phosphatidylcholine	Carvacrol	210 nm	-19.0±3.0	21.0	Solvent displacement	<i>S. epidermidis</i>	Rheological characterization of biofilm	[42]
-	Nitric oxide precursor	172 – 556 nm 2.8 – 9.8 µm	N/A	NP: 0.1-0.5 MP: 0.8-2.3	Emulsion solvent evaporation	<i>S. aureus</i>	MIC MBEC Alamar blue	[43]

Poloxamer-188 Alginate (Alg) PEG Chitosan (CS) Poly(vinyl alcohol) (PVA)	Tobramycin	200 – 1000 nm 11 – 12 µm	All except with CS: App. -36 – 0 With CS: App. 18 – 70	0.8-2.0	Emulsion solvent diffusion followed by spray drying	<i>P. aeruginosa</i>	MIC	[44]
-	Gentamycin	241 – 359 nm	-0.4 – 2.3	0.6-2.2	Emulsion solvent evaporation	<i>P. aeruginosa</i>	MIC MBC MBEC Peritoneal murine infection model	[48]
Chitosan Polyvinyl alcohol (PVA)	Colistin	267 – 330 nm 6.4 – 14.4 µm	CS: 12.4±2.1 PVA: -7.1±1.4	1.3	Emulsion solvent diffusion followed by spray drying	<i>P. aeruginosa</i>	Crystal violet assay	[51]
Acetylcysteine and curcumin	Tobramycin, ciprofloxacin or azithromycin	105 nm 2.2 – 2.6 µm	NP: -9.1±4.6	N/A	Nanoprecipitation followed by spray drying	<i>P. aeruginosa</i>	Dose-kill monitoring	[52]
Pluronic F68	Amikacin	340 – 447 nm	-42.9 – (-29.8)	2.6	Emulsion	<i>P. aeruginosa</i>	MIC MBC MBEC	[54]
PEG	Gentamycin	140 – 919 nm	-5.5 – 0.4	2.9-7.9	Extraction	<i>P. mirabilis</i> <i>E. coli</i> <i>P. aeruginosa</i> <i>S. aureus</i>	MIB MBC	[56]
D-a-tocopherol polyethylene glycol 1000 succinate (TPGS)	Azithromycin	71 – 98 nm	-49.2 – (-26.8)	2.5-5.5	Microfluidic chip	<i>P. aeruginosa</i>	Confocal monitoring in flow chambers	[57]
D-a-tocopherol polyethylene glycol 1000 succinate (TPGS)	Azithromycin	92 – 93 nm	-28 – (-27)	N/A	Microfluidic chip	<i>P. aeruginosa</i>	Confocal monitoring of penetration MIC Prevention of biofilm formation Eradication of pre-formed biofilms Virulence factor monitoring Bacterial motility	[58]
Pyruvate dehydrogenase	-	267 nm	-13.9 – (- 12.3)	0.5-0.8	Emulsion	<i>P. aeruginosa</i>	Confocal microscopy	[62]
-	Bacteriophages	8.0 µm	N/A	2.6×10 <sup>6</sup> p.f.u. mg <sup>-1</sup>	Emulsion	<i>P. aeruginosa</i>	OD growth monitoring in sputum Confocal microscopy <i>In vivo</i> model	[63]



Chitosan	Tobramycin	187 – 575 nm	PLGA: -2.8 CS-functionalized: 33.47 – 50.13	30.8-45.9	Solvent evaporation	<i>P. aeruginosa</i>	MIC MBEC	[87]
-	Imipenem and cilastatin	348 nm	15±0.6	17.2	Emulsion solvent evaporation	<i>K. pneumonia</i> (clinical isolates) <i>P. aeruginosa</i>	Agar well diffusion MIC Mutation prevention concentration Carbapenemase production by Modified Hodge Test (MHT) Time-kill monitoring	[95]
Magnetic particles	Ciprofloxacin	221 nm 1.5 µm	N/A	NP: 2.8 MP: 3.7	Emulsion solvent evaporation	<i>P. aeruginosa</i>	Agar well diffusion	[102]
Methylated β-cyclodextrin (βCD) Hydroxypropyl-β-cyclodextrin (HPβCD)	Chlorhexidine	26.7 – 45.1 µm	N/A	6.1-16.8	Emulsion solvent evaporation	<i>P. gingivalis</i>	Agar well diffusion	[103]
-	Gentamycin	App. 60 µm	N/A	2.5-13.4	Emulsion solvent evaporation	<i>S. aureus</i>	Agar well diffusion	[104]
Chitosan	Clarithromycin	251 – 357 nm	PLGA: -18.2±0.7 CS-functionalized: 17.4±1.2	N/A	Emulsion solvent diffusion	<i>S. epidermidis</i>	Biofilm adhesion MIC MBC Live/dead-monitoring in well plate	[105]
Chitosan	Clarithromycin	358 nm	24.2±0.6	N/A	Emulsion solvent diffusion	<i>S. epidermidis</i>	CFU counting Live/dead-monitoring in well plate FE-TEM imaging of biofilm	[106]

\* Antimicrobial loads are giving as % w/w unless otherwise stated and in certain cases it has been recalculated from a given µg drug per mg polymer

Abbreviations: N/A = non-available or non-applicable, CFU= colony forming units, EPS = extracellular polymeric substances, MIC = minimum inhibitory concentration, MBC = minimum bactericidal concentration, MBEC = minimum biofilm eradication concentration, MBIC = minimum biofilm inhibitory concentration, OD = optical density

**Table 2.** Overview of chitosan (CS) nanoparticles (NPs) and microparticles (MPs) tested for drug delivery to biofilms.

Additional functionalization	Antimicrobial agents	Size	Charge (mV)	Antimicrobial load (% w/w)*	Preparation method	Biofilm	Antibacterial study type	Ref.
Dextran sulfate (DS)	Tobramycin	170 – 1250 nm	DS: -4.9 – 2.4 CS-DS: App. 12-16	N/A	Ionic gelation	<i>P. aeruginosa</i> (PAO1 and PA-nonM)	MIC Crystal violet assay	[19]
DNase I	Ciprofloxacin	197 – 205 nm	14.6 – 15.3	N/A	Ionic gelation followed by freeze drying	<i>P. aeruginosa</i>	MIC MBC MBEC Confocal microscopy of fixed biofilms	[20]
Alginate lyase	Ciprofloxacin	191 – 206 nm	12.2 – 14.6	N/A	Ionotropic gelation followed by freeze drying	<i>P. aeruginosa</i>	MIC MBC MBEC Confocal microscopy of fixed biofilms	[21]
Alginate, DNase I	Tobramycin	505 – 538 nm	-28.0 – (-25.7)	4.1-9.2	Emulsion	<i>P. aeruginosa</i>	MIC <i>Galleria mellonella</i> in vivo model for <i>P. aeruginosa</i> infection	[22]
-	-	249 – 342 nm	14.0 – 15.0	N/A	Ionic gelation	<i>P. aeruginosa</i> (six different strains)	CFU monitoring of planktonic bacteria and biofilms SEM	[69]
-	Ciprofloxacin	712 – 721 nm	32.3 – 48.4	N/A	Ionic gelation	<i>E. coli</i> <i>P. aeruginosa</i> <i>S. aureus</i>	MIC MBC TEM	[75]
Polysorbate 20 micelles	Analog to nifuroxazide	320 – 523 nm	32.3 – 47.1	N/A	Ionic gelation followed by freeze drying	<i>S. aureus</i>	MIC	[76]
-	-	20 – 1000 nm	N/A	N/A	Ionic gelation	<i>S. mutans</i>	Confocal monitoring of biofilms in flow chambers	[82]
-	-	5.6 µm	58.7±3.7	N/A	Spray drying	<i>S. mutans</i>	MIC MBC 5-day in vitro antibiofilm model	[84]

Alginate	-	50 – 100 µm	N/A	N/A	Addition method	<i>S. aureus</i> <i>E. faecalis</i> <i>P. aeruginosa</i> <i>P. vulgaris</i>	Zone of inhibition Crystal violet visualization Confocal microscopy SEM	[85]
Ag/ZnO	-	100 – 200 nm	N/A	N/A	Ionic gelation	<i>B. licheniformis</i> <i>B. cereus</i> <i>V. parahaemolyticus</i> <i>P. vulgaris</i>	MIC Hydrophobicity assay (BATH) EPS production monitoring Crystal violet assay Confocal microscopy monitoring	[90]
Phosphatidylcholine	Gentamycin	76 – 137 nm	CS: App. 33 CS-PC: -26.7 – (-19.5)	N/A	Ionotropic gelation followed by freeze drying	<i>L. monocytogenes</i> <i>S. aureus</i> <i>E. coli</i> <i>P. aeruginosa</i>	MIC Crystal violet assay Fluorescence microscopy	[92]
N,O-octanoyl Leucine	Levofloxacin	137 – 490 nm 3.8 – 5.8 µm	CS/octanoyl: 1.7 – 4.0 Leucine: -11.4±0.6	N/A	Spray drying	<i>P. aeruginosa</i>	MIC	[107]
DNase	Oxacillin	158 – 167 nm	8.3 – 11.4	N/A	Ionic gelation	<i>S. aureus</i> (clinical isolates)	MIC Crystal violet assay Confocal microscopy	[108]

\* Antimicrobial loads are giving as % w/w unless otherwise stated and in certain cases it has been recalculated from a given µg drug per mg polymer

Abbreviations: N/A = non-available or non-applicable, CFU= colony forming units, EPS = extracellular polymeric substances, MIC = minimum inhibitory concentration, MBC = minimum bactericidal concentration, MBEC = minimum biofilm eradication concentration, SEM = Scanning electron microscopy, TEM = Transmission electron microscopy

**Table 3.** Overview of polycaprolactone (PCL) nanoparticles (NPs) and microparticles (MPs) tested for drug delivery to biofilms.

Additional functionalization	Antimicrobial agents	Size	Charge (mV)	Antimicrobial load (% w/w)*	Preparation method	Biofilm	Antibacterial study type	Ref.
-	Daptomycin and vancomycin	1.2 – 1.4 µm	-17.6 – (-15.9)	12.6-18.9	Emulsion solvent evaporation	<i>S. aureus</i> (MRSA) <i>S. epidermidis</i>	MIC MBC MHIC MBIC FISH	[15]
-	Ciprofloxacin or levofloxacin	170 – 230 nm	N/A	0.3-0.5	Emulsion solvent evaporation	<i>E. coli</i>	MIC MBIC Dose-kill monitoring 5-day time-kill study	[24]
-	Levofloxacin	110 – 230 nm	N/A	0.3-0.4	Nanoprecipitation and Emulsion solvent evaporation	<i>E. coli</i>	MIC MBIC Dose-kill monitoring 5-day time-kill study	[27]
Pluronic F-68 Mannitol Lactose Leucine	Levofloxacin	App. 270 nm 4.8 – 6.5 µm	N/A	0.4	Spray drying	<i>E. coli</i>	CFU monitoring	[94]
-	Imipenem and cilastatin	132 nm	17±1.6	17.7	Emulsion solvent evaporation	<i>K. pneumonia</i> (clinical isolates) <i>P. aeruginosa</i>	Agar well diffusion MIC Mutation prevention concentration Carbapenemase production by Modified Hodge Test (MHT) Time-kill monitoring	[95]
Poly ester amine dendrimer (PEA) Methoxypoly(ethylene glycol)-b-poly (ε-caprolactone) (mPEG-b-PCL) linear block polymer	Vancomycin	52 – 59 nm	-7.3±1.3	19.1	Solvent evaporation	<i>S. aureus</i> (SA and MRSA)	MIC TEM Fluorescence microscopy Flow cytometry CFU monitoring <i>In vivo</i> mouse model	[98]
Sorbitan monostearate	Ciprofloxacin	182 nm	-21.3±2.6	1.85	Interfacial deposition of polymer	<i>S. aureus</i> <i>P. aeruginosa</i>	CFU monitoring	[100]

\* Antimicrobial loads are given as % w/w unless otherwise stated and in certain cases it has been recalculated from a given µg drug per mg polymer

Abbreviations: N/A = non-available or non-applicable, CFU= colony forming units, FISH = Fluorescence in situ hybridization, MIC = minimum inhibitory concentration, MBC = minimum bactericidal concentration, MBIC = minimum biofilm eradication concentration, MBIC = minimum biofilm inhibitory concentration, MHIC = Minimal heat inhibitory concentration, TEM = Transmission electron microscopy

## 5. DISCUSSION AND FUTURE OUTLOOK

Since the development of new antibiotics has been stalled for many years, the research within NP- and MP-systems for encapsulation of antibiotics has grown tremendously. The essential key for solving the enigma of fighting bacterial infections and biofilms is still unsolved, and a solution is urgently needed. One of the key elements of antibiotic resistance, besides genetic mutations, is believed to be the mode of growth in biofilms. Biofilms are capable of evading the host immune defense and show an increased tolerance towards antibiotics. There are many promising particle-based strategies towards combating biofilms, but none of the polymeric particulates have succeeded to reach the clinic just yet. The reason could be that the local concentration of the antibiotics in the biofilm is not sufficiently high or long-lasting and strategies to deliver and preserve the activity of existing antibiotics are needed.

A promising approach for eradicating biofilms and bacterial infections is to provide a long retention of sustain release particles. This has been investigated, as an example, for *Helicobacter pylori* treatment in the stomach. Here, CS MPs were prepared and loaded with tetracycline for the purpose of increasing the local drug concentration in the stomach [109]. Unfortunately, in the following study it was seen that the CS MPs did not have a gastric retention when investigating *in vivo* in gerbils. After 2 h, only approximately 10 % of the CS particles with tetracycline were still found in the stomach and the residence time did not seem to be increased compared to controls, and after 6 h post oral dosing the MPs were mainly found in the colon [110]. For Hejazi *et al.* to improve the gastric residence time and thereby, the local delivery of tetracycline, the CS MPs were cross-linked with glyoxal and then tested *in vivo* in gerbils. After 2 h from the oral dosing, 17 % of the cross-linked particles were found in the stomach compared to 10 % of non-cross-linked MPs, however after 6 h, all the CS particles (both cross-linked and non-cross-linked) were in the colon. Hence, the cross-linking improved the retention of the particles in the stomach [111], but the effect should ideally be more pronounced.

### 5.1. Antimicrobial delivery by the use of device-like structures

Yazdi *et al.* have fabricated porous silicon-based MPs and were thereby able to control the release of cefazolin. A high dose of up to 452 µg of cefazolin was loaded into 10<sup>7</sup> mesoporous MPs depending on the porosity, pore size and pore volume of the silicon. All the silicon MPs had, independent of their pore size, a mean size of 3.2 µm [112]. The drug release was tuned depending on the pore size of the material hence, the smaller the pore size the slower the drug release, probably due to limitations of drug diffusion through the small pores (down to 3 nm). At day 5, a complete drug release was obtained and by then the silicon-based material also seemed to be degraded. This sustained drug release resulted in a long-term eradication and prevention of *S. aureus* [112].

One strategy also based on micro- and nanotechnology is the use of microfabricated devices [113,114]. Such devices are *e.g.* shaped as microcontainers. These are cylindrical in shape and only have one side open, providing unidirectional release. They are about 250 µm in diameter and in height, and can

therefore have a much higher drug load (of approximately 4 µg per container) compared to NP and MPs. After loading the microcontainers with ciprofloxacin, they were coated with a lid of either PEG, CS or Eudragit® S100 [115]. One of the features of the microcontainers is that they are known to be engulfed by the mucus layer [116,117] and therefore, they can have great potential in eradicating biofilms [115]. When applying the ciprofloxacin-loaded microcontainers to a PAO1 biofilm, up to 88 % of the biomass close to the opening of the microcontainer was killed, whereas only 26 % of the bacterial cells were killed by a bolus dose of the antibiotic [115]. Furthermore, CS was shown to be the most promising polymer for the lid of the microcontainers. This could be due to the antimicrobial properties of CS but also due to the fact that ciprofloxacin was released in a sustained fashion through the CS lid [115]. This further led to another study where biofilms were grown in mucus and the CS-coated microcontainers, again loaded with ciprofloxacin resulted in 73 % killed biomass, however, interestingly, if the mucolytic agent, N-acetylcysteine, was incorporated into the CS lid coating, killing was improved (88 %) [118].

Giovanni Traverso and co-authors have several publications on different devices providing long gastric retention [119]. These devices are typically in the cm size regime and are as such not a particulated system. However, they show an interesting alternative towards localized delivery. One of such devices is a drug depot system intended for long residence time in the stomach and prolonged drug release. This device was delivered through the nasogastric route and could release high doses of antibiotics over a period of several weeks when tested *in vivo* in pigs [120]. Another type of device, this one for oral administration, was an ultra-long-acting capsule which dissolved in the stomach and then developed into a star-shaped system that could not pass to the intestine due to its size and shape. The device released small molecules in the stomach, for up to weeks, and after releasing, the device was degraded and could then pass through the gastro-intestinal tract [121]. Later, a similar device was developed from the same group. Here, the device had a central core of Elastollan® 1185 from which six arms were pointing out. The arms were made in either PLA or Elastollan® R6000. This delivery system could fold and recoil when reaching the stomach after oral dosing and can contain one drug dose in each arm. Again, this delivery system had a long residence time in the stomach for then to disintegrate whereby the remaining device pieces travelled through the gastro-intestinal tract [122]. Further investigations of the effect on similar devices on gastric biofilms could be of great interest.

## **5.2. Advanced particulated systems for antimicrobial delivery**

Previously, N-acetylcysteine or cysteamine have been incorporated into NEMs, each compound having a specific action in the improvement of pulmonary function in CF patients [123]. The NEMs consisted of a nano-sized polyanion tobramycin complex (PTC) encapsulated in PVA MPs. The NEMs properties were compared to TOBIPodhaler (Novartis), the only commercially available dry powder inhalatory formulation based on porous MPs. Here, an increased drug diffusion through a mucus section was observed while showing a sustained tobramycin release. Moreover, the cysteamine NEMs showed a pronounced antimicrobial activity against *P. aeruginosa* biofilms compared to TOBIPodhaler and free tobramycin [123].

In the literature, there has been promising results on incorporating enzymes such as alcalase into a particulated system also containing antibiotic (Figure 5). Weldrick *et al.* showed great reduction in biofilm mass by incorporating alcalase into a carbopol nanogel. For biofilms composed of *S. aureus*, *P. aeruginosa*, *S. epidermidis*, *E. coli*, and *E. faecalis*, the carbopol-alcalase combination caused over 50 % decrease in the biomass compared to when treating only with alcalase. [124]. Moreover, co-treatment with ciprofloxacin in alcalase-coated carbopol nanogels led to a 3 log<sub>10</sub> reduction in viable biofilm-forming cells when compared to ciprofloxacin treatment alone. Adding alcalase to a formulation can be a good choice as it can degrade alginate and thereby, disrupt the EPS matrix of the bacterial biofilm and thus, reduce mucus viscoelasticity and decrease the biomass of the biofilm [124–127].

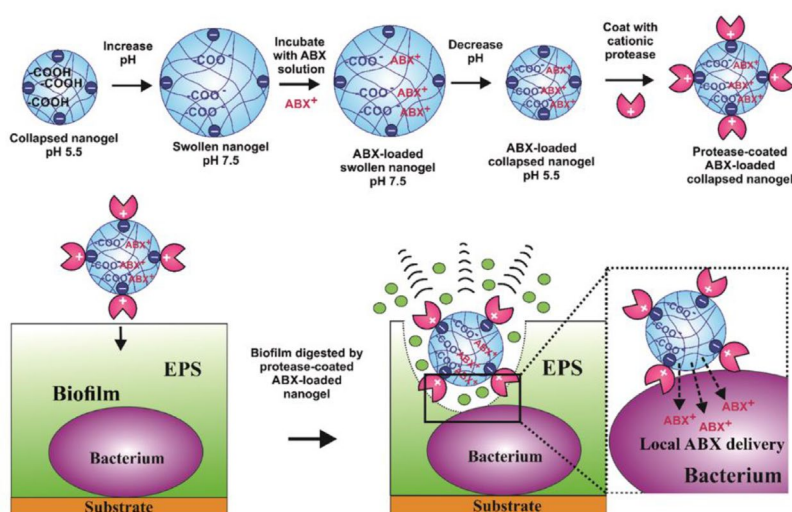


**Figure 5.** Exploiting enzymatic degradation of the biofilm with alcalase loaded nanogel particles. The enzyme alcalase acts as hydrolases, cleaving peptide chains of the extracellular polymeric substances (EPS) matrix, and as an esterase, enabling it to catalyze hydrolysis of some esters including carboxylic esters and amino esters. Carbopol Aqua SF1 nanogels were loaded with ciprofloxacin (ABX+) followed by surface coating with protease (Alcalase 2.4 L FG). Reprinted with permission from [124]. Copyright© 2019, American Chemical Society.

### 5.3. Targeted and/or triggered antimicrobial delivery

Functionalizing the polymeric particulates with targeting ligands can be utilized in obtaining targeted delivery. This may provide additional particle accumulation at the site of the biofilm-embedded bacteria and promote contact between the carrier and the bacteria. The targeting can either be non-specific relying on charge-based or hydrogen-bonding interactions, or specific, in which targeting ligands selectively bind to a target molecule within the biofilm *i.e.* bacterial cell membrane or components of the EPS matrix. Targeting of lipid-based drug delivery systems has been reviewed previously [91], and investigations of specific targeting using drug-loaded polymeric particles remain in their infancy. Recently, polymeric NPs were covered with multiple copies of the galactose-binding lectin LecA (PA-IL), a ligand that has a prominent role in the bacterial virulence of *P. aeruginosa* [128]. The surface-coated NPs bind to *P. aeruginosa* lectin (LecA) with a high potency, inhibiting biofilm formation. Unlike dendrimeric or small molecule inhibitors of LecA, a drug can potentially be encapsulated within their lipophilic core thus, enabling targeted antibiotic delivery, which however, remains to be investigated [128].

An interesting alternative approach to local delivery is triggered release of antibiotics from polymeric particles. This can provide sudden high concentrations avoiding upregulations of resistance mechanisms. When a bacterial infection occurs, the bacteria will secrete many virulence factors, such as phospholipase, phosphatase, lipase, toxins and protease and additionally, an acidic pH will be present [129]. This unique bacterial microenvironment can be utilized as a trigger for release of the antibiotic, thereby improving targeting. This gives a possibility for reaching higher sustained local drug concentrations with fewer side effects and a lowered risk of developing resistance. Until now, only very few, have exploited this opportunity and we believe that this is one of the key areas to be addressed in future research.

One of the few published studies utilized rhamnolipids, a virulence factor of *P. aeruginosa* responsible for maintaining a biofilm structure, to trigger drug release from lipid-polymer hybrid NPs consisting of a PLGA core and a phosphatidylcholine coating. Triggered release was achieved for the low membrane permeability compound calcein, partly for ciprofloxacin, whereas compounds with high membrane permeability (levofloxacin and ofloxacin) already showed a rapid release in the absence of rhamnolipids, an effect attributed to their easy lipid membrane permeabilities [130]. Also a polymeric triple-layered nanogel (TLN) containing bacterial lipase-sensitive PCL interlayers between a cross-linked polyphosphoester core and a shell of PEG was developed [131]. Using *S. aureus* as the model bacterium and vancomycin as the model antibiotic, the authors demonstrated that the PCL 'fence' prevented premature drug release, whereas the TLN released almost all the encapsulated vancomycin within 24 h in the presence of *S. aureus* (lipase-containing environment), significantly inhibiting *S. aureus* growth [131]. Another trigger to be used is the acidic pH of the biofilm (Figure 6). Farokhzad and co-authors developed PLGA-PLG-PEG NPs capable of switching charge with decreasing pH, thus shielding non-targeted interactions at pH 7.4, but binding to bacteria in the acidic pH of the biofilm, showing great potential in biofilm treatment [132]. The pH difference was also utilized by Gao *et al.*, that prepared azithromycin-loaded NPs by electrostatic complexation between azithromycin conjugated amino-ended poly(amidoamine) dendrimer (PAMAM) and 2,3-dimethyl maleic anhydride (DA) modified poly(ethylene glycol)-block-polylysine (PEG-b-PLys). The NPs disassembled in acidic biofilms (pH 6.0), releasing the azithromycin-PAMAM NPs. *In vivo* studies confirmed a reduced bacterial burden and that the particles alleviated inflammation in a chronic lung infection model [133].

As an alternative trigger to the local biochemical microenvironment is the use of external physical stimulus such as heat, electromagnetic radiation or ultrasound [14]. Magnetic NPs have been studied extensively for use in the biomedical field due to multiple factors, one being targeted drug release. Hua *et al.* combined PLGA NPs with magnetic NPs allowing a triggered drug release when exposed to an external oscillating magnetic field, an effect presumably due to a mechanical disruption of the PLGA particles. The antimicrobial activity of ciprofloxacin was kept intact in the presence of the magnetic NP complex while at the same time drug release was fully controllable [102]. Also, carbon quantum dots (CQDs)-PLGA hybrid NPs were recently presented, showing a stimuli-responsive antibiotic release upon laser irradiation and a chemo-photothermally synergistic anti-biofilm effect against *P. aeruginosa* biofilms [134].



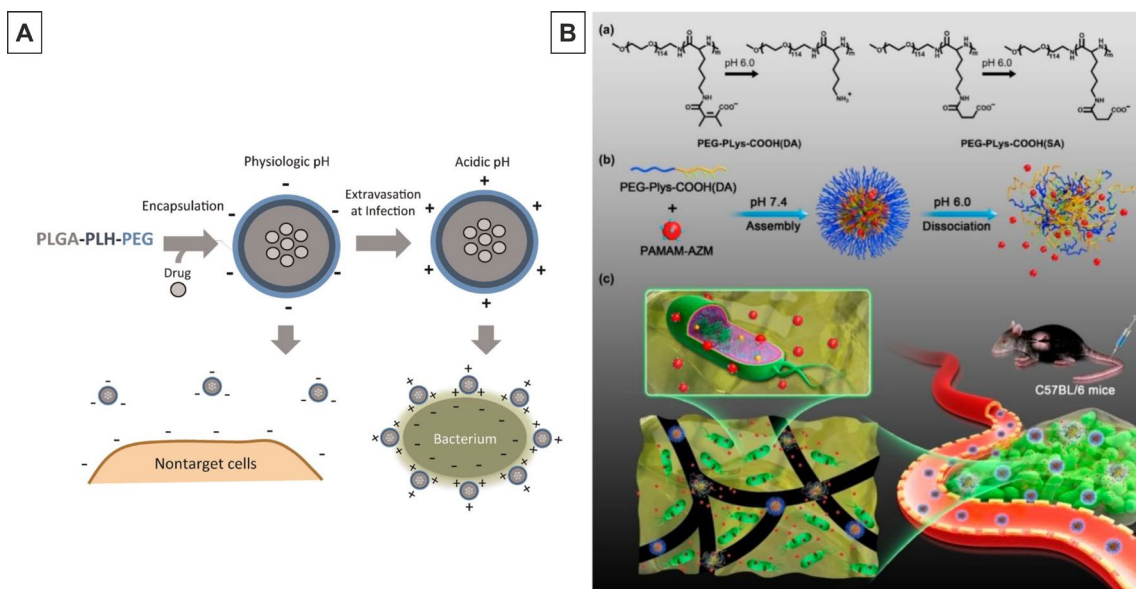


**Figure 6.** Using the weakly acidic pH of biofilms to achieve a triggered release of antibiotics. **(A)** NPs avoid uptake or binding to non-target cells at physiologic pH 7.4 due to a slight negative charge and surface PEGylation. The surface charge-switching mechanism is activated in the weakly acidic biofilm, resulting in NP binding to negatively charged bacteria and a controlled release of the encapsulated vancomycin promoting antibacterial effects. Reprinted with permission from [132]. Copyright© 2020, American Chemical Society. **(B)** NPs self-assemble at pH 7.4, but the chemical structure is modified in the acidic biofilm microenvironment, triggering the release of azithromycin (AZM)-containing NPs. Reprinted with permission from [133]. Copyright© 2020, American Chemical Society.

#### 5.4. *In vitro* and *in vivo* models for improved correlation to the clinic

An important aspect of eradicating biofilms in the clinic is to look into the environment in which the biofilm is growing since this can greatly influence the antimicrobial efficacy of the polymeric drug delivery system. Mucins, present on the mucosal lining of the gastro-intestinal tract and in the lungs, increase the viscosity of the environment thus, preventing penetration [135]. Interestingly, most studies reporting on mucus-penetrative effects have been conducted on native or artificial mucus without the presence of bacteria [100,136–138]. Fewer have reported on biofilm grown in artificial sputum [38,139] and to the best of our knowledge, the behavior in mucus-containing dynamic conditions remains an almost untouched territory [118].

We believe that a main contributor to developing new formulations and/or delivery systems for antibiotics will be *in vitro* and *in vivo* test systems utilized for creating and mimicking the biofilm habitat found in humans. So far, methods applied for antimicrobial susceptibility tests of drug delivery systems can be divided into: <sup>i</sup>static systems, such as those based on microtiter or agar plates, and <sup>ii</sup>dynamic systems including flow cells and bioreactor-based models. Classic static antibiotic susceptibility tests that provide a MIC, is the far most applied method to define susceptibility breakpoints, however, these are performed with bacteria growing in planktonic mode.

As the biofilm-associated bacteria greatly differ from their planktonic counterpart, it may seem to invalidate the planktonic-based biofilm research. However, the ease of planktonic assays makes them a useful tool for screening new antimicrobial drug delivery system as the absence of planktonic efficacy

generally will imply absence of biofilm-associated bacteria that are more difficult to treat. Nevertheless, development of microbial susceptibility tests of bacteria in their biofilm mode of growth is of growing interest. Different biofilm susceptibility endpoints have been suggested including the MBIC, MBEC and biofilm bactericidal concentration (BBC) [140]. Unfortunately, the definition and interpretation of these parameters differ greatly among different publications and none of the official agencies have yet set up standardized definitions of the biofilm endpoints like the guidelines for MIC value. In contrast to the static assays, that only provide an approximation to the complexity of the antibiotic activity against biofilms, the dynamic systems offers the possibility of constantly monitoring biofilm dynamics. Fluorescently-tagged or stained cells are grown under hydrodynamic conditions in flow cells, or in miniature disc-setups, to form mature biofilms [141]. By using CLSM, the behavior and changes after treatment with an antibiotic delivery system can be monitored. This has previously been applied in many studies, however, far most studies, still rely on the use of static assays. Also, pharmacokinetic/pharmacodynamic-simulations can be applied in the flow cells [142], however, these have yet to be applied in the research on antibiotic delivery systems. Moreover, it should be noted that despite the flow cell technology being considered the golden standard for studying biofilm physiology, no *in vitro* models, so far, can fully mimic the complexity of *in vivo* biofilms [142]. Multiple *in vivo* mammalian and non-mammalian animal models have been developed to mimic biofilm infections as reviewed previously [143–146]. However, many of these models do have their drawbacks and development of models correlating well with the infection seen in humans is still lacking. Also, the already existing models have only been applied in a limited amount of studies of polymeric particulates. A few examples include, Deacon *et al.* who used the non-mammalian *Galleria mellonella* model to study tobramycin-loaded, alginate- and DNase-coated CS NPs towards *P. aeruginosa* [22]. In addition, Agarwal *et al.* and Abdelghany *et al.* used an *in vivo* murine peritoneal infection model studying the effect of bacteriophage-loaded PLGA MPs or gentamycin-loaded PLGA NPs, respectively, towards *P. aeruginosa* [48,63]. Previously, also a mouse skin infection model was employed for investigating antimicrobial activity and therapeutic efficacy of a new antibiotic PCL-based formulation [98].

We believe that more attention needs to be paid towards using good *in vivo* models when assessing the effect of potential polymeric drug delivery particulates for biofilm infections.

## 6. CONCLUSION

Bacterial biofilm-related infections are responsible for a considerable global healthcare issue. The low response of biofilms to antibiotic therapy together with the lack of development of new antimicrobial entities only highlight the urgent need for innovative solutions.

This review shows that the use of polymeric nano- and microparticulated delivery systems is a promising approach for antibiotic delivery to biofilm infections as they can protect the antibiotic and potentially deliver sufficiently high local drug concentration. We do believe that emphasis needs to be paid towards optimizing loading efficiency and more work is necessary to push towards combinational strategies utilizing the unique bacterial micro-environment in the biofilm to achieve triggered and targeted release. Until now, there are very few antibiotics on the market formulated within nano- and microparticles. One reason could be that the very majority of the published papers base their conclusions on *in vitro* observations, which are great screening tools, however as the *in vitro* environment is far less complex than the human body, next step needs to be directed towards *in vivo* assessments. This is an essential step for further development of the polymeric particulates and for being able to reach the market.

## ACKNOWLEDGEMENTS

The authors would like to acknowledge the Center for Intelligent Drug Delivery and Sensing Using Microcontainers and Nanomechanics (IDUN) whose research is funded by the Danish National Research Foundation (DNRF122) and Villum Foundation (Grant No. 9301).

## REFERENCES

- [1] J.W. Costerton, P.S. Stewart, E.P. Greenberg, Bacterial Biofilms: A Common Cause of Persistent Infections, *Science*. 284 (1999) 1318–1322. <https://doi.org/10.1126/science.284.5418.1318>.
- [2] L. Hall-Stoodley, J.W. Costerton, P. Stoodley, Bacterial biofilms: From the natural environment to infectious diseases, *Nat. Rev. Microbiol.* 2 (2004) 95–108. <https://doi.org/10.1038/nrmicro821>.
- [3] J.W. Costerton, Introduction to biofilm, *Int. J. Antimicrob. Agents*. 11 (1999) 217–221. [https://doi.org/10.1016/S0924-8579\(99\)00018-7](https://doi.org/10.1016/S0924-8579(99)00018-7).
- [4] D. Davies, Understanding biofilm resistance to antibacterial agents, *Nat. Rev. Drug Discovery*. 2 (2003) 114–122. <https://doi.org/10.1038/nrd1008>.
- [5] T.F.C. Mah, G.A. O'Toole, Mechanisms of biofilm resistance to antimicrobial agents, *Trends Microbiol.* 9 (2001) 34–39. [https://doi.org/10.1016/S0966-842X\(00\)01913-2](https://doi.org/10.1016/S0966-842X(00)01913-2).
- [6] M. Malone, T. Bjarnsholt, A.J. McBain, G.A. James, P. Stoodley, D. Leaper, M. Tachi, G. Schultz, T. Swanson, R.D. Wolcott, The prevalence of biofilms in chronic wounds: a systematic review and meta-analysis of published data, *J. Wound Care*. 26 (2017) 20–25. <https://doi.org/10.12968/jowc.2017.26.1.20>.
- [7] G.A. James, E. Swogger, R. Wolcott, E. deLancey Pulcini, P. Secor, J. Sestrich, J.W. Costerton, P.S. Stewart, Biofilms in chronic wounds, *Wound Repair Regen*. 16 (2008) 37–44. <https://doi.org/10.1111/j.1524-475X.2007.00321.x>.
- [8] M. Burmølle, T.R. Thomsen, M. Fazli, I. Dige, L. Christensen, P. Homøe, M. Tvede, B. Nyvad, T. Tolker-Nielsen, M. Givskov, C. Moser, K. Kirketerp-Møller, H.K. Johansen, N. Høiby, P.Ø. Jensen, S.J. Sørensen, T. Bjarnsholt, Biofilms in chronic infections - A matter of opportunity - Monospecies biofilms in multispecies infections, *FEMS Immunol. Med. Microbiol.* 59 (2010) 324–336. <https://doi.org/10.1111/j.1574-695X.2010.00714.x>.
- [9] L. Hall-Stoodley, F.Z. Hu, A. Gieseke, L. Nistico, D. Nguyen, J. Hayes, M. Forbes, D.P. Greenberg, B. Dice, A. Burrows, P.A. Wackym, P. Stoodley, J.C. Post, G.D. Ehrlich, J.E. Kerschner, Direct Detection of Bacterial Biofilms on the Middle-Ear Mucosa of Children With Chronic Otitis Media, *JAMA*. 296 (2006) 202. <https://doi.org/10.1001/jama.296.2.202>.
- [10] H. Probert, G. Gibson, Bacterial biofilms in the human gastrointestinal tract, *Curr Issues Intest Microbiol*. 3 (2002) 23–27.
- [11] I.S. Ferreira, A. Bettencourt, B. Bétrisey, L.M.D. Gonçalves, A. Trampuz, A.J. Almeida, Improvement of the antibacterial activity of daptomycin-loaded polymeric microparticles by Eudragit RL 100: An assessment by isothermal microcalorimetry, *Int. J. Pharm.* 485 (2015) 171–182. <https://doi.org/10.1016/j.ijpharm.2015.03.016>.
- [12] M. Natan, E. Banin, From Nano to Micro: using nanotechnology to combat microorganisms and their multidrug resistance, *FEMS Microbiol. Rev.* 41 (2017) 302–322. <https://doi.org/10.1093/femsre/fux003>.
- [13] M.H. Xiong, Y. Bao, X.Z. Yang, Y.H. Zhu, J. Wang, Delivery of antibiotics with polymeric particles, *Adv. Drug Delivery Rev.* 78 (2014) 63–76. <https://doi.org/10.1016/j.addr.2014.02.002>.
- [14] K. Forier, K. Raemdonck, S.C. De Smedt, J. Demeester, T. Coenye, K. Braeckmans, Lipid and polymer nanoparticles for drug delivery to bacterial biofilms, *J. Controlled Release*. 190 (2014) 607–623. <https://doi.org/10.1016/j.jconrel.2014.03.055>.

- [15] A. Bettencourt, I. Ferreira, L. Goncalves, S. Kasper, B. Bertrand, J. Kikhney, A. Moter, A. Trampuz, A.J. Almeida, Activity of daptomycin- and vancomycin-loaded poly-epsilon-caprolactone microparticles against mature staphylococcal biofilms, *Int. J. Nanomedicine*. 10 (2015) 4351–4366. <https://doi.org/10.2147/IJN.S84108>.
- [16] C. Martin, W. Low, A. Gupta, M. Amin, I. Radecka, S. Britland, P. Raj, K. Kenward, Strategies for Antimicrobial Drug Delivery to Biofilm, *Curr. Pharm. Des.* 21 (2014) 43–66. <https://doi.org/10.2174/1381612820666140905123529>.
- [17] F. Danhier, E. Ansorena, J.M. Silva, R. Coco, A. Le Breton, V. Préat, PLGA-based nanoparticles: An overview of biomedical applications, *J. Controlled Release*. 161 (2012) 505–522. <https://doi.org/10.1016/j.jconrel.2012.01.043>.
- [18] R. Misra, S. Acharya, F. Dilnawaz, S.K. Sahoo, Sustained antibacterial activity of doxycycline-loaded poly(D,L-lactide-co-glycolide) and poly(epsilon-caprolactone) nanoparticles, *Nanomedicine*. 4 (2009) 519–530. <https://doi.org/10.2217/nnm.09.28>.
- [19] L. Chronopoulou, E.G. Di Domenico, F. Ascenzioni, C. Palocci, Positively charged biopolymeric nanoparticles for the inhibition of *Pseudomonas aeruginosa* biofilms, *J. Nanoparticle Res.* 18 (2016) 1–10. <https://doi.org/10.1007/s11051-016-3611-y>.
- [20] K.K. Patel, A.K. Agrawal, M.M. Anjum, M. Tripathi, N. Pandey, S. Bhattacharya, R. Tilak, S. Singh, DNase-I functionalization of ciprofloxacin-loaded chitosan nanoparticles overcomes the biofilm-mediated resistance of *Pseudomonas aeruginosa*, *Appl. Nanosci.* 10 (2020) 563–575. <https://doi.org/10.1007/s13204-019-01129-8>.
- [21] K.K. Patel, M. Tripathi, N. Pandey, A.K. Agrawal, S. Gade, M.M. Anjum, R. Tilak, S. Singh, Alginate lyase immobilized chitosan nanoparticles of ciprofloxacin for the improved antimicrobial activity against the biofilm associated mucoid *P. aeruginosa* infection in cystic fibrosis, *Int. J. Pharm.* 563 (2019) 30–42. <https://doi.org/10.1016/j.ijpharm.2019.03.051>.
- [22] J. Deacon, S.M. Abdelghany, D.J. Quinn, D. Schmid, J. Megaw, R.F. Donnelly, D.S. Jones, A. Kissenpfennig, J.S. Elborn, B.F. Gilmore, C.C. Taggart, C.J. Scott, Antimicrobial efficacy of tobramycin polymeric nanoparticles for *Pseudomonas aeruginosa* infections in cystic fibrosis: Formulation, characterisation and functionalisation with dornase alfa (DNase), *J. Controlled Release*. 198 (2015) 55–61. <https://doi.org/10.1016/j.jconrel.2014.11.022>.
- [23] A. Baelo, R. Levato, E. Julián, A. Crespo, J. Astola, J. Gavalda, E. Engel, M.A. Mateos-Timoneda, E. Torrents, Disassembling bacterial extracellular matrix with DNase-coated nanoparticles to enhance antibiotic delivery in biofilm infections, *J. Controlled Release*. 209 (2015) 150–158. <https://doi.org/10.1016/j.jconrel.2015.04.028>.
- A paper highlighting great effects of DNase I-functionalization of nanoparticles for antibiotic delivery providing simultaneous biofilm disassembly.**
- [24] W.S.W. Cheow, M.M.W. Chang, K. Hadinoto, Antibacterial efficacy of inhalable antibiotic-encapsulated biodegradable polymeric nanoparticles against *E. coli* biofilm cells, *J. Biomed. Nanotechnol.* 6 (2010) 391–403. <https://doi.org/10.1166/jbn.2010.1116>.
- [25] Y. Il Jeong, H.S. Na, D.H. Seo, D.G. Kim, H.C. Lee, M.K. Jang, S.K. Na, S.H. Roh, S. Il Kim, J.W. Nah, Ciprofloxacin-encapsulated poly(dl-lactide-co-glycolide) nanoparticles and its antibacterial activity, *Int. J. Pharm.* 352 (2008) 317–323. <https://doi.org/10.1016/j.ijpharm.2007.11.001>.

- [26] M.A.D.S. Ramos, P.B. Da Silva, L. Spósito, L.G. De Toledo, B. Vidal Bonifácio, C.F. Rodero, K.C. Dos Santos, M. Chorilli, T.M. Bauab, Nanotechnology-based drug delivery systems for control of microbial biofilms: A review, *Int. J. Nanomedicine*. 13 (2018) 1179–1213. <https://doi.org/10.2147/IJN.S146195>.
- [27] W.S. Cheow, M.W. Chang, K. Hadinoto, Antibacterial efficacy of inhalable levofloxacin-loaded polymeric nanoparticles against *E. coli* biofilm cells: The effect of antibiotic release profile, *Pharm. Res.* 27 (2010) 1597–1609. <https://doi.org/10.1007/s11095-010-0142-6>.
- [28] N. Thomas, C. Thorn, K. Richter, B. Thierry, C. Prestidge, Efficacy of Poly-Lactic-Co-Glycolic Acid Micro- and Nanoparticles of Ciprofloxacin Against Bacterial Biofilms, *J. Pharm. Sci.* 105 (2016) 3115–3122. <https://doi.org/10.1016/j.xphs.2016.06.022>.
- An interesting paper demonstrating the particle size is not a critical parameter in biofilm treatment if antibiotic concentrations are kept constant.**
- [29] S. Tamilvanan, N. Venkateshan, A. Ludwig, The potential of lipid- and polymer-based drug delivery carriers for eradicating biofilm consortia on device-related nosocomial infections, *J. Controlled Release*. 128 (2008) 2–22. <https://doi.org/10.1016/j.jconrel.2008.01.006>.
- [30] S. Tamilvanan, V. Kumar, D. Sharma, A. Thakur, In vitro evaluation of polyethylene glycol based microparticles containing azithromycin, *Drug Delivery Transl. Res.* 4 (2014) 139–148. <https://doi.org/10.1007/s13346-013-0187-2>.
- [31] J. Szczeblinska, K. Fijalkowski, J. Kohn, M. El Fray, Antibiotic loaded microspheres as antimicrobial delivery systems for medical applications, *Mater. Sci. Eng. C*. 77 (2017) 69–75. <https://doi.org/10.1016/j.msec.2017.03.215>.
- [32] A. SMITH, Biofilms and antibiotic therapy: Is there a role for combating bacterial resistance by the use of novel drug delivery systems?, *Adv. Drug Delivery Rev.* 57 (2005) 1539–1550. <https://doi.org/10.1016/j.addr.2005.04.007>.
- [33] K. Bazaka, M. V. Jacob, R.J. Crawford, E.P. Ivanova, Efficient surface modification of biomaterial to prevent biofilm formation and the attachment of microorganisms, *Appl. Microbiol. Biotechnol.* 95 (2012) 299–311. <https://doi.org/10.1007/s00253-012-4144-7>.
- [34] Y. Li, R. Na, X. Wang, H. Liu, L. Zhao, X. Sun, G. Ma, F. Cui, Fabrication of Antimicrobial Peptide-Loaded PLGA/Chitosan Composite Microspheres for Long-Acting Bacterial Resistance, *Molecules*. 22 (2017) 1637. <https://doi.org/10.3390/molecules22101637>.
- [35] M.-L. Manca, S. Mourtas, V. Dracopoulos, A.M. Fadda, S.G. Antimisiaris, PLGA, chitosan or chitosan-coated PLGA microparticles for alveolar delivery?, *Colloids Surfaces B Biointerfaces*. 62 (2008) 220–231. <https://doi.org/10.1016/j.colsurfb.2007.10.005>.
- [36] M.M. Arnold, E.M. Gorman, L.J. Schieber, E.J. Munson, C. Berkland, NanoCipro encapsulation in monodisperse large porous PLGA microparticles, *J. Controlled Release*. 121 (2007) 100–109. <https://doi.org/10.1016/j.jconrel.2007.05.039>.
- [37] A. Kumari, S.K. Yadav, S.C. Yadav, Biodegradable polymeric nanoparticles based drug delivery systems, *Colloids Surfaces B Biointerfaces*. 75 (2010) 1–18. <https://doi.org/10.1016/j.colsurfb.2009.09.001>.

- [38] J. Ernst, M. Klinger-Strobel, K. Arnold, J. Thamm, A. Hartung, M.W. Pletz, O. Makarewicz, D. Fischer, Polyester-based particles to overcome the obstacles of mucus and biofilms in the lung for tobramycin application under static and dynamic fluidic conditions, *Eur. J. Pharm. Biopharm.* 131 (2018) 120–129. <https://doi.org/10.1016/j.ejpb.2018.07.025>.

**A study on PEG-functionalized PLGA particles showing increased mucus penetration and effectiveness in biofilm eradication.**

- [39] N. Günday Türeli, A. Torge, J. Juntke, B.C. Schwarz, N. Schneider-Daum, A.E. Türeli, C.-M. Lehr, M. Schneider, Ciprofloxacin-loaded PLGA nanoparticles against cystic fibrosis *P. aeruginosa* lung infections, *Eur. J. Pharm. Biopharm.* 117 (2017) 363–371. <https://doi.org/10.1016/j.ejpb.2017.04.032>.
- [40] I. Coowanitwong, V. Arya, P. Kulvanich, G. Hochhaus, Slow Release Formulations of Inhaled Rifampin, *AAPS J.* 10 (2008) 342–348. <https://doi.org/10.1208/s12248-008-9044-5>.
- [41] L.L. Chaves, S.A. Costa Lima, A.C.C. Vieira, L. Barreiros, M.A. Segundo, D. Ferreira, B. Sarmiento, S. Reis, Development of PLGA nanoparticles loaded with clofazimine for oral delivery: Assessment of formulation variables and intestinal permeability, *Eur. J. Pharm. Sci.* 112 (2018) 28–37. <https://doi.org/10.1016/j.ejps.2017.11.004>.
- [42] A. Iannitelli, R. Grande, A. di Stefano, M. di Giulio, P. Sozio, L.J. Bessa, S. Laserra, C. Paolini, F. Protasi, L. Cellini, Potential antibacterial activity of carvacrol-loaded poly(DL-lactide-co-glycolide) (PLGA) nanoparticles against microbial biofilm, *Int. J. Mol. Sci.* 12 (2011) 5039–5051. <https://doi.org/10.3390/ijms12085039>.
- [43] S. Hasan, N. Thomas, B. Thierry, C.A. Prestidge, Biodegradable nitric oxide precursor-loaded micro- and nanoparticles for the treatment of *Staphylococcus aureus* biofilms, *J. Mater. Chem. B.* 5 (2017) 1005–1014. <https://doi.org/10.1039/c6tb03290g>.
- [44] F. Ungaro, I. D'Angelo, C. Coletta, R. D'Emmanuele Di Villa Bianca, R. Sorrentino, B. Perfetto, M.A. Tufano, A. Miro, M.I. La Rotonda, F. Quaglia, Dry powders based on PLGA nanoparticles for pulmonary delivery of antibiotics: Modulation of encapsulation efficiency, release rate and lung deposition pattern by hydrophilic polymers, *J. Controlled Release.* 157 (2012) 149–159. <https://doi.org/10.1016/j.jconrel.2011.08.010>.
- [45] B. Brauner, C. Schuster, M. Wirth, F. Gabor, Trimethoprim-Loaded Microspheres Prepared from Low-Molecular- Weight PLGA as a Potential Drug Delivery System for the Treatment of Urinary Tract Infections, *ACS Omega.* 5 (2020) 9013–9022. <https://doi.org/10.1021/acsomega.0c00981>.
- [46] F. Mohamed, C.F. van der Walle, Engineering Biodegradable Polyester Particles With Specific Drug Targeting and Drug Release Properties, *J. Pharm. Sci.* 97 (2008) 71–87. <https://doi.org/10.1002/jps.21082>.
- [47] D. Essa, P.P.D. Kondiah, Y.E. Choonara, V. Pillay, The Design of Poly(lactide-co-glycolide) Nanocarriers for Medical Applications, *Front. Bioeng. Biotechnol.* 8 (2020) 1–20. <https://doi.org/10.3389/fbioe.2020.00048>.
- [48] S.M. Abdelghany, D.J. Quinn, R.J. Ingram, B.F. Gilmore, R.F. Donnelly, C.C. Taggart, C.J. Scott, Gentamicin-loaded nanoparticles show improved antimicrobial effects towards *Pseudomonas aeruginosa* infection, *Int. J. Nanomedicine.* 7 (2012) 4053–4063. <https://doi.org/10.2147/IJN.S34341>.

- [49] F. Masood, T. Yasin, H. Bukhari, M. Mujahid, Characterization and application of roxithromycin loaded cyclodextrin based nanoparticles for treatment of multidrug resistant bacteria, *Mater. Sci. Eng. C*. 61 (2016) 1–7. <https://doi.org/10.1016/j.msec.2015.11.076>.
- [50] N.R. Labiris, M.B. Dolovich, Pulmonary drug delivery. Part I: Physiological factors affecting therapeutic effectiveness of aerosolized medications, *Br. J. Clin. Pharmacol.* 56 (2003) 588–599. <https://doi.org/10.1046/j.1365-2125.2003.01892.x>.
- [51] I. D'Angelo, B. Casciaro, A. Miro, F. Quaglia, M.L. Mangoni, F. Ungaro, Overcoming barriers in *Pseudomonas aeruginosa* lung infections: Engineered nanoparticles for local delivery of a cationic antimicrobial peptide, *Colloids Surfaces B Biointerfaces*. 135 (2015) 717–725. <https://doi.org/10.1016/j.colsurfb.2015.08.027>.
- [52] N. Lababidi, C.V. Montefusco-Pereira, C. de Souza Carvalho-Wodarz, C.M. Lehr, M. Schneider, Spray-dried multidrug particles for pulmonary co-delivery of antibiotics with N-acetylcysteine and curcumin-loaded PLGA-nanoparticles, *Eur. J. Pharm. Biopharm.* 157 (2020) 200–210. <https://doi.org/10.1016/j.ejpb.2020.10.010>.
- [53] C. Takahashi, N. Ogawa, Y. Kawashima, H. Yamamoto, Observation of antibacterial effect of biodegradable polymeric nanoparticles on *Staphylococcus epidermidis* biofilm using FE-SEM with an ionic liquid, *Microscopy*. 64 (2015) 169–180. <https://doi.org/10.1093/jmicro/dfv010>.
- [54] P. Sabaeifard, A. Abdi-Ali, M.R. Soudi, C. Gamazo, J.M. Irache, Amikacin loaded PLGA nanoparticles against *Pseudomonas aeruginosa*, *Eur. J. Pharm. Sci.* 93 (2016) 392–398. <https://doi.org/10.1016/j.ejps.2016.08.049>.
- [55] Q. Xu, L.M. Ensign, N.J. Boylan, A. Schön, X. Gong, J.-C. Yang, N.W. Lamb, S. Cai, T. Yu, E. Freire, J. Hanes, Impact of Surface Polyethylene Glycol (PEG) Density on Biodegradable Nanoparticle Transport in Mucus *ex Vivo* and Distribution in Vivo, *ACS Nano*. 9 (2015) 9217–9227. <https://doi.org/10.1021/acsnano.5b03876>.
- [56] R. Dorati, A. DeTrizio, M. Spalla, R. Migliavacca, L. Pagani, S. Pisani, E. Chiesa, B. Conti, T. Modena, I. Genta, Gentamicin Sulfate PEG-PLGA/PLGA-H Nanoparticles: Screening Design and Antimicrobial Effect Evaluation toward Clinic Bacterial Isolates, *Nanomaterials*. 8 (2018) 37. <https://doi.org/10.3390/nano8010037>.
- [57] F. Wan, S.S.R. Bohr, S.N. Kłodzińska, H. Jumaa, Z. Huang, T. Nylander, M.B. Thygesen, K.K. Sørensen, K.J. Jensen, C. Sternberg, N. Hatzakis, H. Mørck Nielsen, Ultrasmall TPGS–PLGA Hybrid Nanoparticles for Site-Specific Delivery of Antibiotics into *Pseudomonas aeruginosa* Biofilms in Lungs, *ACS Appl. Mater. Interfaces*. 12 (2020) 380–389. <https://doi.org/10.1021/acsnano.9b19644>.
- This study reports on TPGS-PLGA nanoparticles that are enzymatically cleaved by esterases in the biofilm, thus allowing site-specific delivery of antibiotics. Moreover, the particles penetrate and accumulate in the deep layers of the biofilm.**
- [58] S.N. Kłodzińska, F. Wan, H. Jumaa, C. Sternberg, T. Rades, H.M. Nielsen, Utilizing nanoparticles for improving anti-biofilm effects of azithromycin: A head-to-head comparison of modified hyaluronic acid nanogels and coated poly (lactic-co-glycolic acid) nanoparticles, *J. Colloid Interface Sci.* 555 (2019) 595–606. <https://doi.org/10.1016/j.jcis.2019.08.006>.
- [59] L. Drago, L. Cappelletti, E. De Vecchi, L. Pignataro, S. Torretta, R. Mattina, Antiadhesive and antibiofilm activity of hyaluronic acid against bacteria responsible for respiratory tract infections, *APMIS*. 122 (2014) 1013–1019. <https://doi.org/10.1111/apm.12254>.



- [60] W.S. Cheow, K. Hadinoto, Factors affecting drug encapsulation and stability of lipid-polymer hybrid nanoparticles, *Colloids Surfaces B Biointerfaces*. 85 (2011) 214–220. <https://doi.org/10.1016/j.colsurfb.2011.02.033>.
- [61] N. Højby, T. Bjarnsholt, M. Givskov, S. Molin, O. Ciofu, Antibiotic resistance of bacterial biofilms, *Int. J. Antimicrob. Agents*. 35 (2010) 322–332. <https://doi.org/10.1016/j.ijantimicag.2009.12.011>.
- [62] C. Han, J. Goodwine, N. Romero, K.S. Steck, K. Sauer, A. Doiron, Enzyme-encapsulating polymeric nanoparticles: A potential adjunctive therapy in *Pseudomonas aeruginosa* biofilm-associated infection treatment, *Colloids Surfaces B Biointerfaces*. 184 (2019) 110512. <https://doi.org/10.1016/j.colsurfb.2019.110512>.
- [63] R. Agarwal, C.T. Johnson, B.R. Imhoff, R.M. Donlan, N.A. McCarty, A.J. García, Inhaled bacteriophage-loaded polymeric microparticles ameliorate acute lung infections, *Nat. Biomed. Eng.* 2 (2018) 841–849. <https://doi.org/10.1038/s41551-018-0263-5>.
- [64] D.R. Perinelli, L. Fagioli, R. Campana, J.K.W. Lam, W. Baffone, G.F. Palmieri, L. Casettari, G. Bonacucina, Chitosan-based nanosystems and their exploited antimicrobial activity, *Eur. J. Pharm. Sci.* 117 (2018) 8–20. <https://doi.org/10.1016/j.ejps.2018.01.046>.
- [65] R. Misra, S.K. Sahoo, Antibacterial Activity of Doxycycline-Loaded Nanoparticles, in: *Methods Enzymol.*, 1st ed., Elsevier Inc., 2012: pp. 61–85. <https://doi.org/10.1016/B978-0-12-391858-1.00004-6>.
- [66] A. Grenha, Chitosan nanoparticles: A survey of preparation methods, *J. Drug Target.* 20 (2012) 291–300. <https://doi.org/10.3109/1061186X.2011.654121>.
- [67] R. Osman, P.L. Kan, G. Awad, N. Mortada, A.E. El-Shamy, O. Alpar, Spray dried inhalable ciprofloxacin powder with improved aerosolisation and antimicrobial activity, *Int. J. Pharm.* 449 (2013) 44–58. <https://doi.org/10.1016/j.ijpharm.2013.04.009>.
- [68] Y. Liu, L. Shi, L. Su, H.C. van der Mei, P.C. Jutte, Y. Ren, H.J. Busscher, Nanotechnology-based antimicrobials and delivery systems for biofilm-infection control, *Chem. Soc. Rev.* 48 (2019) 428–446. <https://doi.org/10.1039/C7CS00807D>.
- [69] A. Machul, D. Mikołajczyk, A. Regiel-Futyra, P.B. Heczko, M. Strus, M. Arruebo, G. Stochel, A. Kyzioł, Study on inhibitory activity of chitosan-based materials against biofilm producing *Pseudomonas aeruginosa* strains, *J. Biomater. Appl.* 30 (2015) 269–278. <https://doi.org/10.1177/0885328215578781>.
- [70] R. Cheung, T. Ng, J. Wong, W. Chan, Chitosan: An Update on Potential Biomedical and Pharmaceutical Applications, *Mar. Drugs*. 13 (2015) 5156–5186. <https://doi.org/10.3390/md13085156>.
- [71] Z. Ma, A. Garrido-Maestu, K.C. Jeong, Application, mode of action, and in vivo activity of chitosan and its micro- and nanoparticles as antimicrobial agents: A review, *Carbohydr. Polym.* 176 (2017) 257–265. <https://doi.org/10.1016/j.carbpol.2017.08.082>.
- [72] C.M. Lehr, J.A. Bouwstra, E.H. Schacht, H.E. Junginger, In vitro evaluation of mucoadhesive properties of chitosan and some other natural polymers, *Int. J. Pharm.* 78 (1992) 43–48. [https://doi.org/10.1016/0378-5173\(92\)90353-4](https://doi.org/10.1016/0378-5173(92)90353-4).
- [73] B. Jamil, H. Habib, S. Abbasi, H. Nasir, A. Rahman, A. Rehman, H. Bokhari, M. Imran, Cefazolin loaded chitosan nanoparticles to cure multi drug resistant Gram-negative pathogens, *Carbohydr. Polym.* 136 (2015) 682–691. <https://doi.org/10.1016/j.carbpol.2015.09.078>.

- [74] L. Qi, Z. Xu, X. Jiang, C. Hu, X. Zou, Preparation and antibacterial activity of chitosan nanoparticles, *Carbohydr. Res.* 339 (2004) 2693–2700. <https://doi.org/10.1016/j.carres.2004.09.007>.
- [75] V. Kucukoglu, H. Uzuner, H. Kenar, A. Karadenizli, In vitro antibacterial activity of ciprofloxacin loaded chitosan microparticles and their effects on human lung epithelial cells, *Int. J. Pharm.* 569 (2019) 118578. <https://doi.org/10.1016/j.ijpharm.2019.118578>.
- [76] L.F. de Andrade, A.C. Apolinário, C.O. Rangel-Yagui, M.A. Stephano, L.C. Tavares, Chitosan nanoparticles for the delivery of a new compound active against multidrug-resistant *Staphylococcus aureus*, *J. Drug Deliv. Sci. Technol.* 55 (2020) 101363. <https://doi.org/10.1016/j.jddst.2019.101363>.
- [77] L.T.K. Ngan, S.L. Wang, I.M. Hiep, P.M. Luong, N.T. Vui, T.M. Crossed D Signinh, N.A. Dzung, Preparation of chitosan nanoparticles by spray drying, and their antibacterial activity, *Res. Chem. Intermed.* 40 (2014) 2165–2175. <https://doi.org/10.1007/s11164-014-1594-9>.
- [78] L. Keawchaon, R. Yoksan, Preparation, characterization and in vitro release study of carvacrol-loaded chitosan nanoparticles, *Colloids Surfaces B Biointerfaces.* 84 (2011) 163–171. <https://doi.org/10.1016/j.colsurfb.2010.12.031>.
- [79] N. Liu, X.G. Chen, H.J. Park, C.G. Liu, C.S. Liu, X.H. Meng, L.J. Yu, Effect of MW and concentration of chitosan on antibacterial activity of *Escherichia coli*, *Carbohydr. Polym.* 64 (2006) 60–65. <https://doi.org/10.1016/j.carbpol.2005.10.028>.
- [80] X. Fei Liu, Y. Lin Guan, D. Zhi Yang, Z. Li, K. De Yao, Antibacterial action of chitosan and carboxymethylated chitosan, *J. Appl. Polym. Sci.* 79 (2001) 1324–1335. [https://doi.org/10.1002/1097-4628\(20010214\)79:7<1324::AID-APP210>3.0.CO;2-L](https://doi.org/10.1002/1097-4628(20010214)79:7<1324::AID-APP210>3.0.CO;2-L).
- [81] A.J. Huh, Y.J. Kwon, “Nanoantibiotics”: A new paradigm for treating infectious diseases using nanomaterials in the antibiotics resistant era, *J. Controlled Release.* 156 (2011) 128–145. <https://doi.org/10.1016/j.jconrel.2011.07.002>.
- [82] L.E. Chávez de Paz, A. Resin, K.A. Howard, D.S. Sutherland, P.L. Wejse, Antimicrobial Effect of Chitosan Nanoparticles on *Streptococcus mutans* Biofilms, *Appl. Environ. Microbiol.* 77 (2011) 3892–3895. <https://doi.org/10.1128/AEM.02941-10>.
- [83] M. Kong, X.G. Chen, Y.P. Xue, C.S. Liu, L.J. Yu, Q.X. Ji, D.S. Cha, H.J. Park, Preparation and antibacterial activity of chitosan microspheres in a solid dispersing system, *Front. Mater. Sci. China.* 2 (2008) 214–220. <https://doi.org/10.1007/s11706-008-0036-2>.
- [84] E.R.H. Kawakita, A.C.S. Ré, M.P.G. Peixoto, M.P. Ferreira, A.P. Ricomini-Filho, O. Freitas, C.P. Aires, Effect of chitosan dispersion and microparticles on older *streptococcus mutans* biofilms, *Molecules.* 24 (2019) 1–11. <https://doi.org/10.3390/molecules24091808>.
- [85] R. Thaya, B. Vaseeharan, J. Sivakamavalli, A. Iswarya, M. Govindarajan, N.S. Alharbi, S. Kadaikunnan, M.N. Al-anbr, J.M. Khaled, G. Benelli, Synthesis of chitosan-alginate microspheres with high antimicrobial and antibiofilm activity against multi-drug resistant microbial pathogens, *Microb. Pathog.* 114 (2018) 17–24. <https://doi.org/10.1016/j.micpath.2017.11.011>.
- [86] S. Shak, D.J. Capon, R. Hellmiss, S.A. Marsters, C.L. Baker, Recombinant human DNase I reduces the viscosity of cystic fibrosis sputum, *Proc. Natl. Acad. Sci. U. S. A.* 87 (1990) 9188–9192. <https://doi.org/10.1073/pnas.87.23.9188>.

- [87] N. Al-Nemrawi, N. Alshraiedeh, A. Zayed, B. Altaani, Low Molecular Weight Chitosan-Coated PLGA Nanoparticles for Pulmonary Delivery of Tobramycin for Cystic Fibrosis, *Pharmaceutics*. 11 (2018) 28. <https://doi.org/10.3390/ph11010028>.
- [88] A. Regiel, S. Irusta, A. Kyzioł, M. Arruebo, J. Santamaria, Preparation and characterization of chitosan–silver nanocomposite films and their antibacterial activity against *Staphylococcus aureus*, *Nanotechnology*. 24 (2013) 015101. <https://doi.org/10.1088/0957-4484/24/1/015101>.
- [89] X. Wang, Y. Du, H. Liu, Preparation, characterization and antimicrobial activity of chitosan-Zn complex, *Carbohydr. Polym.* 56 (2004) 21–26. <https://doi.org/10.1016/j.carbpol.2003.11.007>.
- [90] R. Thaya, B. Malaikozhundan, S. Vijayakumar, J. Sivakamavalli, R. Jeyasekar, S. Shanthi, B. Vaseeharan, P. Ramasamy, A. Sonawane, Chitosan coated Ag/ZnO nanocomposite and their antibiofilm, antifungal and cytotoxic effects on murine macrophages, *Microb. Pathog.* 100 (2016) 124–132. <https://doi.org/10.1016/j.micpath.2016.09.010>.
- [91] Z. Rukavina, Ž. Vanić, Current Trends in Development of Liposomes for Targeting Bacterial Biofilms, *Pharmaceutics*. 8 (2016) 18. <https://doi.org/10.3390/pharmaceutics8020018>.
- [92] Y. Qiu, D. Xu, G. Sui, D. Wang, M. Wu, L. Han, H. Mu, J. Duan, Gentamicin decorated phosphatidylcholine-chitosan nanoparticles against biofilms and intracellular bacteria, *Int. J. Biol. Macromol.* 156 (2020) 640–647. <https://doi.org/10.1016/j.ijbiomac.2020.04.090>.
- [93] S. Sreekumar, F.M. Goycoolea, B.M. Moerschbacher, G.R. Rivera-Rodriguez, Parameters influencing the size of chitosan-TPP nano- and microparticles, *Sci. Rep.* 8 (2018) 1–11. <https://doi.org/10.1038/s41598-018-23064-4>.
- [94] K. Kho, W.S. Cheow, R.H. Lie, K. Hadinoto, Aqueous re-dispersibility of spray-dried antibiotic-loaded polycaprolactone nanoparticle aggregates for inhaled anti-biofilm therapy, *Powder Technol.* 203 (2010) 432–439. <https://doi.org/10.1016/j.powtec.2010.06.003>.
- [95] M.I. Shaaban, M.A. Shaker, F.M. Mady, Imipenem/cilastatin encapsulated polymeric nanoparticles for destroying carbapenem-resistant bacterial isolates, *J. Nanobiotechnology*. 15 (2017) 1–12. <https://doi.org/10.1186/s12951-017-0262-9>.
- [96] T.K. Dash, V.B. Konkimalla, Poly-ε-caprolactone based formulations for drug delivery and tissue engineering: A review, *J. Controlled Release*. 158 (2012) 15–33. <https://doi.org/10.1016/j.jconrel.2011.09.064>.
- [97] L. Peltonen, J. Aitta, S. Hyvönen, M. Karjalainen, J. Hirvonen, Improved entrapment efficiency of hydrophilic drug substance during nanoprecipitation of poly(l)lactide nanoparticles, *AAPS PharmSciTech*. 5 (2004) 115–120. <https://doi.org/10.1208/pt050116>.
- [98] C.A. Omolo, R.S. Kalhapure, N. Agrawal, M. Jadhav, S. Rambharose, C. Mocktar, T. Govender, A hybrid of mPEG-b-PCL and G1-PEA dendrimer for enhancing delivery of antibiotics, *J. Controlled Release*. 290 (2018) 112–128. <https://doi.org/10.1016/j.jconrel.2018.10.005>.

**The development of novel materials is essential for the efficient drug delivery. In this paper a linear polymer dendrimer hybrid star polymer (3-mPEA) comprising of a poly (ester-amine) dendrimer (G1-PEA) and a diblock copolymer of methoxy poly (ethylene glycol)-b-poly(ε-caprolactone) (mPEG-b-PCL) was synthesized for vancomycin delivery showing great effects both *in vitro* and *in vivo*.**

- [99] R. Misra, S. Acharya, F. Dilnawaz, S.K. Sahoo, Sustained antibacterial activity of doxycycline-loaded poly(D,L-lactide-co-glycolide) and poly( $\epsilon$ -caprolactone) nanoparticles, *Nanomedicine*. 4 (2009) 519–530. <https://doi.org/10.2217/nnm.09.28>.
- [100] A. Torge, S. Wagner, P.S. Chaves, E.G. Oliveira, S.S. Guterres, A.R. Pohlmann, A. Titz, M. Schneider, R.C.R. Beck, Ciprofloxacin-loaded lipid-core nanocapsules as mucus penetrating drug delivery system intended for the treatment of bacterial infections in cystic fibrosis, *Int. J. Pharm.* 527 (2017) 92–102. <https://doi.org/10.1016/j.ijpharm.2017.05.013>.
- [101] A. Bettencourt, I. Ferreira, L. Goncalves, S. Kasper, B. Bertrand, J. Kikhney, A. Moter, A. Trampuz, A.J. Almeida, Activity of daptomycin- and vancomycin-loaded poly-epsilon-caprolactone microparticles against mature staphylococcal biofilms, *Int. J. Nanomedicine*. 10 (2015) 4351. <https://doi.org/10.2147/IJN.S84108>.
- [102] X. Hua, S. Tan, H.M.H.N. Bandara, Y. Fu, S. Liu, H.D.C. Smyth, Externally controlled triggered-release of drug from PLGA micro and nanoparticles, *PLoS One*. 9 (2014) 1–17. <https://doi.org/10.1371/journal.pone.0114271>.
- [103] I.C. Yue, J. Poff, M.E. Cortés, R.D. Sinisterra, C.B. Faris, P. Hildgen, R. Langer, V.P. Shastri, A novel polymeric chlorhexidine delivery device for the treatment of periodontal disease, *Biomaterials*. 25 (2004) 3743–3750. <https://doi.org/10.1016/j.biomaterials.2003.09.113>.
- [104] C. Flores, S. Degoutin, F. Chai, G. Raoul, J.C. Hornez, B. Martel, J. Siepmann, J. Ferri, N. Blanchemain, Gentamicin-loaded poly(lactic-co-glycolic acid) microparticles for the prevention of maxillofacial and orthopedic implant infections, *Mater. Sci. Eng. C*. 64 (2016) 108–116. <https://doi.org/10.1016/j.msec.2016.03.064>.
- [105] C. Takahashi, S. Saito, A. Suda, N. Ogawa, Y. Kawashima, H. Yamamoto, Antibacterial activities of polymeric poly(DL-lactide-co-glycolide) nanoparticles and Soluplus® micelles against *Staphylococcus epidermidis* biofilm and their characterization, *RSC Adv*. 5 (2015) 71709–71717. <https://doi.org/10.1039/C5RA13885J>.
- [106] C. Takahashi, Y. Akachi, N. Ogawa, K. Moriguchi, T. Asaka, M. Tanemura, Y. Kawashima, H. Yamamoto, Morphological study of efficacy of clarithromycin-loaded nanocarriers for treatment of biofilm infection disease, *Med. Mol. Morphol.* 50 (2017) 9–16. <https://doi.org/10.1007/s00795-016-0141-8>.
- [107] Z. Merchant, K.M.G. Taylor, P. Stapleton, S.A. Razak, N. Kunda, I. Alfagih, K. Sheikh, I.Y. Saleem, S. Somavarapu, Engineering hydrophobically modified chitosan for enhancing the dispersion of respirable microparticles of levofloxacin, *Eur. J. Pharm. Biopharm.* 88 (2014) 816–829. <https://doi.org/10.1016/j.ejpb.2014.09.005>.
- [108] Y. Tan, S. Ma, M. Leonhard, D. Moser, G.M. Haselmann, J. Wang, D. Eder, B. Schneider-Stickler, Enhancing antibiofilm activity with functional chitosan nanoparticles targeting biofilm cells and biofilm matrix, *Carbohydr. Polym.* 200 (2018) 35–42. <https://doi.org/10.1016/j.carbpol.2018.07.072>.
- [109] R. Hejazi, M. Amiji, Stomach-specific anti-*H. pylori* therapy. I: Preparation and characterization of tetracycline-loaded chitosan microspheres, *Int. J. Pharm.* 235 (2002) 87–94. [https://doi.org/10.1016/S0378-5173\(01\)00985-1](https://doi.org/10.1016/S0378-5173(01)00985-1).
- [110] R. Hejazi, M. Amiji, Stomach-specific anti-*H. pylori* Therapy. II. Gastric residence studies of tetracycline-loaded chitosan microspheres in gerbils, *Pharm. Dev. Technol.* 8 (2003) 253–262. <https://doi.org/10.1081/PDT-120022154>.

- [111] R. Hejazi, M. Amiji, Stomach-specific anti-H. pylori therapy. Part III: Effect of chitosan microspheres crosslinking on the gastric residence and local tetracycline concentrations in fasted gerbils, *Int. J. Pharm.* 272 (2004) 99–108. <https://doi.org/10.1016/j.ijpharm.2003.12.001>.
- [112] I.K. Yazdi, M.B. Murphy, C. Loo, X. Liu, M. Ferrari, B.K. Weiner, E. Tasciotti, Cefazolin-loaded mesoporous silicon microparticles show sustained bactericidal effect against *Staphylococcus aureus*, *J. Tissue Eng.* 5 (2014) 204173141453657. <https://doi.org/10.1177/2041731414536573>.
- [113] L.H. Nielsen, S.S. Keller, A. Boisen, Microfabricated devices for oral drug delivery, *Lab Chip.* 18 (2018) 2348–2358. <https://doi.org/10.1039/C8LC00408K>.
- [114] N.K. Mandsberg, J.F. Christfort, K. Kamguyan, A. Boisen, S.K. Srivastava, Orally ingestible medical devices for gut engineering, *Adv. Drug Delivery Rev.* (2020) 1–2. <https://doi.org/10.1016/j.addr.2020.05.004>.
- [115] S.E. Birk, J.A.J. Haagensen, H.K. Johansen, S. Molin, L.H. Nielsen, A. Boisen, Microcontainer Delivery of Antibiotic Improves Treatment of *Pseudomonas aeruginosa* Biofilms, *Adv. Healthc. Mater.* 9 (2020) 1–10. <https://doi.org/10.1002/adhm.201901779>.
- This is the first report showing that microdevices can be useful for antibiotic delivery in treatment of biofilms by providing high local drug concentrations, and thereby a more effective treatment and reduced use of antibiotics.**
- [116] L.H. Nielsen, A. Meleró, S.S. Keller, J. Jacobsen, T. Garrigues, T. Rades, A. Müllertz, A. Boisen, Polymeric microcontainers improve oral bioavailability of furosemide, *Int. J. Pharm.* 504 (2016) 98–109. <https://doi.org/10.1016/j.ijpharm.2016.03.050>.
- [117] C. Mazzoni, F. Tentor, S.A. Strindberg, L.H. Nielsen, S.S. Keller, T.S. Alstrøm, C. Gundlach, A. Müllertz, P. Marizza, A. Boisen, From concept to in vivo testing: Microcontainers for oral drug delivery, *J. Controlled Release.* 268 (2017) 343–351. <https://doi.org/10.1016/j.jconrel.2017.10.013>.
- [118] S.E. Birk, L. Seriola, V. Cavallo, J.A.J. Haagensen, S. Molin, L.H. Nielsen, K. Zór, A. Boisen, Enhanced Eradication of Mucin-embedded Bacterial Biofilm by Locally Delivered Antibiotics in Functionalized Microcontainers, Submitted. (2020).
- [119] D.H. Altreuter, A.R. Kirtane, T. Grant, C. Kruger, G. Traverso, A.M. Bellinger, Changing the pill: developments toward the promise of an ultra-long-acting gastroretentive dosage form, *Expert Opin. Drug Deliv.* 15 (2018) 1189–1198. <https://doi.org/10.1080/17425247.2018.1544615>.
- [120] M. Verma, K. Vishwanath, F. Eweje, N. Roxhed, T. Grant, M. Castaneda, C. Steiger, H. Mazdiyasni, T. Bense, D. Minahan, V. Soares, J.A.F. Salama, A. Lopes, K. Hess, C. Cleveland, D.J. Fulop, A. Hayward, J. Collins, S.M. Tamang, T. Hua, C. Ikeanyi, G. Zeidman, E. Mule, S. Boominathan, E. Popova, J.B. Miller, A.M. Bellinger, D. Collins, D. Leibowitz, S. Batra, S. Ahuja, M. Bajija, S. Batra, R. Sarin, U. Agarwal, S.D. Khaparde, N.K. Gupta, D. Gupta, A.K. Bhatnagar, K.K. Chopra, N. Sharma, A. Khanna, J. Chowdhury, R. Stoner, A.H. Slocum, M.J. Cima, J. Furin, R. Langer, G. Traverso, A gastric resident drug delivery system for prolonged gram-level dosing of tuberculosis treatment, *Sci. Transl. Med.* 11 (2019) eaau6267. <https://doi.org/10.1126/scitranslmed.aau6267>.
- [121] A.M. Bellinger, M. Jafari, T.M. Grant, S. Zhang, H.C. Slater, E.A. Wenger, S. Mo, Y.-A.L. Lee, H. Mazdiyasni, L. Kogan, R. Barman, C. Cleveland, L. Booth, T. Bense, D. Minahan, H.M. Hurowitz, T. Tai, J. Daily, B. Nikolic, L. Wood, P.A. Eckhoff, R. Langer, G. Traverso, Oral, ultra-long-lasting drug delivery: Application toward malaria elimination goals, *Sci. Transl. Med.* 8 (2016) 365ra157-365ra157. <https://doi.org/10.1126/scitranslmed.aag2374>.

- [122] A.R. Kirtane, O. Abouzid, D. Minahan, T. Bensele, A.L. Hill, C. Selinger, A. Bershteyn, M. Craig, S.S. Mo, H. Mazdiyasi, C. Cleveland, J. Rogner, Y.-A.L. Lee, L. Booth, F. Javid, S.J. Wu, T. Grant, A.M. Bellinger, B. Nikolic, A. Hayward, L. Wood, P.A. Eckhoff, M.A. Nowak, R. Langer, G. Traverso, Development of an oral once-weekly drug delivery system for HIV antiretroviral therapy, *Nat. Commun.* 9 (2018) 2. <https://doi.org/10.1038/s41467-017-02294-6>.

**This paper presents encapsulated, gastric-resident dosage forms for ultra-long-acting drug delivery, a device that we believe could have great potential in treatment of gastric biofilms.**

- [123] B. Porsio, M.G. Cusimano, D. Schillaci, E.F. Craparo, G. Giammona, G. Cavallaro, Nano into Micro Formulations of Tobramycin for the Treatment of *Pseudomonas aeruginosa* Infections in Cystic Fibrosis, *Biomacromolecules*. 18 (2017) 3924–3935. <https://doi.org/10.1021/acs.biomac.7b00945>.

**An interesting study comparing nano in micro (NiM) particulated formulations to a dry powder inhalator. The NiMs facilitated slow tobramycin release due to incorporation in a core polyanion complex and drug diffusion through the mucus mesh was achieved by incorporation of N-acetylcysteine, l-arginine or cysteamine.**

- [124] P.J. Weldrick, M.J. Hardman, V.N. Paunov, Enhanced Clearing of Wound-Related Pathogenic Bacterial Biofilms Using Protease-Functionalized Antibiotic Nanocarriers, *ACS Appl. Mater. Interfaces*. 11 (2019) 43902–43919. <https://doi.org/10.1021/acsami.9b16119>.
- [125] R.A. Hatch, N.L. Schiller, Alginate lyase promotes diffusion of aminoglycosides through the extracellular polysaccharide of mucoid *Pseudomonas aeruginosa*, *Antimicrob. Agents Chemother.* 42 (1998) 974–977. <https://doi.org/10.1128/aac.42.4.974>.
- [126] G.A. Islan, V.E. Bosio, G.R. Castro, Alginate lyase and ciprofloxacin co-immobilization on biopolymeric microspheres for cystic fibrosis treatment, *Macromol. Biosci.* 13 (2013) 1238–1248. <https://doi.org/10.1002/mabi.201300134>.
- [127] K.M. El-Say, H.S. El-Sawy, Polymeric nanoparticles: Promising platform for drug delivery, *Int. J. Pharm.* 528 (2017) 675–691. <https://doi.org/10.1016/j.ijpharm.2017.06.052>.
- [128] T.R. Flockton, L. Schnorbus, A. Araujo, J. Adams, M. Hammel, L.J. Perez, Inhibition of *Pseudomonas aeruginosa* biofilm formation with surface modified polymeric nanoparticles, *Pathogens*. 8 (2019). <https://doi.org/10.3390/pathogens8020055>.
- [129] L. Rahme, E. Stevens, S. Wolfort, J. Shao, R. Tompkins, F. Ausubel, Common virulence factors for bacterial pathogenicity in plants and animals, *Science*. 268 (1995) 1899–1902. <https://doi.org/10.1126/science.7604262>.
- [130] W.S. Cheow, K. Hadinoto, Lipid-polymer hybrid nanoparticles with rhamnolipid-triggered release capabilities as anti-biofilm drug delivery vehicles, *Particuology*. 10 (2012) 327–333. <https://doi.org/10.1016/j.partic.2011.08.007>.
- [131] M.H. Xiong, Y. Bao, X.Z. Yang, Y.C. Wang, B. Sun, J. Wang, Lipase-sensitive polymeric triple-layered nanogel for “on-demand” drug delivery, *J. Am. Chem. Soc.* 134 (2012) 4355–4362. <https://doi.org/10.1021/ja211279u>.

**Reports on a novel lipase-sensitive polymeric triple-layered nanogel as drug carrier – a new strategy utilizing the unique bacterial biofilm microenvironment to target the drug delivery.**

- [132] A.F. Radovic-Moreno, T.K. Lu, V.A. Puscasu, C.J. Yoon, R. Langer, O.C. Farokhzad, Surface charge-switching polymeric nanoparticles for bacterial cell wall-targeted delivery of antibiotics, *ACS Nano*. 6 (2012) 4279–4287. <https://doi.org/10.1021/nn3008383>.
- [133] Y. Gao, J. Wang, M. Chai, X. Li, Y. Deng, Q. Jin, J. Ji, Size and Charge Adaptive Clustered Nanoparticles Targeting the Biofilm Microenvironment for Chronic Lung Infection Management, *ACS Nano*. 14 (2020) 5686–5699. <https://doi.org/10.1021/acsnano.0c00269>.
- A paper presenting an innovative size and charge adaptive particulated system that disassemble in the weakly acidic biofilm-microenvironment whereafter nanoparticles are released showing penetration and long-term retention within the biofilm.**
- [134] Z. Huang, T. Zhou, Y. Yuan, S. Natalie Klodzińska, T. Zheng, C. Sternberg, H. Mørck Nielsen, Y. Sun, F. Wan, Synthesis of carbon quantum dot-poly lactic-co-glycolic acid hybrid nanoparticles for chemo-photothermal therapy against bacterial biofilms., *J. Colloid Interface Sci.* 577 (2020) 66–74. <https://doi.org/10.1016/j.jcis.2020.05.067>.
- [135] L. Müller, X. Murgia, L. Siebenbürger, C. Börger, K. Schwarzkopf, K. Sewald, S. Häussler, A. Braun, C. Lehr, M. Hittinger, S. Wronski, Human airway mucus alters susceptibility of *Pseudomonas aeruginosa* biofilms to tobramycin, but not colistin, *J. Antimicrob. Chemother.* 73 (2018) 2762–2769. <https://doi.org/10.1093/jac/dky251>.
- [136] F. Wan, T. Nylander, S.N. Klodzinska, C. Foged, M. Yang, S.G. Baldursdottir, H. M. Nielsen, Lipid Shell-Enveloped Polymeric Nanoparticles with High Integrity of Lipid Shells Improve Mucus Penetration and Interaction with Cystic Fibrosis-Related Bacterial Biofilms, *ACS Appl. Mater. Interfaces*. 10 (2018) 10678–10687. <https://doi.org/10.1021/acsami.7b19762>.
- [137] J.S. Suk, S.K. Lai, Y.Y. Wang, L.M. Ensign, P.L. Zeitlin, M.P. Boyle, J. Hanes, The penetration of fresh undiluted sputum expectorated by cystic fibrosis patients by non-adhesive polymer nanoparticles, *Biomaterials*. 30 (2009) 2591–2597. <https://doi.org/10.1016/j.biomaterials.2008.12.076>.
- [138] P. Li, X. Chen, Y. Shen, H. Li, Y. Zou, G. Yuan, P. Hu, H. Hu, Mucus penetration enhanced lipid polymer nanoparticles improve the eradication rate of *Helicobacter pylori* biofilm, *J. Controlled Release*. 300 (2019) 52–63. <https://doi.org/10.1016/j.jconrel.2019.02.039>.
- [139] M. Klinger-Strobel, J. Ernst, C. Lautenschläger, M.W. Pletz, D. Fischer, O. Makarewicz, A blue fluorescent labeling technique utilizing micro-and nanoparticles for tracking in LIVE/DEAD® stained pathogenic biofilms of staphylococcus aureus and burkholderia cepacia, *Int. J. Nanomedicine*. 11 (2016) 575–583. <https://doi.org/10.2147/IJN.S98401>.
- [140] O. Ciofu, E. Rojo-Molinero, M.D. Macià, A. Oliver, Antibiotic treatment of biofilm infections, *Apmis*. 125 (2017) 304–319. <https://doi.org/10.1111/apm.12673>.
- [141] L. Seriola, T.Z. Laksafoss, J.A.J. Haagensen, C. Sternberg, M.P. Soerensen, S. Molin, K. Zór, A. Boisen, Bacterial Cell Cultures in a Lab-on-a-Disc: A Simple and Versatile Tool for Quantification of Antibiotic Treatment Efficacy, *Anal. Chem.* 92 (2020) 13871–13879. <https://doi.org/10.1021/acs.analchem.0c02582>.
- [142] J.A.J. Haagensen, D. Verotta, L. Huang, A. Spormann, K. Yang, New *In Vitro* Model To Study the Effect of Human Simulated Antibiotic Concentrations on Bacterial Biofilms, *Antimicrob. Agents Chemother.* 59 (2015) 4074–4081. <https://doi.org/10.1128/AAC.05037-14>.
- [143] D. Lebeaux, A. Chauhan, O. Rendueles, C. Beloin, From in vitro to in vivo models of bacterial biofilm-related infections, *Pathogens*. 2 (2013) 288–356. <https://doi.org/10.3390/pathogens2020288>.

- [144] R.A. Gabrielska, K.P. Rumbaugh, Biofilm models of polymicrobial infection, *Future Microbiol.* 10 (2015) 1997–2015. <https://doi.org/10.2217/fmb.15.109>.
- [145] S. Edwards, B. V. Kjellerup, Exploring the applications of invertebrate host-pathogen models for in vivo biofilm infections, *FEMS Immunol. Med. Microbiol.* 65 (2012) 205–214. <https://doi.org/10.1111/j.1574-695X.2012.00975.x>.
- [146] T. Coenye, H.J. Nelis, In vitro and in vivo model systems to study microbial biofilm formation, *J. Microbiol. Methods.* 83 (2010) 89–105. <https://doi.org/10.1016/j.mimet.2010.08.018>.



# APPENDIX II

PAPER II

**Microcontainer delivery of antibiotic improves treatment of *Pseudomonas aeruginosa* biofilms**

S.E. Birk, J.A.J. Haagenen, H.K. Johansen, S. Molin, L.H. Nielsen, A. Boisen

*Advanced Healthcare Materials*, 2020, 9 (10): 1901779

# Microcontainer Delivery of Antibiotic Improves Treatment of *Pseudomonas aeruginosa* Biofilms

Stine Egebro Birk,\* Janus Anders Juul Haagenen, Helle Krogh Johansen, Søren Molin, Line Hagner Nielsen, and Anja Boisen

**Biofilm-associated infections are difficult to treat effectively with antibiotics despite repeated treatments. Polymeric microdevices (microcontainers) have previously been shown to engulf in mucus layers and to provide tunable release. Such devices may overcome the challenge of delivering antibiotics into the biofilm, increasing the local drug concentration and hence improve local bacterial killing. In this work, microcontainers are loaded with the antibiotic, ciprofloxacin hydrochloride, and functionalized with polymeric lids of polyethylene glycol (PEG), chitosan, or Eudragit S100. The PEG lid gives rise to a drug release comparable to uncoated microcontainers showing complete release after 8 h, whereas chitosan and Eudragit S100 lids result in continuous release during the course of 24 h. All antibiotic-containing microcontainers inhibit planktonic growth of *Pseudomonas aeruginosa* (PAO1) cells, but the degree of inhibition depends on the coating. Microcontainers with ciprofloxacin hydrochloride kill about three times more biofilm-associated PAO1 cells compared with a single standard bolus. Moreover, the use of microcontainers in biofilm result in bacterial killing equal to a constant flow of a three times higher concentration of solubilized antibiotics. These studies suggest that microcontainers can be useful for antibiotic delivery in treatment of biofilm-associated infections, resulting in more effective treatment and reduced use of antibiotics.**

## 1. Introduction

A biofilm is a consortium of bacteria living together in a self-produced extracellular polymeric substances (EPS) matrix consisting of various polysaccharides, proteins, and DNA.<sup>[1,2]</sup> The


bacteria adhere to each other and to surfaces, aggregates develop, and the biofilm promotes bacterial survival in otherwise hostile environments.<sup>[3,4]</sup> Biofilm-associated infections are difficult to treat, and they are often associated with chronic infections, resulting in recurrent inflammation and exacerbations despite intense treatment with antibiotics. In contrast, bacteria living as planktonic, single-cell populations in suspension show decreased tolerance toward antibiotics, and hence are easier to treat.<sup>[1,2,5]</sup>

*Pseudomonas aeruginosa* is a Gram-negative pathogenic bacterial species forming biofilms and causing devastating chronic infections in immunocompromised individuals.<sup>[3,6]</sup> *P. aeruginosa* can cause serious intestinal infections, where it for example has been isolated from patients suffering from inflammatory bowel disease and cancer patients.<sup>[7,8]</sup> The gastrointestinal tract is often considered to be an important reservoir for *P. aeruginosa* and the presence in the intestines is responsible for increased mortality in

gut-derived sepsis and bacteremia and facilitates hematogenous spread of infections to other organs.<sup>[8]</sup> *P. aeruginosa* often causes chronic lung infections in patients suffering from cystic fibrosis due to the accumulation of thick, sticky mucus and to the consequentially impaired mucociliary clearance.<sup>[4,5]</sup>

S. E. Birk, Dr. L. H. Nielsen, Prof. A. Boisen  
The Danish National Research Foundation and Villum Foundation's  
Center for Intelligent Drug Delivery and Sensing Using Microcontainers  
and Nanomechanics (IDUN)  
Department of Health Technology  
Technical University of Denmark  
Ørstedes Plads 345C, Kongens Lyngby 2800, Denmark  
E-mail: stegha@dtu.dk  
Dr. J. A. J. Haagenen, Prof. S. Molin  
Novo Nordisk Foundation Center for Biosustainability  
Technical University of Denmark  
Kemitorvet 220, Kongens Lyngby 2800, Denmark

Prof. H. K. Johansen  
Department of Clinical Microbiology, Section 9301  
Copenhagen University Hospital Rigshospitalet Henrik Harpestrengs  
Vej 4A  
Copenhagen Ø 2100, Denmark  
Prof. H. K. Johansen  
Department of Clinical Medicine  
Faculty of Health and Medical Sciences  
University of Copenhagen  
Blegdamsvej 9, Copenhagen Ø 2100, Denmark

 The ORCID identification number(s) for the author(s) of this article can be found under <https://doi.org/10.1002/adhm.201901779>

DOI: 10.1002/adhm.201901779

Antibiotic treatment is the standard therapy for chronic infections with *P. aeruginosa*, but it is difficult to fully combat *P. aeruginosa* infections.<sup>[9]</sup> One of the most often used antibiotics is ciprofloxacin. This is a broad spectrum second generation fluoroquinolone with a reported low frequency of spontaneous bacterial resistance.<sup>[10,11]</sup> Delivery of several antibiotics to biofilm-associated infections is, however, obstructed by the EPS matrix. This viscous structure creates diffusional barriers that may deactivate the antibiotics in the outer layers of the biofilm faster than they diffuse, leading to insufficient antimicrobial effects.<sup>[4,12,13]</sup> Also, the EPS allows development of phenotypically different subpopulations with reduced metabolic activities and growth properties, making the bacteria more tolerant to antibiotic treatment.<sup>[2]</sup>

Standard delivery of antibiotics is usually untargeted, and will result in distribution of the drugs to all parts of the body. Consequently, the efficacy of the antibiotics may decrease, since reduced concentrations of the antibiotics may reach the actual site of the infection.<sup>[14]</sup> The recalcitrance of infectious biofilms toward antibiotics may be overcome by the use of a local antibiotic delivery system creating a high local concentration, and hence a more effective treatment. In recent years, nanotechnology-based drug delivery systems such as mesoporous silica nanoparticles, polymeric nanoparticles, and liposomes have been broadly studied as antibiotic carriers facilitating penetration and ultimately killing of infectious biofilms.<sup>[13]</sup> However, many of these formulations suffer from poor storage stability,<sup>[13]</sup> versatility may be limited and usage depends on the properties of the active pharmaceutical drug, that is, charge, size, and hydrophilicity. Microfabricated drug delivery devices have shown promise toward increasing local drug concentration,<sup>[15,16]</sup> and might as well be a suitable system for delivering antibiotics to specific sites of infection. One of such devices is a microcontainer, which is a micrometer sized polymeric device mainly developed for oral delivery of therapeutics.<sup>[17]</sup> Microcontainers have proven to be able to improve oral bioavailability of small drugs, most likely due to the fact that microcontainers have mucoadhesive properties and are engulfed within the intestinal mucus.<sup>[18,19]</sup> In addition, microcontainers have the benefit of being very versatile and can be used for delivery of any active pharmaceutical ingredient no matter size, charge, or hydrophilicity. The microcontainers can be functionalized by applying a polymeric lid onto the cavity of drug-loaded microcontainers.<sup>[20]</sup> Polymers with different properties can be used, for example, to control the drug release profiles, to achieve additional mucoadhesive or mucus penetrating effects, and/or to provide additional antibacterial activity. Polyethylene glycol (PEG) is an uncharged hydrophilic polymer

that has been shown to possess either mucoadhesive or mucus penetrating properties, depending on the surface density and the molecular weight.<sup>[21,22]</sup> Wang et al. documented improved mucus penetration of polystyrene nanoparticles coated with low molecular weight (MW) PEG, whereas higher MW PEG improved mucoadhesion.<sup>[23]</sup> Chitosan is a cationic polysaccharide that has been widely explored as a mucoadhesive polymer. In addition, it provides controlled drug release, prolonging the therapeutic effect of the drug,<sup>[24,25]</sup> and has also been reported to possess antimicrobial properties.<sup>[26]</sup> Previously, the inhibitory effect of chitosan solutions and nanoparticles without antibiotics against *P. aeruginosa* clinical isolates in planktonic and biofilm conditions was investigated, and it was shown that planktonic bacteria were more effectively eradicated than biofilm-associated bacteria.<sup>[27]</sup> Eudragit S100 is an anionic co-polymer widely used for pH-responsive formulations as it dissolves at pH values above 7.<sup>[28,29]</sup> It has previously been reported that using Eudragit microparticles for antibiotic delivery caused a significant reduction in adherent methicillin-resistant *Staphylococcus aureus* compared to treatment with free antibiotics.<sup>[30]</sup>

The aim of this study is to investigate the potential impact of using microcontainers in the treatment of *P. aeruginosa* biofilms. The microcontainers are suggested to adhere to the biofilm and release the loaded ciprofloxacin in a controlled and localized manner. Ciprofloxacin-loaded microcontainers were coated with polymeric lids of PEG, chitosan, and Eudragit S100. Together with investigating the drug release, the resulting antimicrobial activity obtained from the functionalized microcontainers were tested on planktonic bacterial cells as well as on biofilm consortia of *P. aeruginosa* (PAO1) and compared to delivery of unconfined antibiotic.

## 2. Results and Discussion

### 2.1. Loading of Antibiotic into Microcontainers and Lid Depositing

Microcontainers (Figure 1A; Figure S1, Supporting Information) with an inner diameter of  $232 \pm 1 \mu\text{m}$  and an inner height of  $214 \pm 3 \mu\text{m}$  (mean  $\pm$  SD,  $n = 3$ ) were produced and successfully loaded with  $2.75 \pm 0.48 \text{ mg}$  ( $n = 44$  chips, mean  $\pm$  SD) ciprofloxacin hydrochloride (CIP) per chip corresponding to  $4.39 \pm 0.77 \mu\text{g}$  in each microcontainer. The loaded microcontainers were visualized using scanning electron microscopy (SEM), which confirmed efficient loading (Figure 1B). Following the drug loading, the microcontainers were coated on the cavity

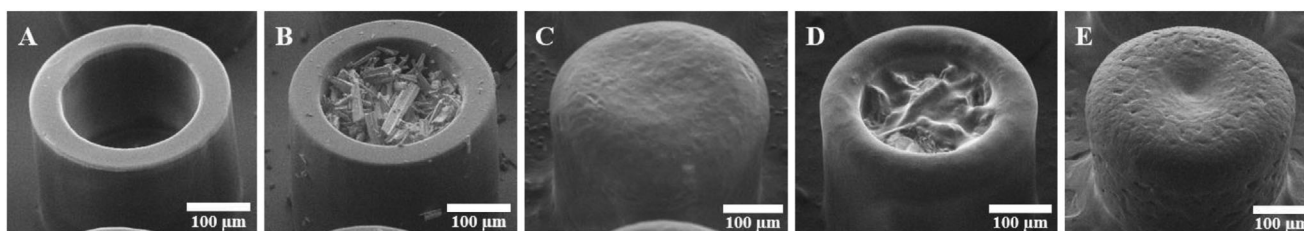


**Figure 1.** Scanning electron microscopy (SEM) images of a microcontainer A) empty, B) loaded with ciprofloxacin hydrochloride (CIP), C) coated with polyethylene glycol (PEG), D) coated with chitosan, and E) coated with Eudragit S100.

with either PEG, chitosan, or Eudragit S100, and the height and morphology of the spray coated lids were characterized by profilometry and SEM. Coating with PEG resulted in a uniform lid (Figure 1C), which was also confirmed by profilometry measurements revealing a low surface roughness and a coating thickness of  $32.4 \pm 1.9 \mu\text{m}$  (mean  $\pm$  SD,  $n = 3$ ). Mazzoni et al. reported a coating thickness of  $17.0 \pm 5.6 \mu\text{m}$  when coating microcontainers using 0.7% w/v PEG dissolved in dichloromethane.<sup>[20]</sup> In this study, 2.66% w/v of PEG has been utilized with water as solvent, and it was observed that these changes increased the coating thickness with a factor two. The chitosan coating (Figure 1D) resulted in the thinnest lid among the three polymers, since the polymer concentration was lower and the spray coating parameters were different. The chitosan lid did not cover the open cavity of the microcontainer completely, and structures of the CIP crystals were still visible. However, we aimed for a thin layer as chitosan is hygroscopic and quickly swells when in contact with water, hence creating a hydrogel lid affecting the release of CIP.<sup>[31,32]</sup> The thickness of the chitosan coating was  $8.9 \pm 0.7 \mu\text{m}$  (mean  $\pm$  SD,  $n = 6$ ), in accordance with previously reported heights.<sup>[20]</sup> Eudragit S100 coating was shown to cover the entire opening of the microcontainer and to be homogeneously distributed (Figure 1E), and the height was  $25.0 \pm 5.3 \mu\text{m}$  (mean  $\pm$  SD,  $n = 6$ ).

## 2.2. In Vitro Release of Ciprofloxacin Hydrochloride from Microcontainers

The release of CIP from uncoated and coated microcontainers was evaluated in a modified minimal medium, FAB medium.<sup>[33]</sup> When no coating was applied onto the microcontainers, it appears that two types of release kinetics apply. Within the first minute an initial burst release of  $42.1 \pm 4.5\%$  of CIP occurred, followed by 7 h sustained release before reaching a plateau (Figure 2A). Applying a PEG lid on the microcontainers resulted in a lower initial release ( $31.5 \pm 1.9\%$  CIP released from PEG-coated microcontainers after 10 min compared to  $44.7 \pm 4.9\%$  CIP released from uncoated microcontainers). However, after 90 min no significant differences in the release profiles were observed (Figure 2A). This is consistent with PEG being a water-soluble polymer,<sup>[34]</sup> which quickly solubilizes in the aqueous FAB medium. Chitosan coating gave rise to an initial release of  $25.9 \pm 5.6\%$  CIP after 90 min, followed by a subsequent sustained release with  $99.5 \pm 9.1\%$  being released after 28 h (Figure 2B). In accordance, it has previously been shown that chitosan nanoparticles also provide a burst release of CIP followed by a sustained release behavior.<sup>[35]</sup> SEM images confirmed swelling and after 28 h the hydrogel was still present on the microcontainers (data not shown), presumably due to the limited solubility of chitosan at physiological pH.<sup>[32]</sup> The sustained release profiles are likely caused by a slow but constant diffusion of entrapped CIP through the chitosan hydrogel. Eudragit S100 was included as a coating to provide protection of CIP until the microcontainers had reached the biofilm growing bacteria in the flow cell system, and fast release could be induced by increasing the pH of the FAB medium. As can be seen from Figure 2C, the coating was kept intact for up to 15 min, and release was triggered when increasing the pH from 6.8 to 7.4. This is in accordance with Eudragit S100 being

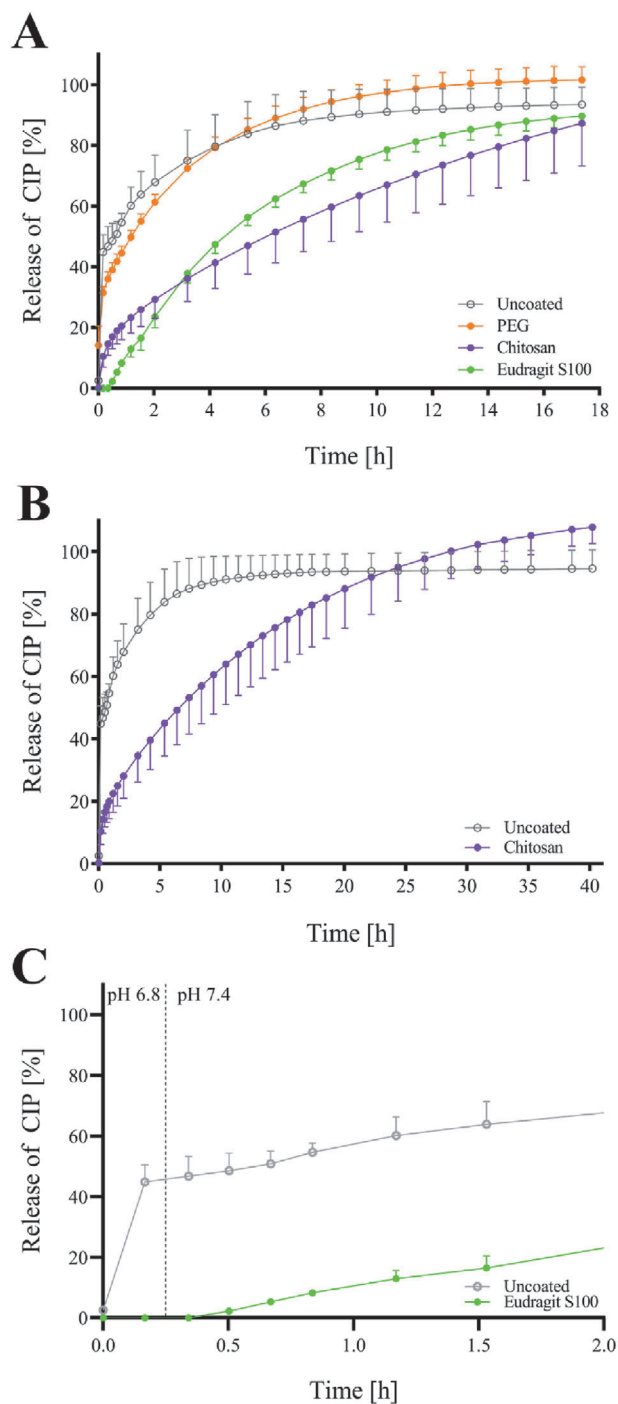


**Figure 2.** In vitro cumulative release of ciprofloxacin hydrochloride (CIP) from microcontainers in FAB medium as a function of time. A) Uncoated microcontainers compared to microcontainers coated with polyethylene glycol (PEG), chitosan, or Eudragit S100. Release differed significantly from uncoated microcontainers until  $t = 90$  min (PEG),  $t = 11$  h (Eudragit S100), and  $t = 13$  h (chitosan). B) Zoom-out depicting the release of CIP during 40 h with chitosan coating. C) Magnified view showing the initial release of CIP with Eudragit S100 coating. In experiments with Eudragit S100 the chips were placed in FAB medium at pH 6.8 for 15 min followed by immersion in FAB medium at pH 7.4. Data are presented as mean  $\pm$  SD ( $n = 3-6$ ) and an unpaired  $t$ -test was applied for determination of significant difference (with statistical significance defined as  $p < 0.05$ ).

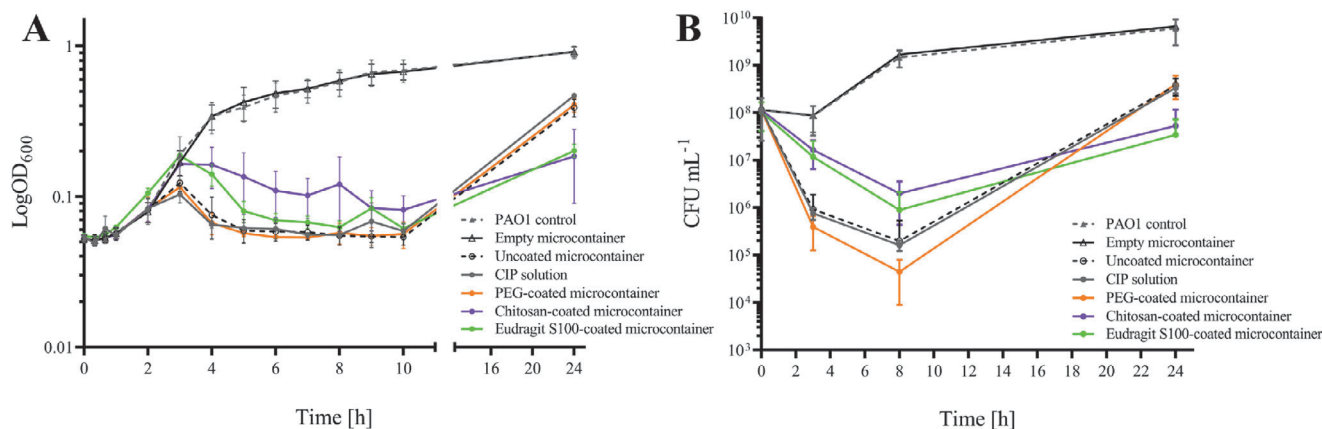


**Figure 3.** Impact of the microcontainers on planktonic growth inhibition of PAO1 cells. A) Measurement of the optical density (log OD<sub>600</sub>) as a function of time. Significant difference after  $t = 3$  h (CIP solution; uncoated; PEG) and  $t = 4$  h (chitosan, Eudragit S100) when compared to PAO1 control growth. B) Viable counts measured as CFU mL<sup>-1</sup> as a function of time. Color codes represent microcontainers loaded with ciprofloxacin hydrochloride (CIP) and coated with polyethylene glycol (PEG), chitosan, or Eudragit S100. Controls include PAO1 growth control without microcontainer addition, empty microcontainers, uncoated microcontainers as well as CIP in solution. Data are depicted as mean  $\pm$  SD ( $n = 3-4$ ) and one-way ANOVA with Tukey's multiple comparison was applied for determination of significant difference (with statistical significance defined as  $p < 0.05$ ).

solubilized at pH values above 7.<sup>[29]</sup> To facilitate inoculation of the microcontainers into a flow cell system, they were shortly embedded in a gelatin hydrogel at pH 6.8. The release data support that the lid was kept intact during the time in the hydrogel, and that release was triggered in the growth medium with a pH of 7.4. However, the release of CIP from Eudragit S100-coated microcontainers was sustained, with only  $46.1 \pm 3.0\%$  being released after 4 h and  $90.2 \pm 2.8\%$  after 18 h. This complies with previous findings in the literature, observing that albumin-containing microspheres coated with Eudragit S100 showed a sustained release in intestinal pH reaching complete release after 16 h.<sup>[36]</sup>

### 2.3. Impact of Microcontainers on Planktonic Growth of PAO1 Cells

The impacts of empty, CIP-loaded and polymer-coated microcontainers on bacterial growth inhibition were determined from addition of these to planktonic PAO1 cultures. Bacterial growth inhibition observed for CIP-loaded uncoated and PEG-coated microcontainers, respectively, differed significantly after 3 h from the PAO1 control growth ( $p$  value  $\leq 0.0017$ ), whereas CIP mediated bacterial growth inhibition with chitosan and Eudragit S100, respectively, differed significantly from control after 4 h ( $p$  values  $\leq 0.0013$ ; **Figure 3A**). These results align with the release data (cf. **Figure 2**), in which only limited differences in release profiles were observed for uncoated and PEG-coated microcontainers, whereas delayed releases of CIP were observed for both chitosan and Eudragit S100. Addition of all loaded and polymer-coated microcontainers led to reductions in viable counts of PAO1, reaching the lowest bacterial viability after 8 h of treatment with viable counts reduced from  $\approx 10^9$  colony forming units (CFU) mL<sup>-1</sup> (control) to between  $10^4-10^6$  CFU mL<sup>-1</sup> (**Figure 3B**). The increase of OD<sub>600</sub> during the first 3 h after addition of the microcontainers seemingly conflicts with the decrease in CFU during this period. We suggest that this "conflict" is a reflection of a reduced plating efficiency of the treated bacteria,

which shows that although the antibiotic exerts its inhibitory effect of reducing viability of the bacteria, it takes time to stop increase of the optical density. This increase most likely reflects that the cells may continue to grow in size without dividing and quickly lose the capacity to form colonies on plates. The delayed cell lysis is observed later as a decrease in OD<sub>600</sub>. After 24 h, regrowth of viable cells was observed in all treated cultures, reaching an average of  $1.73 \times 10^8$  CFU mL<sup>-1</sup> (**Figure 3B**). Regrowth may be due to a subpopulation of resistant cells not affected by the applied CIP concentrations. The empty microcontainers had no effect on growth of PAO1 cells (**Figure 3A,B**). Treating the planktonic bacterial suspension with 20  $\mu$ L of a 0.22 mg mL<sup>-1</sup> CIP solution (same amount as confined in one microcontainer) resulted in identical growth inhibition (**Figure 3A,B**), proving that administration of CIP in microcontainers did not decrease the efficacy of the antibiotic toward planktonic suspensions of PAO1.

### 2.4. Impact of Microcontainers on Biofilm Growth of PAO1 Cells

Antibiotics, which normally inhibit growth and kill bacteria in suspended cultures, have been shown to be much less efficient in bacterial biofilms.<sup>[1]</sup> This specific behavior of biofilm bacteria is a serious medical problem, since many infections are characterized by biofilm growth in the human body. Microcontainers potentially may deliver a large dose of antibiotics into close contact with a localized infection, increasing the local concentration of antibiotics, which may improve the chance of eradicating the bacteria in the biofilm. Controlling the release rate by the use of different coatings makes it possible to expose the biofilm to specific concentrations of CIP over time. PAO1 biofilms were allowed to mature for 96 h in flow cell chambers, reaching a biomass of  $5.35 \pm 3.74 \mu\text{m}^3 \mu\text{m}^{-2}$  (**Figure S2**, Supporting Information). Subsequently, microcontainers were successfully introduced into the flow cell biofilm. A bright field image of the top



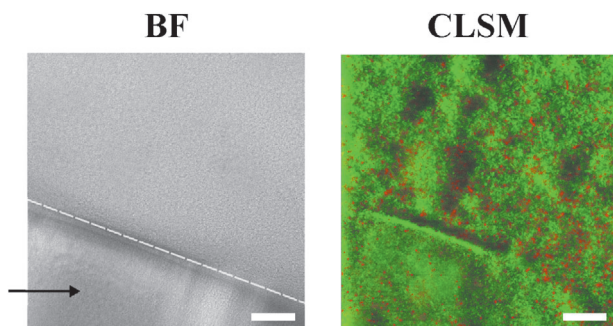


**Figure 4.** Example of a bright field (BF) image of a microcontainer (located below the dotted line and marked with an arrow) and the corresponding confocal laser scanning microscopy (CLSM) image of a 96 h old biofilm after 7 h of treatment with CIP-loaded and polyethylene glycol (PEG)-coated microcontainers. Green represents live GFP fluorescent bacteria. Red represents dead bacteria after PI staining. Scale bar: 30  $\mu\text{m}$ .

of a PEG-coated microcontainer together with a corresponding confocal laser scanning microscopy image is shown in **Figure 4**.

To determine efficacies of PEG-, chitosan-, or Eudragit S100-coated microcontainers on killing of biofilm-associated PAO1 cells, confocal images were acquired at locations in close proximity to the microcontainers (**Figure 5**).

After 2 h of treatment with CIP-loaded microcontainers, containing  $\approx 120 \mu\text{g}$  CIP in total, limited bacterial killing occurred, with an average dead biomass of  $11.1 \pm 14.2\%$ ,  $3.3 \pm 1.5\%$ , and  $8.5 \pm 12.2\%$  for PEG, chitosan, and Eudragit S100 coatings, respectively. At this time point, PEG coating led to the greatest amount of CIP release (61.3%) compared to chitosan and Eudragit S100 (28.1% and 23.6%, respectively) (cf. **Figure 2A**). The differences in amount of released CIP were paralleled by the mean killing of biofilm-associated PAO1 cells after 2 h. Note, however, that utilizing a PEG coating with a faster release did not significantly improve the killing compared to the sustained release achieved with chitosan and Eudragit S100. After 7 h, the dead bacterial fraction increased to  $19.7 \pm 16.2\%$ ,  $23.5 \pm 19.6\%$  and  $13.5 \pm 10.2\%$  for PEG, chitosan and Eudragit S100, respectively. All coatings reduced bacterial motility after 7 h compared to 2 h. In addition, bacterial morphology changed as the bacteria appeared coccoid, a sign of slow growth and starvation.<sup>[37]</sup> At the same time many bacteria appeared extremely elongated indicating that they are stressed and still metabolically active, but cell division is inhibited.<sup>[37]</sup> This observation correlates with the reported mechanism of ciprofloxacin, which interferes with DNA replication and transcription by inhibition of topoisomerase II (also known as DNA gyrase) and topoisomerase IV, thereby inhibiting cell division.<sup>[11]</sup> When planktonic PAO1 cells were treated with coated microcontainers, a significant killing was observed after 8 h (cf. **Figure 3**). Microcontainer therefore had a faster and more effective impact on planktonic cell inhibition, which correlates with previously reported decreased antibiotic tolerance of planktonic bacteria compared to the biofilm-associated cells.<sup>[11]</sup> After treating for 24 h, in which almost all antibiotic had been released from the microcontainers, the live population of PAO1 were significantly reduced and the dead biomass increased to  $75.7 \pm 16.2\%$ ,  $88.2 \pm 5.3\%$ , and  $73.6 \pm 14.8\%$  for PEG, chitosan, and Eudragit S100, respectively.

Altogether, the uncharged PEG coating did not appear to improve the antimicrobial effect compared to the anionic, non-mucoadhesive Eudragit S100 coating, whereas the cationic chitosan coating appeared to be the most promising coating (**Figure 5**). Interestingly, the charge of the polymers did not appear to have any prominent effect on the eradication of the biofilm. Du et al. reported a 3.2-fold increase in elimination of an established *P. aeruginosa* biofilm when treated with PEG-conjugated tobramycin compared to the effect of a solution of the antibiotic.<sup>[38]</sup> Moreover, Suk et al. showed that low MW PEG-coated nanoparticles moved through undiluted cystic fibrosis sputum up to 90-fold faster than uncoated particles, but the penetration of identically coated larger nanoparticles were strongly hindered.<sup>[39]</sup> For this reason, larger particles or devices like the microcontainers coated with PEG are likely to be mostly mucoadhesive, however, this did not improve the bacterial killing as no difference between PEG and Eudragit S100 coating was observed. Chitosan has previously been shown to be mucoadhesive presumably due to hydrogen bonding and ionic interactions with the negatively charged mucins.<sup>[26]</sup> The same mechanism may be relevant in the biofilm, in which the positively charged chitosan can interact with the negatively charged components of the EPS (such as alginate),<sup>[40]</sup> hence increasing adhesion. In addition, Machul et al. reported an inhibitory effect of chitosan on both planktonic as well as biofilm-associated *P. aeruginosa*.<sup>[27]</sup> The chitosan may interact with the negatively charged microbial cell membranes causing leakage of the intracellular components hence cell disintegration.<sup>[24,26]</sup> Both the additional antimicrobial effect as well as improved adhesion might have contributed to the enhanced killing observed when using chitosan coating in this study.

#### 2.4.1. Impact of One Bolus Dose or Constant Perfusion of Ciprofloxacin Hydrochloride on PAO1 Biofilm

To determine whether CIP confined in microcontainers would provide improved killing compared to the same dose of unconfined antibiotic given as one bolus injection, a 96 h old PAO1 biofilm was treated with one bolus dose of  $120 \mu\text{g}$  CIP and images were acquired 2, 7, and 24 h after exposure. After 2 h,  $26.7 \pm 25.4\%$  was found dead and no significant change occurred in the following 24 h (**Figure 6**). In absence of antibiotics, the biofilm biomass showed minimal killing after 24 h as expected. These findings indicate that using the same dose of CIP but confining it in microcontainers improved the in vitro antibacterial properties of CIP significantly.

Moreover, a 96 h old PAO1 biofilm was perfused with CIP in a concentration of  $4 \mu\text{g mL}^{-1}$  for 24 h, corresponding to a total amount of  $330 \mu\text{g}$  CIP delivered to the biofilm. The perfusion resulted in  $82.0 \pm 6.2\%$  killing of the total amount of biomass after 24 h (**Figure 7**). In control chambers, PAO1 cells were still alive and the biomass increased over 24 h as expected. Comparing these results to biofilm treatment with CIP confined in microcontainers (cf. **Figure 5E**), it was found that microcontainers provided bacterial killing similar to a 2.75 times higher concentration of solubilized antibiotic constantly perfused. Therefore, it appears that confining CIP in microcontainers is a promising strategy, providing the same antibacterial effect with a significantly reduced amount of antibiotic.

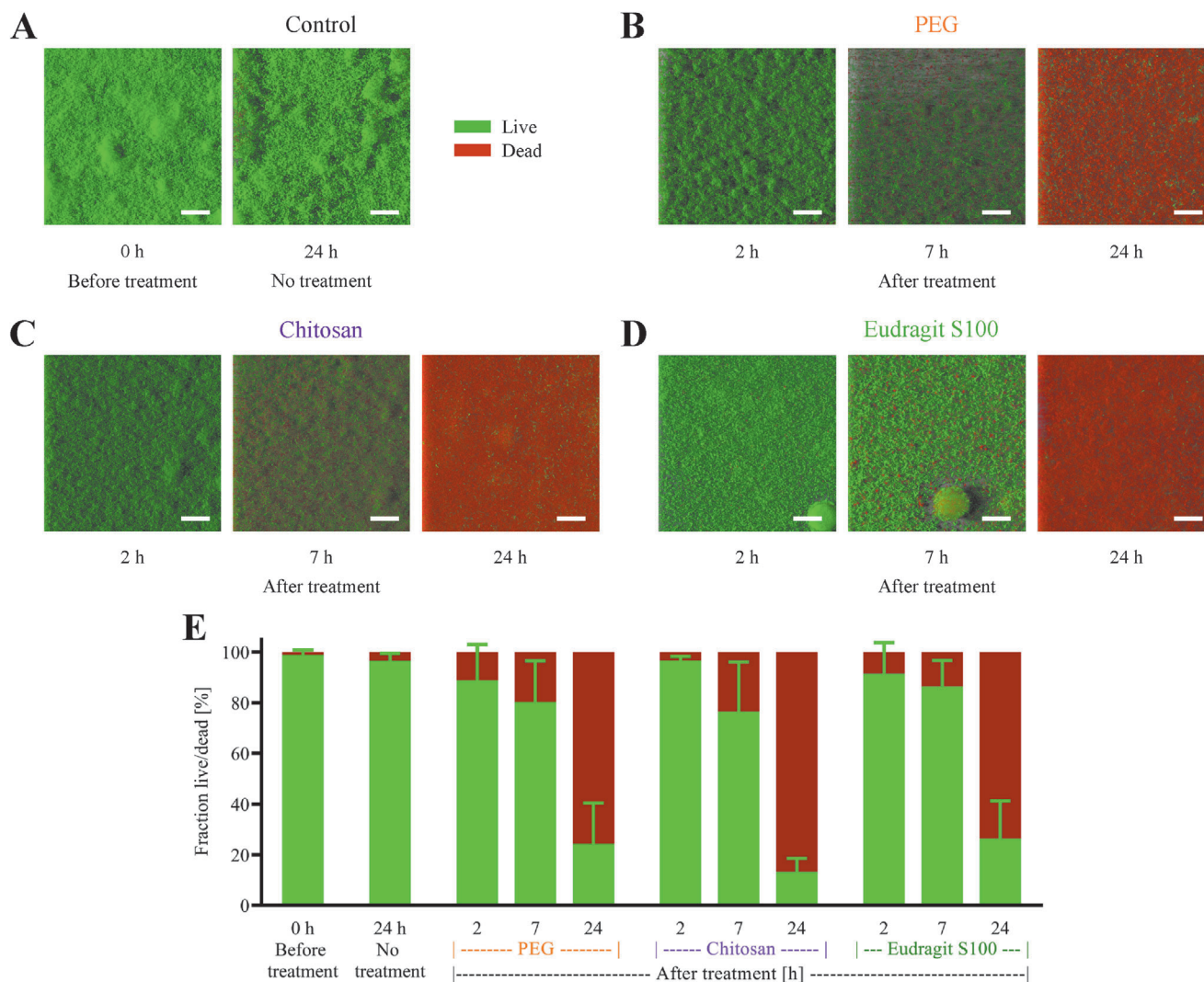


**Figure 5.** PAO1 biofilm grown for 96 h under flow to a mature state, and thereafter exposed to  $\approx 120 \mu\text{g}$  ciprofloxacin hydrochloride (CIP) confined in microcontainers coated with either polyethylene glycol (PEG), chitosan, or Eudragit S100. A–D) Confocal laser scanning microscopy (CLSM) images of mature biofilm before treatment and 2, 7, and 24 h after treatment with polymer-coated microcontainers as well as a 24 h untreated control. Scale bar:  $30 \mu\text{m}$ . E) Quantitative analysis of the biomass ( $\mu\text{m}^3 \mu\text{m}^{-2}$ ) converted to the fraction of live/dead (%). Green represents live bacteria. Red represents dead bacteria. Data are depicted as mean + SD ( $n = 4\text{--}24$ ).

No complete eradication of PAO1 biofilm was observed in any of the treatments tested, since 10–20% of the biomass remained alive despite treatment with CIP confined in microcontainers or as constant perfusion. The remaining fraction might be a subpopulation of antibiotic-tolerant persister cells in a temporary dormant state in which cell division is minimized.<sup>[41,42]</sup> Many antibiotics (including ciprofloxacin) require a certain degree of metabolic activity in the cells to be effective as the mechanism of action often involves disruption of the cellular processes.<sup>[4]</sup> To achieve a full eradication therapy on the biofilm cells with microcontainers, it is possible that delivery of a nutrition-rich compound prior to antibiotic therapy may stimulate bacterial growth, and thus improve the antibiotic efficacy.

Using microcontainers to achieve a site-specific delivery of antibiotics could potentially reduce the required dose, and thereby reduce the risk of resistance development. The local delivery

would also prevent antibiotic exposure in the gastrointestinal tract and its microbiota, thereby decreasing the risk of gastrointestinal side effects often seen for patients needing antibiotics for extended time periods.<sup>[9]</sup> The microcontainers could potentially be used to prevent recurring infections and to treat initial and chronic infections. An additional benefit of the microcontainers is the possibility of personalizing the treatment, by dosing the amount of microcontainers needed for treatment of a certain infection in different patients.

### 3. Conclusion

Microcontainers were successfully loaded with CIP and functionalized with lids of PEG, chitosan, or Eudragit S100. Release profiles from coated microcontainers showed that PEG

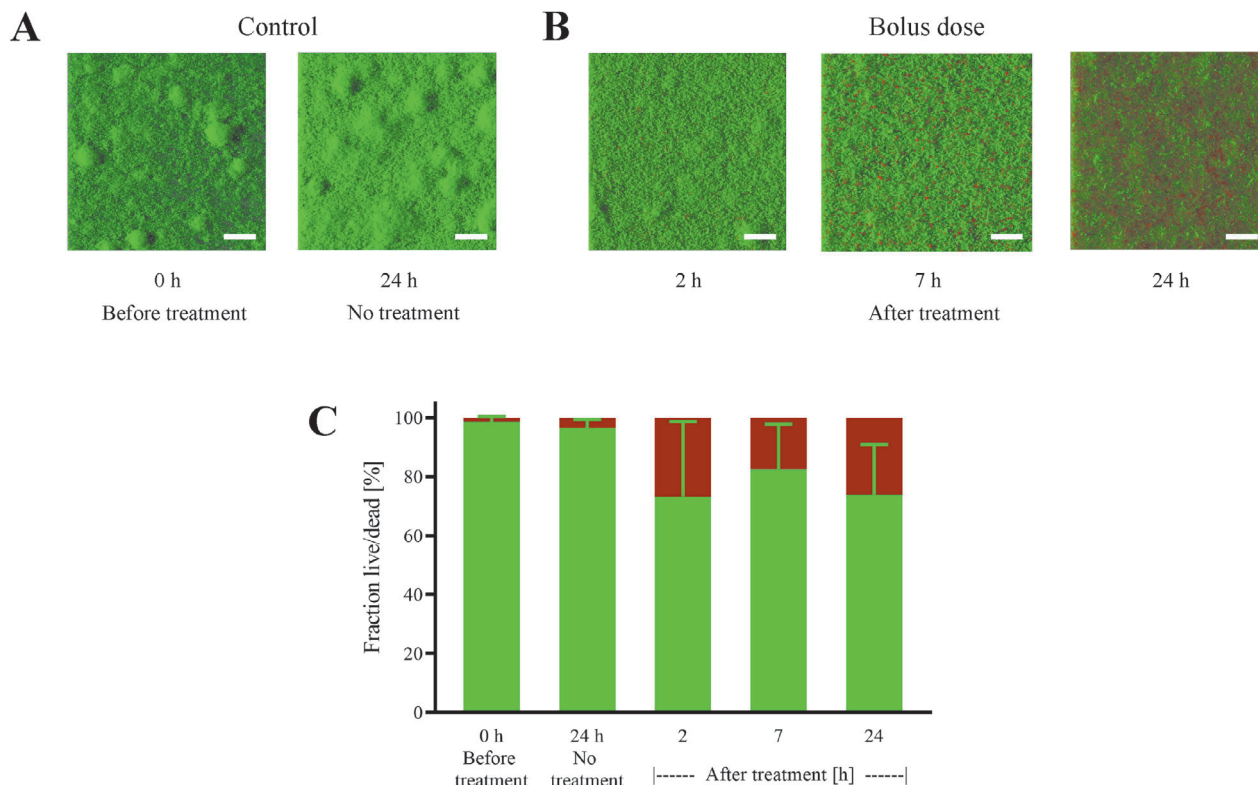


**Figure 6.** PAO1 biofilm grown for 96 h under flow to a mature state and thereafter exposed to one bolus injection of  $60 \mu\text{g mL}^{-1}$  ciprofloxacin hydrochloride (CIP) with a total dose of  $120 \mu\text{g}$ . A,B) Confocal laser scanning microscopy (CLSM) images of the biofilm before treatment and 2, 7, and 24 h after treatment as well as a 24 h control biofilm not treated. Scale bar:  $30 \mu\text{m}$ . C) Quantitative analysis of the biomass ( $\mu\text{m}^3 \mu\text{m}^{-2}$ ) converted to the fraction of live/dead (%). Green represents live bacteria. Red represents dead bacteria. Data are depicted as mean + SD ( $n = 3$ ).

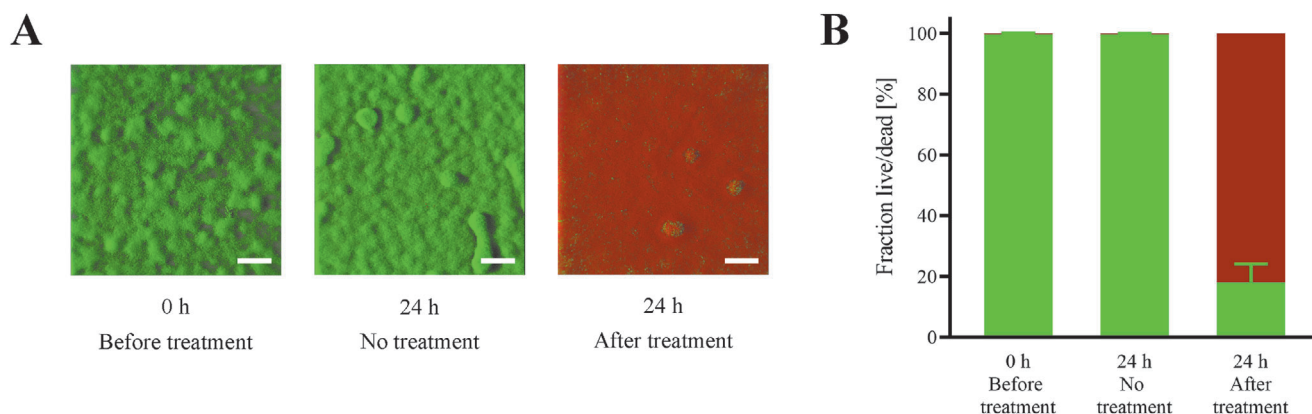


**Figure 7.** PAO1 biofilm grown for 96 h under flow to a mature state and thereafter exposed to perfusion of  $4 \mu\text{g mL}^{-1}$  ciprofloxacin hydrochloride (CIP) for 24 h corresponding to a total amount of  $330 \mu\text{g}$  CIP delivered to the biofilm. A) Confocal laser scanning microscopy (CLSM) images of the biofilm before treatment, after 24 h with no treatment, and after 24 h treatment with CIP. Scale bar:  $30 \mu\text{m}$ . B) Quantitative analysis of the biomass ( $\mu\text{m}^3 \mu\text{m}^{-2}$ ) converted to the fraction of live/dead (%). Green represents live bacteria. Red represents dead bacteria. Data are depicted as mean + SD ( $n = 5$ ).

facilitated a faster release of CIP, whereas Eudragit S100 and chitosan gave rise to a sustained release. All antibiotic containing microcontainers inhibit planktonic growth of PAO1 cells, but the degree of inhibition depends on the choice of coating. Treating a mature PAO1 biofilm with a bolus dose of CIP only resulted in killing of a  $26.1 \pm 16.9\%$  of the biofilm cells after 24 h. The same dose confined in coated microcontainers killed  $75.7 \pm 16.2\%$ ,

$88.2 \pm 5.3\%$ , and  $73.6 \pm 14.8\%$  of the biomass in close proximity to the microcontainer, when using PEG, chitosan, and Eudragit S100 coatings, respectively. Microcontainers provided bacterial killing similar to a 2.75 times higher concentration of solubilized antibiotic constantly perfused. This proves that using microcontainers as a delivery system for antibiotic treatment of biofilm-associated infections could be a promising new strategy.



## 4. Experimental Section

**Fabrication of Microcontainers:** Microcontainers were fabricated on silicon wafers as previously described with two-steps of photolithography using the negative epoxy-based photoresist SU-8.<sup>[43]</sup> Silicon wafers (4-in. b100N n-type) were supplied by Okmetic, Vantaa, Finland, whereas SU-8 2075 and SU-8 developer were purchased from Microresist Technology GmbH (Berlin, Germany). For biofilm assays, the microcontainers were fabricated on top of a fluorocarbon coated silicon wafer enabling detachment of single microcontainers from the wafer,<sup>[44]</sup> whereas for the other studies, the microcontainers were fabricated directly on the silicon wafer.<sup>[43]</sup> The wafers with the fabricated microcontainers were cut into chips of 12.8 × 12.8 mm<sup>2</sup> containing 625 microcontainers on each chip, using a laser cutter (microSTRUCT vario, 3D Microac AG, Chemnitz, Germany). The dimensions of the microcontainers were measured on an Alpha-Step IQ Stylus Profilometer (KLA-Tencor Corporation, Milpitas, USA).

**Loading Ciprofloxacin Hydrochloride in Microcontainers:** A mask was used to cover the gaps between the microcontainers to allow only drug loading in the cavity of the microcontainers.<sup>[45]</sup> The microcontainers were then manually loaded with CIP (Fagron, Uitgeest, The Netherlands) by distributing powder over a chip with microcontainers using a small brush. The mask was gently removed after loading and any excess of drug in between the microcontainers was removed with pressurized air. The chips with microcontainers were weighed before and after loading to determine the amount of drug loaded into the microcontainers

**Deposition of a Lid on Ciprofloxacin Hydrochloride-Loaded Microcontainers:** The microcontainers were coated with three different lids of either PEG, chitosan, or Eudragit S100. A 2.66% w/v solution of low molecular weight 11–15 kDa PEG (Sigma-Aldrich, St. Louis, USA) in water was made. The chitosan solution was prepared in a 0.5% w/v concentration by dissolving low molecular weight chitosan (12 kDa, 75–85% deacetylated, Sigma-Aldrich, St. Louis, USA) in 0.1 M acetic acid (Sigma-Aldrich, St. Louis, USA). After dissolving, the chitosan solution was filtered using a 5–13 μm filter with vacuum suction. A solution of 1% w/v Eudragit S100 (Evonik Industries, Darmstadt, Germany) and 5% w/w in relation to the polymer of dibutyl sebacate (Sigma Aldrich, St. Louis, USA) was dissolved in isopropanol (Honeywell, Muskegon, USA). The solutions were sprayed on top of the CIP-loaded microcontainers using a spray coating system equipped with an ultrasonic nozzle actuated at 120 kHz (ExactaCoat, Sono Tek, USA). The nozzle of the spray coater moved across the microcontainer chip in a x–y path covering the area of the chip. One loop corresponded to the nozzle moving across the sample twice, with an offset of 2 mm in the x direction the second time as the beam diameter was 4 mm. Z-distance represents the distance between the spray nozzle and the sample (Table 1).

The thickness of the coatings was evaluated using a contact profilometer (Alpha-Step IQ Stylus Profilometer, KLA-Tencor, Corporation, Milpitas, USA). Each of the polymers was sprayed on top of a flat silicon chip covered with a layer of SU-8. Half of the chip was covered by a glass cover slip hence, enabling coating of only half a chip suitable for height evaluation.

**Table 1.** Parameters used for ultrasonic spray coating with either 2.66% w/v polyethylene glycol (PEG), 0.5% w/v chitosan, or 1% w/v Eudragit S100 applied on ciprofloxacin hydrochloride (CIP)-loaded microcontainers.

Coating parameters	PEG	Chitosan	Eudragit S100
Path speed [mm s <sup>-1</sup> ]	20	25	10
Infusion rate [mL min <sup>-1</sup> ]	0.1	0.1	0.1
Generator power [W]	1.3	1.3	2.2
Shaping air pressure [kPa]	0.02	0.03	0.02
Heat plate temperature [°C]	40	50	40
Z-distance from nozzle to sample [cm]	6.0	5.5	3.0
No. of loops	150	120	30

The height profiles were measured using an 8 mg tip force with a scan speed of 50 μm s<sup>-1</sup> and a sampling rate of 50 Hz. Measurements were conducted at three different locations on each coated chip and presented as mean ± SD.

**Scanning Electron Microscopy of the Microcontainers:** The quality of the loading and the coating was evaluated using a tabletop SEM (Hitachi High-Technologies Europe GmbH, Krefeld, Germany). The chips with microcontainers were placed on a 30° tilted holder and SEM images were acquired using the scattered electron (SE) detector and an accelerating voltage of 15 kV for highest quality images.

**In Vitro Release of Ciprofloxacin Hydrochloride from Microcontainers:** The in vitro release of CIP from the microcontainers was measured using a μDiss Profiler (Pion Inc. Woburn, MA, USA) at a constant temperature of 37 °C. Stirring rate was kept at 100 RPM and the absorbance was measured in situ at 350 nm. The path length of the UV probes was 5 mm. Each probe of the μDiss was calibrated prior to each release study. Each chip with CIP-loaded microcontainers was attached to cylindrical magnetic stirrers with carbon tape and placed in a glass vial. Modified FAB medium was prepared as described in Table S1, Supporting Information, with a pH of 6.8 and pH 7.4. The chips were covered with 20 mL of FAB medium with pH 6.8 and CIP release from microcontainers was measured for 18–40 h depending on the polymer coating. For Eudragit S100, the chips were placed in FAB medium at pH 6.8 for 15 min and subsequently, in FAB medium adjusted to pH 7.4. The percentage of drug release at each time point was calculated from the known amount of drug loaded per chip and presented as mean ± SD. The release studies were in 3–6 replicates for uncoated microcontainers and microcontainers coated with either PEG, chitosan, or Eudragit S100.

**Bacterial Strain and Media Preparation:** *P. aeruginosa* PAO1 was genetically modified to express green fluorescent protein (GFP) constitutively by insertion into a neutral intergenic region in the genome with no impact on the cell growth physiology.<sup>[6,46,47]</sup> An overnight culture of PAO1 was prepared from a –80 °C stock by inoculating a small amount into 5 mL LB and allowing growth until stationary phase for 12–16 h at 37 °C at 150 RPM. Plate assays were conducted in LB medium. Biofilms were grown in modified FAB minimal medium with trace metals suitable for PAO1 growth and with glucose as the only carbon source (Table S1, Supporting Information).<sup>[33]</sup>

**Planktonic Growth of PAO1 and Growth Inhibition Testing:** To study the ability of microcontainers to inhibit bacterial growth, a PAO1 overnight culture was diluted to an optical density (OD<sub>600</sub>) of 0.05 in 20 mL of LB medium adjusted to pH 6.8, except when used with Eudragit S100 where pH was pH 7.4. One microcontainer either being empty or loaded with CIP or loaded with CIP and coated with PEG, chitosan, or Eudragit S100 was added to each flask. For the control with CIP in solution, 20 μL of a 0.22 mg mL<sup>-1</sup> CIP solution was added to the flask. The flasks were placed in a 37 °C incubator at 150 RPM. Samples were taken at selected time points between 20 min and 24 h after introduction of the microcontainer. Bacterial density was monitored using OD measurements at 600 nm on an automated plate reader (Synergy H1, BioTek, USA). Viable counts were obtained after 3, 8 and 24 h by serial dilution followed by spot plating on LB agar plates. The plates were left to incubate overnight at 37 °C and CFU were counted the following day.

**Setup of Flow System to Grow Biofilms:** Biofilms of PAO1 were grown at 37 °C under laminar flow in flow chambers at 58.4 μL min<sup>-1</sup> with a 16-channel Watson Marlow pump as described by Tolker–Nielsen et al.<sup>[48]</sup> However, the flow cells were slightly modified implementing an inlet channel on the side of the flow chamber to allow inoculation of the microcontainers. Sterilization of the flow system was performed by pumping 1 L of 0.5% v/v hypochlorite through the system over a period of 4 h followed by a cleaning procedure with filling and emptying the system three times with 2 L of autoclaved MilliQ water. Thereafter, the system was filled with FAB medium at pH 6.8 and left with a flow of 58.4 μL min<sup>-1</sup> overnight to allow saturation of the tubings with the medium. The medium flow in the system was stopped and inlet was clamped to avoid backflow. The inlet silicone tube was wiped with 70% v/v ethanol and 250 μL of a diluted overnight culture (with 0.9% NaCl to OD<sub>600</sub> of 0.05) was inoculated carefully into the flow chamber. The inlet needle hole was wiped with ethanol and

resealed with a thin layer of silicone glue. To allow the bacteria to attach to the glass surface the flow chambers were left for 1 h without flow before medium flow was resumed. Bacterial biofilms were allowed to develop for 96 h before antibiotic treatment.

**Treating PAO1 Biofilm with Ciprofloxacin Hydrochloride Confined in Coated Microcontainers:** For inoculation of microcontainers, a solution of 2.5% w/v gelatin (Sigma-Aldrich Chemie GmbH, Steinheim, Germany) was used to allow the microcontainer to be dispersed in the syringe instead of sticking to the walls. The gelatin was weighed into sterile tubes and dissolved in 100 mM phosphate-buffered saline (adjusted to pH 6.8) in a water bath at 37 °C and 100 RPM. For sterilization purposes, chloroform (Sigma-Aldrich, St. Louis, USA) was added to the gelatin solution with a final concentration of 0.5% v/v. The tubes were stored at room temperature. Chloroform evaporation was allowed and the microcontainers coated with either PEG, chitosan, or Eudragit S100 were added to the gelatin just prior to the experiment. Microcontainers loaded with  $\approx 120 \mu\text{g}$  CIP in total were introduced into the flow cell and the system was left without flow for 15 min before starting the flow again. In Eudragit S100 channels the pH of the medium was increased to 7.4. Images used for quantification purposes were acquired at a distance of 140–320  $\mu\text{m}$  from the open side of the microcontainer, as the presence of the microcontainer in the image would interfere with the quantitative COMSTAT analysis (see Microscopy Parameters, Image Acquisition, and Analysis).

**Treating PAO1 Biofilm with Unconfined Ciprofloxacin Hydrochloride as Bolus Dose or as Constant Perfusion:** A 96 h old PAO1 biofilm was treated with unconfined CIP in two ways: 1) as a single bolus dose or 2) as a constant perfusion. When treated with one bolus dose, the tubing after the bubble traps were clamped off and 2 mL of a 60  $\mu\text{g mL}^{-1}$  CIP solution were introduced into the system, corresponding to a total dose of 120  $\mu\text{g}$  of CIP. Tubings were afterward sealed with silicone. For the perfusion study, the medium bottle was changed with a medium bottle containing 4  $\mu\text{g mL}^{-1}$  of CIP and medium in bubble traps was exchanged with antibiotic-containing medium. The biofilm was treated for 24 h corresponding to a total delivered dose of 330  $\mu\text{g}$ .

**Microscopy Parameters, Image Acquisition, and Analysis:** Microscopic observations of bacterial biofilms and microcontainers were completed using an inverted Leica TCS SP8 confocal laser scanning microscope (Mannheim, Germany) equipped with an argon/krypton laser and detectors and filter sets for simultaneous monitoring of GFP (excitation: 488 nm, emission: 493–558 nm) for live cell imaging and propidium iodide (excitation: 543 nm, emission: 558–700 nm) for dead cell staining. Sequential line scanning was used to avoid cross talk. Images were obtained using an HC PL Apo CS2 63 $\times$  oil objective (numerical aperture 1.4). Propidium iodide was injected into the top of the bubble traps and allowed to flow into the flow chambers for 10 min prior to image acquisition. Images were acquired with z-intervals of 1  $\mu\text{m}$ . As control, six biological experiments were performed acquiring two images (technical replicates) of non-treated biofilm in each experiment at random positions within the flow cell to account for any heterogeneity within the biofilm. Stacked images were generated using Imaaris software (Version 7.7.1, Bitplane AG, Zürich, Switzerland). Volume of biomass was calculated using the image-analysis COMSTAT version 2.1 software.<sup>[33,49]</sup> Graphs depicting the fraction of live/dead biomass were generated by calculating the percentage of live/dead in relation to the total biomass measured either before treatment (0 h), after 24 h without treatment as control, or 2, 7 and 24 h after treatment.

**Statistical Analysis:** Data are expressed as the mean  $\pm$  SD unless otherwise noted. For comparison of two individual mean values an unpaired *t*-test was applied, whereas a one-way ANOVA with Tukey's multiple comparison was used if more than two mean values were compared. Graphs and tests were conducted in GraphPad Prism (Version 8.0.1, GraphPad Software, CA, USA) and *p*-values were considered statistically significant when below 5% ( $p < 0.05$ ).

## Supporting Information

Supporting Information is available from the Wiley Online Library or from the author.

## Acknowledgements

The authors would like to acknowledge the Center for Intelligent Drug Delivery and Sensing Using Microcontainers and Nanomechanics (IDUN) whose research is funded by the Danish National Research Foundation (DNRF122) and Villum Foundation (Grant No. 9301). Micro- and nanofabrication specialist Lasse Højlund Eklund Thamdrup, DTU Health Tech is thanked for help with fabrication of the microcontainers. Furthermore, Associate Professor Claus Sternberg, DTU Bioengineering is greatly acknowledged for providing access to the confocal laser scanning microscope as well as help with the quantitative program Comstat. In addition, Nanna Bild, DTU Health Tech is acknowledged for her kind help with drawing of the graphical abstract. Helle Krogh Johansen was supported by The Novo Nordisk Foundation as a clinical research stipend (NNF12OC1015920), by Rigshospitalets Rammebevilling 2015–17 (R88-A3537), by Lundbeck-fonden (R167-2013-15229), by Novo Nordisk Fonden (NNF15OC0017444, NNF18OC0052776), by RegionH Rammebevilling (R144-A5287), and by Independent Research Fund Denmark/Medical and Health Sciences (FSS-4183-00051, DFF-9039-00037A).

## Conflict of Interest

The authors declare no conflict of interest.

## Keywords

bacterial biofilm, ciprofloxacin, drug delivery, microdevices, polymeric coatings

Received: December 12, 2019

Revised: March 4, 2020

Published online:

- [1] D. Davies, *Nat. Rev. Drug Discovery* **2003**, *2*, 114.
- [2] N. Høiby, T. Bjarnsholt, M. Givskov, S. Molin, O. Ciofu, *Int. J. Antimicrob. Agents* **2010**, *35*, 322.
- [3] J. W. Costerton, P. S. Stewart, E. P. Greenberg, *Science* **1999**, *284*, 1318.
- [4] L. Hall-Stoodley, J. W. Costerton, P. Stoodley, *Nat. Rev. Microbiol.* **2004**, *2*, 95.
- [5] M. Burmølle, T. R. Thomsen, M. Fazli, I. Dige, L. Christensen, P. Homøe, M. Tvede, B. Nyvad, T. Tolker-Nielsen, M. Givskov, C. Moser, K. Kirketerp-Møller, H. K. Johansen, N. Høiby, P. Ø. Jensen, S. J. Sørensen, T. Bjarnsholt, *FEMS Immunol. Med. Microbiol.* **2010**, *59*, 324.
- [6] C. K. Stover, X. Q. Pham, A. L. Erwin, S. D. Mizoguchi, P. Warrenner, M. J. Hickey, F. S. Brinkman, W. O. Hufnagle, D. J. Kowalik, M. Lagrou, R. L. Garber, L. Goltry, E. Tolentino, S. Westbrock-Wadman, Y. Yuan, L. L. Brody, S. N. Coulter, K. R. Folger, A. Kas, K. Larbig, R. Lim, K. Smith, D. Spencer, G. K. Wong, Z. Wu, I. T. Paulsen, J. Reizer, M. H. Saier, R. E. Hancock, S. Lory, M. V. Olson, *Nature* **2000**, *406*, 959.
- [7] P. Markou, Y. Apidianakis, *Front. Cell. Infect. Microbiol.* **2014**, *3*, 1.
- [8] I. Y. Hwang, E. Koh, A. Wong, J. C. March, W. E. Bentley, Y. S. Lee, M. W. Chang, *Nat. Commun.* **2017**, *8*, 1.
- [9] S. Kłodzińska, P. Priemel, T. Rades, H. Mørck Nielsen, *Int. J. Mol. Sci.* **2016**, *17*, 1688.
- [10] R. Osman, P. L. Kan, G. Awad, N. Mortada, A. E. El-Shamy, O. Alpar, *Int. J. Pharm.* **2013**, *449*, 44.
- [11] K. J. Aldred, R. J. Kerns, N. Osheroff, *Biochemistry* **2014**, *53*, 1565.
- [12] X. Li, Y. C. Yeh, K. Giri, R. Mout, R. F. Landis, Y. S. Prakash, V. M. Rotello, *Chem. Commun.* **2015**, *51*, 282.
- [13] Y. Liu, L. Shi, L. Su, H. C. Van der Mei, P. C. Jutte, Y. Ren, H. J. Busscher, *Chem. Soc. Rev.* **2019**, *48*, 428.

- [14] T. Bjarnsholt, P. Ø. Jensen, M. J. Fiandaca, J. Pedersen, C. R. Hansen, C. B. Andersen, T. Pressler, M. Givskov, N. Høiby, *Pediatr. Pulmonol.* **2009**, *44*, 547.
- [15] J. R. Jørgensen, M. L. Jepsen, L. H. Nielsen, M. Dufva, H. M. Nielsen, T. Rades, A. Boisen, A. Müllertz, *Eur. J. Pharm. Biopharm.* **2019**, *143*, 98.
- [16] K. M. Ainslie, C. M. Kraning, T. A. Desai, *Lab Chip* **2008**, *8*, 1042.
- [17] L. H. Nielsen, S. S. Keller, A. Boisen, *Lab Chip* **2018**, *18*, 2348.
- [18] L. H. Nielsen, A. Melero, S. S. Keller, J. Jacobsen, T. Garrigues, T. Rades, A. Müllertz, A. Boisen, *Int. J. Pharm.* **2016**, *504*, 98.
- [19] C. Mazzoni, F. Tentor, S. A. Strindberg, L. H. Nielsen, S. S. Keller, T. S. Alstrøm, C. Gundlach, A. Müllertz, P. Marizza, A. Boisen, *J. Controlled Release* **2017**, *268*, 343.
- [20] C. Mazzoni, R. D. Jacobsen, J. Mortensen, J. R. Jørgensen, L. Vaut, J. Jacobsen, C. Gundlach, A. Müllertz, L. H. Nielsen, A. Boisen, *Macromol. Biosci.* **2019**, *1900004*, 1.
- [21] S. K. Lai, Y.-Y. Wang, J. Hanes, *Adv. Drug Delivery Rev.* **2009**, *61*, 158.
- [22] M. Liu, J. Zhang, W. Shan, Y. Huang, *Asian J. Pharm. Sci.* **2014**, *10*, 275.
- [23] Y. Y. Wang, S. K. Lai, J. S. Suk, A. Pace, R. Cone, J. Hanes, *Angew. Chem., Int. Ed.* **2008**, *47*, 9726.
- [24] T. M. Ways, W. Lau, V. Khutoryanskiy, *Polymer* **2018**, *10*, 267.
- [25] P. S. Pourshahab, K. Gilani, E. Moazeni, H. Eslahi, M. R. Fazeli, H. Jamalifar, *J. Microencapsulation* **2011**, *28*, 605.
- [26] E. I. Rabea, M. E. Badawy, C. V. Stevens, G. Smagge, W. Steurbaut, *Biomacromolecules* **2003**, *4*, 1457.
- [27] A. Machul, D. Mikołajczyk, A. Regiel-Futyr, P. B. Heczko, M. Strus, M. Arruebo, G. Stochel, A. Kyzioł, *J. Biomater. Appl.* **2015**, *30*, 269.
- [28] L. Liu, W. D. Yao, Y. F. Rao, X. Y. Lu, J. Q. Gao, *Drug Delivery* **2017**, *24*, 569.
- [29] V. K. Nikam, K. B. Kotade, V. M. Gaware, R. T. Dolas, K. B. Dhamak, S. B. Somwanshi, A. N. Khadse, V. A. Kashid, *Pharmacologyonline* **2011**, *1*, 152.
- [30] A. K. Woischnig, L. M. Gonçalves, M. Ferreira, R. Kuehl, J. Kikhney, A. Moter, I. A. C. Ribeiro, A. J. Almeida, N. Khanna, A. F. Bettencourt, *Int. J. Pharm.* **2018**, *550*, 372.
- [31] F. Ahmadi, Z. Oveisi, S. M. Samani, Z. Amoozgar, *Res. Pharm. Sci.* **2015**, *10*, 1.
- [32] M. Mohammed, J. Syeda, K. Wasan, E. Wasan, *Pharmaceutics* **2017**, *9*, 53.
- [33] A. Heydorn, A. T. Nielsen, M. Hentzer, C. Sternberg, M. Givskov, B. K. Ersbøll, S. Molin, *Microbiology* **2000**, *146*, 2395.
- [34] K. Knop, R. Hoogenboom, D. Fischer, U. S. Schubert, *Angew. Chem., Int. Ed.* **2010**, *49*, 6288.
- [35] Z. Sobhani, S. M. Samani, H. Montaseri, E. Khezri, *Adv. Pharm. Bull.* **2017**, *7*, 427.
- [36] P. Shastri, R. Ubale, M. D'Souza, *Drug Dev. Ind. Pharm.* **2013**, *39*, 164.
- [37] D. A. Gray, G. Dugar, P. Gamba, H. Strahl, M. J. Jonker, L. W. Hamoen, *Nat. Commun.* **2019**, *10*, 1.
- [38] J. Du, H. M. Bandara, P. Du, H. Huang, K. Hoang, D. Nguyen, S. V. Mogarala, H. D. C. Smyth, *Mol. Pharmaceutics* **2015**, *12*, 1544.
- [39] J. S. Suk, S. K. Lai, Y.-Y. Wang, L. M. Ensign, P. L. Zeitlin, M. P. Boyle, J. Hanes, *Biomaterials* **2009**, *30*, 2591.
- [40] E. E. Mann, D. J. Wozniak, *FEMS Microbiol. Rev.* **2012**, *36*, 893.
- [41] A. Brauner, O. Fridman, O. Gefen, N. Q. Balaban, *Nat. Rev. Microbiol.* **2016**, *14*, 320.
- [42] K. Lewis, *Nat. Rev. Microbiol.* **2007**, *5*, 48.
- [43] L. H. Nielsen, S. S. Keller, K. C. Gordon, A. Boisen, T. Rades, A. Müllertz, *Eur. J. Pharm. Biopharm.* **2012**, *81*, 418.
- [44] L. H. Nielsen, S. S. Keller, A. Boisen, A. Müllertz, T. Rades, *Drug Delivery Transl. Res.* **2014**, *4*, 268.
- [45] Z. Abid, C. Gundlach, O. Durucan, C. von Halling Laier, L. H. Nielsen, A. Boisen, S. S. Keller, *Microelectron. Eng.* **2017**, *171*, 20.
- [46] B. W. Holloway, A. F. Morgan, *Annu. Rev. Microbiol.* **1986**, *40*, 79.
- [47] M. Klausen, A. Heydorn, P. Ragas, L. Lambertsen, A. Aaes-Jørgensen, S. Molin, T. Tolker-Nielsen, *Mol. Microbiol.* **2003**, *48*, 1511.
- [48] T. Tolker-Nielsen, C. Sternberg, *Curr. Protoc. Microbiol.* **2011**, *21*, 1B.2.1.
- [49] M. Vorregaard, *Comstat2 – A Modern 3D Image Analysis Environment for Biofilms*, Technical University of Denmark (DTU), Kgs. Lyngby, Denmark, **2008**.

## Supporting Information

Microcontainer Delivery of Antibiotic Improves Treatment of *Pseudomonas aeruginosa*

## Biofilms

Stine Egebro Birk\*, Janus Anders Juul Haagensen, Helle Krogh Johansen, Søren Molin, Line Hagner

Nielsen and Anja Boisen

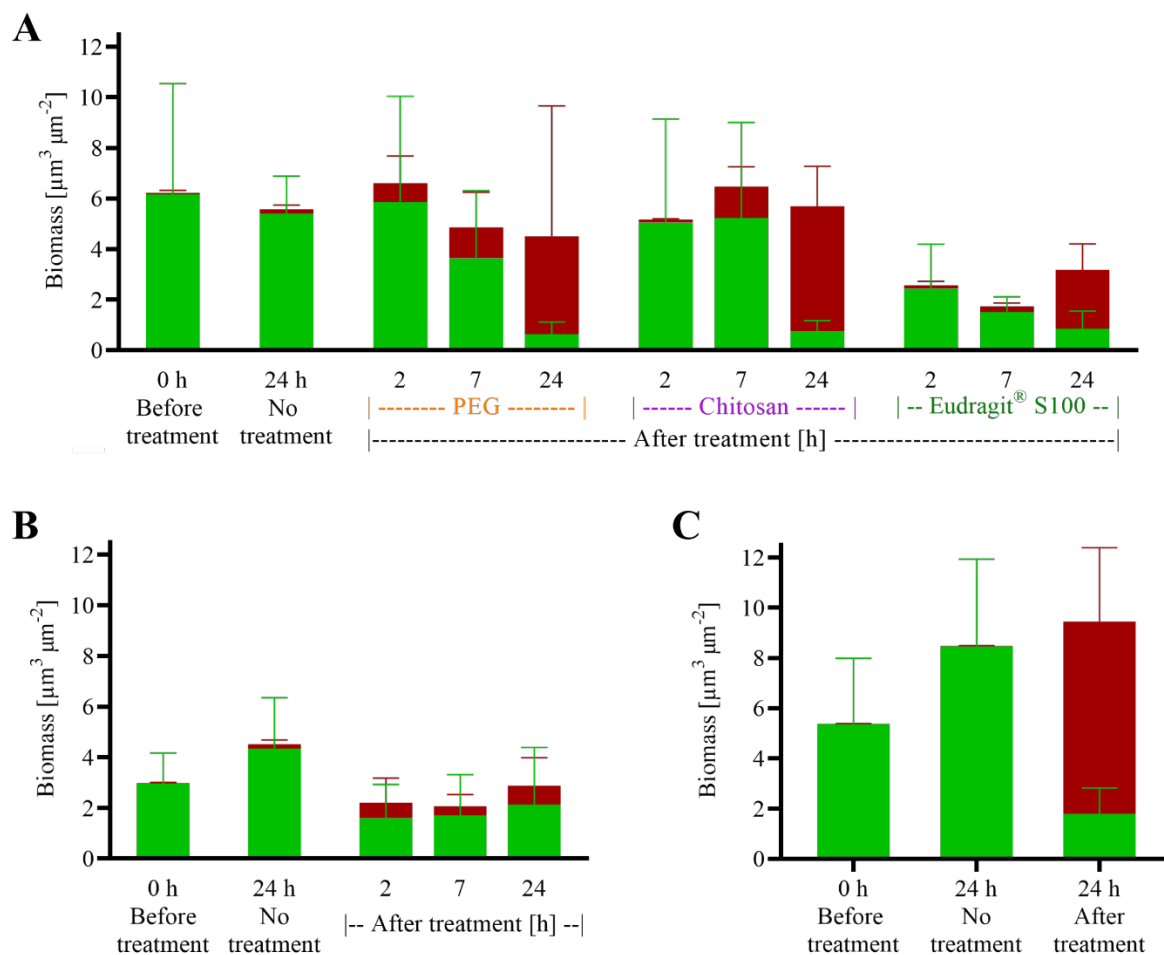


**Figure S1.** Graphs depicting the biomasses of PAO1 biofilm grown under flow for 96 h to a mature state and thereafter exposed to ciprofloxacin hydrochloride (CIP)-loaded microcontainers coated with either polyethylene glycol (PEG), chitosan or Eudragit<sup>®</sup> S100 (A) or a bolus dose of CIP (B) or constant perfusion of CIP (C). Green represents live bacteria. Red represents dead bacteria. Data are depicted as mean $\pm$ SD (n=4-24).

**Table S1.** The composition of modified FAB medium. A10 buffer, FB minimal medium with trace metals and the carbon source were autoclaved separately and mixed afterwards. Concentrations are given as final concentrations.

<b>A10 buffer</b>	<b>FB minimal medium with trace metals</b>		<b>Carbon source</b>
33.7 mM Na <sub>2</sub> HPO <sub>4</sub> ·2H <sub>2</sub> O	1 mM MgCl <sub>2</sub>	2 μg L <sup>-1</sup> CuSO <sub>4</sub> ·5H <sub>2</sub> O	0.3 mM glucose
22.0 mM KH <sub>2</sub> PO <sub>4</sub>	0.1 mM CaCl <sub>2</sub>	2 μg L <sup>-1</sup> ZnSO <sub>4</sub> ·7H <sub>2</sub> O	
15.1 mM (NH <sub>4</sub> ) <sub>2</sub> SO <sub>4</sub>	20 μg L <sup>-1</sup> CaSO <sub>4</sub> ·2H <sub>2</sub> O	1 μg L <sup>-1</sup> CoSO <sub>4</sub> ·7H <sub>2</sub> O	
51 mM NaCl	20 μg L <sup>-1</sup> FeSO <sub>4</sub> ·7H <sub>2</sub> O	1 μg L <sup>-1</sup> NaMoO <sub>4</sub> ·H <sub>2</sub> O	
	2 μg L <sup>-1</sup> MnSO <sub>4</sub> ·H <sub>2</sub> O	0.5 μg L <sup>-1</sup> H <sub>3</sub> BO <sub>3</sub>	

# APPENDIX III

## PAPER III

### **Co-delivery of ciprofloxacin and colistin using microcontainers for bacterial biofilm treatment**

S.E. Birk, C. Mazzoni, M.M. Javed, M.B. Hansen, H.K. Johansen, J.A.J. Haagensen, S. Molin, L.H. Nielsen, A. Boisen

*International Journal of Pharmaceutics, 2021 (submitted)*

# Co-delivery of ciprofloxacin and colistin using microcontainers for bacterial biofilm treatment

*Stine Egebro Birk<sup>a\*</sup>, Chiara Mazzoni<sup>a</sup>, Madeeha Mobasharah Javed<sup>a</sup>, Morten Borre Hansen<sup>b</sup>, Helle Krogh Johansen<sup>d,e</sup>, Janus Anders Juul Haagensen<sup>c</sup>, Søren Molin<sup>c</sup>, Line Hagner Nielsen<sup>a</sup>, Anja Boisen<sup>a</sup>*

<sup>a</sup>The Danish National Research Foundation and Villum Foundation's Center for Intelligent Drug Delivery and Sensing Using Microcontainers and Nanomechanics (IDUN), Department of Health Technology, Technical University of Denmark, Ørsteds Plads 345C, 2800 Kongens Lyngby, Denmark

<sup>b</sup>Novo Nordisk Foundation Center for Intestinal Absorption and Transport of Biopharmaceuticals, Department of Health Technology, Technical University of Denmark, Produktionstorvet 423, 2800 Kongens Lyngby, Denmark

<sup>c</sup>Novo Nordisk Foundation Center for Biosustainability, Technical University of Denmark, Kemitorvet 220, 2800 Kongens Lyngby, Denmark

<sup>d</sup>Department of Clinical Microbiology, Section 9301 Copenhagen University Hospital Rigshospitalet, Henrik Harpestrangs Vej 4A, Copenhagen Ø 2100, Denmark

<sup>e</sup>Department of Clinical Medicine Faculty of Health and Medical Sciences University of Copenhagen, Blegdamsvej 3B, Copenhagen N 2200, Denmark

\*Corresponding author: Stine Egebro Birk, e-mail: stegha@dtu.dk

## ABSTRACT

In many infected patients, bacterial biofilms represent a mode of growth that significantly enhances the tolerance to antimicrobials, leaving the patients with difficult-to-cure infections. Therefore, there is a growing need for effective treatment strategies to combat biofilm infections. In this work, reservoir-based microdevices, also known as microcontainers (MCs), are co-loaded with two antibiotics: ciprofloxacin hydrochloride (CIP) and colistin sulfate (COL), targeting both metabolically active and dormant subpopulations of the biofilm. We assess the synergistic effect of the two drugs in a time-kill study of planktonic *P. aeruginosa* and find that co-loaded MCs are superior to monotherapy, resulting in complete killing of the entire population. Biofilm consortia of *P. aeruginosa* grown in flow chambers were not fully eradicated. However, antibiotics in MCs work significantly faster than simple perfusion of antibiotics (62.5±8.3 % versus 10.6±10.1 % after 5 h) in biofilm consortia, showing the potential of the MC-based treatment to minimize the use of antimicrobials in future therapies.

## KEYWORDS

Microdevices; Drug delivery; Antimicrobials; Antibiotics; Chitosan; *Pseudomonas aeruginosa*

## 1. INTRODUCTION

Antibiotic resistance is one of the greatest challenges facing the global healthcare system (Davies and Davies, 2010). Microbes are developing resistance at an alarming rate, while the 'golden era' of antibiotic discovery is long over (O'Neill, 2016). This leaves us with a clear demand for novel strategies to combat multi-drug resistant (MDR) bacterial infections (Parish, 2019).

Besides from MDR, it has become evident that the ability of bacteria to organize themselves into matrix-enclosed aggregates, also known as biofilm, is responsible for most chronic bacterial infections (Hall-Stoodley et al., 2004). In fact, it has been shown that the biofilm-lifestyle renders the bacteria with a 10-1,000-fold higher tolerance towards antibiotics than their planktonic counterparts (Mah and O'Toole, 2001; Stewart, 2002). Gradients of nutrients and oxygen exist from the top to the bottom of the biofilm, with oxygen levels being high at the surface and low in the center of the biofilm. Similarly, metabolic activity is stratified with high activity at the surface and low or no growth in the center (Ciofu and Tolker-Nielsen, 2019; Pamp et al., 2008). As the antimicrobial effect of antibiotics often depends on the metabolic activity of the bacteria, this dormancy-phenomenon is one of the explanations for the reduced susceptibility of biofilm-associated bacteria towards antibiotics (Høiby et al., 2010). Consequently, monotherapy with antibiotics, which are only active against growing cells, leads to a reduction of bacteria without complete eradication of the biofilm (Anwar and Costerton, 1990).

Combining antibiotics with different cellular targets is widely recognized as a useful strategy to increase the likelihood of achieving early adequate bacterial eradication of infections, where monotherapy has failed, and at the same time minimizing the risk of resistance development (Tamma et al., 2012; Traugott et al., 2011). Ciprofloxacin is a fluoroquinolone antibiotic showing broad activity mainly against Gram-negative bacteria, such as *Pseudomonas aeruginosa* that are associated with debilitating infections in the airways (Bjarnsholt, 2011; Schwerdt et al., 2018) and wounds (Pastar et al., 2013). Ciprofloxacin exhibits bacteriostatic and bactericidal effects by inhibiting the DNA gyrase and topoisomerase IV enzymes essential for DNA replication (Aldred et al., 2014; Silva et al., 2011), thus targeting mainly the actively dividing cells found in the outer edges of the biofilm (Høiby et al., 2010). The cyclic cationic lipopeptide, colistin, belonging to the family of polymyxins, has recently received raising attention because of its significant effect on MDR Gram-negative bacteria (Li et al., 2006; Nation et al., 2015). Colistin binds to the lipid A component in lipopolysaccharides disordering the cell membrane structure, making it more permeable (a detergent-like effect), which ultimately results in cellular death (Bialvaei and Samadi Kafil, 2015). This means that colistin kills dormant bacterial subpopulations found in the core of the biofilm (Haagensen et al., 2007; Pamp et al., 2008). The use of colistin was originally hampered due to its serious nephrotoxicity, but the limited therapeutic options have driven its revival as a last line of defense against severe *P. aeruginosa* infections (Li et al., 2006). Colistin has shown attractive synergistic antimicrobial activity against *P. aeruginosa* when combined with antibiotics such as azithromycin (Lin et al., 2015), rifampicin (Giamarellos-Bourboulis et al., 2003), and ciprofloxacin (Buyck et al., 2015).



Recently it was documented that liposomes co-loaded with ciprofloxacin and colistin showed an increase in of the antimicrobial efficacy against *P. aeruginosa* compared to monotherapies, while, at the same time, showing no toxicity towards the pulmonary epithelial cells (Chai et al., 2019; Wang et al., 2018; Yu et al., 2020). Liposomes are one example of a particulated drug delivery system, which are gaining considerable attention to improve the therapeutic efficacy of antibiotic treatments (Gao et al., 2018). By using particulates to deliver antibiotics, a sufficiently high drug concentration can be achieved at the site of infection, while reducing the administered dose, keeping systemic toxicity at a minimum as well as limiting the risk of development of resistance (Liu et al., 2019). However, many of these formulations suffer from poor drug loading capabilities as well as from restrictions concerning which drugs that can be encapsulated into the particles.

Recent and promising approaches have focused on reservoir-based polymeric microdevices serving as drug carriers for oral drug delivery (Nielsen et al., 2018). The microdevices have shown a promising potential towards prolonging the retention of drugs at the site of absorption as well as providing a higher local drug concentration (Ainslie et al., 2009; Chirra et al., 2014; Nielsen et al., 2016). Previously, we have proposed microcontainers (MCs), which are polymeric cylindrical structures, as a means to deliver high loads of antibiotics to the site of infection (Birk et al., 2020). Compared to other drug delivery systems, such as liposomes, the MCs possess the unique capability of allowing delivery of any antibiotic no matter the size, charge or lipo-/hydrophilicity. Therefore, the ratio between co-loaded antibiotics can easily be adjusted as desired. Moreover, MCs have demonstrated mucoadhesive properties as they can embed and engulf in mucus (a habitat which biofilms reside in) (Mazzoni et al., 2017; Mosgaard et al., 2019; Nielsen et al., 2016). Moreover, adhesion was shown to be further promoted by coating the MCs with a lid of chitosan (Mazzoni et al., 2019). Previously we have shown that local delivery of ciprofloxacin hydrochloride (CIP) confined in MCs resulted in eradication of *P. aeruginosa* biofilm equal to a constant flow of an about three times higher concentration of the solubilized antibiotic. However, 10-20 % of the biomass remained alive despite treatment with CIP (Birk et al., 2020).

The aim of the present study was to exploit the potential of using MCs for co-delivery of synergistic antibiotics as a more efficient treatment of *P. aeruginosa* biofilms compared to monotherapies. CIP and colistin sulfate (COL) were co-loaded in MCs and coated with a mucoadhesive coating of chitosan. *In vitro* release kinetics were characterized together with time-kill investigations of planktonic *P. aeruginosa* and compared to antibiotic monotherapy. Lastly, the impacts of co-loaded MCs were investigated on biofilm consortia of *P. aeruginosa* and compared to single-loaded MCs and simple antibiotic perfusion.

## **2. MATERIALS AND METHODS**

### **2.1. Materials**

Silicon (Si) wafers (4" (100) n-type) were acquired from Okmetic (Vantaa, Finland), while the SU-8 constituents (SU-8 2075 and SU-8 Developer) were purchased from Micro Resist Technology (Berlin, Germany). Ciprofloxacin HCl (CIP) was from Fagron (Uitgeest, The Netherlands), while colistin sulfate (COL), chitosan (low MW 50-190 kDa, 75-85 % deacetylation), acetic acid, Luria Bertani (LB) medium, potassium phosphate, disodium phosphate, sodium chloride, calcium chloride, ammonium sulfate, magnesium chloride, trace metals, glucose, propidium iodide and glutaraldehyde (25 % solution) were all bought from Sigma-Aldrich (St. Louis, MO USA). Osmium tetroxide (4 % in water) was acquired from ACROS Organics. Ultrapure water was obtained from a Q-POD® dispenser (Merck Millipore, Burlington, MA, USA).

### **2.2. Fabrication of MCs**

MCs were fabricated on silicon wafers using a mask-based two-step photolithography process, an approach originally introduced for drug delivery devices by Tao *et al.* and later modified by Nielsen *et al.* (Nielsen *et al.*, 2012; Tao *et al.*, 2007). Starting out with clean Si substrates, a release layer consisting of 5 nm titanium (Ti) and 20 nm gold (Au) was deposited (Temescal FC-2000, Ferrotec Corporation, Santa Clara, CA, USA) using electron beam evaporation. The release layer ensured adequate adhesion of the MCs to the chip during loading and coating, while simultaneously enabling the detachment of MCs from the chip without damaging them (Nielsen *et al.*, 2016). Subsequently, the Ti/Au-Si wafers were covered with a layer of the negative epoxy photoresist SU-8 and exposed to a number of baking steps allowing the formation of the bottom and the side walls of the MCs. After fabrication, the wafers were diced (Automatic Dicing Saw DAD 321, DISCO, Tokyo, Japan) into squared chips (12.8 × 12.8 mm<sup>2</sup>), with each chip containing 625 individual MCs. The inner and outer diameters of the individual MCs were determined with an Eclipse L200 bright-field optical microscope (Nikon, Tokyo, Japan), whereas the inner and outer heights were evaluated by vertical scanning interferometry using a PLu Neox 3D Optical Profiler (Sensofar, Terrassa, Spain).

### **2.3. Loading of CIP and COL into MCs and coating with chitosan**

Prior to drug loading, a shadow mask was aligned on top of the chip containing MCs in order to minimize the amount of drug powder being distributed into the gaps between the MCs, as previously described (Abid *et al.*, 2017).

For the co-loading, CIP and COL powders were mixed in a 1:8 w/w ratio. CIP:COL or pure COL powder was loaded into MCs using a centrifuge method previously described (Jørgensen *et al.*, 2019). In brief, the powder was distributed on top of the mask and the chip was subsequently centrifuged in a flat-bottomed Falcon tube using a Heraeus Megafuge 16R Centrifuge (Thermo Fisher Scientific, Waltham, MA, USA) at 3720 g for 120 s at room temperature. Following this, the chip was removed from the Falcon tube and

additional powder was embossed into the cavity of the MCs by applying a pressure of  $0.49 \cdot 10^{-1}$  Torr for 15 s with a compact digital pressure controlled electric crimper-MSK-160E (MTI Corporation, Richmond, CA, USA). The centrifugation and compression steps were conducted twice to ensure adequate drug loading. Afterwards, the shadow mask was removed and any excess drug around the MCs was gently removed using pressurized air. CIP was loaded into the MCs using only compression.

The chips were weighed before and after loading to quantify the amount of loaded drug. Drug loading capacity was calculated as the amount of loaded drug relative to the weight of a drug-loaded MC. CIP:COL- and COL-loaded chips were stored in the freezer at  $-18$  °C until usage to ensure drug stability, whereas CIP-loaded chips were stored at room temperature.

Functionalization of the drug-loaded MCs was achieved by spray coating a lid of a chitosan solution over the chip using an Exacta Coat Ultrasonic Spray System (Sonotek, USA) with an accumist nozzle operating at 120 kHz. The chitosan solution was prepared by dissolving 0.5 % w/v chitosan in 0.1 M acetic acid, heated overnight at 50°C and subsequently, filtered using a 5-13 µm filter with vacuum suction. Each chip was coated with two alternating spray paths having an offset of 2 mm, resulting in a total of 90 passages for CIP:COL and COL, and 120 passages for CIP. To facilitate solvent evaporation, the plate underneath the chip was heated to 50°C. Generator power was kept at 1.3 W, path speed at 25 mm/s and infusion rate at 0.1 mL/min. The applied shaping air pressure was 0.020 bar for CIP:COL and for COL MCs, and 0.028 bar for CIP-loaded MCs. The distance between the spray nozzle and the sample was set to 5.5 cm.

The quality of the loading and the coating of the MCs was evaluated using a tabletop scanning electron microscope (SEM) (Hitachi High-Technologies Europe GmbH, Krefeld, Germany). The MC chips were placed on a 30° tilted holder and SEM images were acquired using the scattered electron (SE) detector and an accelerating voltage of 15 kV.

#### **2.4. Characterization of *in vitro* drug release from MCs using LC-MS**

The *in vitro* release from co-loaded MCs was investigated using liquid chromatography-mass spectrometry (LC-MS), and the MCs loaded with either CIP or COL were utilized as controls. A chip containing 625 MCs was diced into mini-chips containing 100-110 MCs using a diamond cutter. The mini-chip was placed in a Falcon™ tube containing 5 mL FAB medium (buffered minimal medium used for bacterial growth; for preparation see **Supp. Materials, Table S1**) at 100 rpm and 37°C. Samples of 200 µL were taken at specified time points over the course of 48 h and replaced with 200 µL blank FAB medium. Samples with drug concentrations above the upper limit of detection for the LC-MS assay were diluted with FAB medium as appropriate. All samples were stored at  $-18$  °C prior to the analysis.

Standards (0-50 µM CIP or COL) and samples were analyzed with a Shimadzu Nexera X2/Prominence HPLC (Shimadzu Europe, Duisburg, Germany) and ESI micrOTOF-Q III (Bruker Daltonics, Bremen, Germany) LC-MS setup. The LC was performed by a 5 µL injection of the analyte on a Poroshell 120 SB-C8 column, 2.7 µm, 2.1x50 mm (Agilent, Santa Clara, CA, USA) followed by elution with a linear gradient of MeCN and 2.5 mM NH<sub>4</sub>OH in water with 0.1 % formic acid (from 0 to 100 % over 9 min) at a flow rate of 0.4 mL/min. The chromatographic front (1.75 min) was diverted to waste, while the remaining run was injected into

the ESI microTOF-Q III mass spectrometer. A calibration solution consisting of 2.5 mM NaOH, 2.25 mM formic acid in 90 % *i*-PrOH/water was injected into the ion source between 1.75 and 1.85 min at a flowrate of 30  $\mu$ L/h for internal calibration of the spectra. MS analysis was performed in positive mode in the range of 50-3,000 *m/z* at a rate of 2 Hz. For COL, a capillary potential of 5,000 V was employed, the nebulization pressure was 1.5 bar and the drying gas flow was set to 3 L/min at 180°C. For CIP, the parameters were 4,500 V, 0.3 bar and 4 L/min at 200°C. All mass spectra were analyzed with the software QuantAnalysis (Bruker Daltonics, Bremen, Germany) to generate extracted ion chromatograms for 332.16 $\pm$ 0.05 *m/z* (for CIP) and 1155.7 $\pm$ 0.1 *m/z* (for COL) and the resulting peaks were integrated.

All experiments were carried out in 3-6 replicates and data were normalized to 100 % in relation to the measured amount of drug release after 48 h.

## **2.5. Bacterial strains and overnight culturing**

For all bacterial studies, a *P. aeruginosa* PAO1 strain (Klockgether et al., 2010) genetically modified to express green fluorescent protein (GFP) constitutively by insertion into a neutral intergenic region in the genome was used (Holloway and Morgan, 1986; Klausen et al., 2003; Stover et al., 2000). Overnight cultures of PAO1 were grown in lysogeny broth (LB) at 150 rpm at 37°C for 18-20 h.

## **2.6. Time-kill studies of planktonic *P. aeruginosa* using co-loaded MCs**

For studying the ability of co-loaded MCs to inhibit bacterial growth, an inoculation of PAO1 overnight culture was diluted to a final concentration of approximately  $1 \times 10^6$  cells/mL. As controls, single loaded MCs were used in the same set-up. To each vial containing 10 mL culture, treatment was added as either uncoated MCs, coated MCs or antibiotic solution (for concentrations see **Figure 1**). PAO1 in LB without treatment and pure LB were used as negative control. The number of added MCs varied according to the difference in antibiotic loading per MC (determined per individual chip) and the minimum inhibitory concentration (MIC) values of the antibiotics (aiming for reaching 4xMIC for each antibiotic). Vials were stored at 150 rpm and 37 °C during the course of the experiment. Samples were taken at 0, 3, 8 and 24 h, and viable counts were obtained by serial dilution followed by spot plating on LB agar plates. The plates were left to incubate overnight at 37 °C and colony forming units (CFU) were counted the following day.

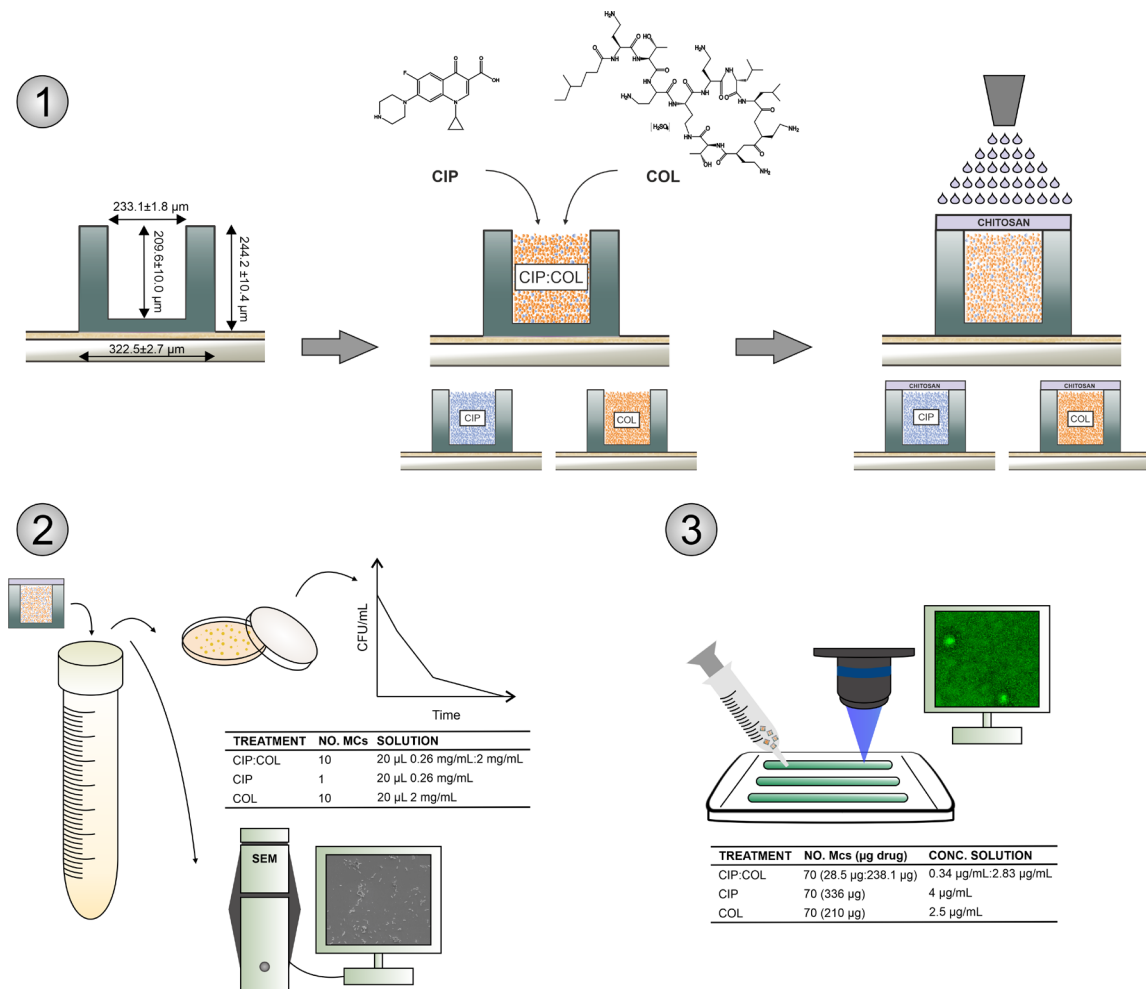


**Figure 1.** Schematic presentation of the production of microcontainers (MCs) and the conducted experiments on *P. aeruginosa* PAO1. **1)** Dimensions of fabricated MCs (mean±SD, n=6-12), co-loading or single-loading of ciprofloxacin hydrochloride (CIP) and/or colistin sulfate (COL) followed by coating with chitosan. **2)** MCs were tested against PAO1 cultures in shaken LB medium. Samples were taken over time for counting the colony forming units (CFU/mL). MCs were tested both with and without chitosan coating and compared to treatment with antibiotic in solution. See table for applied concentrations. Scanning electron microscopy (SEM) was applied as a visual assessment of bacterial killing after 24 h. **3)** MCs were tested against PAO1 in biofilm mode of growth using flow-chambers and with confocal microscopy monitoring. See table for applied concentrations.

## 2.7. SEM observation of *P. aeruginosa* cells post treatment with MCs

A qualitative study was performed to investigate the ability of the coated CIP:COL, CIP or COL MCs to inhibit biofilm formation on glass slides over 24 h. Microscopic glass slides were cut into smaller rectangles of approximately 3x7 mm size using a diamond cutter. The glass slides were sterilized in ethanol for 20 min, left to air dry and subsequently, mounted onto vials with Pressure Sensitive Adhesive (PSA) tape. Growth and treatment were conducted as described in Section 2.6.

Sample fixation was completed as previously described by Weber *et al.* (Weber *et al.*, 2014). In brief, the samples were covered with 2.5 % glutaraldehyde for 2 h, washed three times in phosphate buffered saline (PBS) and then transferred to wells containing 0.5 mL 1 % osmium tetroxide for 1 h. Thereafter, the

samples were dehydrated in solutions with increasing ethanol percentages (35 %, 50 %, 75 %, 2x90 %, and 2x100 %) for 30 min in each solution. After the last dehydration step, the samples were placed in a critical point dryer (Leica EM CPD300 Critical point dryer, Germany) for 2 h to allow further dehydration of the sample without causing structural changes to the bacteria. Lastly, the samples were placed in a desiccator overnight.

Prior to SEM analysis, the biofilm samples on glass slides were coated with a thin conducting layer of gold (Quorum Q150T ES Coater, Quorum Technologies, Lewes, United Kingdom) to prevent sample charging with the electron beam. Tooling factor was 2.3. Sputter current was kept at 20 mA and a sputter time of 65 s were used, whereas the clean current was 60 mA and clean time of 30 s. The stage was rotating at a speed of 30 rpm. SEM images were acquired using a QFEG 200 Cryo-ESEM (FEI Company, USA) using the Everhart-Thornley (ETD) detector with high vacuum mode and a voltage of 5 kV.

## **2.8. Growth of *P. aeruginosa* biofilms in flow chambers and treatment with antibiotics**

### *2.8.1. Growth of PAO1 biofilms*

The PAO1 biofilm growth was conducted in flow chambers suitable for MCs inoculation as previously described (Birk et al., 2020), with the only change that treatment was performed on a 72 h old biofilm. A sterile system was achieved by pumping 0.5 % v/v hypochlorite through the system over a period of 4 h followed by a cleaning procedure with filling and emptying the system three times with autoclaved MilliQ water. The system was perfused overnight with modified FAB minimal medium with trace metals (for preparation see **Supp. Materials, Table S1**), the flow was stopped, and the tubings were clamped and sterilized on the outside. Thereafter, 250  $\mu$ L of a diluted overnight culture (with 0.9 % NaCl to OD<sub>600</sub> of 0.05) was inoculated carefully into the flow chamber and resealed with silicone glue. Flow chambers were left without flow for 1 h to allow bacterial attachment to the glass surface, before medium flow was resumed. Temperature was kept at 37°C throughout the entire experiment.

### *2.8.2. Treatment with antibiotics*

Treatment with CIP and COL were conducted in two ways: I) as confined in coated MCs (either as co-loaded or as single-loaded as controls), or II) as a constant perfusion. 70 MCs were added to each flow chamber, and constant perfusion was achieved by adding CIP and/or COL to the medium bottle (see **Figure 1** for concentrations). To allow inoculation of MCs, a solution of 2.5% w/v gelatin (Sigma-Aldrich Chemie GmbH, Steinheim, Germany) was used to disperse the microcontainer in the syringe instead of sticking to the walls of the syringe as described previously (Birk et al., 2020). Biofilms were treated for 24 h, after which images were acquired at a distance of 140-320  $\mu$ m from the open side of the MCs and in case of perfusion at random locations in the flow chamber.

### 2.8.3. Microscopy parameters, image acquisition and analysis

Biofilms were monitored using an inverted Leica TCS SP8 CLSM (Mannheim, Germany) equipped with an argon/krypton laser and detectors and filter set for sequential monitoring of GFP (excitation wavelength: 488 nm, emission range: 493-558 nm) for live cell imaging and propidium iodide (excitation wavelength: 543 nm, emission range: 558-700 nm) for dead cell staining. Images were obtained in z-intervals of 1  $\mu\text{m}$  using an HC PL Apo CS2 63x oil objective (numerical aperture 1.4). PAO1 expressed GFP consecutively, and propidium iodide had to be injected into the bubble trap. As control, four biological experiments were performed acquiring two images (technical replicates) of non-treated biofilm in each experiment at random positions within the flow chamber. For each treatment, 3-5 biological replicates with 3-5 technical replicates were acquired. Stacked images and 3D images were generated using Imaris software (Version 7.7.1, Bitplane AG, Zürich, Switzerland). Volume of biomass was calculated using the image analysis software COMSTAT version 2.1 (Heydorn et al., 2000; Vorregaard, 2008). Graphs depicting the fraction of live/dead biomass were generated by calculating the percentage of live/dead in relation to the total biomass measured at the specified time-point.

### 2.9. Statistical analysis

Data are expressed as the mean $\pm$ SD, unless otherwise stated. For comparison of two individual mean values an unpaired t-test was applied, whereas a one-way ANOVA with Tukey's multiple comparison was used if more than two mean values were compared. Graphs and tests were conducted in GraphPad Prism (Version 8.0.1, GraphPad Software, CA, USA) and p-values were considered statistically significant when below 1 % ( $p < 0.01$ ).

## 3. RESULTS AND DISCUSSION

### 3.1. Loading of antibiotics into MCs and coating depositing

MCs were produced with good reproducibility in the desired dimensions (see **Figure 1** for dimensions). For the co-loading of CIP:COL, we chose a 1:8 w/w ratio based on the MIC values of the individual antibiotics towards PAO1 cells (0.125  $\mu\text{g}/\text{mL}$  for CIP (Soares et al., 2019); 1  $\mu\text{g}/\text{mL}$  of COL (Bergen et al., 2010)). The loading resulted in  $3.85\pm 0.37$   $\mu\text{g}/\text{MC}$  CIP:COL,  $5.16\pm 0.54$   $\mu\text{g}/\text{MC}$  CIP or  $3.32\pm 0.57$   $\mu\text{g}/\text{MC}$  COL ( $n=12-18$ , mean $\pm$ SD), corresponding to a drug loading capacity of 14.6-21.0 % w/w. Efficient loading was confirmed with SEM (**Figure 2A** and **Supp. Materials, Figure S1**). After drug loading, the cavity of the MCs was coated with a layer of chitosan, serving to promote bioadhesion. Moreover, chitosan is known to contribute to the killing of *P. aeruginosa* (Perinelli et al., 2018). The coating of CIP:COL- and COL-loaded MCs resulted in a uniform, fully covering lid, whereas the coating of CIP-loaded MCs was less uniform, a tendency also previously observed (Birk et al., 2020) (**Figure 2B** and **Supp. Materials, Figure S1**).

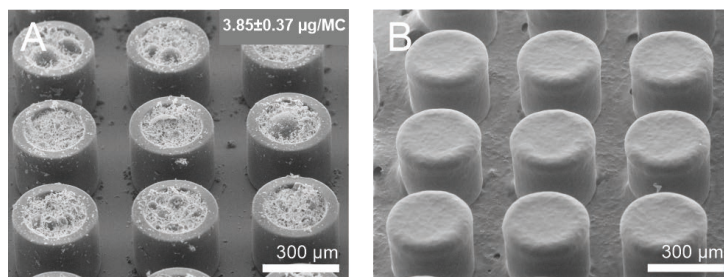


**Figure 2.** Scanning electron microscope (SEM) images of microcontainers (MCs) co-loaded with ciprofloxacin hydrochloride and colistin sulfate (1:8 w/w) (A) and subsequently coated with chitosan (B).

### 3.2. *In vitro* drug release from MCs

The release of CIP and/or COL from chitosan-coated MCs was evaluated at 37 °C in FAB medium at pH 6.8 (Figure 3) (for release from uncoated MCs, see **Supp. Materials Figure S2**).

The co-loaded chitosan-coated MCs released their entire COL cargo within the first 30 min reaching a release of  $98.7 \pm 5.7$  %. This was similar to what was observed from the single-loaded COL MCs ( $105.2 \pm 8.8$  %), and co-loading therefore did not influence the release profile of COL. The release of CIP was significantly accelerated from the co-loaded MCs ( $79.0 \pm 6.4$  % within 30 min) as compared to when CIP was single-loaded ( $13.8 \pm 1.2$  % within 30 min). This tendency was also observed in a previous study with liposomes, where incorporation of COL significantly accelerated the CIP release compared to liposomes loaded only with CIP (Wang et al., 2018). Sustained release from chitosan particles is a well-known phenomenon (Mohammed et al., 2017) and has previously been shown for CIP-loaded chitosan NPs (Patel et al., 2019) and CIP- or lysozyme loaded MCs (Birk et al., 2020; Mazzoni et al., 2019). The chitosan lid is shown to swell due to the hydrogel properties of chitosan (Ahmadi et al., 2015) creating pores which allows diffusion of CIP and COL. The diffusion rate depends on the hydrophilicity of the drugs, and the different release profiles can therefore be attributed to the higher aqueous solubility of COL (50 mg/ml (Wang et al., 2016)) compared to CIP (varying solubilities reported: 0.17-30 mg/mL (Olivera et al., 2011; Ross and Riley, 1994; Varanda et al., 2006)). Moreover, it is well known that surfactants influence the degree of hydrogel swelling and can provide micellar solubilization of poorly water-soluble drugs (Gunathilake et al., 2018; Wallace et al., 2010). As COL is amphiphilic in nature, we believe that COL served as a surfactant, affecting the swelling of chitosan and the associated drug release. In the current study, COL constituted approximately 90 % of the co-loaded MC (due to the large difference in MIC values of CIP and COL). Seemingly, the water soluble and fast-releasing COL drove the release of the otherwise less soluble CIP.



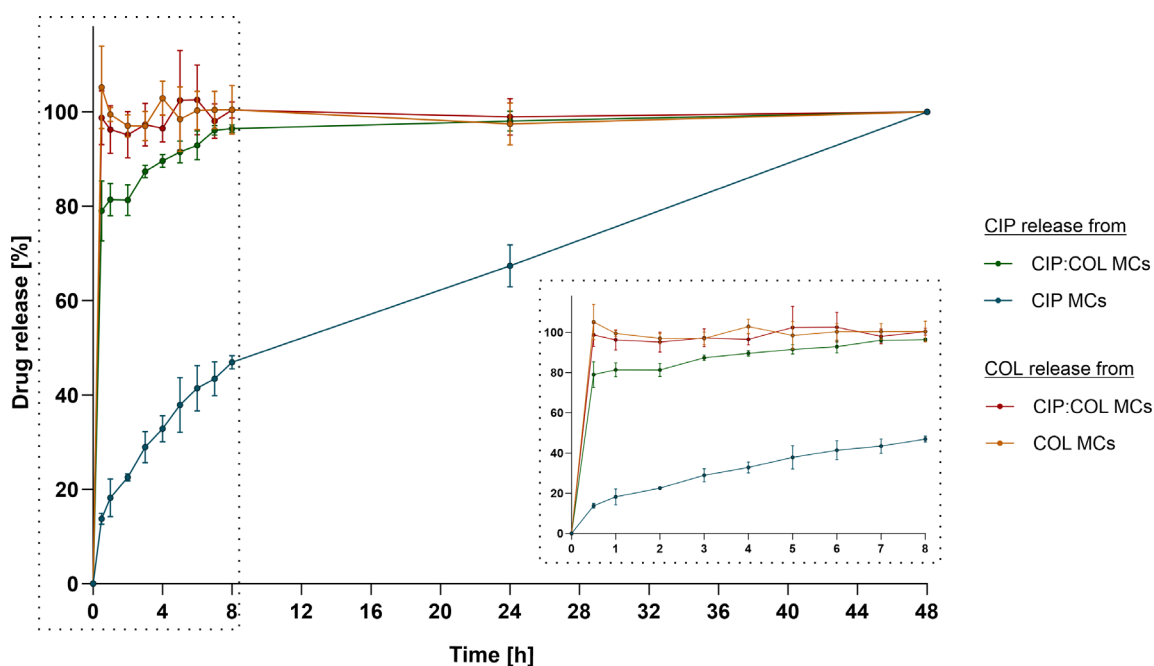


**Figure 3.** *In vitro* release of ciprofloxacin hydrochloride (CIP) and colistin sulfate (COL) from co-loaded or single-loaded microcontainers (MCs) coated with chitosan. Release study was performed at 37 °C in FAB medium at pH 6.8 and quantified by LC-MS. Data was normalized to 100 % and presented as mean±SD, n=3-4.

### 3.3. Time-kill of planktonic *P. aeruginosa* using co-loaded MCs

The capabilities of the drug-loaded and coated MCs to inhibit and kill planktonic bacteria were investigated by adding MCs to a growing population of *P. aeruginosa* (Figure 4) (for effect of uncoated MCs, see **Supp. Materials Figure S3**). Treatment with CIP:COL, CIP or COL significantly reduced bacterial growth compared to the PAO1 growth control ( $p \leq 0.0001$ ).

For co-loaded MCs, growth inhibition was increased compared to the monotherapies. The three types of treatments for the co-loaded MCs (uncoated, coated and solution) resulted in similar viable counts, which is in accordance with the rapid release of CIP:COL from the MCs (Figure 3 and **Supp. Materials Figure S2**). After 8 h, no growth was observed except for the coated MCs (note: only 1 out of 4 replicates showed growth). At 24 h, no growth was observed for any of the treatments.

When treating with CIP in MCs or in solution, the maximum killing was reached at 8 h and regrowth was observed at 24 h, indicating a possible resistant subpopulation. No differences were observed between CIP in solution or confined in MCs throughout the 24 h period ( $p \geq 0.36$ ). Presumably, the starting bacterial density was sufficiently low to allow a similar inhibition despite the sustained release observed with the chitosan coating (Figure 3).

Similar reductions in viable counts were observed when treating with COL confined in MCs or in solution, which correlates with the release data showing that all COL was released within the first 30 min. In contrast to CIP treatment, treating with COL generally did not give rise to a significant difference ( $p \geq 0.02$ ) between the viable counts after 3, 8, and 24 h, thus indicating that the amount of COL was sufficient to prevent further regrowth.

Altogether, the combination CIP:COL showed greater inhibition effect on PAO1 compared to single-loaded MCs, a synergistic effect of the two antibiotics reaching levels where all subpopulations were killed with no regrowth. The synergistic mechanism of CIP and COL on planktonic cells is not yet completely understood, but may be attributed to the ability of COL to enhance the uptake of CIP by destabilizing the outer membrane of the Gram-negative bacterium (Buyck et al., 2015). Recently, Yu *et al.* treated two COL-resistant *P. aeruginosa* strains with 8 mg/L CIP and 2 mg/L COL delivered in a liposomal formulations and found an enhanced *in vitro* antimicrobial activity compared to the monotherapies (Yu et al., 2020). However, one strain showed regrowth after 24 h despite treating with the two antibiotics, whereas the other only showed a 2-log reduction. In our study (treating PAO1 with 0.5 mg/L CIP: 4 mg/L COL), we observed a full eradication, and the difference may be attributed to the selection of the strain or the applied ratio of antibiotics.

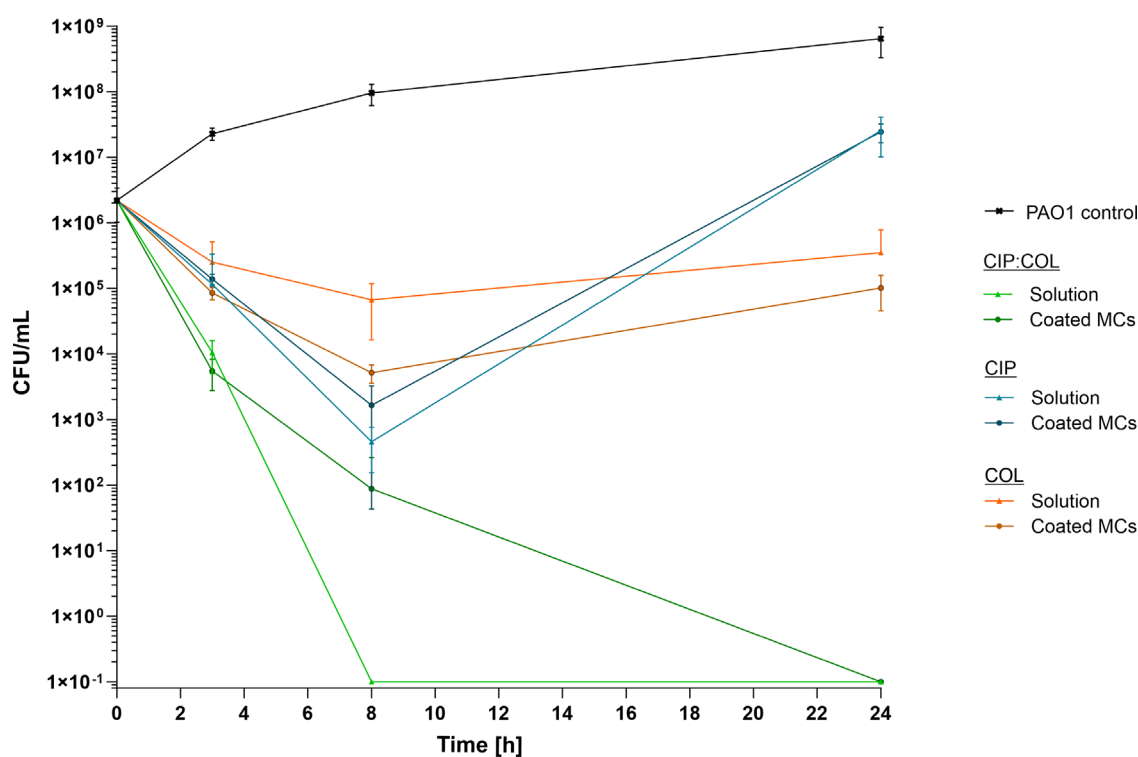


**Figure 4.** Inhibition of planktonic growth of *P. aeruginosa* (PAO1) over time when co-delivering ciprofloxacin hydrochloride (CIP) and colistin sulfate (COL) in chitosan-coated microcontainers (MCs) or as antibiotic solution. As controls, treatment with CIP or COL alone (as coated MCs or antibiotic solutions) as well as a positive control for PAO1 growth were included. Data is presented as mean±SD (n=3-6).

### 3.4. SEM observation of *P. aeruginosa* cells post treatment with MCs

SEM imaging of *P. aeruginosa* biofilms supported the viable counting results. Non-treated biofilms grew unevenly across the glass slide with certain areas containing huge and thick clusters (**Figure 5A**). These clusters were not found in the MC-treated samples, but instead single bacteria or small clusters were spread almost uniformly across the glass surface. However, the bacteria exposed to co-loaded and coated MCs were clearly affected by the treatment, and morphological changes appeared to correlate well with

the mechanism of action of the individual antibiotics. For the co-loaded CIP:COL MCs, the predominant effect on bacterial morphology originated from COL as cellular debris and deformed bacteria were observed (**Figure 5B**), yet, single bacteria did also appear elongated as evident from the zoom-in. When the biofilm was treated with CIP-loaded MCs, the bacteria appeared elongated, which is in accordance with the mechanism of CIP, inhibiting DNA replication and ultimately cellular division (**Figure 5C**) (Aldred et al., 2014). Also, the membrane disordering effect of COL (Bialvaei and Samadi Kafil, 2015) was evident in the samples treated with COL-loaded MCs, as extracellular material could be observed between the bacteria (**Figure 5D**). Moreover, the cell length appeared to be diminished and the bacteria to be collapsed. This is in accordance with previous results from the investigation of the effect of COL on the cellular structure of *P. aeruginosa* using atomic force microscopy (Mortensen et al., 2009). They observed that after only 3 h of COL treatment, the cells had almost completely lost their morphological structure. The visual assessment after treatment with CIP:COL MCs revealed that COL had the biggest impact on the bacteria, a tendency which is probably a consequence of two factors. Firstly, that the co-loaded CIP:COL MCs contained significantly more COL than CIP, and secondly, that COL quickly destabilizes the membrane thereby, evading the cellular elongation as otherwise observed after the treatment with only CIP.

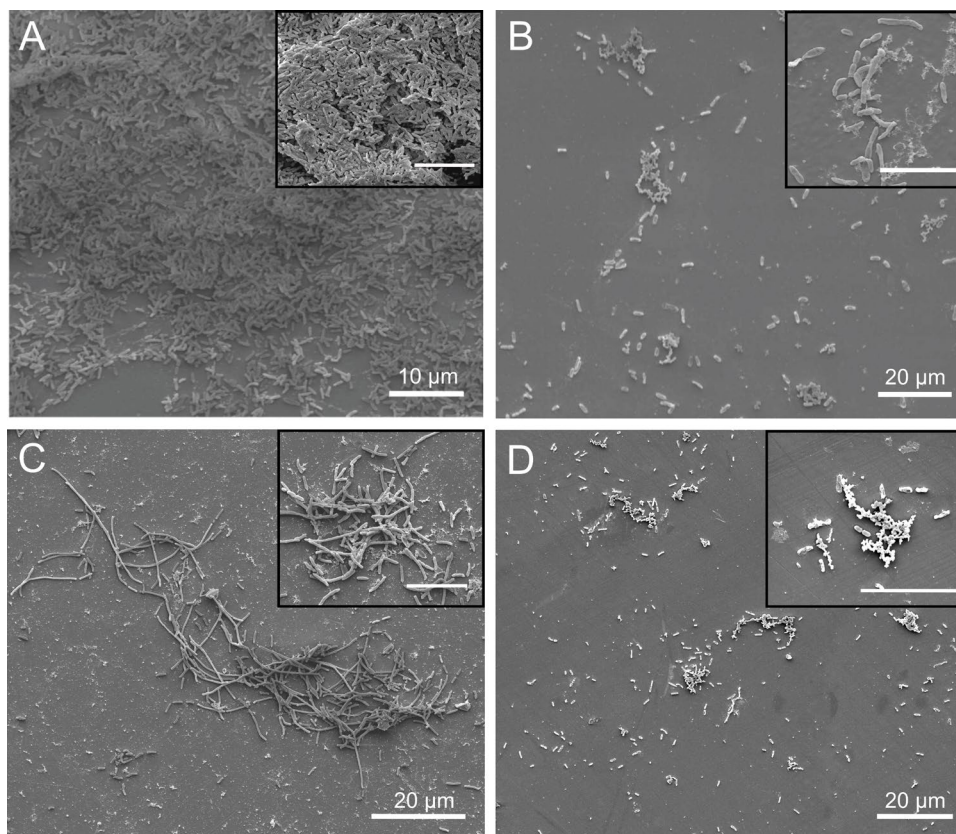


**Figure 5.** Scanning electron microscopy (SEM) images of a *P. aeruginosa* PAO1 biofilm grown for 24 h and **A**) left without antibiotic treatment, **B**) treated with coated co-loaded ciprofloxacin hydrochloride (CIP) and colistin sulfate (COL) MCs, **C**) CIP MCs and **D**) COL MCs. Scale bars on the inserts are 10 µm.

### 3.5. Eradication of pre-formed *P. aeruginosa* biofilms

The combination of COL targeting the metabolically inactive subpopulations with CIP being active against the metabolically active subpopulation has been shown to enable eradication of *P. aeruginosa* biofilms *in vitro* (Pamp et al., 2008). As previously reported, MC-based delivery increased the local antibiotic concentration, thus improving eradication (Birk et al., 2020). In this study, we evaluated the effect of co-delivering CIP and COL in MCs on biofilm eradication. Before treatment, biofilms were grown for 72 h resulting in a biomass of  $5.39 \pm 3.31 \mu\text{m}^3/\mu\text{m}^2$  (n=43).

CIP:COL co-loaded in MCs worked significantly faster than CIP:COL in solution, as a much larger fraction of the biomass was found dead after 5 h ( $62.5 \pm 8.3$  % versus  $10.6 \pm 10.1$  %,  $p \leq 0.0001$ ), which is also evident from the confocal images (**Figure 6**). We believe this effect is due to the burst release of the antibiotics from the MCs (**Figure 3**) creating an immediate high local drug concentration and ultimately more dead biomass. After 24 h,  $69.6 \pm 13.8$  % and  $74.1 \pm 20.4$  % of dead biomass was found for CIP:COL in MCs and for CIP:COL in solution, respectively, showing no significant difference (p-value of 0.4653). Interestingly, the biomass did not regrow after 24 h, showing, that despite all drug being released within 30 min from the MCs, a long-lasting effect still applies.

COL in MCs worked significantly faster than COL in solution ( $56.3 \pm 12.3$  % versus  $3.7 \pm 5.1$  % dead biomass after 5 h,  $p \leq 0.0001$ ) (**Supp. Materials, Figure S4**). No regrowth occurred after 24 h, and confocal images revealed dead biomass only in the core of the biofilm cluster. Notably, COL in MCs gave rise to a larger dead biomass than COL in solution ( $56.8 \pm 17.4$  % versus  $29.2 \pm 18.0$  %,  $p \leq 0.0001$ ), which may indicate that less COL could be used to achieve the same bacterial killing.

Treatment with CIP monotherapy for 5 h and 24 h resulted in a dead biomass of  $14.1 \pm 10.8$  % and  $81.9 \pm 9.8$  % with CIP in MCs and  $26.8 \pm 13.9$  % and  $85.8 \pm 10.5$  % with CIP in solution, showing no statistical difference ( $p \geq 0.05$ , **Supp. Materials, Figure S4**) despite the local and sustained CIP release observed from the MCs. As evident from the confocal cross-section (**Supp. Materials, Figure S4**), CIP killed the bacteria in the periphery of the biofilm clusters. Previously, we reported that  $88.2 \pm 5.3$  % of the biomass was killed, when exposing the biofilm to MCs loaded with about one-third of the CIP dose administered in the present study ( $\sim 120 \mu\text{g}$  versus  $336 \mu\text{g}$ ) (Birk et al., 2020). This is very interesting, as no further improvement in the bacterial killing was found despite the increased concentration of CIP. This proves that CIP-loaded MCs are effective even with less antibiotic used. However, they are not able, despite increasing the dose, to eradicate the remaining fraction, which might be due to a dormant or resistant subpopulation not affected by CIP. To address this subpopulation, we aimed at delivering a synergistic CIP and COL therapy, but, as evident from the present study, no full biofilm eradication occurred neither with the solutions nor when confined in MCs.

Only few studies have been published employing drug delivery carriers for co-delivery of CIP and COL, and these all involve liposomes (Chai et al., 2019; Wang et al., 2018; Yu et al., 2020). This focus on liposomes is likely due to their biocompatibility combined with a unique property allowing fusion with bacterial phospholipid bilayers, whereby channels to release their antimicrobial cargo directly into the intracellular

space of the bacterium are created (Forier et al., 2014). However, liposomes often suffer from a poor drug loading capacity, which is usually much lower than 10 % w/w (Lee, 2020), and as a result, the quantity of drug is not sufficient to reach therapeutic levels in the body, or the amount of the carrier material required is too high which may cause undesirable side-effects (Couvreur, 2013).

This is the first time that two synergistic antibiotics have been delivered in microfabricated devices such as MCs. The drug loading capacity of the applied MCs varied between 14.6-21.0 % w/w, being considerably higher than loading values reported for liposomes. Our results clearly prove that the antibiotics confined in MCs works significantly faster than the antibiotic solutions. This shows the potential of the MCs in delivery of immediate high local concentrations of multiple antibiotics at the site of infection. Future studies will include a detailed investigation of the influence of varying antibiotic concentrations as well as treatment with antibiotics with other mechanisms of actions. Pamp *et al.* showed that a combined treatment with CIP and COL was able to kill almost all cells in a *P. aeruginosa* biofilm as less than 10 cell/mL survived the combinational treatment compared to  $3.80 \times 10^5$ - $2.25 \times 10^7$  cells/mL on average in separately treated biofilm (Pamp et al., 2008). The concentrations of applied antibiotics were significantly higher than the concentrations applied in this study (60 µg/mL CIP and 25 µg/mL COL versus 4 µg/mL CIP and 2.5 µg/mL COL) and a full eradication may therefore be achieved by increasing the drug concentrations. Moreover, to achieve full biofilm eradication other combinational strategies may be included such as incorporation of agents that degrade the extracellular matrix, promoting disruption of biofilms. Such a mechanism might promote phenotypical alterations making the otherwise tolerant dormant cells more susceptible.

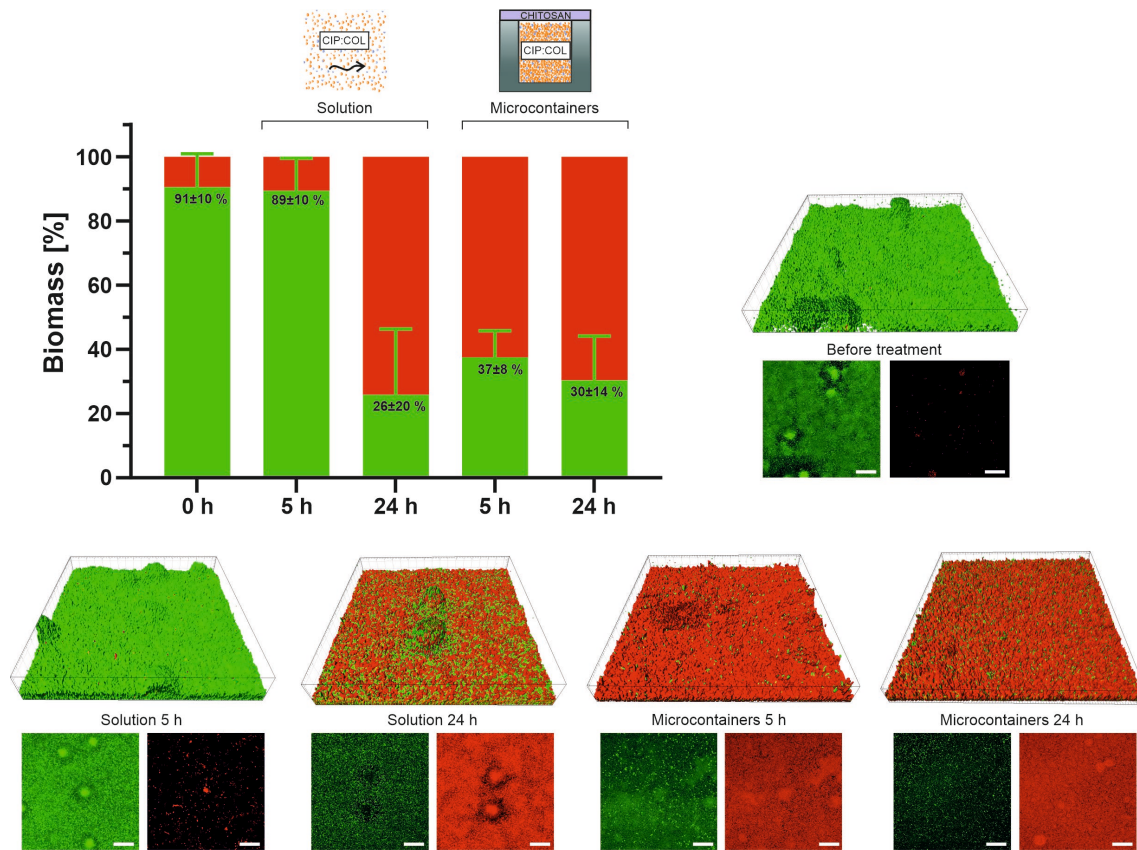


**Figure 6.** 72 h old *P. aeruginosa* (PAO1) biofilm treated with ciprofloxacin hydrochloride and colistin sulfate (CIP:COL) confined in MCs coated with chitosan or as a solution. Quantitative analysis of the biomass ( $\mu\text{m}^3/\mu\text{m}^2$ ) converted to the fraction of live/dead (%) cells. Data is depicted as mean+SD (n=4-5 biological replicates with 3-5 technical replicates for each type of treatment). Representative confocal laser scanning microscopy (CLSM) images of the biofilm before treatment, and 5 and 24 h post treatment with CIP:COL in MCs or as a solution. Green represents live bacteria and red shows dead bacteria. Scale bars: 30  $\mu\text{m}$ .

## 4. CONCLUSION

Previous studies utilizing MCs have primarily focused on delivery of single drug entities. In this study, we exploited the potential of co-delivery of two synergistic antibiotics, namely CIP and COL using MCs. We demonstrated that the activity of the antibiotics was retained while loaded in MCs. Combining CIP:COL in MCs showed greater effects on the killing of planktonic *P. aeruginosa* than the monotherapies, thus the two antibiotics synergistically killed all subpopulations as no regrowth occurred. In contrast, full eradication could not be achieved when treating a 72 h old biofilm with MCs, yet the MCs worked significantly faster than the solution. These results show that the MCs have a great potential as delivery system for biofilm treatment by reaching immediate high local drug concentration of multiple drugs at the site of infection.

## AUTHOR CONTRIBUTIONS

Conceptualization and methodology, S.E.B., C.M., H.K.J., J.A.J.H., S.M., L.H.N. and A.B.; supervision, S.E.B., C.M., J.A.J.H., S.M., L.H.N. and A.B; investigation, S.E.B., C.M., M.M.J., M.B.H.; resources, S.M. and A.B.; writing—original draft preparation, S.E.B.; writing—review and editing, all authors; funding acquisition, A.B. All authors have read and agreed to the published version of the manuscript.

## ACKNOWLEDGEMENTS AND FUNDING

The authors would like to acknowledge the Center for Intelligent Drug Delivery and Sensing Using Microcontainers and Nanomechanics (IDUN) whose research is funded by the Danish National Research Foundation (DNRF122) and Villum Foundation (Grant No. 9301). Micro- and nanofabrication specialist Lasse Højlund Eklund Thamdrup, DTU Health Tech is thanked for help with fabrication of the microcontainers. Furthermore, associate Professor Claus Sternberg, DTU Bioengineering is greatly acknowledged for providing access to the confocal scanning laser microscope. Helle Krogh Johansen was supported by The Novo Nordisk Foundation as a clinical research stipend (NNF12OC1015920), by Rigshospitalets Rammebevilling 2015–17 (R88-A3537), by Lundbeckfonden (R167-2013-15229), by Novo Nordisk Fonden (NNF15OC0017444, NNF18OC0052776), by RegionH Rammebevilling (R144-A5287) and by Independent Research Fund Denmark/Medical and Health Sciences (FSS-4183-00051, DFF-9039-00037A).

## 5. REFERENCES

- Abid, Z., Gundlach, C., Durucan, O., von Halling Laier, C., Nielsen, L.H., Boisen, A., Keller, S.S., 2017. Powder embossing method for selective loading of polymeric microcontainers with drug formulation. *Microelectron. Eng.* 171, 20–24. <https://doi.org/10.1016/j.mee.2017.01.018>
- Ahmadi, F., Oveisi, Z., Samani, S.M., Amoozgar, Z., 2015. Chitosan based hydrogels: characteristics and pharmaceutical applications. *Res. Pharm. Sci.* 10, 1–16.
- Ainslie, K.M., Lowe, R.D., Beaudette, T.T., Petty, L., Bachelder, E.M., Desai, T.A., 2009. Microfabricated Devices for Enhanced Bioadhesive Drug Delivery: Attachment to and Small-Molecule Release Through a Cell Monolayer Under Flow. *Small* 5, 2857–2863. <https://doi.org/10.1002/smll.200901254>
- Aldred, K.J., Kerns, R.J., Osheroff, N., 2014. Mechanism of quinolone action and resistance. *Biochemistry* 53, 1565–1574. <https://doi.org/10.1021/bi5000564>
- Anwar, H., Costerton, J.W., 1990. Enhanced activity of combination of tobramycin and piperacillin for eradication of sessile biofilm cells of *Pseudomonas aeruginosa*. *Antimicrob. Agents Chemother.* 34, 1666–1671. <https://doi.org/10.1128/AAC.34.9.1666>
- Bergen, P.J., Bulitta, J.B., Forrest, A., Tsuji, B.T., Li, J., Nation, R.L., 2010. Pharmacokinetic/Pharmacodynamic Investigation of Colistin against *Pseudomonas aeruginosa* Using an In Vitro Model. *Antimicrob. Agents Chemother.* 54, 3783–3789. <https://doi.org/10.1128/AAC.00903-09>
- Bialvaei, A.Z., Samadi Kafil, H., 2015. Colistin, mechanisms and prevalence of resistance. *Curr. Med. Res. Opin.* 31, 707–721. <https://doi.org/10.1185/03007995.2015.1018989>
- Birk, S.E., Haagensen, J.A.J., Johansen, H.K., Molin, S., Nielsen, L.H., Boisen, A., 2020. Microcontainer Delivery of Antibiotic Improves Treatment of *Pseudomonas aeruginosa* Biofilms. *Adv. Healthcare Mater.* 9, 1901779. <https://doi.org/10.1002/adhm.201901779>
- Bjarnsholt, T., 2011. *Pseudomonas aeruginosa* Biofilms in the Lungs of Cystic Fibrosis Patients, in: Moser, C., Jensen, P.Ø., Høiby, N. (Eds.), *Biofilm Infections*. Springer, pp. 167–185. <https://doi.org/10.1007/978-1-4419-6084-9>
- Buyck, J.M., Tulkens, P.M., Van Bambeke, F., 2015. Activities of Antibiotic Combinations against Resistant Strains of *Pseudomonas aeruginosa* in a Model of Infected THP-1 Monocytes. *Antimicrob. Agents Chemother.* 59, 258–268. <https://doi.org/10.1128/AAC.04011-14>
- Chai, G., Park, H., Yu, S., Zhou, F., Li, J., Xu, Q., Zhou, Q. (Tony), 2019. Evaluation of co-delivery of colistin and ciprofloxacin in liposomes using an in vitro human lung epithelial cell model. *Int. J. Pharm.* 569, 118616. <https://doi.org/10.1016/j.ijpharm.2019.118616>
- Chirra, H.D., Shao, L., Ciaccio, N., Fox, C.B., Wade, J.M., Ma, A., Desai, T.A., 2014. Planar Microdevices for Enhanced In Vivo Retention and Oral Bioavailability of Poorly Permeable Drugs. *Adv. Healthcare Mater.* 3, 1648–1654. <https://doi.org/10.1002/adhm.201300676>
- Ciofu, O., Tolker-Nielsen, T., 2019. Tolerance and Resistance of *Pseudomonas aeruginosa* Biofilms to Antimicrobial Agents—How *P. aeruginosa* Can Escape Antibiotics. *Front. Microbiol.* 10, 1–15. <https://doi.org/10.3389/fmicb.2019.00913>
- Couvreur, P., 2013. Nanoparticles in drug delivery: Past, present and future. *Adv. Drug Delivery Rev.* 65, 21–23. <https://doi.org/10.1016/j.addr.2012.04.010>
- Davies, J., Davies, D., 2010. Origins and Evolution of Antibiotic Resistance. *Microbiol. Mol. Biol. Rev.* 74, 417–433. <https://doi.org/10.1128/MMBR.00016-10>
- Foier, K., Raemdonck, K., De Smedt, S.C., Demeester, J., Coenye, T., Braeckmans, K., 2014. Lipid and polymer nanoparticles for drug delivery to bacterial biofilms. *J. Controlled Release* 190, 607–623.



<https://doi.org/10.1016/j.jconrel.2014.03.055>

- Gao, W., Chen, Y., Zhang, Y., Zhang, Q., Zhang, L., 2018. Nanoparticle-based local antimicrobial drug delivery. *Adv. Drug Delivery Rev.* 127, 46–57. <https://doi.org/10.1016/j.addr.2017.09.015>
- Giamarellos-Bourboulis, E.J., Sambatakou, H., Galani, I., Giamarellou, H., 2003. In Vitro Interaction of Colistin and Rifampin on Multidrug-Resistant *Pseudomonas aeruginosa*. *J. Chemother.* 15, 235–238. <https://doi.org/10.1179/joc.2003.15.3.235>
- Gunathilake, T.M.S.U., Ching, Y.C., Chuah, C.H., Illias, H.A., Ching, K.Y., Singh, R., Nai-Shang, L., 2018. Influence of a nonionic surfactant on curcumin delivery of nanocellulose reinforced chitosan hydrogel. *Int. J. Biol. Macromol.* 118, 1055–1064. <https://doi.org/10.1016/j.ijbiomac.2018.06.147>
- Haagensen, J.A.J., Klausen, M., Ernst, R.K., Miller, S.I., Folkesson, A., Tolker-Nielsen, T., Molin, S., 2007. Differentiation and distribution of colistin- and sodium dodecyl sulfate-tolerant cells in *Pseudomonas aeruginosa* biofilms. *J. Bacteriol.* 189, 28–37. <https://doi.org/10.1128/JB.00720-06>
- Hall-Stoodley, L., Costerton, J.W., Stoodley, P., 2004. Bacterial biofilms: From the natural environment to infectious diseases. *Nat. Rev. Microbiol.* 2, 95–108. <https://doi.org/10.1038/nrmicro821>
- Heydorn, A., Nielsen, A.T., Hentzer, M., Sternberg, C., Givskov, M., Ersbøll, B.K., Molin, S., 2000. Quantification of biofilm structures by the novel computer program comstat. *Microbiology* 146, 2395–2407. <https://doi.org/10.1099/00221287-146-10-2395>
- Høiby, N., Bjarnsholt, T., Givskov, M., Molin, S., Ciofu, O., 2010. Antibiotic resistance of bacterial biofilms. *Int. J. Antimicrob. Agents* 35, 322–332. <https://doi.org/10.1016/j.ijantimicag.2009.12.011>
- Holloway, B.W., Morgan, A.F., 1986. Genome Organization in *Pseudomonas*. *Annu. Rev. Microbiol.* 40, 79–105. <https://doi.org/10.1146/annurev.mi.40.100186.000455>
- Jørgensen, J.R., Jepsen, M.L., Nielsen, L.H., Dufva, M., Nielsen, H.M., Rades, T., Boisen, A., Müllertz, A., 2019. Microcontainers for oral insulin delivery – In vitro studies of permeation enhancement. *Eur. J. Pharm. Biopharm.* 143, 98–105. <https://doi.org/10.1016/j.ejpb.2019.08.011>
- Klausen, M., Heydorn, A., Ragas, P., Lambertsen, L., Aaes-Jørgensen, A., Molin, S., Tolker-Nielsen, T., 2003. Biofilm formation by *Pseudomonas aeruginosa* wild type, flagella and type IV pili mutants. *Mol. Microbiol.* 48, 1511–1524. <https://doi.org/10.1046/j.1365-2958.2003.03525.x>
- Klockgether, J., Munder, A., Neugebauer, J., Davenport, C.F., Stanke, F., Larbig, K.D., Heeb, S., Schöck, U., Pohl, T.M., Wiehlmann, L., Tümmler, B., 2010. Genome Diversity of *Pseudomonas aeruginosa* PAO1 Laboratory Strains. *J. Bacteriol.* 192, 1113–1121. <https://doi.org/10.1128/JB.01515-09>
- Lee, M.-K., 2020. Liposomes for Enhanced Bioavailability of Water-Insoluble Drugs: In Vivo Evidence and Recent Approaches. *Pharmaceutics* 12, 264. <https://doi.org/10.3390/pharmaceutics12030264>
- Li, J., Nation, R., Turnidge, J., Milne, R., Coulthard, K., Rayner, C., Paterson, D., 2006. Colistin: the re-emerging antibiotic for multidrug-resistant Gram-negative bacterial infections. *Lancet Infect Dis* 6, 589–601. [https://doi.org/10.1016/S1473-3099\(06\)70580-1](https://doi.org/10.1016/S1473-3099(06)70580-1)
- Lin, L., Nonejuie, P., Munguia, J., Hollands, A., Olson, J., Dam, Q., Kumaraswamy, M., Rivera, H., Corriden, R., Rohde, M., Hensler, M.E., Burkart, M.D., Pogliano, J., Sakoulas, G., Nizet, V., 2015. Azithromycin Synergizes with Cationic Antimicrobial Peptides to Exert Bactericidal and Therapeutic Activity Against Highly Multidrug-Resistant Gram-Negative Bacterial Pathogens. *EBioMedicine* 2, 690–698. <https://doi.org/10.1016/j.ebiom.2015.05.021>
- Liu, Y., Shi, L., Su, L., van der Mei, H.C., Jutte, P.C., Ren, Y., Busscher, H.J., 2019. Nanotechnology-based antimicrobials and delivery systems for biofilm-infection control. *Chem. Soc. Rev.* 48, 428–446. <https://doi.org/10.1039/C7CS00807D>
- Mah, T.F.C., O’Toole, G.A., 2001. Mechanisms of biofilm resistance to antimicrobial agents. *Trends Microbiol.* 9, 34–39. [https://doi.org/10.1016/S0966-842X\(00\)01913-2](https://doi.org/10.1016/S0966-842X(00)01913-2)
- Mazzoni, C., Jacobsen, R.D., Mortensen, J., Jørgensen, J.R., Vaut, L., Jacobsen, J., Gundlach, C., Müllertz,

- A., Nielsen, L.H., Boisen, A., 2019. Polymeric Lids for Microcontainers for Oral Protein Delivery. *Macromol. Biosci.* 19, 1900004. <https://doi.org/10.1002/mabi.201900004>
- Mazzoni, C., Tentor, F., Strindberg, S.A., Nielsen, L.H., Keller, S.S., Alstrøm, T.S., Gundlach, C., Müllertz, A., Marizza, P., Boisen, A., 2017. From concept to in vivo testing: Microcontainers for oral drug delivery. *J. Controlled Release* 268, 343–351. <https://doi.org/10.1016/j.jconrel.2017.10.013>
- Mohammed, M., Syeda, J., Wasan, K., Wasan, E., 2017. An Overview of Chitosan Nanoparticles and Its Application in Non-Parenteral Drug Delivery. *Pharmaceutics* 9, 53. <https://doi.org/10.3390/pharmaceutics9040053>
- Mortensen, N.P., Fowlkes, J.D., Sullivan, C.J., Allison, D.P., Larsen, N.B., Molin, S., Doktycz, M.J., 2009. Effects of Colistin on Surface Ultrastructure and Nanomechanics of *Pseudomonas aeruginosa* Cells. *Langmuir* 25, 3728–3733. <https://doi.org/10.1021/la803898g>
- Mosgaard, M.D., Strindberg, S., Abid, Z., Petersen, R.S., Thamdrup, L.H.E., Andersen, A.J., Keller, S.S., Müllertz, A., Nielsen, L.H., Boisen, A., 2019. Ex vivo intestinal perfusion model for investigating mucoadhesion of microcontainers. *Int. J. Pharm.* 570, 118658. <https://doi.org/10.1016/j.ijpharm.2019.118658>
- Nation, R.L., Li, J., Cars, O., Couet, W., Dudley, M.N., Kaye, K.S., Mouton, J.W., Paterson, D.L., Tam, V.H., Theuretzbacher, U., Tsuji, B.T., Turnidge, J.D., 2015. Framework for optimisation of the clinical use of colistin and polymyxin B: the Prato polymyxin consensus. *Lancet Infect. Dis.* 15, 225–234. [https://doi.org/10.1016/S1473-3099\(14\)70850-3](https://doi.org/10.1016/S1473-3099(14)70850-3)
- Nielsen, L.H., Keller, S.S., Boisen, A., 2018. Microfabricated devices for oral drug delivery. *Lab Chip* 18, 2348–2358. <https://doi.org/10.1039/C8LC00408K>
- Nielsen, L.H., Keller, S.S., Gordon, K.C., Boisen, A., Rades, T., Müllertz, A., 2012. Spatial confinement can lead to increased stability of amorphous indomethacin. *Eur. J. Pharm. Biopharm.* 81, 418–425. <https://doi.org/10.1016/j.ejpb.2012.03.017>
- Nielsen, L.H., Melero, A., Keller, S.S., Jacobsen, J., Garrigues, T., Rades, T., Müllertz, A., Boisen, A., 2016. Polymeric microcontainers improve oral bioavailability of furosemide. *Int. J. Pharm.* 504, 98–109. <https://doi.org/10.1016/J.IJPHARM.2016.03.050>
- O'Neill, J., 2016. Tackling drug-resistant infections globally, Review on Antimicrobial Resistance. <https://doi.org/10.4103/2045-080X.186181>
- Olivera, M.E., Manzo, R.H., Junginger, H.E., Midha, K.K., Shah, V.P., Stavchansky, S., Dressman, J.B., Barends, D.M., 2011. Biowaiver monographs for immediate release solid oral dosage forms: Ciprofloxacin hydrochloride. *J. Pharm. Sci.* 100, 22–33. <https://doi.org/10.1002/jps.22259>
- Pamp, S.J., Gjermansen, M., Johansen, H.K., Tolker-Nielsen, T., 2008. Tolerance to the antimicrobial peptide colistin in *Pseudomonas aeruginosa* biofilms is linked to metabolically active cells, and depends on the *pmr* and *mexAB-oprM* genes. *Mol. Microbiol.* 68, 223–240. <https://doi.org/10.1111/j.1365-2958.2008.06152.x>
- Parish, T., 2019. Steps to address anti-microbial drug resistance in today's drug discovery. *Expert Opin. Drug Discov.* 14, 91–94. <https://doi.org/10.1080/17460441.2019.1550481>
- Pastar, I., Nusbaum, A.G., Gil, J., Patel, S.B., Chen, J., Valdes, J., Stojadinovic, O., Plano, L.R., Tomic-Canic, M., Davis, S.C., 2013. Interactions of Methicillin Resistant *Staphylococcus aureus* USA300 and *Pseudomonas aeruginosa* in Polymicrobial Wound Infection. *PLoS One* 8, e56846. <https://doi.org/10.1371/journal.pone.0056846>
- Patel, K.K., Tripathi, M., Pandey, N., Agrawal, A.K., Gade, S., Anjum, M.M., Tilak, R., Singh, S., 2019. Alginate lyase immobilized chitosan nanoparticles of ciprofloxacin for the improved antimicrobial activity against the biofilm associated mucoid *P. aeruginosa* infection in cystic fibrosis. *Int. J. Pharm.* 563, 30–42. <https://doi.org/10.1016/j.ijpharm.2019.03.051>
- Perinelli, D.R., Fagioli, L., Campana, R., Lam, J.K.W., Baffone, W., Palmieri, G.F., Casettari, L., Bonacucina,

- G., 2018. Chitosan-based nanosystems and their exploited antimicrobial activity. *Eur. J. Pharm. Sci.* 117, 8–20. <https://doi.org/10.1016/j.ejps.2018.01.046>
- Ross, D.L., Riley, C.M., 1994. Dissociation and complexation of the fluoroquinolone antimicrobials - an update. *J. Pharm. Biomed. Anal.* 12, 1325–1331. [https://doi.org/10.1016/0731-7085\(94\)00081-6](https://doi.org/10.1016/0731-7085(94)00081-6)
- Schwerdt, M., Neumann, C., Schwartbeck, B., Kampmeier, S., Herzog, S., Görlich, D., Dübbers, A., Große-Onnebrink, J., Kessler, C., Küster, P., Schültingkemper, H., Treffon, J., Peters, G., Kahl, B.C., 2018. *Staphylococcus aureus* in the airways of cystic fibrosis patients - A retrospective long-term study. *Int. J. Med. Microbiol.* 308, 631–639. <https://doi.org/10.1016/j.ijmm.2018.02.003>
- Silva, F., Lourenço, O., Queiroz, J.A., Domingues, F.C., 2011. Bacteriostatic versus bactericidal activity of ciprofloxacin in *Escherichia coli* assessed by flow cytometry using a novel far-red dye. *J. Antibiot. (Tokyo)*. 64, 321–325. <https://doi.org/10.1038/ja.2011.5>
- Soares, A., Alexandre, K., Lamoureux, F., Lemée, L., Caron, F., Pestel-Caron, M., Etienne, M., 2019. Efficacy of a ciprofloxacin/amikacin combination against planktonic and biofilm cultures of susceptible and low-level resistant *Pseudomonas aeruginosa*. *J. Antimicrob. Chemother.* 74, 3252–3259. <https://doi.org/10.1093/jac/dkz355>
- Stewart, P.S., 2002. Mechanisms of antibiotic resistance in bacterial biofilms. *Int. J. Med. Microbiol.* 292, 107–113. <https://doi.org/10.1078/1438-4221-00196>
- Stover, C.K., Pham, X.Q., Erwin, A.L., Mizoguchi, S.D., Warrener, P., Hickey, M.J., Brinkman, F.S., Hufnagle, W.O., Kowalik, D.J., Lagrou, M., Garber, R.L., Goltry, L., Tolentino, E., Westbrock-Wadman, S., Yuan, Y., Brody, L.L., Coulter, S.N., Folger, K.R., Kas, A., Larbig, K., Lim, R., Smith, K., Spencer, D., Wong, G.K., Wu, Z., Paulsen, I.T., Reizer, J., Saier, M.H., Hancock, R.E., Lory, S., Olson, M. V., 2000. Complete genome sequence of *Pseudomonas aeruginosa* PAO1, an opportunistic pathogen. *Nature* 406, 959–64. <https://doi.org/10.1038/35023079>
- Tamma, P.D., Cosgrove, S.E., Maragakis, L.L., 2012. Combination Therapy for Treatment of Infections with Gram-Negative Bacteria. *Clin. Microbiol. Rev.* 25, 450–470. <https://doi.org/10.1128/CMR.05041-11>
- Tao, S.L., Papat, K., Desai, T.A., 2007. Off-wafer fabrication and surface modification of asymmetric 3D SU-8 microparticles. *Nat. Protoc.* 1, 3153–3158. <https://doi.org/10.1038/nprot.2006.451>
- Traugott, K.A., Echevarria, K., Maxwell, P., Green, K., Lewis, J.S., 2011. Monotherapy or Combination Therapy? The *Pseudomonas aeruginosa* Conundrum. *Pharmacotherapy* 31, 598–608. <https://doi.org/10.1592/phco.31.6.598>
- Varanda, F., Pratas De Melo, M.J., Caço, A.I., Dohrn, R., Makrydaki, F.A., Voutsas, E., Tassios, D., Marrucho, I.M., 2006. Solubility of antibiotics in different solvents. 1. Hydrochloride forms of tetracycline, moxifloxacin, and ciprofloxacin. *Ind. Eng. Chem. Res.* 45, 6368–6374. <https://doi.org/10.1021/ie060055v>
- Vorregaard, M., 2008. Comstat2 - A Modern 3D Image Analysis Environment for Biofilms. Technical University of Denmark, DTU.
- Wallace, S.J., Li, J., Nation, R.L., Prankerd, R.J., Velkov, T., Boyd, B.J., 2010. Self-Assembly Behavior of Colistin and Its Prodrug Colistin Methanesulfonate: Implications for Solution Stability and Solubilization. *J. Phys. Chem. B* 114, 4836–4840. <https://doi.org/10.1021/jp100458x>
- Wang, S., Yu, S., Lin, Y., Zou, P., Chai, G., Yu, H.H., Wickremasinghe, H., Shetty, N., Ling, J., Li, J., Zhou, Q., 2018. Co-Delivery of Ciprofloxacin and Colistin in Liposomal Formulations with Enhanced In Vitro Antimicrobial Activities against Multidrug Resistant *Pseudomonas aeruginosa*. *Pharm. Res.* 35, 187. <https://doi.org/10.1007/s11095-018-2464-8>
- Wang, W., Zhou, Q.T., Sun, S.P., Denman, J.A., Gengenbach, T.R., Barraud, N., Rice, S.A., Li, J., Yang, M., Chan, H.K., 2016. Effects of Surface Composition on the Aerosolisation and Dissolution of Inhaled Antibiotic Combination Powders Consisting of Colistin and Rifampicin. *AAPS J.* 18, 372–384. <https://doi.org/10.1208/s12248-015-9848-z>

- Weber, K., Delben, J., Bromage, T.G., Duarte, S., 2014. Comparison of SEM and VPSEM imaging techniques with respect to *Streptococcus mutans* biofilm topography. *FEMS Microbiol. Lett.* 350, 175–179. <https://doi.org/10.1111/1574-6968.12334>
- Yu, S., Wang, S., Zou, P., Chai, G., Lin, Y.W., Velkov, T., Li, J., Pan, W., Zhou, Q.T., 2020. Inhalable liposomal powder formulations for co-delivery of synergistic ciprofloxacin and colistin against multi-drug resistant gram-negative lung infections. *Int. J. Pharm.* 575, 118915. <https://doi.org/10.1016/j.ijpharm.2019.118915>

## Supplementary materials

### **Co-delivery of ciprofloxacin and colistin using microcontainers for bacterial biofilm treatment**

Stine Egebro Birk, Chiara Mazzoni, Madeeha Mobasharah Javed, Morten Borre Hansen, Helle Krogh Johansen, Søren Molin, Janus Anders Juul Haagenen, Line Hagner Nielsen, Anja Boisen

<b>TABLE S1</b>	Media preparation
<b>FIGURE S1</b>	SEM images of single-loaded coated MCs
<b>FIGURE S2</b>	Release from uncoated MCs
<b>FIGURE S3</b>	Effect of uncoated MCs on planktonic <i>P. aeruginosa</i> growth
<b>FIGURE S4</b>	Effect of single-loaded coated MCs on <i>P. aeruginosa</i> biofilms

**Table S1.** The composition of modified FAB medium. A10 buffer, FB minimal medium with trace metals and the carbon source were autoclaved separately and mixed afterwards. Concentrations are given as final concentrations. \*Carbon source was not added for the release studies to avoid unintentional growth.

A10 buffer	FB minimal medium with trace metals	Carbon source*
33.7 mM Na <sub>2</sub> HPO <sub>4</sub> ·2H <sub>2</sub> O	1 mM MgCl <sub>2</sub>	2 µg L <sup>-1</sup> CuSO <sub>4</sub> ·5H <sub>2</sub> O
22.0 mM KH <sub>2</sub> PO <sub>4</sub>	0.1 mM CaCl <sub>2</sub>	2 µg L <sup>-1</sup> ZnSO <sub>4</sub> ·7H <sub>2</sub> O
15.1 mM (NH <sub>4</sub> ) <sub>2</sub> SO <sub>4</sub>	20 µg L <sup>-1</sup> CaSO <sub>4</sub> ·2H <sub>2</sub> O	1 µg L <sup>-1</sup> CoSO <sub>4</sub> ·7H <sub>2</sub> O
51 mM NaCl	20 µg L <sup>-1</sup> FeSO <sub>4</sub> ·7H <sub>2</sub> O	1 µg L <sup>-1</sup> NaMoO <sub>4</sub> ·H <sub>2</sub> O
	2 µg L <sup>-1</sup> MnSO <sub>4</sub> ·H <sub>2</sub> O	0.5 µg L <sup>-1</sup> H <sub>3</sub> BO <sub>3</sub>

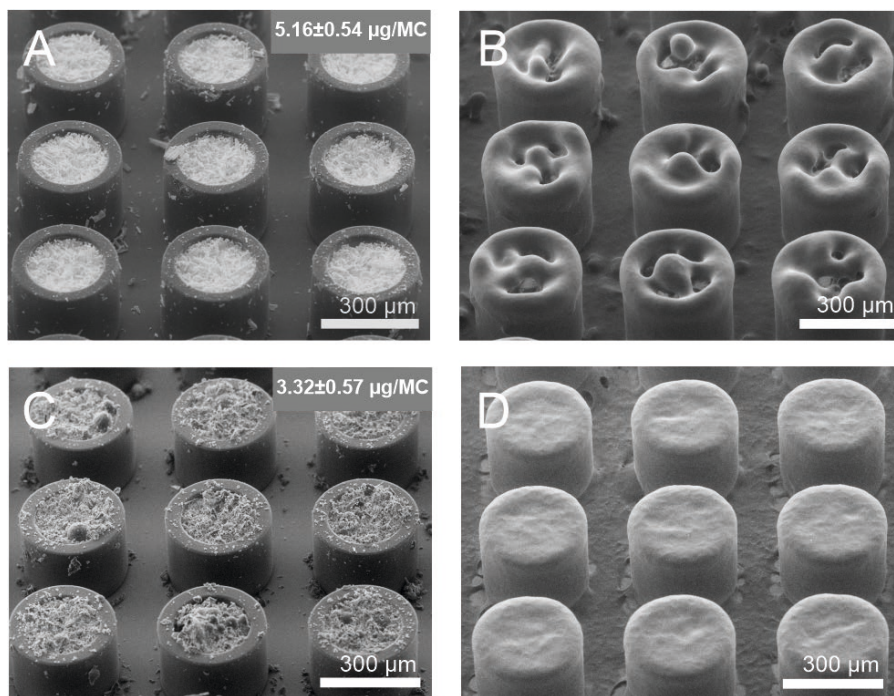


**Figure S1.** Scanning electron microscope (SEM) images of microcontainers (MCs) loaded with ciprofloxacin hydrochloride (A) or colistin sulfate (C) and subsequently coated with chitosan (B,D). Amount of loaded drug per MC is given as the mean±SD calculated based on the known amount loaded into one chip.

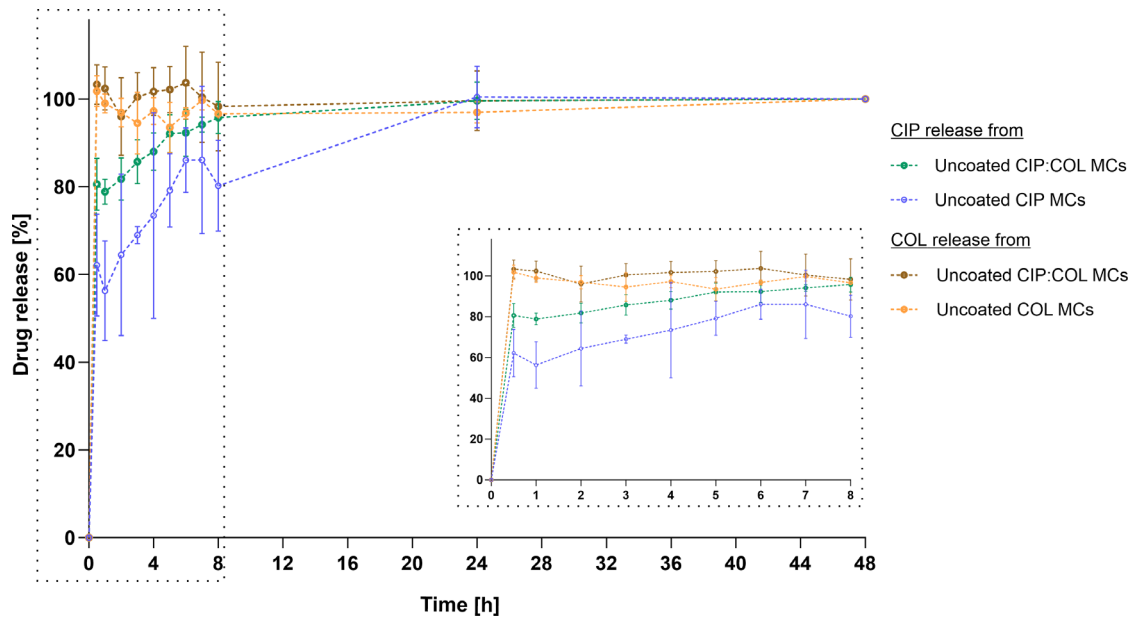


**Figure S2.** *In vitro* release of ciprofloxacin hydrochloride (CIP) and colistin sulfate (COL) from co-loaded or single-loaded microcontainers (MCs) without chitosan coating. Release study was performed at 37 °C in FAB medium pH 6.8 and quantified by LC-MS. Data was normalized to 100 % and presented as mean±SD, n=3-4.

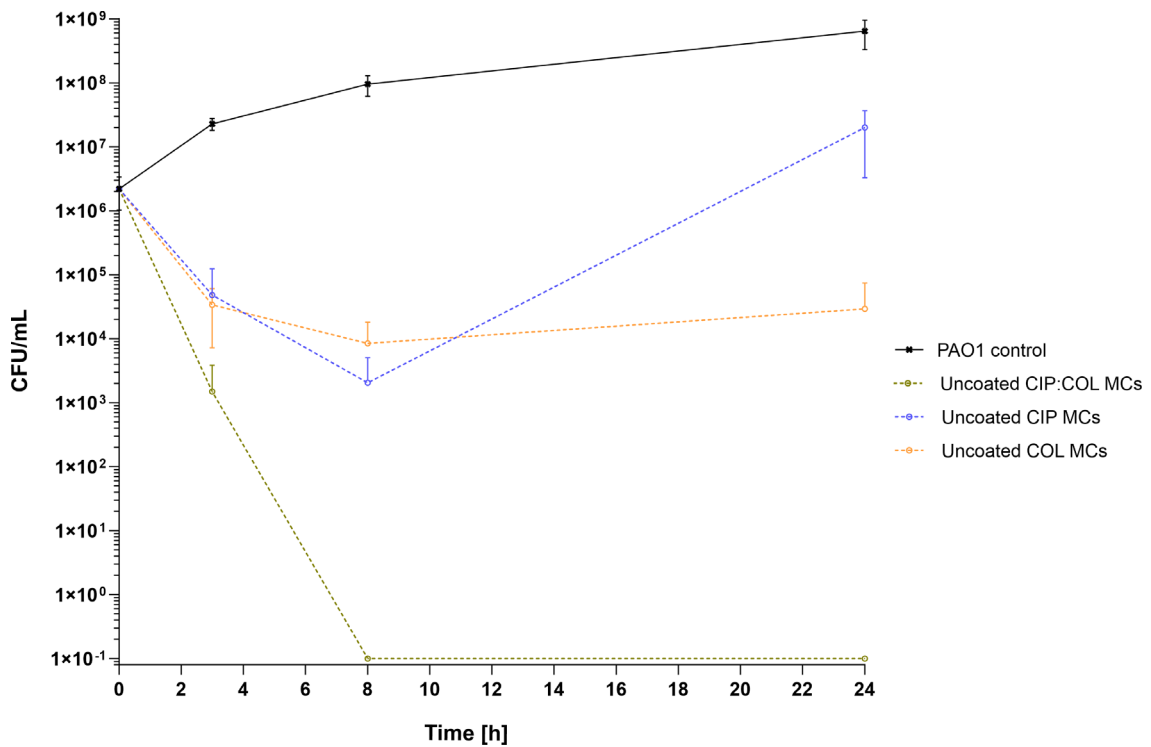


**Figure S3.** Inhibition of planktonic growth of *P. aeruginosa* (PAO1) over time when co-delivering ciprofloxacin hydrochloride (CIP) and colistin sulfate (COL) in uncoated microcontainers (MCs). As controls, treatment with CIP or COL alone in uncoated MCs as well as a positive control for PAO1 growth was included. Data is presented as mean±SD (n=3-6).

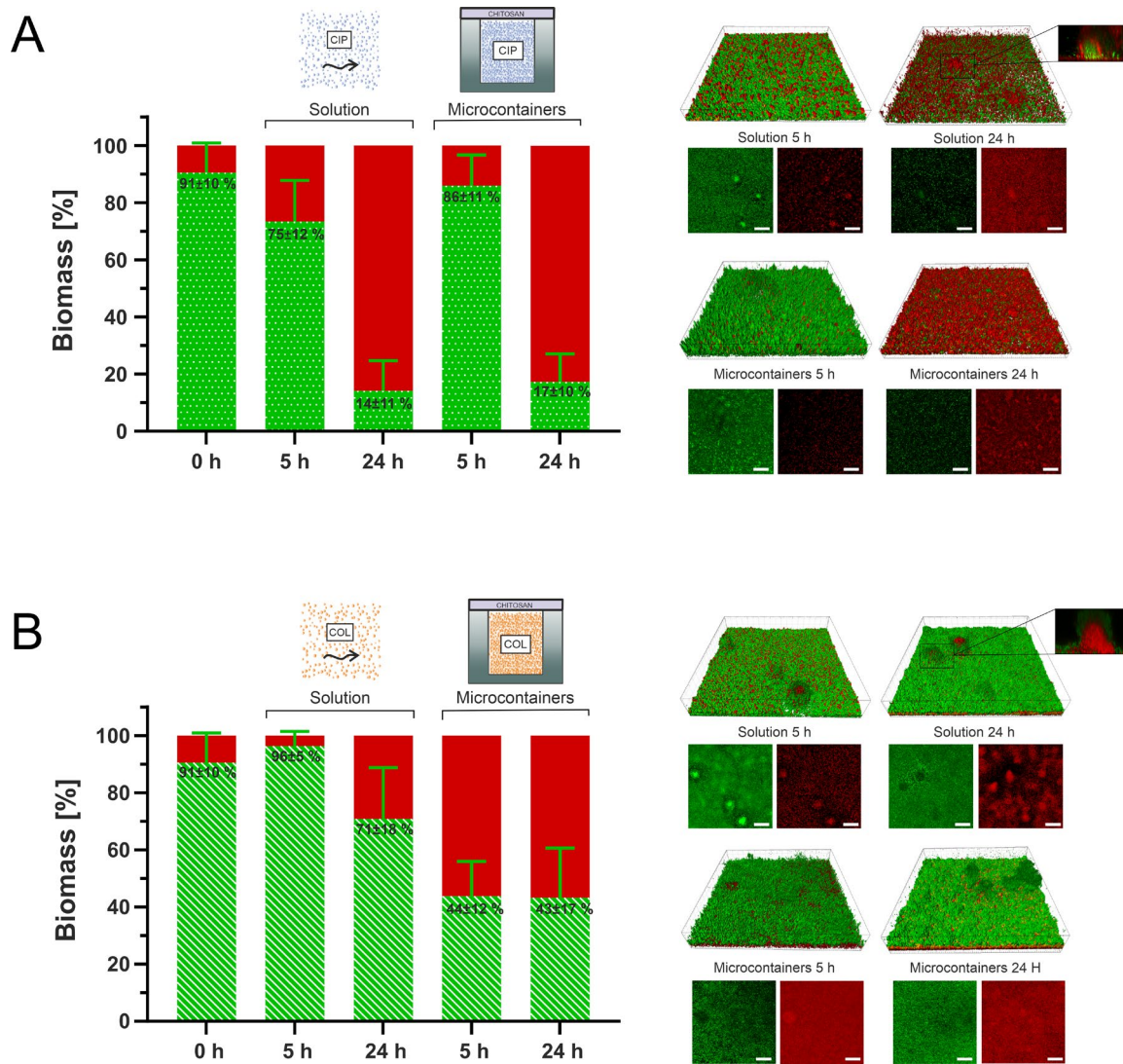


**Figure S4.** 72 h old *P. aeruginosa* (PAO1) biofilm treated with ciprofloxacin hydrochloride (CIP) (A) or colistin sulfate (COL) (B) either as solution or confined in MCs coated with chitosan. Quantitative analysis of the biomass ( $\mu\text{m}^3/\mu\text{m}^2$ ) converted to the fraction of live/dead (%). Data is depicted as mean+SD ( $n=3-5$  biological replicates with 3-5 technical replicates for each type of treatment). Representative confocal laser scanning microscopy (CLSM) images of biofilm before treatment, and 5 and 24 h post treatment with CIP or COL solution or MCs. Vertical sections show how the two different antimicrobials targets metabolically active cells versus dormant cells. Green represents live bacteria. Red represents dead bacteria. Scale bars: 30  $\mu\text{m}$ .



# APPENDIX IV

## PAPER IV

### **Enhanced eradication of mucin-embedded bacterial biofilm by locally delivered antibiotics in functionalized microcontainers**

S.E. Birk<sup>\*</sup>, L. Seriola<sup>\*</sup>, V. Cavallo, J.A.J. Haagensen, S. Molin, L.H. Nielsen, K. Zór, A. Boisen

*Journal of Controlled Release, 2020 (submitted, <sup>\*</sup>The authors contributed equally to the work)*

# Enhanced eradication of mucin-embedded bacterial biofilm by locally delivered antibiotics in functionalized microcontainers

*Stine Egebro Birk<sup>a\*\*†</sup>, Laura Seriola<sup>a\*\*†</sup>, Valentina Cavallo<sup>a</sup>, Janus Anders Juul Haagensen<sup>b</sup>, Søren Molin<sup>b</sup>, Line Hagner Nielsen<sup>a</sup>, Kinga Zór<sup>a\*</sup>, Anja Boisen<sup>a</sup>*

<sup>a</sup>The Danish National Research Foundation and Villum Foundation's Center for Intelligent Drug Delivery and Sensing Using Microcontainers and Nanomechanics (IDUN), Department of Health Technology, Technical University of Denmark, Ørsteds Plads 345C, 2800 Kgs. Lyngby, Denmark.

<sup>b</sup>Novo Nordisk Foundation Center for Biosustainability, Technical University of Denmark, Kemitorvet 220, 2800 Kgs. Lyngby, Denmark.

† The authors contributed equally to the work.

\*Corresponding authors: Stine Egebro Birk, e-mail: stegha@dtu.dk; Laura Seriola, e-mail: lauser@dtu.dk; Kinga Zór, e-mail: kinzo@dtu.dk

## ABSTRACT

Bacterial biofilm-related infections are difficult to eradicate and require repeated treatments with high doses of antibiotics. Thus, there is an urgent need for new and robust treatment strategies that can minimize the use of antibiotics and at the same time enhance eradication of biofilm. Functionalized reservoir-based microdevices, such as microcontainers (MCs), offer high drug loading capacity, mucus embedment and tunable drug release, therefore making them interesting candidates for local delivery of antibiotics into biofilm. Here, MCs are loaded with the antibiotic ciprofloxacin, and subsequently sealed with a lid consisting of chitosan (CHI) and a mucolytic agent, N-acetylcysteine (NAC). We find that CHI and NAC work synergistically, showing improved mucoadhesive and mucolytic properties. The CHI/NAC functionalization significantly accelerates ciprofloxacin release from MCs, with 100 % release within 1 h, whereas MCs only functionalized with CHI reach full release within 40 h. We show for the first time, that it is possible to use mucin-containing medium in a perfusion microfluidic platform, an essential factor for better mimicking of the *in vivo* habitat of the bacteria. When evaluating the effect of MCs on *Pseudomonas aeruginosa* (*P. aeruginosa*) biofilms grown in a newly developed *in vitro* centrifugal microfluidic system with a mucin-containing medium, we find that the CHI/NAC coated MCs improve eradication of biofilm (88.22±2.89 %) compared to CHI-coated MCs (72.68±3.73 %) or bolus injection (39.86±13.28 %). Our findings suggest that MCs are significantly more efficient than a bolus treatment. Furthermore, CHI/NAC functionalized MCs are able to kill most of the biomass already after 5 h (80.75±3.50 %), mainly due to a fast drug release. This is to the best of our knowledge, the first time where CHI/NAC has been combined to explore mucolytic properties on bacterial biofilms. These results show an effective MC-based treatment strategy which potentially can limit side effects and lead to a reduced use of antibiotic in future therapies.

## KEYWORDS

Microdevices; *In vitro* perfusion system; Artificial sputum medium; N-acetylcysteine; Chitosan; *Pseudomonas aeruginosa* biofilm

## 1. INTRODUCTION

Bacterial biofilms are 10-1000 times more tolerant towards antimicrobial agents compared to their planktonic counterparts [1–4]. Reportedly, up to 80 % of bacterial infections in humans are associated with biofilms [5] resulting in a substantial economic burden and healthcare cost [6]. Biofilms are aggregations, where microbial cells adhere to each other and produce a matrix of extracellular polymeric substances (EPS) consisting of DNA, proteins and polysaccharides [7]. Due to the nature and structure of the EPS matrix, it is one of the main protections of the bacteria, capable of decreasing the diffusion of antimicrobial agents through the biofilm layers [3,8,9].

One of the most studied pathogenic biofilm-forming species is the Gram negative bacterium *Pseudomonas aeruginosa* (*P. aeruginosa*) [10]. This pathogen often creates highly recalcitrant infections in people with chronic wounds [11] and with a compromised host defense such as in patients with cystic fibrosis [12] or AIDS [13,14]. These infections are associated with a high rate of morbidity and a mortality [15]. The mucosal epithelial surfaces of our human body are covered with layers of viscous mucus, in which pathogens can reside and develop serious infections [16,17]. It has specifically been shown that mucins [17,18], which are glycoproteins produced by epithelial goblet cells and the main gel-forming component of mucus, help biofilm formation of *P. aeruginosa* [19].

Depending on the type of bacterial infection, patients are treated with antibiotics with different mechanism of action. Quinolones are widely used in clinics since they inhibit bacterial DNA synthesis by blocking DNA gyrase and topoisomerase IV, ultimately causing bacterial death [20]. Ciprofloxacin hydrochloride (CIP) is a second-generation quinolone commonly used to treat *P. aeruginosa* biofilm infections [21,22]. Intravenous or oral administrations of antibiotics often fail as they cannot be dosed in concentrations that are sufficiently high to eradicate biofilms, considering the risk of side effects as well as the threat of developing antibiotic resistance [23].

Therefore, the use of antimicrobial delivery systems, which can create high local drug concentrations and enhance penetration through the EPS, thereby leading to enhanced eradication of bacteria in biofilm, has gained great interest [9,24]. Reservoir-based polymeric microdevices, with a large drug loading capacity, ensuring the local delivery of high drug concentrations in the intestinal mucosa or in close proximity of biofilms, have been proposed as promising tools for drug delivery [24–26]. Microcontainers (MCs), which are polymeric cylindrical microdevices, have been shown to increase oral bioavailability of small drugs, possibly due to mucoadhesion and engulfment in the intestinal mucus [27,28]. After drug loading, the MCs can be sealed and functionalized with a polymeric coating, designed to protect the drug from the exterior environment and to enable tailored and controlled release [27,29–31]. Moreover, our latest findings show that local delivery of CIP by the use of MCs promoted eradication of *P. aeruginosa* biofilms with the use of substantially lower antibiotic concentrations compared to bulk delivery [24].

There are various strategies to improve the effect of antibiotic treatment. For instance chitosan (CHI), a cationic polysaccharide, has been widely used as a mucoadhesive polymer increasing the residence time of drug formulations at the site of action, caused by electrostatic interactions and hydrogen bonding [32]. Moreover, CHI can provide a controlled antibiotic release [33,34]. Earlier, we found that CIP-loaded MCs

functionalized with CHI, showed slightly higher average biofilm eradication than other polymeric coatings, such as polyethylene glycol and Eudragit S100 [24]. The effect can be attributed to the known antimicrobial activity of CHI [35,36].

In order to further increase the efficacy of treatment, mucolytic agents are often used in diseases such as cystic fibrosis, in order to reduce the bulk viscoelasticity of the thick mucus layer in the lungs [37]. N-acetylcysteine (NAC) is one of these mucolytic agents, that has proven to be beneficial in inhibiting biofilm adherence and development, as well as in disrupting pre-formed mature *P. aeruginosa* biofilms [38–42]. NAC is a drug approved by the U.S. Food and Drug Administration (FDA) [43], and is widely used in connection with a number of clinical conditions, including chronic bronchitis, due to its inherent mucolytic and antioxidant effects [44]. NAC selectively breaks the thiol-disulfide bonds between the glycoproteins in the mucin, ultimately reducing the degree of cross-linking and thereby, the viscosity of the mucus [45]. The synergistic use of CHI and NAC has previously been studied, however mostly in lipid-based carriers. For instance, Hamedinasab *et al.*, demonstrated prolonged release of NAC from liposomes in the lungs after inhalation [46], and it has also been shown that nanostructured lipid carriers improve ophthalmic bioavailability within the ocular mucosa [47]. Additionally, CHI-based nanomicelles functionalized with NAC provide improved bioadhesion, mucus penetration and ultimately enhanced oral absorption of hydrophobic drugs with an otherwise poor penetrative profile [48].

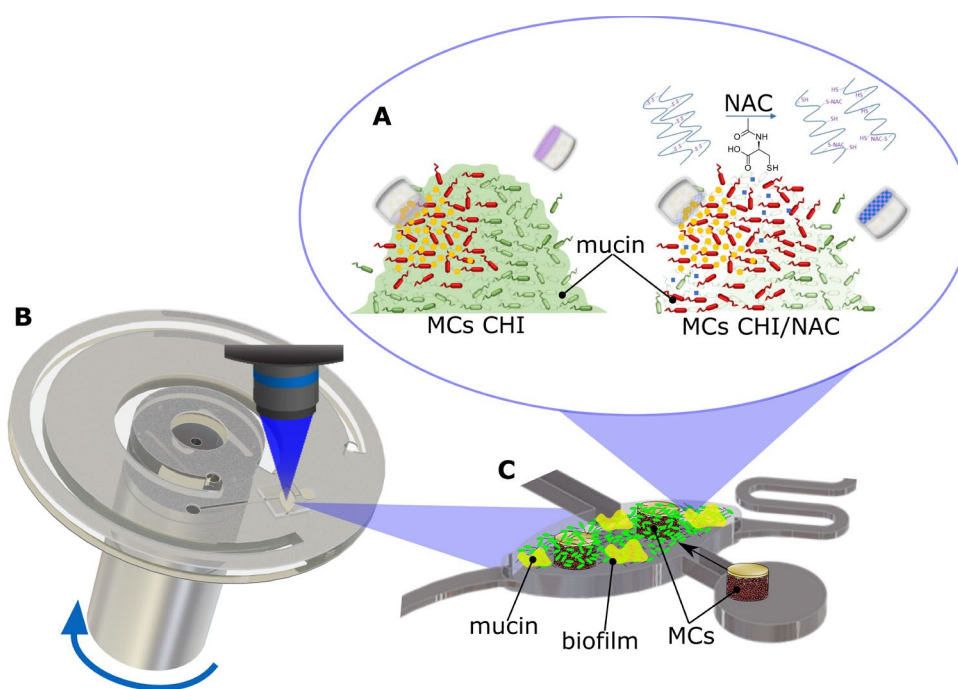


**Figure 1.** Schematic representation of the functionalized microcontainers (MCs) for local delivery of antibiotics to the mucin-embedded biofilm and the in vitro centrifugal system: Bacterial Culture on Disc (BCoD). Illustration of the proposed effect of the functionalized MCs on the biofilm (red are killed and green are live bacteria), where chitosan (CHI) (purple) may provide a prolonged residence time of the MCs, while the combination of CHI and N-acetylcysteine (NAC) (blue) coating may further improve biofilm eradication, due to the mucolytic effect of NAC (A). The BCoD system (B) and close-up of the bacterial culture chamber, where *P. aeruginosa* biofilm (green) is grown in the presence of mucin (yellow) and treated with antibiotics loaded in functionalized MCs (C).

Here, we investigate whether functionalization with CHI/NAC of CIP-loaded MCs can further improve eradication of *P. aeruginosa* biofilms. Our hypothesis is that the CHI/NAC coating can have a dual effect on eradication of biofilms by enhancing (i) *local delivery*, due to the mucoadhesive properties of CHI and (ii) *improve drug diffusion* into the biofilm, thanks to the mucolytic effect of NAC (Figure 1A). Although, there are a few studies, evaluating the mucoadhesive properties of CHI/NAC [48], this is, to the best of our knowledge, the first time where the combination of these two compounds is used to explore the mucolytic properties on bacterial biofilms.

In this study the mucolytic effect of NAC, as well as the mucoadhesive effect of the CHI/NAC blend is evaluated with Quartz Crystal Microbalance (QCM) and we assess the effect of the CHI/NAC functionalized, CIP-loaded MCs on biofilms in a novel *in vitro* system (Figure 1B).

The centrifugal microfluidic-based *in vitro* system, the bacterial culture on disc (BCoD) platform (Figure 1B), provides a unique possibility to perform studies on biofilms embedded in mucin (Figure 1C), often unachievable with commonly available *in vitro* platforms [49]. *In vitro*, the *P. aeruginosa* biofilm is grown under flow condition in artificial sputum medium (ASM) [49], mimicking the sputum of cystic fibrosis patients and providing a microenvironment similar to *in vivo* condition [50]. As other microfluidic systems, the BCoD works with small reagents volumes (from  $\mu\text{L}$  to few mL), enabling the use of complex and expensive growth media such as ASM, and additionally does not necessitate the use of auxiliary pumps [49]. Pumps and tubing introduce additional reagent consumption. Thus, the BCoD is ideal for minimizing reagent consumption and to the best of our knowledge, ASM has never previously been used in perfusion microfluidic bacterial culture platforms. In the BCoD, the antimicrobial activity of the developed CHI/NAC and CHI-functionalized MCs is compared to bulk delivery of unconfined antibiotics.

## 2. MATERIALS AND METHODS

### 2.1. Materials

Silicon (Si) wafers (4" (100) n-type) were acquired from Okmetic (Vantaa, Finland), while the SU-8 constituents (SU-8 2075 and SU-8 Developer) were obtained from Micro Resist Technology (Berlin, Germany). CIP were from Fagron (Uitgeest, The Netherlands), while CHI (low MW 50-190 kDa, 75-85 % deacetylation), acetic acid, NAC, citric acid, sodium hydroxide, disodium hydrogen phosphate, sodium chloride, hydrogen chloride, mucin powder from porcine stomach (Type II), Luria Bertani (LB) medium, propidium iodide (label for identification of dead cells) and Alcian blue (label for identification of mucin) were all acquired from Sigma-Aldrich (St. Louis, MO, USA). All components used for FAB medium and ASM medium (composition and preparation in Supporting Information, Table S1 and Table S2) were bought from Sigma-Aldrich (St. Louis, MO, USA). Gold sensors (QSX 301 Gold) were acquired from Biolin Scientific AB (Västra Frölunda, Sweden). Poly(methyl methacrylate) (PMMA) with a thickness of 5 mm was purchased from Nordisk plast (Randers, Denmark), while PMMA with a thickness of 0.5 mm was from PSC A/S (Brønderslev, Denmark). ARcare 7840 pressure sensitive double adhesive tape (PSA) was purchased from Adhesive Research (Limerick, Ireland), and cover glass was obtained from Gerhard Menzel B.V.&Co.KG (Braunschweig, Germany). Syringes and needles were acquired from Hounisen

Laboratorieudstyr A/S (Jystrup, Denmark), whereas filters were from CHROMAFIL®, Macherey-Nagel (Düren, Germany). Ultrapure water was obtained from a Q-POD® dispenser (Merck Millipore, Burlington, MA, USA).

## **2.2. Characterization of the mucolytic activity of CHI/NAC by the use of quartz crystal microbalance with dissipation (QCM-D)**

The mucolytic effect of NAC in the presence of CHI was monitored in real-time as changes in frequency and dissipation shifts of a mucin layer dispersed onto gold sensors QSX 301 in a Q-Sense E1 Analyzer (Q-Sense AB, Gothenburg, Sweden). The QCM-D experiments were performed at room temperature using 0.1 M citric acid/0.2 M isotonic phosphate buffer adjusted to pH 4 at a flow rate of 0.1 mL/min. A 25 mg/L mucin solution was freshly prepared by dissolving mucin powder in the citric acid/phosphate buffer with gently stirring at 100 rpm for 1 h. The control solutions, containing 0.4 or 20 mg/mL NAC in citric acid/phosphate buffer, were stirred for 1.5 h before use. The CHI solution was prepared in a concentration of 100 mg/L and stirred at 50°C overnight. To prepare the CHI/NAC solution, 0.4 mg/mL NAC was added to an already solubilized CHI solution and dissolved by stirring for 1.5 h, giving rise to a concentration similar to the one applied for the spray coating process (20 mg/mL NAC in 0.5 % w/v CHI, see section "Functionalization and coating of MCs"). Each solution of NAC and CHI were manually filtered using a 0.8 µm pore size syringe filter and subsequently degassed.

Prior to each QCM-D experiment, the flow module and gold sensors were cleaned multiple times by rinsing with Milli-Q water, ethanol and acetone and dried with pressurized air. Citric acid/phosphate buffer was flown in the detection chamber for 30 min in order to obtain a stable frequency and dissipation baseline on the QCM. The mucin solution was introduced onto the sensor for 1.5 h to allow absorption of a mucin layer on the gold sensor. Subsequently, the system was rinsed for approximately 15 min with buffer to remove any unbound mucins. CHI, NAC, or CHI/NAC solutions were added for 1 h and changes in frequency and dissipation was monitored. Lastly, any unbound molecules were removed by rinsing the gold sensor with a buffer solution for 30 min. For each step in the assay, the flow rate was kept at 0.1 mL/min for the entire experiment. All data was subsequently fitted in a Voigt Kelvin model providing information on the viscoelastic properties, i.e. dissipation behaviour, of the layer. Data in the 3<sup>rd</sup> overtone was used for analysis in the QTools software (Version 3, Q-Sense AB, Sweden). All experiments were performed in duplicates and results normalized to start at 0 in frequency and dissipation.

## **2.3. Fabrication and antibiotic loading of MCs**

MCs were fabricated using a two-step photolithography process originally described by Tao *et al.* and later modified by Nielsen *et al.* [51,52]. In brief, Si wafers were covered with a layer of the negative epoxy photoresist SU-8 and subsequently, exposed to a number of baking steps allowing the formation of the bottom and the side walls of the MCs. After fabrication, the wafers were diced into chips (12.8×12.8 mm<sup>2</sup>), with each chip containing 625 individual MCs. For the biofilm assays, harvesting of individual MCs was enabled by addition of a release layer under the MCs, made by electron beam deposition of 5 nm titanium

and 20 nm gold on the Si wafer prior to baking (Temescal FC-2000, Ferrotec Corporation, USA). The inner and outer diameters of the individual MCs were determined with an Eclipse L200 bright-field optical microscope (Nikon, Tokyo, Japan), whereas the inner and outer heights were evaluated by vertical scanning interferometry using a PLu Neox 3D Optical Profiler (Sensofar, Terrassa, Spain).

MCs were loaded with the antibiotic, CIP, using an embossing method as previously described [53]. In short, a shadow mask was attached on top of the chip to cover the gaps between the MCs. CIP was distributed on the chip with a brush and subsequently embossed into the cavity of the MCs by applying a pressure of  $0.49 \cdot 10^{-1}$  T with a compact digital pressure controlled electric crimper-MSK-160E (MTI Corporation, Richmond, CA, USA). Afterwards, the shadow mask was removed and any excess of CIP outside the MCs were gently removed with pressurized air. The chips were weighted before and after loading to quantify the amount of drug.

#### **2.4. Functionalization and coating of MCs**

After loading, the opening of the MCs was coated with CHI and NAC. Coating was achieved by spraying the solution over the chip with MCs using an ExactaCoat Ultrasonic Spray System (Sonotek, USA) with an accumist nozzle operating at 120 kHz. 0.5 % w/v CHI was dissolved in 0.1 M acetic acid by heating overnight (50°C) and subsequently, filtered using a 5-13  $\mu$ m filter with vacuum suction. For the CHI/NAC coating solution, NAC was added in concentrations of 10, 20, or 40 mg/mL, corresponding to CHI/NAC ratios of 1:2, 1:4, or 1:8 w/w.

Each chip was coated with either CHI or the CHI/NAC-mixture with two alternating spray paths having an offset of 2 mm, resulting in a total of 120 passages. To allow solvent evaporation, the plate underneath the chip was heated to 50°C. Generator power was kept at 1.3 W, path speed at 25 mm/s, infusion rate at 0.1 mL/min and the air pressure at 0.026 bar. The distance between the spray nozzle and the sample was set to 5.5 cm.

#### **2.5. Surface characterization of loaded and coated MCs**

Visualization of the MCs after loading and coating was carried out by scanning electron microscopy (SEM) using a Hitachi Tabletop Microscope (Hitachi High-Technologies Europe GmbH, Krefeld, Germany). The chips were observed on a 30° tilted holder and images were acquired using the scattered electron (SE) detector and an accelerating voltage of 15 kV for highest quality images. The thickness of the CHI and CHI/NAC coatings was assessed by spraying the solutions onto flat Si chips with a layer of SU-8 deposited on top, half covered with a glass slip. Subsequently, measurements were conducted with an Alpha-Step IQ Stylus Profilometer (KLA-Tencor, Corporation, Milpitas, USA) using a scan speed of 50  $\mu$ m/s and a tip force of 8.17 mg. Measurements were conducted at three different locations on each coated chip and presented as mean $\pm$ standard deviation (SD).



## 2.6. *In vitro* release of CIP from MCs

The release of CIP from the functionalized MCs was studied using a  $\mu$ Diss Profiler (Pion Inc. Woburn, MA, USA). Initially, a calibration curve for each probe was prepared by adding specified volumes of a 2 mg/mL CIP solution in MilliQ to 20 mL of FAB medium (composition in Supporting Information, Table S1) and monitored by UV-absorbance.

For the release study, a chip with MCs was attached to a cylindrical magnetic stirrer with carbon tape, placed in a glass vial and subsequently, covered with 20 mL FAB medium. All studies were performed at 37°C with a stirring rate of 100 rpm and with UV in situ probes with a path length of 5 mm. Second derivative UV spectra in the range of 350-355 nm were collected over a period of 40 h. The percentage of released CIP was calculated from the known amount of drug loaded per chip. All experiments were carried out in 3-6 replicates and data were normalized to 100 % in relation to the total drug release after 40 h.

## 2.7. Bacterial strain and culture condition

The *P. aeruginosa* (PAO1) [54] strain was genetically modified by introducing a gene encoding green fluorescent protein (GFP) in the chromosome at a neutral site using Tn7 tagging [55], making the bacteria fluoresce green under the microscope when exposed to a 488 nm light source. Overnight cultures of PAO1 were prepared in LB medium at 37°C, and 40  $\mu$ L culture diluted to a final concentration of approximately  $1 \times 10^8$  cells/mL ( $OD_{600}$  of 0.05) was used as inoculum.

## 2.8. *In vitro* microfluidics platform for bacterial growth and monitoring

The BCoD (Figure 2A) was designed and fabricated as described in details by Seriola *et al.* [49]. Briefly, the platform consists of three PMMA layers bonded together by two PSA layers, and is composed of an inlet and waste reservoir together with a cell culture chamber (Figure 2A, insert). A detailed description of the fabrication and assembly is provided in the Supporting information, BCoD fabrication (Figure S1). Figure 2A shows the stack of BCoD placed in an incubation room, where it can be observed that the opening in the BCoD is closed with sterile filters (Figure 2A). The cell culture chamber (Figure 2B) has a depth of 1 mm with an inner volume of 32  $\mu$ L and is closed with a cover glass (described in the Supporting Information, BCoD fabrication, Figure S1), to achieve optimum imaging with an upright Leica SP5 CLSM confocal laser scanning microscope (Leica Microsystems, Mannheim, Germany). For this application, compared to the previous design [49], the cell culture chamber was modified in order to be able to allow the insertion of the MCs and to maximize their contact with the formed biofilm attached on the glass lid (Figure 2B, close-up).

More specifically, the size of the chamber was halved (1 mm, 32  $\mu$ L) and an opening close to the cell chamber was created as shown in Figure 2B. In the *in vitro* system (Figure 2A and 2B), the culture medium flows from the inlet reservoir and reaches the cell chamber through a serpentine channel. The shape of the channel was designed in order to enable good mixing of nutrients, without sharp edges, and to avoid trapping of bubbles. Waste products and detached clusters of bacteria moved from the cell chamber to the waste reservoir through a straight channel. Prior to inoculation with bacteria, the disc was sterilized

for 20 min with 0.5 M sodium hydroxide and carefully rinsed with sterile water and FAB minimal medium (without glucose). After sterilization, the platform was filled with medium and placed on the spin stand (rotation was achieved with a spindle motor, RE 35, Maxon motor AG, Sachseln, Switzerland) as shown in Figure 2A. The rotational frequency was set to 2 Hz for a few seconds to prime the cell culture chamber and to create the front of the liquid, then the rotation of the disc was stopped, and PAO1 was inoculated into the cell chamber through an inoculation channel using a syringe needle. During inoculation, the opening of the inlet reservoir was closed in order to avoid contamination of bacteria in the inlet reservoir. After 1 h in static condition, the disc was spun with a defined rotational frequency to achieve the required flow rate of 1  $\mu\text{L}/\text{min}$  (calibration curve of the BCoD is presented in Figure S2). The flow rate was kept constant throughout the experiment if not otherwise specified.

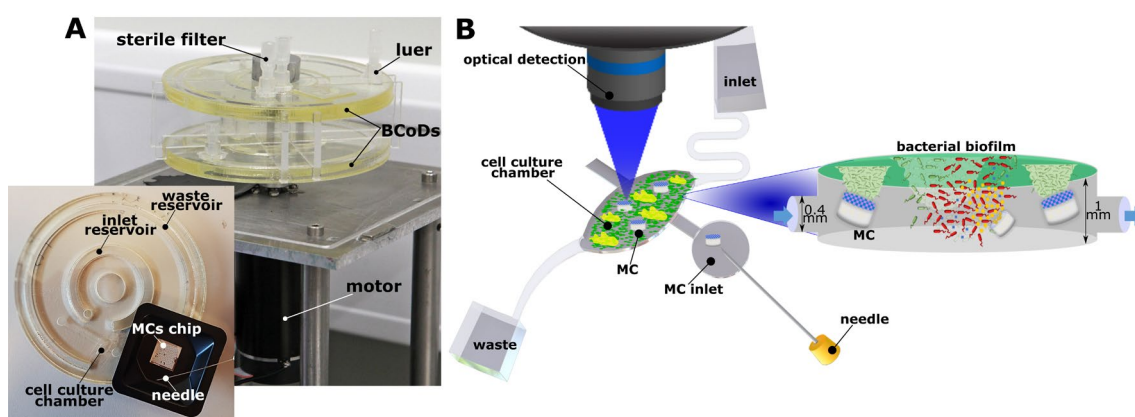


**Figure 2.** Bacterial culture on disc (BCoD) systems stacked on a spin stand with sterile filters, placed in the opening of the BCoD via luer connectors, in an incubation room. The insert shows the main operational units on the BCoD, the microcontainers (MCs) on the chip and the syringe needle used for the removal of MCs from the chip (A). Graphical representation of the cell culture chamber on the BCoD and the illustration of the addition of the MCs in the chamber. The close-up depicts the cell culture chamber with the formed bacterial biofilm in the presence of mucin and the effect of the antibiotics delivered with the functionalized MCs (B).

## 2.9. PAO1 growth and antibiotic treatment monitoring in BCoD

PAO1 was grown from single cells to a biofilm using two different dilutions of ASM: i) 100 times diluted mucin and nutrients (following called “mucin poor ASM”) and ii) 10 times diluted mucin and 100 times diluted nutrients (following called “mucin rich ASM”) (preparation in Supporting Information, Media preparation). The selected flow rate was 1  $\mu\text{L}/\text{min}$ . The biofilm was monitored during formation and before and after antibiotic treatment with confocal microscopy. To be able to detect dead cells, 2  $\mu\text{L}$  of propidium iodide (20 mM) was introduced in the inlet reservoir. After formation of the biofilm, antibiotic treatment was administered either as I) bolus injection (antibiotic introduced directly in the cell chamber), II) CHI-coated MCs or III) CHI/NAC (1:8 w/w)-coated MCs (Figure 3). For comparison, the antibiotic treatment was carried out with same final concentration (4  $\mu\text{g}/\text{mL}$ ) of CIP in the cell culture chamber. The effect of the treatment was evaluated 5 h and/or 24 h after introduction of antibiotic. The bolus injection and the quantity of MCs introduced into the cell chamber were calculated (Supporting Information

Calculation S1) considering the concentration used in previous studies [49].

In all experiments, the bacterial biofilm was grown for 48 h, when cultured in mucin rich medium, while for 72 h in mucin poor medium, followed by CIP treatment for 24 h. When the MCs were introduced in the disc, images were collected near and far from the MC in order to cover the entire cell chamber.

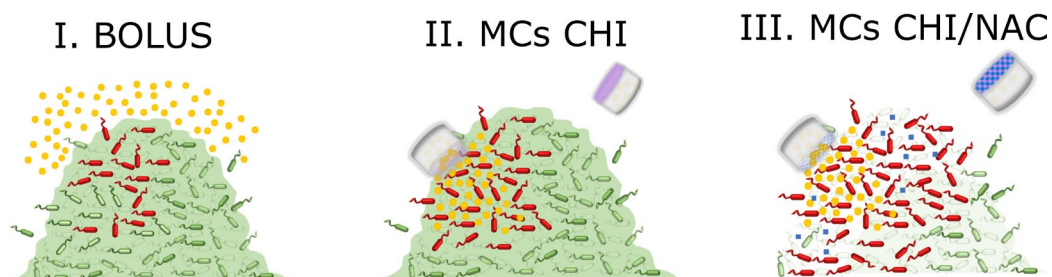


**Figure 3.** Schematic representation of the strategies for mucin embedded biofilm eradication, illustrating the expected effect of the treatment, when ciprofloxacin hydrochloride (CIP) was administered directly as bolus (I) and when delivered in functionalized MCs, namely chitosan (CHI) (II) and chitosan/N-acetylcysteine (CHI/NAC) coated MCs (III).

#### 2.10. Data collection and statistics

GraphPad Prism (Version 8.0.1, GraphPad Software, CA, USA) and Origin(Pro) 2019b (OriginLab Corp, Northampton, USA) was used to analyze and display the data. All data are expressed as mean $\pm$ SD, unless otherwise stated. Microscopic monitoring of bacterial biofilms and effect of MCs were completed using an upright Leica equipped with an argon/krypton laser and detectors and filter sets for simultaneous monitoring of GFP (excitation: 488 nm, emission: 493–558 nm) for live cell imaging and propidium iodide (excitation: 543 nm, emission: 558–700 nm) for dead cell staining. Sequential line scanning was used to avoid cross talk. Images were obtained using a 50x water objective (numerical aperture 0.75). The microscopy images were collected throughout the cell culture chamber in order to cover the entire chamber. The confocal images were treated using IMARIS software (Bitplane AG) and the collected images were used to calculate the bacterial biomass using Comstat (Comstat, Technical University of Denmark) [56]. For the evaluation of the effect of treatment on biofilms, two biological replicates were used for each treatment strategy with eighteen technical replicates in each case. Statistical analysis were conducted using GraphPad Prism (Version 8.0.1, GraphPad Software, CA, USA). p-values were calculated using the unpaired t-test ( $p \leq 0.05$  was considered significant).

### 3. RESULTS & DISCUSSION

#### 3.1. Characterization of the mucolytic activity of CHI/NAC coating

NAC has proven to be beneficial for disruption of mature biofilms due to its mucolytic effect [38–40], but we also found it important to test if this effect was compromised when used in combination with CHI. Therefore, the mucolytic activity of NAC, in the presence of CHI, was investigated using a QCM-D-based assay, monitoring changes in frequency ( $\Delta f$ ) and dissipation ( $\Delta d$ ) (Supporting Information, QCM-D results, Figure S3 and Figure S4). We observed that the addition of 0.4 mg/mL NAC gave rise to a slightly increased frequency and dissipation ( $\Delta f=0.59$  and  $\Delta d=0.2$ ) (detailed explanation in Supporting Information, QCM-D results). When 100 mg/L CHI was introduced onto the sensor, this caused an immediate decrease in frequency ( $\Delta f=6.19$ ) indicating a higher mass due to CHI absorption onto mucins. Moreover an increased dissipation ( $\Delta d=0.77$ ) was observed, demonstrating a softer mucin layer. When applying 100 mg/L CHI with 0.4 mg/mL NAC (ratio of 1:4 w/w) onto the mucin layer, we observed a decreased frequency ( $\Delta f=13.79$ ) and an increased dissipation ( $\Delta d=1.89$ ), both values being higher than the ones measured after addition of only NAC or CHI. CHI adhesion and entrapment of water led to an increased mass, which was larger than observed for CHI alone, suggesting that relatively more water was taken up.

Moreover, the covalent attachment of NAC to the sulfide-groups of the mucin chains may have contributed to the increase in mass, indicating an improved mucoadhesion. This was also observed by Lian *et al.*, who designed nano-micelles based on a CHI-vitamin E succinate copolymer conjugated with NAC (CS-VES-NAC). The nano-micelles exhibited a two-fold stronger mucoadhesive force compared to CS-VES, probably due to the covalent attachment [48]. Most importantly, an increased dissipation was also observed in our study, which is a result of a much softer and less viscous mucin layer, proving the mucolytic effect of NAC and demonstrating a clear synergistic effect of NAC and CHI. The latter can be explained by the fact that the adhesive CHI may entrap NAC and bring it in close contact with the mucins, where in contrast, NAC by itself has no ionic interaction mechanisms with the mucins and therefore it can easier be flushed away. The obtained results confirm the mucolytic effect of NAC even in the presence of CHI.

#### 3.2. Loading and coating of MCs

Based on the QCM-D studies, we could conclude that the mixture of CHI and NAC displays both the mucoadhesive effect from CHI and the mucolytic effect from NAC. Therefore, CHI/NAC was used for the coating and functionalization of the MCs. Additionally, as control, MCs were also coated with CHI alone. The fabrication process of the MCs proved to be reproducible, considering that the inner and overall height was  $232.1 \pm 1.7 \mu\text{m}$  and  $267.4 \pm 2.1 \mu\text{m}$  (mean $\pm$ SD,  $n=24$ ), respectively, and the inner and outer diameter was found to be  $236.5 \pm 0.6 \mu\text{m}$  and  $322.2 \pm 0.7 \mu\text{m}$  (mean $\pm$ SD,  $n=9$ ), respectively (Figure 4A).

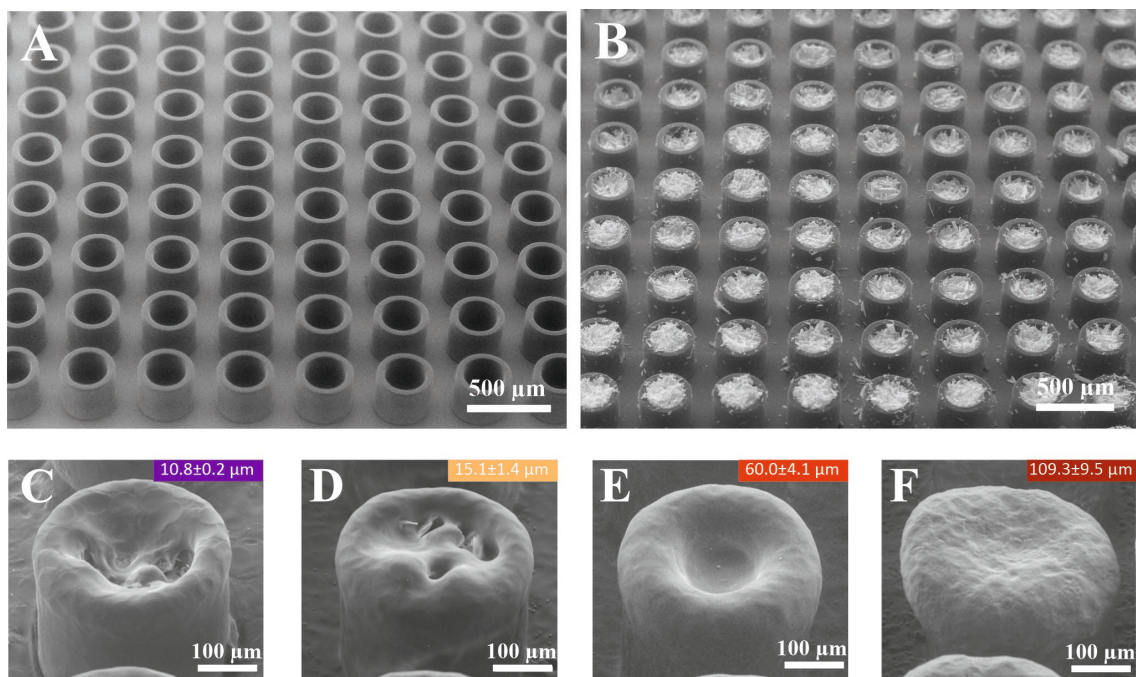


**Figure 4.** Scanning electron microscopy (SEM) images of empty MCs (A), loaded with ciprofloxacin hydrochloride (CIP) (B), and coated with 0.5 % w/v chitosan (CHI) (C) in combination with N-acetylcysteine (NAC) in ratios of 1:2 w/w (D), 1:4 w/w (E), or 1:8 w/w (F). The thickness of the coatings were measured using optical profilometry on a coating deposited on a flat Si wafer. Coating thicknesses are reported in respectively colored boxes (expressed as mean±SD, n=3).

MCs were loaded with  $2.18 \pm 0.47$  mg CIP per chip (mean±SD, n=32 chips) corresponding to  $3.54 \pm 0.72$  μg in each MC (Figure 4B). After loading, the openings of the MCs were successfully coated with a solution containing only CHI or a combination of CHI/NAC 1:2 w/w, 1:4 w/w or 1:8 w/w (Figure 4C-F). Optical profilometry revealed coating thicknesses of  $10.8 \pm 0.2$  μm,  $15.1 \pm 1.4$  μm,  $60.0 \pm 4.1$  μm and  $109.3 \pm 9.5$  μm for CHI, CHI/NAC 1:2, 1:4 and 1:8 w/w, respectively, showing that addition of NAC significantly increased the thickness of the coatings. The CHI-coating and CHI/NAC (1:2 w/w)-coating did not cover the entire opening of the MC, and structures of the CIP crystals were still visible, whereas CHI/NAC (1:4 w/w) and CHI/NAC (1:8 w/w)-coatings completely sealed the cavity.

### 3.3. Effect of CHI and CHI/NAC coating on *in vitro* release of CIP from MCs

To investigate the effect of CHI and CHI/NAC-functionalization of MCs, *in vitro* release of CIP from uncoated and coated MCs was evaluated using a μDiss Profiler in FAB medium (Figure 5).

As shown in Figure 5A, the CHI/NAC functionalization led to  $88.9 \pm 2.2$  %,  $97.9 \pm 2.4$  % and  $99.1 \pm 0.8$  % CIP release after 1 h with 1:2, 1:4 and 1:8 w/w CHI/NAC in the coating solution, respectively. Uncoated MCs displayed an initial burst release of  $81.4 \pm 6.8$  % in 5 min and the remaining cargo was slowly released over the course of 40 h. In contrast, CHI-coated MCs exhibited a constant sustained release with only  $4.2 \pm 7.2$  % CIP released after 1 h (Figure 5B). When in contact with water at physiological pH, CHI did not dissolve but instead formed a hydrogel [57]. This is in accordance with previous studies on CHI-MCs showing a sustained release [24], and also with CHI-NPs where CIP exhibited sustained diffusion-controlled release

behaviour [58,59]. Addition of NAC accelerated full drug release compared to both uncoated and CHI-coated MCs and no large differences were observed between the different NAC concentrations. NAC is highly water soluble and incorporation of NAC in the CHI-coating might have led to water-pores in the hydrogel, facilitating a faster release of CIP. The fast release of CIP provided an immediate high local antibiotic concentration in the surrounding area of the MC. Thus, levels above the minimal biofilm eradication concentration may be achieved leading to an improved biofilm treatment, and therefore, for further studies, we evaluated the effect of coatings containing CHI/NAC (1:8 w/w) in comparison with CHI alone.

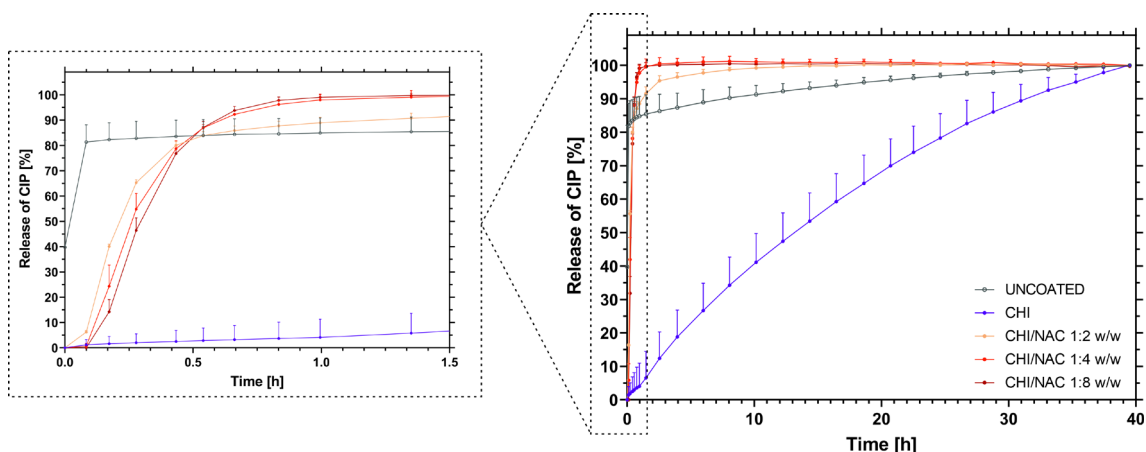


**Figure 5.** *In vitro* cumulative release of ciprofloxacin hydrochloride (CIP) from microcontainers (MCs) in FAB medium as a function of time. Uncoated MCs compared to MCs coated with 0.5 % w/v chitosan (CHI) alone or in combination with N-acetylcysteine (NAC) in ratios of 1:2 w/w, 1:4 w/w, or 1:8 w/w. Left graph (dotted line) shows a zoom-in on the initial release within the first 1.5 h. Data were normalized to 100 % in relation to drug release after 40 h and is presented as mean+SD (n=3-6).

### 3.4. Development and growth of PAO1 biofilm in ASM in the microfluidic platform

The BCoD provides a steady platform for culturing in perfusion of nutrients. It has previously been shown that flow based models represent better conditions [60–64] compared to static setups [65]. In an earlier study, we showed that PAO1 can be cultured for up to 72 h (flow rate of 1  $\mu\text{L}/\text{min}$ ) in 100 times diluted ASM in the BCoD [49]. The length of culture time is adjustable. Usually, in glucose minimal medium, PAO1 requires 2-4 days to develop a mature biofilm [66]. Moreover, the flow rate was found optimal in the BCoD platform [49], as it provides sufficient amounts of nutrients and oxygen to support a multilayered biofilm development.

The main components of ASM are various nutrients and mucin (Table S2), which influence the biofilm development and adherence to surfaces. In initial studies using pure ASM, we observed that PAO1 preferred to grow in the mucin matrix, as in the lungs of cystic fibrosis patients, without adhering to the glass in the culture chamber [49]. However, this made biomass quantification with Comstat impossible, since the software is meant to quantify biomass when attached to a solid surface as, in this case, to the lid of the cell culture chamber. Therefore, the composition of the ASM was optimized (mucin poor and



rich ASM) in order to facilitate adherence of bacteria to the glass lid and formation of biofilm on the glass in the presence of mucins. In Figure S5A and B, the growth of the bacterial biofilm over time can be observed in a mucin poor ASM. When culturing the PAO1 in a mucin rich ASM the bacterial biofilm developed faster (Figure 6), in fact the biomass at 48 h (Figure 6A) was comparable to the biomass obtained at 72 h when PAO1 was grown in mucin poor ASM (Figure S5).

We observed that increasing the mucin in the medium did not alter the initial amount of biomass attached to the cover glass, since after 1 h from inoculation, the biomass was comparable between the two different ASM dilutions. Differences started to be visible after 6 h, where biomass increased 4 times (from  $0.57 \pm 0.37 \mu\text{m}^3/\mu\text{m}^2$  to  $2.36 \pm 0.73 \mu\text{m}^3/\mu\text{m}^2$ ) between 1 h and 6 h when using the mucin rich ASM, while it increased only 2.5 times when using the mucin poor ASM (Figure 6A vs Figure S5A). The confocal images (Figure 6B) show that bacteria started to create aggregates already at 6 h. At 24 h, the biomass doubled ( $5.21 \pm 1.49 \mu\text{m}^3/\mu\text{m}^2$ ) and created a uniform multilayered biofilm in the cell chamber, reaching a total biomass of  $6.35 \pm 2.28 \mu\text{m}^3/\mu\text{m}^2$  after 48 h.

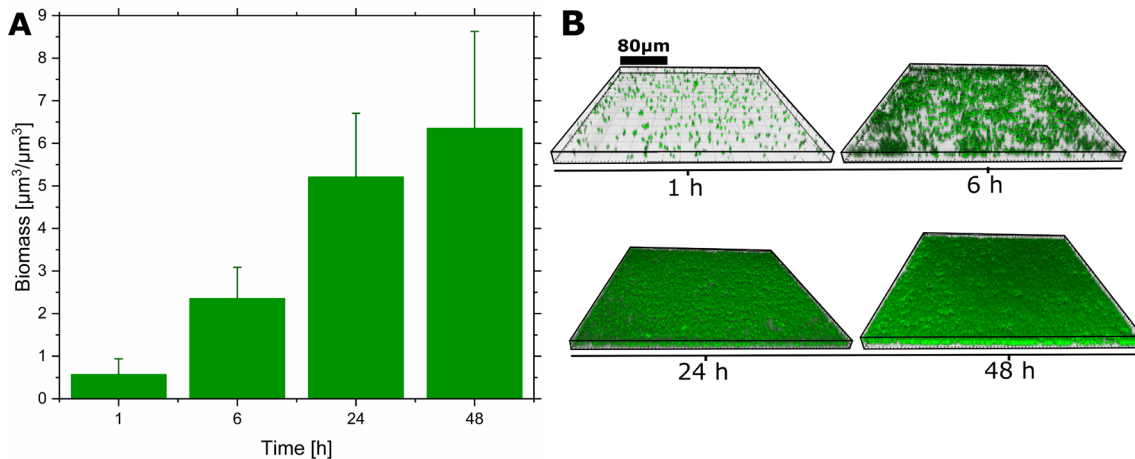


**Figure 6.** PAO1 average biomass growth using a flow of  $1 \mu\text{L}/\text{min}$  in 10 times diluted mucin and 100 times diluted nutrients ASM. (A). Representative images of bacterial growth observed with confocal microscope at different time points at the same location in the cell chamber (B). Data presented as mean+SD is based on 6 biological replicates, each with 9 technical replicates resulting in a total of  $n=54$  confocal images.

It is important to mention that when culturing the biofilm for up to 72 h using less diluted mucin, the bacteria started to grow embedded in the mucin matrix (Figure S6). The data presented in Figure 6, indicate that the presence of mucin facilitated cluster formation by decreasing bacterial motility as proposed earlier [19]. A clear example of mucin effect on PAO1 growth is shown in Figure S7 where PAO1 was grown in different dilutions of mucin using ASM. Additionally, we also found that the biofilm formation was rather uniform in the culture chamber (Figure 6A) and the biomass growth was comparable between discs ( $n=6$ ), with a 15.81 % relative SD in average biomass.

### 3.5. CIP treatment and impact of MCs on PAO1 biofilms

The efficacy of CIP-loaded functionalized MCs was evaluated on biofilms grown in mucin rich ASM (10 times diluted) at 48 h, by quantifying the amount of live or dead biomass after each treatment strategy (Figure 3). For comparison, we also studied the effect of the treatment when PAO1 was grown on mucin poor ASM (100 times diluted ASM) as shown in Figure S5 C and D. As shown in Figure 7A, at 48 h, before treatment,  $97.44 \pm 2.31$  % of the biomass was alive. We observed that the percentage of live biomass was higher compared to the mucin poor ASM (Figure S5C). This is probably due to the fact that in the presence of more mucin (Figure S8), bacteria stick better to the surface and suffer less from the effect of flow velocity.

Figure 7B shows confocal images of the bacterial biofilm in the *in vitro* system and the killing effect of the different treatments after 5 and 24 h. We found that  $61.14 \pm 8.40$  % of the biomass was still live after 5 h from the CIP bolus injection and  $60.13 \pm 13.28$  % after 24 h. The amount of mucin present in the culture medium does not have an effect, in the case of bolus, since the dead biomass was comparable to the mucin poor ASM (Figure S5C). Regarding the CHI-coated MCs, an average of  $39.12 \pm 3.35$  % of the biofilm was killed after 5 h in the entire cell culture chamber. However, if considering only the area in close proximity of the MC, significantly more biomass ( $72.76 \pm 1.52$  %) was killed. Having more biomass killed in vicinity of the MCs could be due to the fact that MCs coated with CHI have a slow release of CIP (Figure 5B) and therefore, only a small quantity of antibiotic was released after 5 h, affecting only bacteria close to the MCs. In fact, after 24 h, when almost all CIP was released in the cell chamber, the average of live biomass was decreased to  $27.32 \pm 3.73$  %.

The MCs coated and functionalized with CHI/NAC (1:8 w/w) proved to be more efficient than the other treatments evaluated in this study. As it can be seen in Figure 7A, after 5 h, only  $19.25 \pm 3.50$  % of the biomass was alive, showing that the fast release of CIP from these MCs (Figure 5B) and the capacity of NAC to decrease the viscosity of the EPS facilitating CIP dispersion in the biofilm, has an effect.

After 24 h, the live biomass further decreased to  $11.78 \pm 2.89$  %. Even if the antibiotic was completely released after approximately 1 h, the biofilm did not regrow after 24 h, indicating a great potential of the NAC-functionalized MCs.

When comparing our observed effects with the results on biofilm grown in mucin poor ASM, we found that there was an interesting difference for the CHI/NAC-coated MCs at 24 h (Figure S5C). Namely, the live biomass was 18 % lower, when PAO1 was grown in mucin rich medium (Figure 7A), which could be due to the mucolytic properties of NAC.



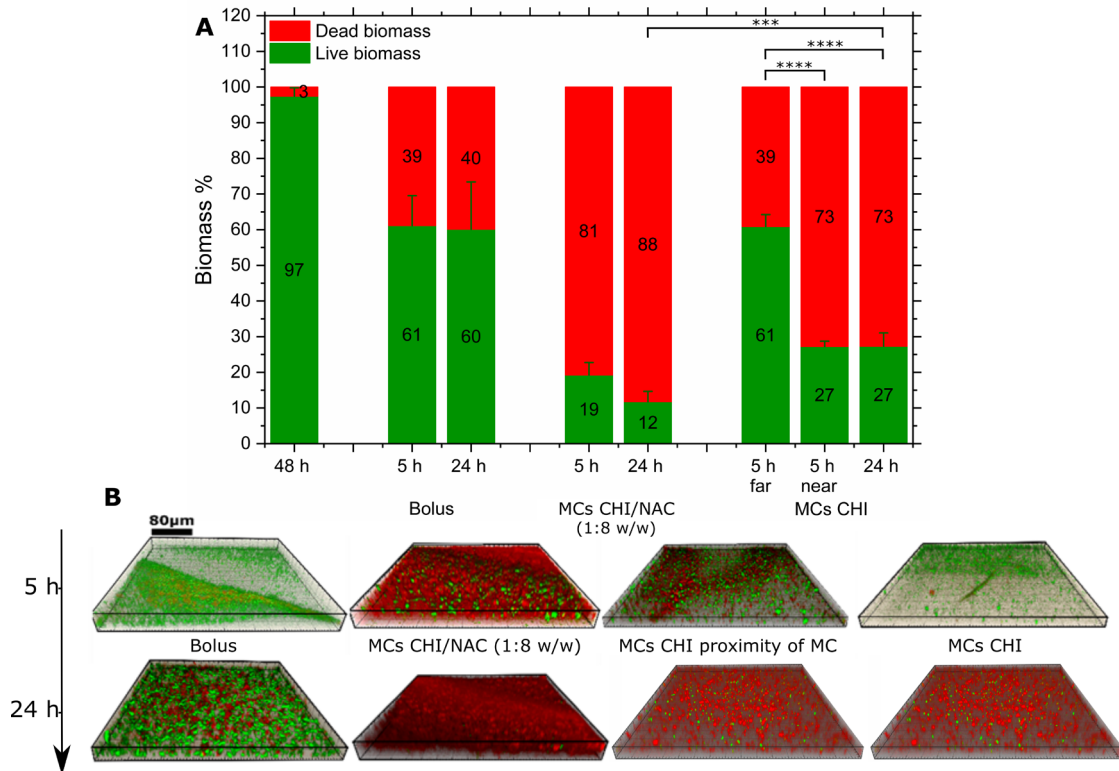


**Figure 7.** Comparison between different antibiotic administration strategies, namely bolus injection, chitosan (CHI) coated and chitosan/ N-acetylcysteine (CHI/NAC 1:8 w/w) coated MCs. Biomass viability was calculated before treatment at 48 h and after 5 and 24 h after treatment. Data presented as mean+SD (n=18). Statistical comparisons were performed based on the absolute live biomass. \*\*\*, p-value < 0.001; \*\*\*\*, p-value < 0.0001 (A). Representative confocal images of the treatments (B).

#### **4. CONCLUSION**

We find that a combination of NAC and CHI in the coating of antibiotic-loaded MCs, provides a synergistic effect with improved mucoadhesion and mucolytic properties and that the presence of NAC significantly accelerates CIP release. Our new *in vitro* BCoD facilitates bacteria culturing in ideal conditions (low/stable flow and possibility of using ASM growth medium). When testing the functionalized MCs in the *in vitro* BCoD platform, containing a PAO1 biofilm, we observed that the effect of CIP delivered in CHI/NAC-coated MCs increase PAO1 eradication with 42 % and 48 % at 5 h and 24 h respectively, compared to bolus. This improved eradication can be contributed to a mucolytic effect of NAC. Moreover, CHI functionalized MCs also enhance eradication, with 33 % higher dead biomass compared to bolus. This effect, we attribute to the mucoadhesive properties of CHI. Our studies show that a combinational strategy of using CHI/NAC-coated MCs in antibiotic delivery for biofilm eradication is a promising approach hence, evaluation of CHI/NAC-coated MCs on clinical isolates would be of great interest as a next step.

#### **ACKNOWLEDGEMENTS**

The authors would like to acknowledge the Center for Intelligent Drug Delivery and Sensing Using Microcontainers and Nanomechanics (IDUN) whose research is funded by the Danish National Research Foundation (DNRF122) and Villum Foundation (Grant No. 9301). Micro- and nanofabrication specialist Lasse Højlund Eklund Thamdrup, DTU Health Tech is acknowledged for help with fabrication of the microcontainers. Moreover, PhD student Khorshid Kamguyan is thanked for her help with QCM data interpretation. Lastly, Associate Professor Claus Sternberg, DTU Bioengineering is thanked for providing access to the confocal scanning laser microscope.

## 5. REFERENCES

- [1] H. Anwar, J.W. Costerton, Enhanced activity of combination of tobramycin and piperacillin for eradication of sessile biofilm cells of *Pseudomonas aeruginosa*., *Antimicrob. Agents Chemother.* 34 (1990) 1666–1671. <https://doi.org/10.1128/AAC.34.9.1666>.
- [2] H. Kumon, K. Tomochika, T. Matunaga, M. Ogawa, H. Ohmori, A Sandwich Cup Method for the Penetration Assay of Antimicrobial Agents through *Pseudomonas Exopolysaccharides*, *Microbiol. Immunol.* 38 (1994) 615–619. <https://doi.org/10.1111/j.1348-0421.1994.tb01831.x>.
- [3] D. Davies, Understanding biofilm resistance to antibacterial agents, *Nat. Rev. Drug Discovery.* 2 (2003) 114–122. <https://doi.org/10.1038/nrd1008>.
- [4] T.C. Mah, G.A. O’Toole, Mechanisms of biofilm resistance to antimicrobial agents, *Trends Microbiol.* 9 (2001) 34–39. [https://doi.org/10.1016/S0966-842X\(00\)01913-2](https://doi.org/10.1016/S0966-842X(00)01913-2).
- [5] U. Römling, C. Balsalobre, Biofilm infections, their resilience to therapy and innovative treatment strategies, *J. Intern. Med.* 272 (2012) 541–561. <https://doi.org/10.1111/joim.12004>.
- [6] U. Römling, S. Kjelleberg, S. Normark, L. Nyman, B.E. Uhlin, B. Åkerlund, Microbial biofilm formation: a need to act, *J. Intern. Med.* 276 (2014) 98–110. <https://doi.org/10.1111/joim.12242>.
- [7] W. Costerton, R. Veeh, M. Shirtliff, M. Pasmore, C. Post, G. Ehrlich, The application of biofilm science to the study and control of chronic bacterial infections, *J. Clin. Invest.* 112 (2003) 1466–1477. <https://doi.org/10.1172/JCI200320365>.
- [8] M. Jamal, U. Tasneem, T. Hussain, A. Saadia, Bacterial Biofilm: Its Composition, Formation and Role in Human Infections, *J. Microbiol. Biotechnol.* 4 (2015) 1–14. <http://www.rroij.com/open-access/bacterial-biofilm-its-composition-formation-and-role-in-human-infections.pdf>.
- [9] Y. Liu, L. Shi, L. Su, H.C. Van der Mei, P.C. Jutte, Y. Ren, H.J. Busscher, Nanotechnology-based antimicrobials and delivery systems for biofilm-infection control, *Chem. Soc. Rev.* 48 (2019) 428–446. <https://doi.org/10.1039/c7cs00807d>.
- [10] H.S. Sader, M.D. Huband, M. Castanheira, R.K. Flamm, *Pseudomonas aeruginosa* Antimicrobial Susceptibility Results from Four Years (2012 to 2015) of the International Network for Optimal Resistance Monitoring Program in the United States, *Antimicrob. Agents Chemother.* 61 (2017) 1–9. <https://doi.org/10.1128/AAC.02252-16>.
- [11] G.A. James, E. Swogger, R. Wolcott, E.D. Pulcini, P. Secor, J. Sestrich, J.W. Costerton, P.S. Stewart, Biofilms in chronic wounds, *Wound Repair Regen.* 16 (2008) 37–44. <https://doi.org/10.1111/j.1524-475X.2007.00321.x>.
- [12] J.R.W. Govan, V. Deretic, Microbial Pathogenesis in Cystic Fibrosis: Mucoid *Pseudomonas aeruginosa* and *Burkholderia cepacia*, *Microbiol. Rev.* 60 (1996) 539–574. <http://mmb.asm.org/>.
- [13] A.B. Lang, M.P. Horn, M.A. Imboden, A.W. Zuercher, Prophylaxis and therapy of *Pseudomonas aeruginosa* infection in cystic fibrosis and immunocompromised patients, *Vaccine.* 22 (2004) S44–S48. <https://doi.org/10.1016/j.vaccine.2004.08.016>.
- [14] F. Franzetti, M. Cernuschi, R. Esposito, M. Moroni, *Pseudomonas* infections in patients with AIDS and AIDS-related complex, *J. Intern. Med.* 231 (1992) 437–443. <https://doi.org/10.1111/j.1365-2796.1992.tb00957.x>.

- [15] C. Kang, S. Kim, H. Kim, S. Park, Y. Choe, M. Oh, E. Kim, K. Choe, *Pseudomonas aeruginosa* Bacteremia: Risk Factors for Mortality and Influence of Delayed Receipt of Effective Antimicrobial Therapy on Clinical Outcome, *Clin. Infect. Dis.* 37 (2003) 745–751. <https://doi.org/10.1086/377200>.
- [16] J.-F. Sicard, G. Le Bihan, P. Vogeleer, M. Jacques, J. Harel, Interactions of Intestinal Bacteria with Components of the Intestinal Mucus, *Front. Cell. Infect. Microbiol.* 7 (2017) 1–15. <https://doi.org/10.3389/fcimb.2017.00387>.
- [17] M.E. V. Johansson, H. Sjövall, G.C. Hansson, The gastrointestinal mucus system in health and disease, *Nat. Rev. Gastroenterol. Hepatol.* 10 (2013) 352–361. <https://doi.org/10.1038/nrgastro.2013.35>.
- [18] S.M. Kreda, C.W. Davis, M.C. Rose, CFTR, Mucins, and Mucus Obstruction in Cystic Fibrosis, *Cold Spring Harb. Perspect. Med.* 2 (2012) a009589–a009589. <https://doi.org/10.1101/cshperspect.a009589>.
- [19] R.M. Landry, D. An, J.T. Hupp, P.K. Singh, M.R. Parsek, Mucin-*Pseudomonas aeruginosa* interactions promote biofilm formation and antibiotic resistance, *Mol. Microbiol.* 59 (2006) 142–151. <https://doi.org/10.1111/j.1365-2958.2005.04941.x>.
- [20] D.C. Hooper, G.A. Jacoby, Topoisomerase Inhibitors: Fluoroquinolone Mechanisms of Action and Resistance, *Cold Spring Harb. Perspect. Med.* 6 (2016) a025320. <https://doi.org/10.1101/cshperspect.a025320>.
- [21] A. Rehman, W.M. Patrick, I.L. Lamont, Mechanisms of ciprofloxacin resistance in *pseudomonas aeruginosa*: New approaches to an old problem, *J. Med. Microbiol.* 68 (2019) 1–10. <https://doi.org/10.1099/jmm.0.000873>.
- [22] K.J. Aldred, R.J. Kerns, N. Osheroff, Mechanism of quinolone action and resistance, *Biochemistry.* 53 (2014) 1565–1574. <https://doi.org/10.1021/bi5000564>.
- [23] M.H. Xiong, Y. Bao, X.Z. Yang, Y.H. Zhu, J. Wang, Delivery of antibiotics with polymeric particles, *Adv. Drug Delivery Rev.* 78 (2014) 63–76. <https://doi.org/10.1016/j.addr.2014.02.002>.
- [24] S.E. Birk, J.A.J. Haagensen, H.K. Johansen, S. Molin, L.H. Nielsen, A. Boisen, Microcontainer Delivery of Antibiotic Improves Treatment of *Pseudomonas aeruginosa* Biofilms, *Adv. Healthc. Mater.* 9 (2020) 1901779. <https://doi.org/10.1002/adhm.201901779>.
- [25] N.M. Elman, Y. Patta, A.W. Scott, B. Masi, H.L. Ho Duc, M.J. Cima, The next generation of drug-delivery microdevices, *Clin. Pharmacol. Ther.* 85 (2009) 544–547. <https://doi.org/10.1038/clpt.2009.4>.
- [26] A. Ahmed, C. Bonner, T.A. Desai, Bioadhesive microdevices with multiple reservoirs: A new platform for oral drug delivery, *J. Controlled Release.* 81 (2002) 291–306. [https://doi.org/10.1016/S0168-3659\(02\)00074-3](https://doi.org/10.1016/S0168-3659(02)00074-3).
- [27] C. Mazzone, F. Tentor, S.A. Strindberg, L.H. Nielsen, S.S. Keller, T.S. Alstrøm, C. Gundlach, A. Müllertz, P. Marizza, A. Boisen, From concept to in vivo testing: Microcontainers for oral drug delivery, *J. Controlled Release.* 268 (2017) 343–351. <https://doi.org/10.1016/j.jconrel.2017.10.013>.
- [28] L.H. Nielsen, A. Melero, S.S. Keller, J. Jacobsen, T. Garrigues, T. Rades, A. Müllertz, A. Boisen, Polymeric microcontainers improve oral bioavailability of furosemide, *Int. J. Pharm.* 504 (2016) 98–109. <https://doi.org/10.1016/j.ijpharm.2016.03.050>.

- [29] C. von H. Laier, B. Gibson, J.A.S. Moreno, T. Rades, S. Hook, L.H. Nielsen, A. Boisen, Microcontainers for protection of oral vaccines, in vitro and in vivo evaluation, *J. Controlled Release*. 294 (2019) 91–101. <https://doi.org/10.1016/j.jconrel.2018.11.030>.
- [30] C. Mazzoni, R.D. Jacobsen, J. Mortensen, J.R. Jørgensen, L. Vaut, J. Jacobsen, C. Gundlach, A. Müllertz, L.H. Nielsen, A. Boisen, Polymeric Lids for Microcontainers for Oral Protein Delivery, *Macromol. Biosci.* 19 (2019) 1900004. <https://doi.org/10.1002/mabi.201900004>.
- [31] L.H. Nielsen, T. Rades, B. Boyd, A. Boisen, Microcontainers as an oral delivery system for spray dried cubosomes containing ovalbumin, *Eur. J. Pharm. Biopharm.* 118 (2017) 13–20.
- [32] T.M. Ways, W. Lau, V. Khutoryanskiy, Chitosan and Its Derivatives for Application in Mucoadhesive Drug Delivery Systems, *Polymer*. 10 (2018) 267. <https://doi.org/10.3390/polym10030267>.
- [33] Z. Merchant, K.M.G. Taylor, P. Stapleton, S.A. Razak, N. Kunda, I. Alfagih, K. Sheikh, I.Y. Saleem, S. Somavarapu, Engineering hydrophobically modified chitosan for enhancing the dispersion of respirable microparticles of levofloxacin, *Eur. J. Pharm. Biopharm.* 88 (2014) 816–829. <https://doi.org/10.1016/j.ejpb.2014.09.005>.
- [34] N. Al-Nemrawi, N. Alshraideh, A. Zayed, B. Altaani, Low Molecular Weight Chitosan-Coated PLGA Nanoparticles for Pulmonary Delivery of Tobramycin for Cystic Fibrosis, *Pharmaceuticals*. 11 (2018) 28. <https://doi.org/10.3390/ph11010028>.
- [35] E.I. Rabea, M.E.-T. Badawy, C. V. Stevens, G. Smagghe, W. Steurbaut, Chitosan as Antimicrobial Agent: Applications and Mode of Action, *Biomacromolecules*. 4 (2003) 1457–1465. <https://doi.org/10.1021/bm034130m>.
- [36] M. Mohammed, J. Syeda, K. Wasan, E. Wasan, An Overview of Chitosan Nanoparticles and Its Application in Non-Parenteral Drug Delivery, *Pharmaceutics*. 9 (2017) 53. <https://doi.org/10.3390/pharmaceutics9040053>.
- [37] J.S. Suk, S.K. Lai, N.J. Boylan, M.R. Dawson, M.P. Boyle, J. Hanes, Rapid transport of muco-inert nanoparticles in cystic fibrosis sputum treated with N-acetyl cysteine, *Nanomedicine*. 6 (2011) 365–375. <https://doi.org/10.2217/nnm.10.123>.
- [38] S. Dinicola, S. De Grazia, G. Carlomagno, J.P. Pintucci, N-acetylcysteine as powerful molecule to destroy bacterial biofilms. A systematic review, *Eur. Rev. Med. Pharmacol. Sci.* 18 (2014) 2942–2948.
- [39] A. Marchese, M. Bozzolasco, L. Gualco, E.A. Debbia, G.C. Schito, A.M. Schito, Effect of fosfomycin alone and in combination with N-acetylcysteine on *E. coli* biofilms, *Int. J. Antimicrob. Agents*. 22 (2003) 95–100. [https://doi.org/10.1016/S0924-8579\(03\)00232-2](https://doi.org/10.1016/S0924-8579(03)00232-2).
- [40] F. Costa, D.M. Sousa, P. Parreira, M. Lamghari, P. Gomes, M.C.L. Martins, N-acetylcysteine-functionalized coating avoids bacterial adhesion and biofilm formation, *Sci. Rep.* 7 (2017) 1–13. <https://doi.org/10.1038/s41598-017-17310-4>.
- [41] T. Zhao, Y. Liu, N-acetylcysteine inhibit biofilms produced by *Pseudomonas aeruginosa*, *BMC Microbiol.* 10 (2010) 140. <https://doi.org/10.1186/1471-2180-10-140>.
- [42] B. Porsio, M.G. Cusimano, D. Schillaci, E.F. Craparo, G. Giammona, G. Cavallaro, Nano into Micro Formulations of Tobramycin for the Treatment of *Pseudomonas aeruginosa* Infections in Cystic Fibrosis, *Biomacromolecules*. 18 (2017) 3924–3935. <https://doi.org/10.1021/acs.biomac.7b00945>.

- [43] Š. Šalamon, B. Kramar, T.P. Marolt, B. Poljšak, I. Milisav, Medical and Dietary Uses of N-Acetylcysteine, *Antioxidants*. 8 (2019) 111. <https://doi.org/10.3390/antiox8050111>.
- [44] Y. Samuni, S. Goldstein, O.M. Dean, M. Berk, The chemistry and biological activities of N-acetylcysteine, *Biochim. Biophys. Acta - Gen. Subj.* 1830 (2013) 4117–4129. <https://doi.org/10.1016/j.bbagen.2013.04.016>.
- [45] G. Aldini, A. Altomare, G. Baron, G. Vistoli, M. Carini, L. Borsani, F. Sergio, N-Acetylcysteine as an antioxidant and disulphide breaking agent: the reasons why, *Free Radic. Res.* 52 (2018) 751–762. <https://doi.org/10.1080/10715762.2018.1468564>.
- [46] H. Hamedinasab, A.H. Rezayan, M. Mellat, M. Mashreghi, M.R. Jaafari, Development of chitosan-coated liposome for pulmonary delivery of N-acetylcysteine, *Int. J. Biol. Macromol.* 156 (2019) 1455–1463. <https://doi.org/10.1016/j.ijbiomac.2019.11.190>.
- [47] D. Liu, J. Li, B. Cheng, Q. Wu, H. Pan, Ex Vivo and in Vivo Evaluation of the Effect of Coating a Coumarin-6-Labeled Nanostructured Lipid Carrier with Chitosan-N-acetylcysteine on Rabbit Ocular Distribution, *Mol. Pharmaceutics*. 14 (2017) 2639–2648. <https://doi.org/10.1021/acs.molpharmaceut.7b00069>.
- [48] H. Lian, T. Zhang, J. Sun, X. Liu, G. Ren, L. Kou, Y. Zhang, X. Han, W. Ding, X. Ai, C. Wu, L. Li, Y. Wang, Y. Sun, S. Wang, Z. He, Enhanced Oral Delivery of Paclitaxel Using Acetylcysteine Functionalized Chitosan-Vitamin E Succinate Nanomicelles Based on a Mucus Bioadhesion and Penetration Mechanism, *Mol. Pharmaceutics*. 10 (2013) 3447–3458. <https://doi.org/10.1021/mp400282r>.
- [49] L. Seriola, T.Z. Laksafoss, J.A.J. Haagensen, C. Sternberg, M.P. Soerensen, S. Molin, K. Zór, A. Boisen, Bacterial Cell Cultures in a Lab-on-a-Disc: A Simple and Versatile Tool for Quantification of Antibiotic Treatment Efficacy, *Anal. Chem.* 92 (2020) 13871–13879. <https://doi.org/10.1021/acs.analchem.0c02582>.
- [50] S. Kirchner, J.L. Fothergill, E.A. Wright, C.E. James, E. Mowat, C. Winstanley, Use of Artificial Sputum Medium to Test Antibiotic Efficacy Against *Pseudomonas aeruginosa* in Conditions More Relevant to the Cystic Fibrosis Lung, *J. Vis. Exp.* 64 (2012) 1–8. <https://doi.org/10.3791/3857>.
- [51] L.H. Nielsen, S.S. Keller, K.C. Gordon, A. Boisen, T. Rades, A. Müllertz, Spatial confinement can lead to increased stability of amorphous indomethacin, *Eur. J. Pharm. Biopharm.* 81 (2012) 418–425. <https://doi.org/10.1016/j.ejpb.2012.03.017>.
- [52] S.L. Tao, K. Popat, T.A. Desai, Off-wafer fabrication and surface modification of asymmetric 3D SU-8 microparticles, *Nat. Protoc.* 1 (2007) 3153–3158. <https://doi.org/10.1038/nprot.2006.451>.
- [53] Z. Abid, C. Gundlach, O. Durucan, C. von Halling Laier, L.H. Nielsen, A. Boisen, S.S. Keller, Powder embossing method for selective loading of polymeric microcontainers with drug formulation, *Microelectron. Eng.* 171 (2017) 20–24. <https://doi.org/10.1016/j.mee.2017.01.018>.
- [54] J. Klockgether, A. Munder, J. Neugebauer, C.F. Davenport, F. Stanke, K.D. Larbig, S. Heeb, U. Schöck, T.M. Pohl, L. Wiehlmann, B. Tümmler, Genome Diversity of *Pseudomonas aeruginosa* PAO1 Laboratory Strains, *J. Bacteriol.* 192 (2010) 1113–1121. <https://doi.org/10.1128/JB.01515-09>.
- [55] M. Klausen, A. Heydorn, P. Ragas, L. Lambertsen, A. Aes-Jørgensen, S. Molin, T. Tolker-Nielsen, Biofilm formation by *Pseudomonas aeruginosa* wild type, flagella and type IV pili mutants, *Mol. Microbiol.* 48 (2003) 1511–1524. <https://doi.org/10.1046/j.1365-2958.2003.03525.x>.
- [56] A. Heydorn, A.T. Nielsen, M. Hentzer, C. Sternberg, M. Givskov, B.K. Ersbøll, S. Molin,

- Quantification of biofilm structures by the novel computer program COMSTAT, *Microbiol. Soc.* 146 (2000) 2395–2407. [www.microbiologyresearch.org](http://www.microbiologyresearch.org).
- [57] F. Ahmadi, Z. Oveisi, S.M. Samani, Z. Amoozgar, Chitosan based hydrogels: characteristics and pharmaceutical applications, *Res. Pharm. Sci.* 10 (2015) 1–16.
- [58] K.K. Patel, M. Tripathi, N. Pandey, A.K. Agrawal, S. Gade, M.M. Anjum, R. Tilak, S. Singh, Alginate lyase immobilized chitosan nanoparticles of ciprofloxacin for the improved antimicrobial activity against the biofilm associated mucoid *P. aeruginosa* infection in cystic fibrosis, *Int. J. Pharm.* 563 (2019) 30–42. <https://doi.org/10.1016/j.ijpharm.2019.03.051>.
- [59] D. Jain, R. Banerjee, Comparison of ciprofloxacin hydrochloride-loaded protein, lipid, and chitosan nanoparticles for drug delivery, *J. Biomed. Mater. Res. Part B Appl. Biomater.* 86B (2008) 105–112. <https://doi.org/10.1002/jbm.b.30994>.
- [60] J. Azeredo, N.F. Azevedo, R. Briandet, N. Cerca, T. Coenye, A. Rita Costa, M. Desvaux, G. Di Bonaventura, M. Hébraud, Z. Jaglic, M. Kačaniová, S. Knøchel, A. Lourenço, F. Mergulhão, R. Louise Meyer, G. Nychas, M. Simões, O. Tresse, C. Sternberg, Critical review on biofilm methods, *Crit. Rev. Microbiol.* 43 (2017) 313–351. <https://doi.org/10.1080/1040841X.2016.1208146>.
- [61] J. Kim, M. Hegde, S.H. Kim, T.K. Wood, A. Jayaraman, A microfluidic device for high throughput bacterial biofilm studies, *Lab Chip*. 12 (2012) 1157. <https://doi.org/10.1039/c2lc20800h>.
- [62] J.A.J. Haagensen, D. Verotta, L. Huang, A. Spormann, K. Yang, New in vitro model to study the effect of human simulated antibiotic concentrations on bacterial biofilms, *Antimicrob. Agents Chemother.* 59 (2015) 4074–4081. <https://doi.org/10.1128/AAC.05037-14>.
- [63] M.R. Benoit, C.G. Conant, C. Ionescu-Zanetti, M. Schwartz, A. Matin, New Device for High-Throughput Viability Screening of Flow Biofilms, *Appl. Environ. Microbiol.* 76 (2010) 4136–4142. <https://doi.org/10.1128/AEM.03065-09>.
- [64] G.A. O’Toole, R. Kolter, Initiation of biofilm formation in *Pseudomonas fluorescens* WCS365 proceeds via multiple, convergent signalling pathways: a genetic analysis, *Mol. Microbiol.* 28 (1998) 449–461. <https://doi.org/10.1046/j.1365-2958.1998.00797.x>.
- [65] A.J. McBain, Chapter 4 In Vitro Biofilm Models, in: *Adv. Appl. Microbiol.*, 2009: pp. 99–132. [https://doi.org/10.1016/S0065-2164\(09\)69004-3](https://doi.org/10.1016/S0065-2164(09)69004-3).
- [66] T. Rasamiravaka, Q. Labtani, P. Duez, M. El Jaziri, The Formation of Biofilms by *Pseudomonas aeruginosa* : A Review of the Natural and Synthetic Compounds Interfering with Control Mechanisms, *Biomed Res. Int.* 1 (2015) 1–17. <https://doi.org/10.1155/2015/759348>.

## Supporting Information

### **Enhanced eradication of mucin-embedded bacterial biofilm by locally delivered antibiotics in functionalized microcontainers**

Stine Egebro Birk, Laura Seriola, Valentina Cavallo, Janus Anders Juul Haagenen, Søren Molin, Line Hagner Nielsen, Kinga Zór, Anja Boisen

<b>TABLE S1 AND S2</b>	Media preparation
<b>FIGURE S1</b>	BCoD fabrication
<b>FIGURE S2</b>	BCoD calibration curve
<b>CALCULATION S1</b>	Calculation of MCs and bolus injection for treatment on BCoD
<b>FIGURES S3 AND S4</b>	QCM-D results
<b>FIGURE S5</b>	Growth and treatment of PAO1 biofilm in 100 times diluted ASM
<b>FIGURE S6</b>	PAO1 72 h growth in 100 times diluted ASM and 10 times diluted mucin
<b>FIGURE S7</b>	Evaluation of PAO1 growth in different ASM dilutions
<b>FIGURE S8</b>	Evaluation of the presence of mucin in different dilutions of ASM and comparison with FAB medium



## Media preparation (Table S1 and S2)

**Table S1.** The composition of modified FAB medium. A10 buffer, FB minimal medium with trace metals and the carbon source were autoclaved separately and mixed afterwards. Concentrations are given as final concentrations.

A10 buffer	FB minimal medium with trace metals	Carbon source
33.7 mM Na <sub>2</sub> HPO <sub>4</sub> ·2H <sub>2</sub> O	1 mM MgCl <sub>2</sub>	2 µg/L CuSO <sub>4</sub> ·5H <sub>2</sub> O
22.0 mM KH <sub>2</sub> PO <sub>4</sub>	0.1 mM CaCl <sub>2</sub>	2 µg/L ZnSO <sub>4</sub> ·7H <sub>2</sub> O
15.1 mM (NH <sub>4</sub> ) <sub>2</sub> SO <sub>4</sub>	20 µg/L CaSO <sub>4</sub> ·2H <sub>2</sub> O	1 µg/L CoSO <sub>4</sub> ·7H <sub>2</sub> O
51 mM NaCl	20 µg/L FeSO <sub>4</sub> ·7H <sub>2</sub> O	1 µg/L NaMoO <sub>4</sub> ·H <sub>2</sub> O
	2 µg/L MnSO <sub>4</sub> ·H <sub>2</sub> O	0.5 µg/L H <sub>3</sub> BO <sub>3</sub>

**Table S2.** The composition of artificial sputum medium (ASM). Concentrations are given as final concentrations and is prior to any dilution with FAB medium.

ASM medium	ASM salt stock solution
16 mg/mL DNA from fish sperm	59 µg mL <sup>-1</sup> Diethylenetriaminepentaacetic acid
20 mg/mL Mucin from porcine stomach (Type II)	50 mg mL <sup>-1</sup> NaCl
2.5 mg/mL Amino acid stock solution	22 mg mL <sup>-1</sup> KCl
10 mg/mL L-cysteine	
10 mg/mL L-tyrosine	
100 mL/L ASM salts stock solution	
5 mL/L Egg yolk	

DNA from fish sperm and mucin from porcine stomach (type II) were dissolved in sterile MilliQ (MQ) water in separate bottles overnight at 150 rpm, 30°C. Next day, the dissolved DNA and mucin were mixed together with an amino acid stock solution (all essential and non-essential amino acids dissolved in sterile water, except L-cysteine and L-tyrosine), L-cysteine (dissolved in 0.5 M potassium hydroxide) and L-tyrosine (dissolved in sterile water), ASM salts stock solution (dissolved in sterile water) and egg yolk. The final solution was sterilized using filtration technique with a filter of 0.22 µm pore size.

For the experiments where ASM was used as 100 times diluted, the dilution was made in FAB medium, while for those which used 10 times diluted mucin and 100 times diluted nutrients the dilution was carried out from the beginning during the ASM preparation.

## BCoD fabrication (Figure S1)

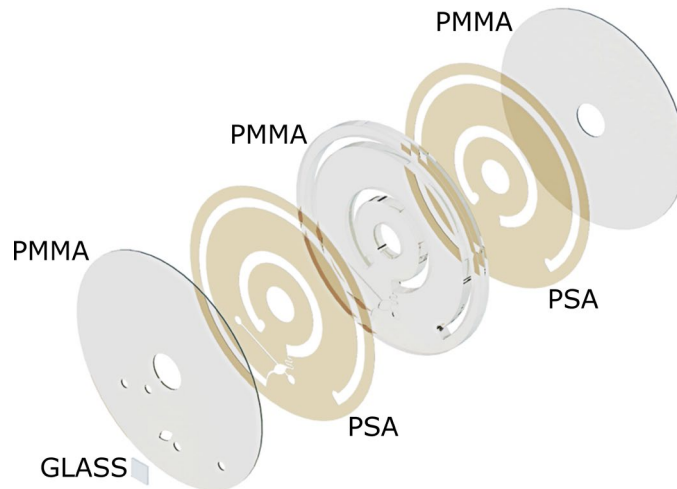


**Figure S1.** Exploded view of the in vitro system with the different PMMA and PSA layers and the cover glass (A).

The platform was designed using Solidworks 2018 (Dassault Systèmes, Vélizy-Villacoublay, France). It consists of six layers; 3 Poly(methyl methacrylate) (PMMA), 2 pressure sensitive double adhesive tape (PSA) and 1 glass. The disc has a 100 mm outer and a 15.35 mm inner diameter. The system was assembled from two layers of 0.5 mm thick PMMA, one layer of 5 mm thick PMMA and two layers of 84  $\mu\text{m}$  thick PSA (Figure S1). A 0.15 mm cover glass was chosen to close the cell chamber (Figure S1) in order to have an optimal imaging for confocal scanning laser microscopy (Leica SP5 CLSM, Leica Microsystems, Mannheim, Germany). The PMMA layers were fabricated using laser ablation technique (Epilog Mini 18 30 W system, Epilog, USA) except for channels and culture chamber which were manufactured with micromilling (Mini-Mill/3, Minitech Machinery Corp, GA, US). PMMA layers, were cleaned with sonication in ultrapure water and ethanol, then assembled with the PSA layers using a bonding press (PW 10 H, P/O/Weber, Germany), with a force of 10 KN for 1 min. The cover glass (Figure S1), was separately glued using a silicone glue (Super Clear Silicone, Versachem, Hartford, Connecticut, USA) and dried overnight. Filters with a 3 mm diameter membrane and a pore size of 0.20  $\mu\text{m}$  were used to maintain a sterile environment in the disc while maintaining an oxygen flow in the platform through the pores. Luer connectors were fabricated in cyclic olefin-copolymer (TOPAS grade 5013L-10, Advanced Polymers GmbH, Frankfurt-Höchst, Germany), using injection molding (Victory Tech 80/ 45, Engel, Schwertberg, Austria) and fixed in the venting and loading openings, facilitating the introduction of sterile filters. Filters and luers are presented in Figure 3 of main text.

## BCoD calibration curve (Figure S2)

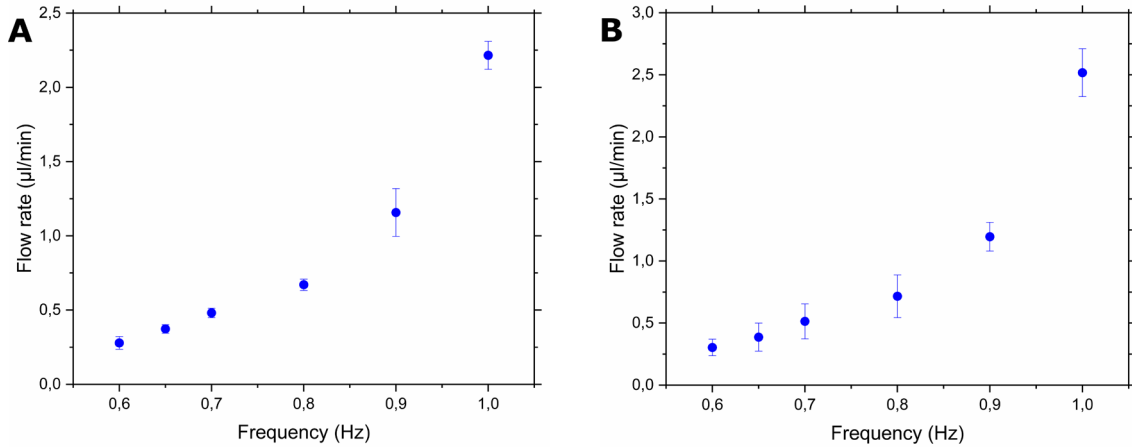


**Figure S2.** Dependency between flow rate and frequency in the platform using 100 times diluted ASM with 100 times diluted mucin (A) and 10 times diluted mucin (B). Standard deviation were calculated based on n=3.

The calibration curve was calculated as described by Seriola *et al.* [1]. ASM medium diluted 100 times was used for performing the calibration showed in Figure S2A, while mucin was diluted only 10 times in the calibration shown in Figure S2B.

## Calculation of MCs and bolus injection for treatment on BCoD (Calculation S1)

In previous studies [1,2] biofilms were treated with a constant perfusion of CIP for 24 h, using a concentration of 4 µg/mL. This is a common concentration used to treat biofilm since it reaches the minimal biofilm inhibitory concentration [3]. In order to have a direct comparison with these studies, the quantity of CIP delivered via MCs and bolus injection were calculated taking into account the amount of CIP delivered with constant perfusion of 4 µg/mL CIP for 24 h.

*For MCs comparison:*

Flow rate used: 1 µL/min

Total amount of medium delivered in 24 h:  $1 \frac{\mu L}{min} \times 60 min \times 24 = 1440 \mu L = 1.44 mL$

Total amount of antibiotic delivered in 24 h in the 1.44 mL:  $1.44 mL \times 4 \frac{\mu g}{mL} = 5.76 \mu g$

Average amount of antibiotic inside 1 MC: 3.54 µg

Amount of MCs to inoculate: 2 (with a total amount of 7.08 µg of antibiotic).

*For bolus injection:*

Total volume of cell chamber: 31.8 µL

Average total amount of antibiotic delivered with MCs: 7.08 µg

CIP concentration of bolus injection to deliver 7.08 µg to the full cell chamber:  $\frac{7.08 \mu g}{31.8 \mu L} = 0.22 \frac{\mu g}{\mu L}$

A 0.22 µg/µL CIP solution was prepared and 31.8 µL inoculated into the cell chamber.

## QCM-D results (Figures S3 and S4)

QCM-D is able to record mass and structural changes, i.e. viscoelastic properties, due to simultaneous monitoring of changes in frequency ( $\Delta f$ ) and dissipation ( $\Delta d$ ) [4,5]. A decrease in frequency of the oscillating sensor indicates an increased mass, and a rise in dissipation indicates a softer layer. QCM-D results can be found below (Figure S3) together with a detailed description of the dataset.

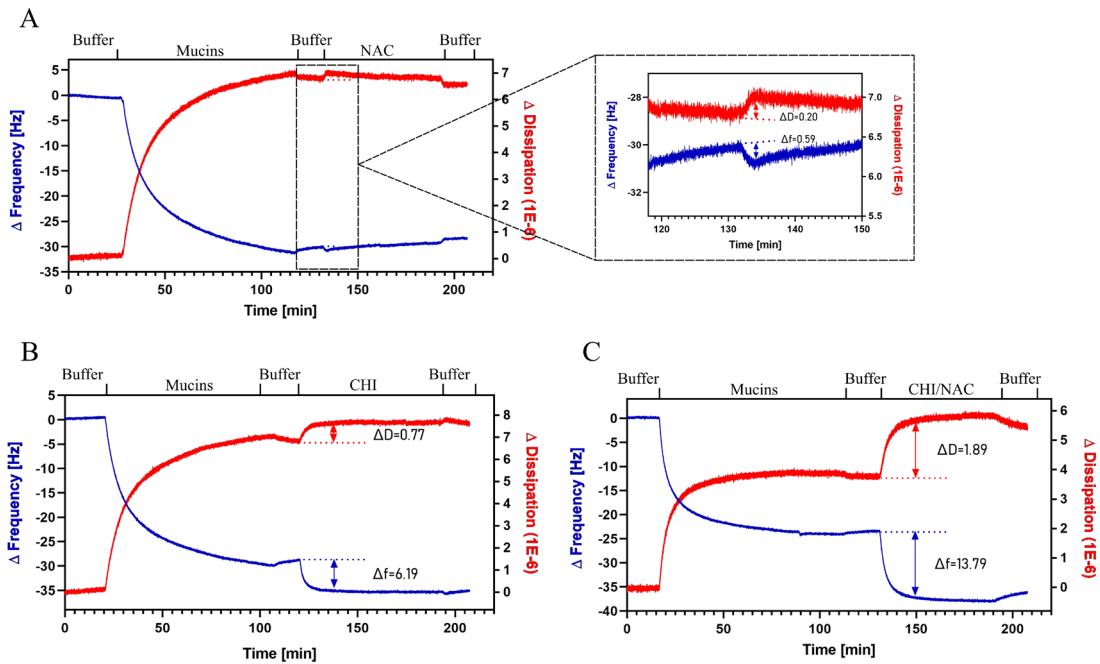


**Figure S3.** QCM-D real-time monitoring of changes in frequency (blue line) and dissipation (red line) of an established mucin layer on gold-coated sensor, in the presence of 0.4 mg/mL N-acetylcysteine (NAC) (A), 100 mg/L chitosan (CHI) (B) or 0.4 mg/mL NAC in 100 mg/mL CHI (C). Results are representative of three independent assays in duplicates.

### *Mucin attachment*

As shown in Figure S3, the mucin layers were rapidly deposited on the sensor as the frequency decreased ( $\Delta f=24-30$ , mass on the sensor increased) and dissipation increased ( $\Delta d=4-7$ , the rigid sensor is covered with a soft mucin layer). This is in accordance with other QCM-D studies reporting on mucin attachment to gold-sensors.[5,6] After the chamber was rinsed with a buffer solution to remove any unbound mucin, there were only negligible change of frequency and dissipation ( $\Delta f \leq 1.19$  and  $\Delta d \leq 0.32$ ), thus confirming the irreversible nature of the covalent mucin-bonding to the sensor.

### *Addition of NAC*

Addition of 0.4 mg/mL NAC resulted in values of  $\Delta f=0.59$  and  $\Delta d=0.2$  (Figure S3A), indicating a slightly increased mass and thereby, a less viscous layer. To confirm the observed mucolytic effect of NAC, an additional study with a higher concentration of NAC (20 mg/mL) was conducted (Figure S4).

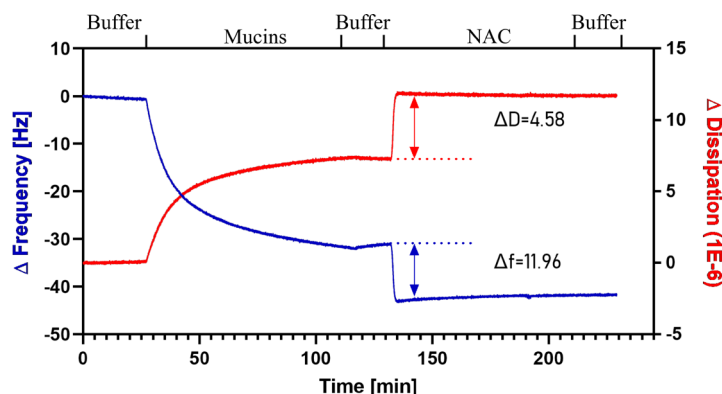


**Figure S4.** Quartz crystal microbalance with dissipation (QCM-D) real-time monitoring of changes in frequency (blue line) and dissipation (red line) of an established mucin layer on gold-coated sensor, when 20 mg/mL N-acetylcysteine (NAC) was applied. Results are representative of an independent assay with 2 replicates.

Changes in frequency and dissipation ( $\Delta f=11.96$  and  $\Delta d=4.58$ ) clearly confirmed the mucolytic effect of NAC on the established mucin layer. As indicated earlier, the mucolytic effect of NAC is caused by a thiol-disulfide exchange reaction in which the disulfide bonds of the otherwise highly cross-linked mucin network are broken, ultimately resulting in lowered viscosity [7]. The increased mass can be explained by NAC remaining attached to the mucin chains, although, it is believed that the main contribution is the entrapment of water into the mucin network, as is also obvious from the increased dissipation. This result is in accordance with the observations made by Cristallini *et al.*, who studied NAC-loaded microparticles and found that they lowered the viscosity of a mucus-containing artificial sputum layer, using standard rheological measurements determining viscosity versus shear rate in the analysis [8].

#### *Addition of CHI*

Applying 100 mg/L of CHI to the layer of mucins caused an immediate decrease in frequency ( $\Delta f=6.19$ ) indicating a higher mass due to CHI being absorbed onto the mucins (Figure S3B). This is due to the mucoadhesive properties of CHI interacting with the negatively charged mucins through ionic and hydrogen bonding [9]. Simultaneously, dissipation increased ( $\Delta d=0.77$ ) indicating a softer layer, presumably caused by the hygroscopic effect of CHI promoting water uptake. Adhesion of CHI did not give rise to as large a change in frequency as observed with the layer-by-layer build-up of mucins on the sensor ( $\Delta f=6.19$  versus  $\Delta f=24-30$ , respectively). This can be explained by the thin CHI layer already attached, shielding the negatively charged mucins from further interaction with more amounts of CHI.

#### *Addition of CHI/NAC*

When adding 0.4 mg/mL NAC in 100 mg/L CHI (CHI/NAC 1:4 w/w) to the mucin layer (Figure S3C), we observed a decrease in frequency ( $\Delta f=13.79$ ) and an increase in dissipation ( $\Delta D=1.89$ ), both values being higher than the ones measured after addition of only NAC or CHI (Figure S3A and S3B).

## Growth and treatment of PAO1 biofilm in ASM diluted 100 times (Figure S5)

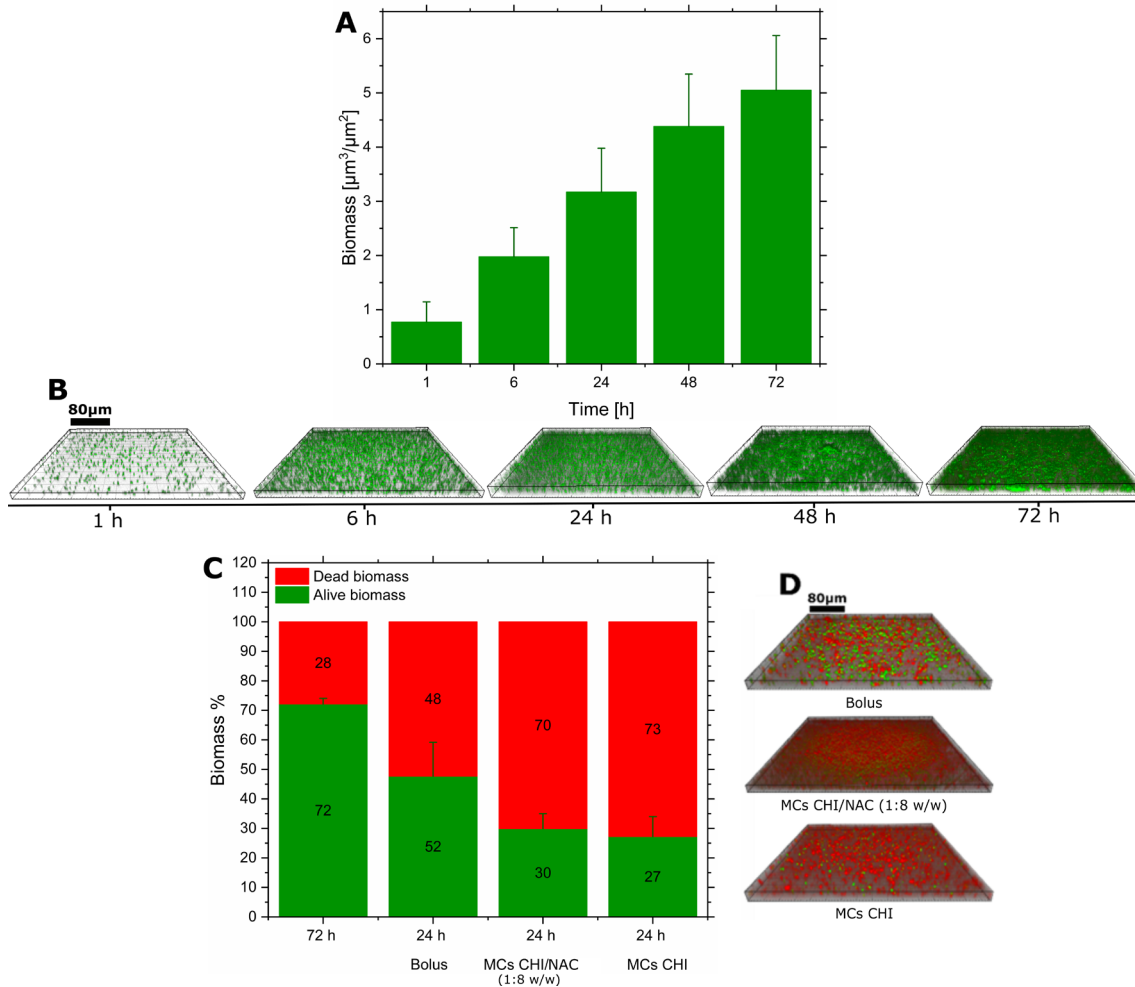


**Figure S5.** PAO1 average biomass growth at 1  $\mu\text{L}/\text{min}$  in 100 times diluted ASM. **(A).** Representative images of bacterial growth observed with confocal microscope at different time points at the same location in the cell chamber **(B)**. Data presented as mean+SD is based on 6 biological replicates, each with 9 technical replicates resulting in a total of  $n=54$  confocal images. Comparison between different antibiotic administration namely bolus injection, MCs CHI-coated and MCs CHI/NAC (1:8 w/w)-coated. Biomass viability was calculated before treatment at 72 h and after 24 h CIP. Data presented as mean+SD ( $n=18$ ) **(C)**. Representative confocal images of different treatments **(D)**.

In Figure S5A the growth of the bacterial biofilm over time can be observed in 100 times diluted ASM. After 6 h, the biomass was more than doubled,  $1.98 \pm 0.54 \mu\text{m}^3/\mu\text{m}^2$ , compared to the initial attachment state, where the biomass was  $0.77 \pm 0.37 \mu\text{m}^3/\mu\text{m}^2$ . After 24 h, the bacteria continued to increase their average biomass ( $3.17 \pm 0.81 \mu\text{m}^3/\mu\text{m}^2$ ) and spread uniformly in the cell chamber (Figure S5B), creating a monolayered biofilm. At 48 h, growth slowed down ( $4.38 \pm 0.96 \mu\text{m}^3/\mu\text{m}^2$ ), the biofilm became multilayered, and bacteria started to form aggregates. After 72 h, the bacterial biofilm average biomass was  $5.05 \pm 1.00 \mu\text{m}^3/\mu\text{m}^2$ , a biomass comparable to what has been observed previously in other flow systems using a conventional laboratory culture medium [1,10,11].

When PAO1 was cultured in 100 times diluted ASM for 72 h, before CIP treatment (Figure S5C),  $72.18 \pm 1.86$  % of the bacterial biofilm cells were alive. After 24 h treatment, only  $52.29 \pm 11.48$  % of the biofilm was killed using a CIP bolus injection (Figure S5C). Local administration of CIP with functionalized MCs resulted in a higher number of dead cells, namely  $70.08 \pm 5.05$  and  $72.76 \pm 6.75$  % dead biomass for CHI and CHI/NAC, respectively. It is clear that when CIP was administered in the MCs, biofilm eradication was more efficient compared to the bolus injection, which was also observed in our previous study [2]. The confocal images show an overview of the cell chamber after treatment, and they confirm that more alive biomass was present in the bolus injection images (Figure S5D). The fact that we were not able to differentiate between the effects of CIP delivered in the CHI vs CHI/NAC-coated MCs, could be due to the fact that the concentrations of mucin in the medium was low, as the ASM was diluted 100 times thus, reducing the opportunity for NAC to show an improvement in the treatment.

### PAO1 72 h growth in 100 times diluted ASM with 10 times diluted mucin (Figure S6)

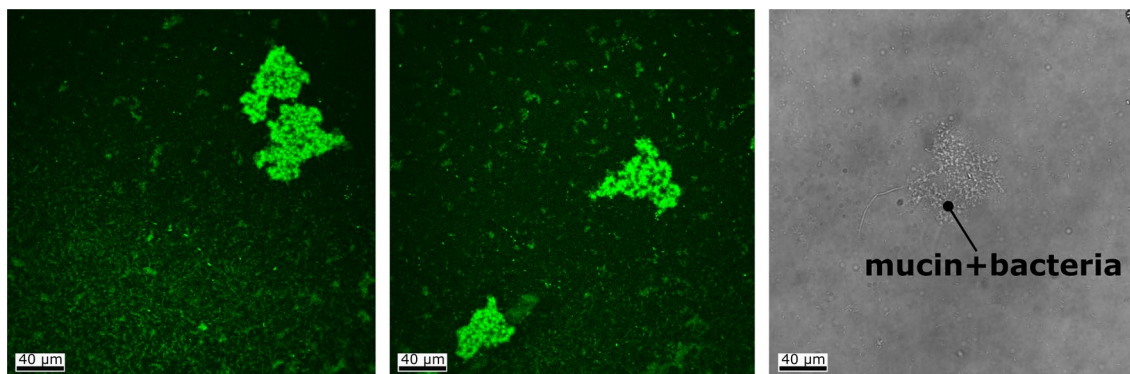


**Figure S6.** Growth of PAO1 in artificial sputum medium (100 times diluted ASM with 10 times diluted mucin) at 72 h. Bacteria started to grow embedded in the mucin and detached from the glass surface. On the right a bright field confocal picture representing bacteria growing in mucin.



### Evaluation of PAO1 growth in different ASM dilutions (Figure S7)

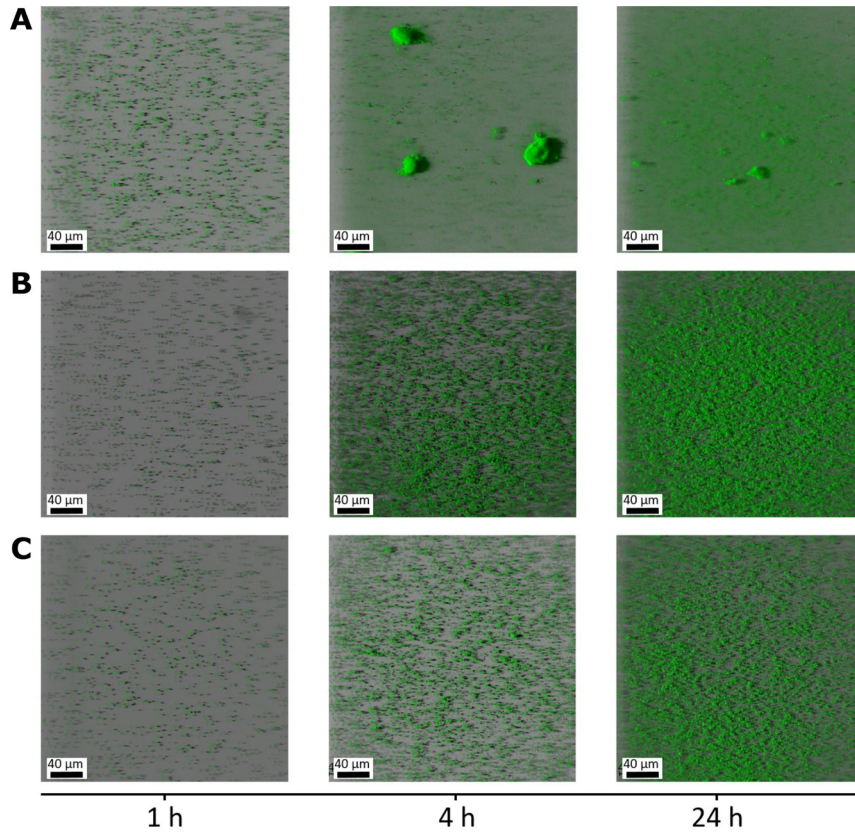


**Figure S7.** Growth of PAO1 after 1 h, 4 h and 24 h in pure artificial sputum medium (ASM) (A), 100 times diluted ASM with 10 times diluted mucin (B) and 100 times diluted ASM (C). It is visible that in pure ASM (A) bacteria grew embedded in the mucin and created clusters already after 4 h which detached from the glass surface after 24 h compromising the quantification and visualization of the biomass. With 10 times diluted mucin (B) bacteria grew faster compared to the 100 times diluted ASM (C).

### Evaluation of the presence of mucin in different dilutions of ASM and comparison with FAB medium (Figure S8)

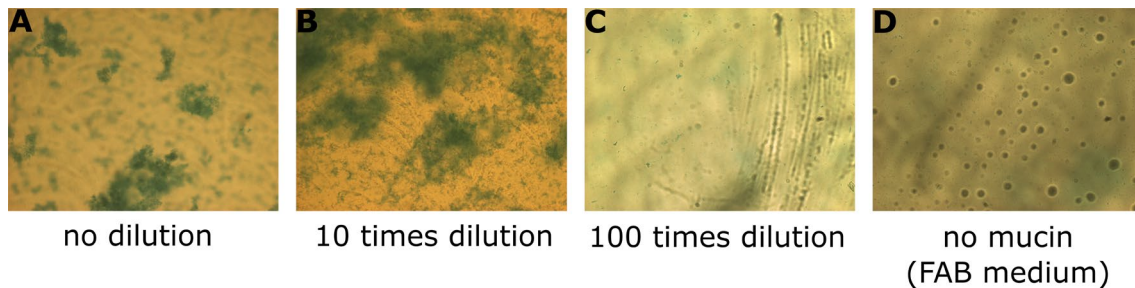


**Figure S8.** Evaluation of the presence of mucin in different dilutions of artificial sputum medium (ASM). The dye, Alcian blue, was applied to detect the presence of mucin in the medium used to culture biofilm for 72 h in vitro. Mucin was visible when ASM was not diluted (A) and it was comparable with the 10 times diluted one (B). When the mucin in ASM was 100 times diluted it was not possible to detect it in the cell culture chamber (C), an observation comparable with FAB medium with no mucin added (D).



## References

- [1] L. Seriola, T.Z. Laksafoss, J.A.J. Haagensen, C. Sternberg, M.P. Soerensen, S. Molin, K. Zór, A. Boisen, Bacterial Cell Cultures in a Lab-on-a-Disc: A Simple and Versatile Tool for Quantification of Antibiotic Treatment Efficacy, *Anal. Chem.* 92 (2020) 13871–13879. <https://doi.org/10.1021/acs.analchem.0c02582>.
- [2] S.E. Birk, J.A.J. Haagensen, H.K. Johansen, S. Molin, L.H. Nielsen, A. Boisen, Microcontainer Delivery of Antibiotic Improves Treatment of *Pseudomonas aeruginosa* Biofilms, *Adv. Healthc. Mater.* 9 (2020) 1901779. <https://doi.org/10.1002/adhm.201901779>.
- [3] H. Wang, H. Wu, Z. Song, N. Høiby, Ciprofloxacin shows concentration-dependent killing of *Pseudomonas aeruginosa* biofilm in vitro, *J. Cyst. Fibros.* 9 (2010) S41. [https://doi.org/10.1016/S1569-1993\(10\)60158-0](https://doi.org/10.1016/S1569-1993(10)60158-0).
- [4] J. Griebinger, S. Dünnhaupt, B. Cattoz, P. Griffiths, S. Oh, S.B.I. Gómez, M. Wilcox, J. Pearson, M. Gumbleton, M. Abdulkarim, I. Pereira De Sousa, A. Bernkop-Schnürch, Methods to determine the interactions of micro- and nanoparticles with mucus, *Eur. J. Pharm. Biopharm.* 96 (2015) 464–476. <https://doi.org/10.1016/j.ejpb.2015.01.005>.
- [5] S. Oh, M. Wilcox, J.P. Pearson, S. Borrós, Optimal design for studying mucoadhesive polymers interaction with gastric mucin using a quartz crystal microbalance with dissipation (QCM-D): Comparison of two different mucin origins, *Eur. J. Pharm. Biopharm.* 96 (2015) 477–483. <https://doi.org/10.1016/j.ejpb.2015.08.002>.
- [6] S. Oh, S. Borrós, Mucoadhesion vs mucus permeability of thiolated chitosan polymers and their resulting nanoparticles using a quartz crystal microbalance with dissipation (QCM-D), *Colloids Surfaces B Biointerfaces.* 147 (2016) 434–441. <https://doi.org/10.1016/j.colsurfb.2016.08.030>.
- [7] G. Aldini, A. Altomare, G. Baron, G. Vistoli, M. Carini, L. Borsani, F. Sergio, N-Acetylcysteine as an antioxidant and disulphide breaking agent: the reasons why, *Free Radic. Res.* 52 (2018) 751–762. <https://doi.org/10.1080/10715762.2018.1468564>.
- [8] C. Cristallini, N. Barbani, L. Ventrelli, C. Summa, S. Filippi, T. Capelôa, E. Vitale, C. Albera, B. Messore, C. Giachino, Biodegradable microparticles designed to efficiently reach and act on cystic fibrosis mucus barrier, *Mater. Sci. Eng. C.* 95 (2019) 19–28. <https://doi.org/10.1016/j.msec.2018.10.064>.
- [9] M. Mohammed, J. Syeda, K. Wasan, E. Wasan, An Overview of Chitosan Nanoparticles and Its Application in Non-Parenteral Drug Delivery, *Pharmaceutics.* 9 (2017) 53. <https://doi.org/10.3390/pharmaceutics9040053>.
- [10] A.R. Varadarajan, R.N. Allan, J.D.P. Valentin, O.E.C. Ocampo, V. Somerville, F. Pietsch, M.T. Buhmann, J. West, P.J. Skipp, H.C. Van Der Mei, Q. Ren, F. Schreiber, J.S. Webb, C.H. Ahrens, An integrated model system to gain mechanistic insights into biofilm formation and antimicrobial resistance development in *Pseudomonas aeruginosa* MPAO1, *BioRxiv.* 1 (2020) 1–34. <https://doi.org/10.1101/2020.02.06.936690>.
- [11] P. Norris, M. Noble, I. Francolini, A.M. Vinogradov, P.S. Stewart, B.D. Ratner, J.W. Costerton, P. Stoodley, Ultrasonically Controlled Release of Ciprofloxacin from Self-Assembled Coatings on Poly(2-Hydroxyethyl Methacrylate) Hydrogels for *Pseudomonas aeruginosa* Biofilm Prevention, *Antimicrob. Agents Chemother.* 49 (2005) 4272–4279. <https://doi.org/10.1128/AAC.49.10.4272-4279.2005>.

# APPENDIX V

PAPER V

**Management of oral biofilms by nisin delivery in adhesive microdevices**

S.E. Birk, M.D. Mosgaard, R.B. Kjeldsen, A. Boisen, R.L. Meyer, L.H. Nielsen

*Research note, 2021*

*Ready for submission to European Journal of Pharmaceutics and Biopharmaceutics*

# Management of oral biofilms by nisin delivery in adhesive microdevices

*Stine Egebro Birk<sup>a\*</sup>, Mette Dalskov Mosgaard<sup>a</sup>, Rolf Bech Kjeldsen<sup>a</sup>, Anja Boisen<sup>a</sup>, Rikke Louise Meyer<sup>b</sup>, Line Hagner Nielsen<sup>a</sup>*

<sup>a</sup>The Danish National Research Foundation and Villum Foundation's Center for Intelligent Drug Delivery and Sensing Using Microcontainers and Nanomechanics (IDUN), Department of Health Technology, Technical University of Denmark, Ørsteds Plads 345C, 2800 Kongens Lyngby, Denmark

<sup>b</sup>Interdisciplinary Nanoscience Center (iNANO), Aarhus University, Gustav Wieds Vej 14, 8000 Aarhus, Denmark

\*Corresponding author: Stine Egebro Birk, e-mail: [stegha@dtu.dk](mailto:stegha@dtu.dk)

## ABSTRACT

Numerous beneficial microbes thrive in the oral cavity where they form biofilms on dental and mucosal surfaces to get access to nutrients, and to avoid being carried away with the saliva. However, biofilm formation is also a virulence factor as it also protects pathogenic bacteria, providing them with an environment for proliferation causing oral infections. Oral hygiene relies on mechanical removal of biofilms. Some oral care products also contain antimicrobials, but effective eradication of biofilms with antimicrobials requires both a high concentration and long exposure time. In the present communication, we investigate the potential of using miniaturized drug delivery devices, known as microcontainers (MCs), to deliver the antimicrobial peptide, nisin to an oral multi-species biofilm. MCs are loaded with nisin and X-ray micro-computed tomography reveals a full release of nisin through a chitosan lid within 15 min. Chitosan-coated MCs display substantial bioadhesion to the buccal mucosa compared to non-coated MCs (68.6±14.3 % vs 33.8±5.2 %). Confocal monitoring of multi-species biofilms reveals antibacterial effects of nisin-loaded chitosan-coated MCs with a faster onset (after 3 h) compared to solution-based delivery (after 9 h). Our study shows the potential of using MCs for treatment of multi-species oral biofilms and is encouraging for further design of drug delivery devices to treat oral diseases.

## KEYWORDS

Microcontainers; Multi-species biofilm; Oromucosal drug delivery; Antimicrobial peptides; Chitosan;  $\mu$ CT; Bioadhesion

## 1. INTRODUCTION

Microbes colonizing the oral cavity are responsible for development of some of the most prevalent oral infections such as periodontal disease and dental caries [1]. The ability of these colonizers to organize themselves in biofilms is their key virulence factor. Biofilms are complex microbial communities encased in a self-produced matrix, in which they exhibit altered phenotypes compared to single planktonic cells. One of the hallmarks of biofilm is their increased tolerance to antibiotics which makes them extremely difficult to treat [1]. Oral bacteria adhere to surfaces coated with saliva, i.e. the salivary pellicle, covering the teeth, tongue, buccal mucosa, soft and hard palate and gingiva, allowing initiation of biofilm formation [2]. Modern genomic analyses have identified more than 700 species of bacteria as well as archaea, fungi, and viruses that comprise the human oral microbiome [2].

To achieve control of the biofilm, development of oral care formulations has been geared towards the incorporation of antimicrobial agents [3]. Antimicrobial peptides have high biocidal activity against several microorganisms. The bacteriocin nisin, is a member of the lantibiotic family of antimicrobial peptides that exhibit antibacterial activity against a wide range of Gram-positive bacteria, including staphylococci, bacilli and clostridia. It is currently used as a food preservative and has GRAS (generally regarded as safe) status [4]. Nisin targets the cell wall precursor lipid II, preventing bacterial cell wall synthesis and forming pores in the membrane, leading to efflux of cell components and ultimately cell death [4,5]. Nisin has shown great effect towards eradication of oral multi-species biofilms [6].

It is, however, not straight forward to deliver antimicrobial peptides to oral biofilms. Current drug delivery formulations to the oral mucosa, such as mouthwash, provide a good initial coverage, but prolonged effects are limited by their short contact time between drug and tissue due to removal with the flow of saliva. Therefore, delivery vehicles capable of retaining the antimicrobial peptide in the oral cavity by improved bioadhesion could be of great value for oral care products. We have previously shown that antibiotic-loaded microcontainers (MCs) improve the eradication of *P. aeruginosa* biofilms by delivering high local concentrations into the biofilm [7]. Moreover, MCs adhere to the intestinal mucus layer [8], and we therefore hypothesize that MCs will adhere to the mucosal surfaces of the oral cavity.

In the present study, MCs were loaded with nisin and functionalized with a mucoadhesive lid of chitosan. Release of nisin was monitored visually in a mucus-saliva blend using scanning electron microscopy (SEM) together with 3D X-ray micro-computed tomography ( $\mu$ CT). To elucidate the bioadhesion properties, chitosan-coated MCs were compared to uncoated MCs using an *ex vivo* flow retention model. Lastly, the impact on biofilm eradication of the chitosan-coated nisin-loaded MCs was studied using confocal microscopy on multi-species biofilms isolated directly from patients.

## **2. MATERIALS AND METHODS**

### **2.1. Materials**

Silicon (Si) wafers (4" (100) n-type) were acquired from Okmetic (Vantaa, Finland), while the SU-8 constituents (SU-8 2075 and SU-8 Developer) were purchased from Micro Resist Technology (Berlin, Germany). Nisin 2.5 % (balance sodium chloride), chitosan (low MW 50-190 kDa, 75-85 % deacetylation), acetic acid, calcium chloride dihydrate, potassium chloride, sodium bicarbonate, sodium dihydrogen phosphate, sodium chloride, sodium hydroxide and porcine gastric mucins (PGM) were all obtained from Sigma-Aldrich (St. Louis, MO USA). Solids for making brain heart infusion (BHI) medium were acquired from Oxoid Ltd. (Hants, UK). Sucrose was bought from Merck KGaA (Darmstadt, Germany). Stainless steel Spectra/Mesh® woven filters with a mesh opening of 213 µm and a thickness of 178 µm were from Spectrum®Labs.com (CA, USA). Ultrapure water was obtained from a Q-POD® dispenser (Merck Millipore, Burlington, MA, USA). The Department of Experimental Medicine, University of Copenhagen, kindly donated the buccal tissue and small intestines from Landrace×Yorkshire×Duroc (LYD) pigs. The pigs were 15–16 weeks of age and the weight was 50–55 kg. Checks were isolated and frozen at -20 °C until further use.

### **2.2. Production of MCs loaded with nisin and coated with chitosan**

MCs were fabricated on chips (each containing 625 MCs) and subsequently, loaded with nisin using a masking- and compression method as described in [7]. Coating of the drug-loaded MCs was achieved by spraying a 1 % w/v chitosan solution (dissolved in 0.5 M acetic acid) over the chip using an Exacta Coat Ultrasonic Spray System (Sono-Tek, Milton, NY, USA). Generator power was 1.5 W to allow proper aerosolization of the chitosan solution. For detailed process parameters, please refer to [7]. The loading and coating quality of the MCs was visualized using a tabletop SEM (TM3030Plus, Hitachi High-Technologies Europe GmbH, Krefeld, Germany). The inspection was performed using the back-scattered electron detector and an acceleration voltage of 15 kV. The chips were stored at 4 °C until usage to ensure drug stability.

### **2.3. X-ray µCT visualization of MCs during release in mucus and saliva mixtures**

To mimic the *in vivo* release-environment, mucus (isolated from intestinal sections) was mixed with sterile human saliva (50:50 % w/w). The chip with MCs was positioned upside down in the mucus:saliva blend in petri-dishes. Release was monitored for 24 h, taking samples after 0, 15 min, 2 h, 5 h and 24 h, and visualized with SEM and in 3D using µCT scanning (ZEISS XRadia 410 Versa, ZEISS, Pleasanton, CA, USA). For µCT scanning, X-rays were generated using a voltage of 60 kV and a power of 10 W (current of 0.17 mA). The 3D visualizations were created from single planar scans using 3201 projections with 1 frame

per projection and an exposure time of 5 s. The final scan time was 6 h and 10 min. The distance between the X-ray probe and the samples was set to obtain a voxel size, which corresponds to the spatial scan resolution, of 3.016  $\mu\text{m}$ . A Feldkamp, Davis and Kress filtered back-projection algorithm was used for the subsequent tomographic reconstructions made in the software provided by the  $\mu\text{CT}$  scanner system (Scout-and-Scan Control System Reconstructor, ZEISS, Pleasanton, CA, USA). The reconstructed data were processed and investigated using a 3D visualization and analysis software (Avizo, Thermo Fisher Scientific Inc., Waltham, MA, USA).

#### **2.4. Adhesion of MCs to the buccal mucosa**

The buccal mucosal tissue was thawed at room temperature. Skin and connective tissue were removed using a scissor, leaving only the buccal mucosa. Mucosa samples had a length of  $4.4\pm 0.5$  cm and a width of  $3.2\pm 0.2$  cm (mean $\pm$ SD, n=10). Gåserød buffer (a solution simulating the electrolyte composition of human whole saliva) was prepared with the composition of: 0.21 g/L sodium bicarbonate, 0.43 g/L sodium chloride, 0.75 g/L potassium chloride, 0.22 g/L calcium chloride dihydrate, 0.91 g/L sodium dihydrogen phosphate and 2.5 % w/v porcine gastric mucins in deionized water adjusted to pH 6.8 [9]. The mucosa was kept moist using the Gåserød buffer during the entire procedure.

To study the bioadhesion of the MCs on porcine buccal mucosa, a custom-made retention measurement setup by Vaut *et al.* was utilized [10]. Humidity was kept at  $89.0\pm 2.3$  % and temperature at  $32.6\pm 0.5$  °C mimicking the oromucosal environment. The buccal mucosa was attached to the tissue holder, kept at an angle of 30°, connected to tubings and a peristaltic pump (Watson Marlow 120S/DV, Falmouth, UK). At the end of the tissue holder, a beaker with a woven stainless steel filter with a pore size of 213  $\mu\text{m}$  was placed to collect non-adhering MCs (Figure 1). The mucosa was flushed with buffer for 10 min (5 rpm, 4.1 mL/min). After the washing procedure, approximately 150 uncoated or coated MCs (counted in a woven mesh under the microscope), was placed 0.5-1 cm from the top of the buccal mucosa. The MCs were allowed to become wetted and adhere to the tissue for 5 min before flow was resumed. After 20 min of flow, the tissue was gently detached from the holder, and dried in air overnight. The amount of MCs on the buccal mucosa, on the tissue holder as well as on the filter paper were counted the following day using a light microscope (Zeiss Axio Scope.A1, Carl Zeiss, Göttingen, Germany) with a C-DIC filter. Recoveries within a single replicate was accepted if between 90-110 %.

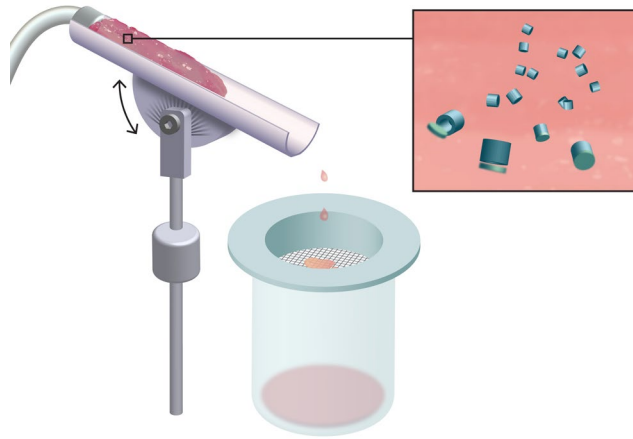


**Figure 1.** Schematic of the *ex vivo* flow retention model applied for testing the bioadhesion of the microcontainers (MCs). The buccal tissue was attached on a tissue holder, which was connected to tubing providing a flow of the buffer. MCs were gently positioned at the top part of the buccal tissue. A beaker with a mesh ensured collection of non-adhering MCs.

## 2.5. Treatment of multi-species oral biofilms

### 2.5.1. Collection, growth and treatment of biofilm

Saliva was collected from volunteers at the Dental School, Aarhus. Samples were mixed well to obtain an average microbiological composition, and afterwards diluted to 50 % in equal volumes of phosphate buffered saline and glycerol. Final stocks were frozen and kept at  $-80^{\circ}\text{C}$  until further use. Sterile saliva was produced by sterile filtering and kept at  $-20^{\circ}\text{C}$ . Multi-species biofilms were grown in 8-wells  $\mu$ -slides (Ibidi GmbH, Gräfelting, Germany) allowing microscopic monitoring of biofilm development. Growth was initiated by inoculating 10 % v/v saliva stock with 10 % v/v sterile saliva, 8 % v/v 50 % sucrose and 72 % v/v brain heart infusion (BHI) medium. Biofilm formation was allowed for 24 h at  $37^{\circ}\text{C}$ . The following day, the growth medium was replaced and supplemented with  $20\ \mu\text{M}$  SYTO 12 and  $2\ \mu\text{M}$  TOTO-3 (Invitrogen, CA, USA) for enabling visualization of live and dead biomass. To initiate treatment,  $15\ \mu\text{L}$  of a  $20\ \text{mg/mL}$  nisin solution (2.5 %) or 35 loaded and coated MCs were added to the individual wells.

### 2.5.2. Microscope parameters, image acquisition and analysis

Biofilms were monitored over the course of 24 h, keeping them incubated at  $37^{\circ}\text{C}$  (H301-K-Frame incubator, Oko-lab, Ottaviano, Italy). Visualization was conducted using a Zeiss LSM700 CLS microscope (Carl Zeiss, Oberkochen, Germany) equipped with lasers, detectors and filter sets for sequential monitoring of the membrane-permeable DNA-binding stain SYTO 12 (excitation: 488 nm, emission: 300-630 nm) for live cell imaging and the membrane-impermeable DNA-binding stain TOTO-3 (excitation: 639 nm, emission: 640-800 nm) for dead cell imaging. Images were obtained in z-intervals of  $1\ \mu\text{m}$  using an HC PL Apo 63x oil objective (numerical aperture 1.4). Stacked images were generated using

Fiji and volume of biomass was calculated using the image-analysis software COMSTAT version 2.1. Graphs were prepared by calculating the percentage of dead biomass in relation to the total biomass measured at the specified time-point, and normalized to zero in order to be able to compare between the different treatments.

## 2.6. Statistical analysis

Data are expressed as the mean $\pm$ standard deviation (SD). For comparison of two individual mean values, an unpaired t-test was applied. Graphs and tests were conducted in GraphPad Prism (Version 8.0.1, GraphPad Software, CA, USA) and p-values were considered statistically significant when below 5 % ( $p < 0.05$ ).

## 3. RESULTS AND DISCUSSION

SEM- and  $\mu$ CT-imaging confirmed efficient loading of nisin into MCs (Figure 2A and 2C). A chip of MCs was loaded with  $5.43\pm 0.59$  mg nisin powder (mean $\pm$ SD,  $n = 18$ ), corresponding to a drug loading of  $8.69\pm 0.95$   $\mu$ g per individual MC. Chitosan-coating of the MCs resulted in a uniform lid covering the cavity (Figure 2B-C). High-resolution  $\mu$ CT, together with SEM, enabled visualization of the lid morphology as well as release of nisin over time from the MCs when embedded in mucus and human whole saliva. Chitosan quickly swelled on top of the MCs, forming a hydrogel-lid, after being wetted for 15 min (Figure 2D). The hydrogel-lid stayed morphologically intact until 24 h, where large holes occurred in the lid (Figure 2E-G). Interestingly,  $\mu$ CT also revealed an intact lid after 15 min, but it was evident from the imaging that no nisin was left inside the MCs (Figure 2H). Therefore, we concluded that nisin released fully from the MCs through the chitosan hydrogel within the first 15 min.

To test the adhesion of chitosan-coated MCs to the buccal mucosa, we used a custom-designed *ex vivo* flow retention model, enabling control of humidity and temperature. The movement of the MCs is an estimate of the bioadhesion, meaning that the shorter distance they move, the more adhesive they are. Coating of MCs with chitosan increased their adhesiveness to the buccal tissue two-fold from  $33.8\pm 5.2$  % to  $68.6\pm 14.3$  % (Figure 3A). Previously, it has been shown that MCs might orient themselves in different orientations on intestinal tissue [8]. When investigating this phenomenon on buccal tissue, we found no significant differences between the orientations of the coated or uncoated MCs (Figure 3B). The majority of MCs were partly embedded in mucus, being either positioned on the side or facing up/down. The mucus layer in the oral cavity is about 70-100  $\mu$ m [11], why very few MCs were be deeply embedded in the mucus (uncoated MCs: none, coated MCs:  $10.0\pm 7.4$  %). The recovery (the number of MCs found after the experiment compared to the number added to the tissue at the beginning of the experiment) was high ( $98.6\pm 5.0$  %,  $n=8$ ).

We compared the antimicrobial effect of nisin-loaded MCs with free nisin in solution, by exposing



multi-species oral biofilms for 24 h (Figure 4). When treating with MCs, the dead biomass increased significantly after 3 h ( $p=0.0091$ ). In contrast, the dead biomass only started increasing significantly in biofilms treated with soluble nisin after 9 h ( $p=0.017$ ). This demonstrates that the MCs worked faster compared to delivery of nisin in solution. Moreover, a tendency showed higher absolute changes in dead biomass after treating with MCs ( $\Delta=24.05\pm 3.83\%$ ) compared to nisin in solution ( $\Delta=14.02\pm 4.56\%$ ) (not significant,  $p=0.054$ ). All nisin cargo was released from the MCs after 15 min, why we did not expect any large differences in efficacy between the MC-based treatment and nisin solution. However, the better effect can imply that the MCs, as many of them are in direct contact with the biofilm, may deliver initial high local drug concentrations in the biofilm, thereby resulting in a faster and better killing.

This is the first time that MCs have been loaded with an antimicrobial peptide and investigated for treatment of oral multi-species biofilms. Previous results focused on antibiotic-loaded MCs towards eradication of mono-species *P. aeruginosa* biofilms [7]. Our results show that nisin was released from the MCs within 15 min. In order to obtain a proper oral formulation, further investigations on how to achieve sustained release of nisin using alternative polymers in combination with chitosan is needed. The chitosan-coated MCs provided a significant bioadhesion proving the great benefit of using devices for delivery to the oral cavity compared to liquid-based formulations which are easily removed by the flow of saliva. Nisin-loaded MCs worked significantly faster than the nisin in solution. Moreover, we observed a slight tendency in increased dead biomass with MCs after 24 h. The results confirm the potential use of MC-based delivery of antimicrobial peptides to multi-species biofilms and are encouraging for the future design of sustained delivery devices maintaining a healthy microbiome of the oral cavity, ultimately improving the life-quality of many patients world-wide.

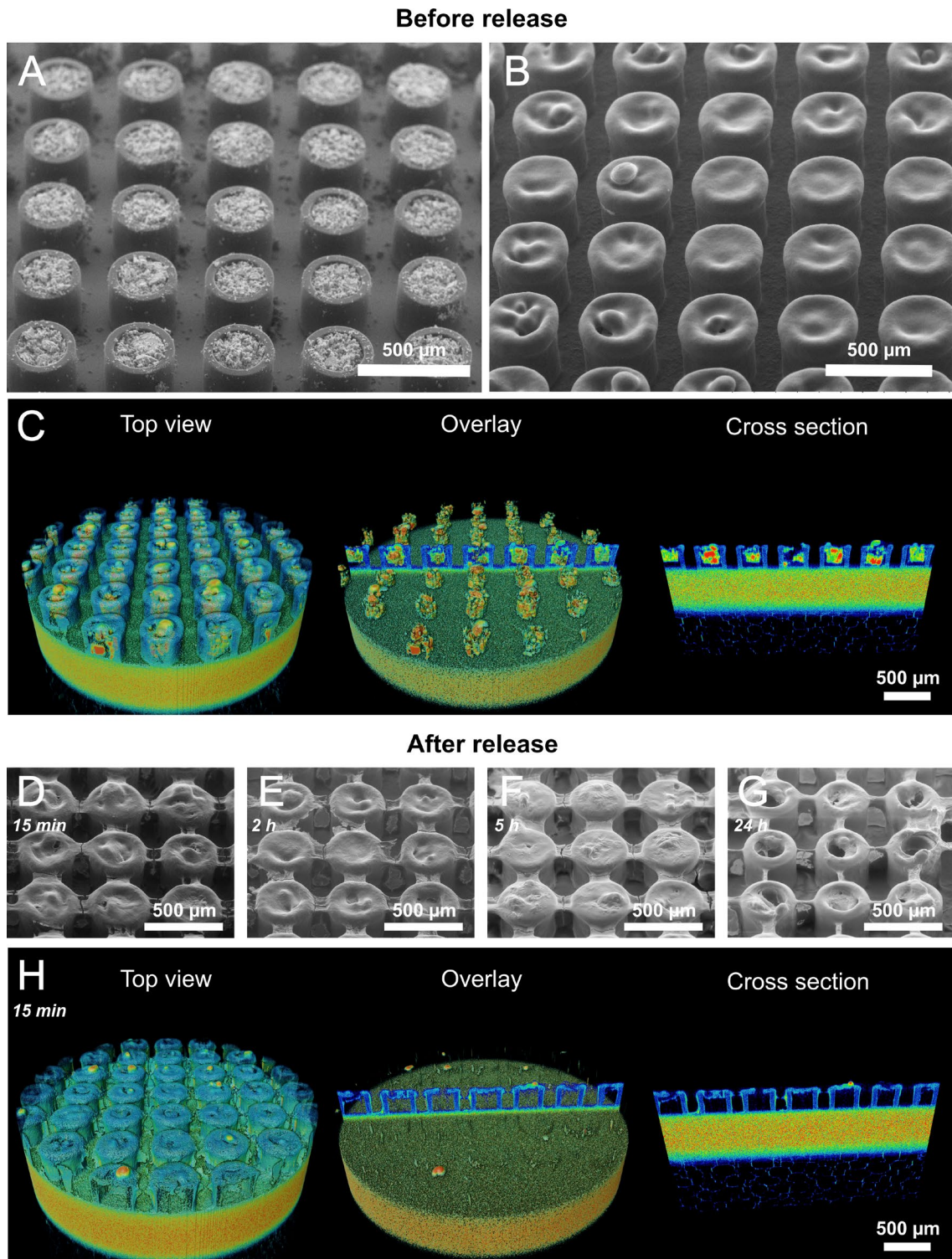


**Figure 2.** Scanning electron microscopy (SEM) images of **A)** microcontainers (MCs) loaded with nisin and **B)** coated with 1 % w/v chitosan. **C)** X-ray micro-computed tomography ( $\mu$ CT) images of MCs before release. **D-G)** SEM images of MCs during release. **H)**  $\mu$ CT images of MCs after 15 min release.

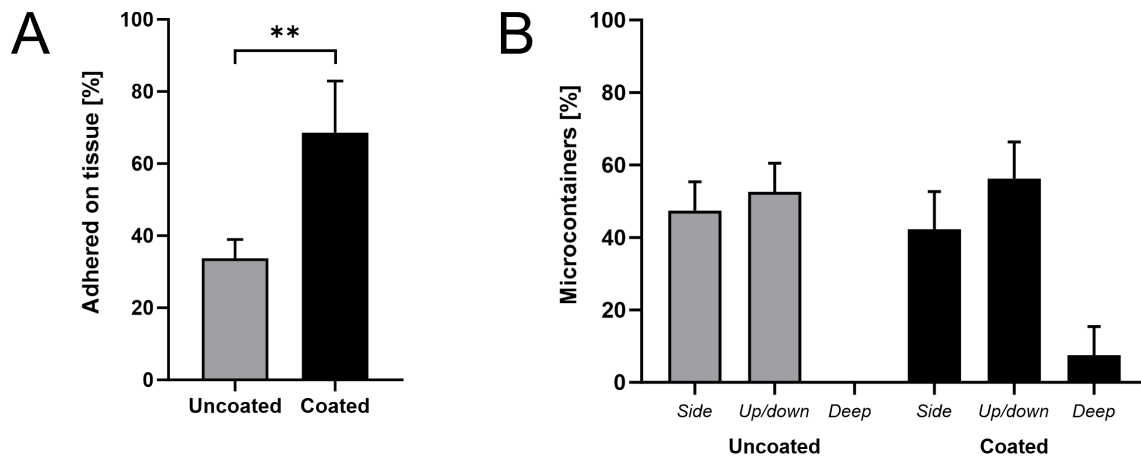


**Figure 3.** Adhesion of microcontainers (MCs) to porcine buccal mucosa. **A)** Percentage of uncoated or chitosan coated MCs adhering. **B)** Orientation in percentage of uncoated and chitosan coated MCs after ended experiment. The following orientations were stated; sideways, open cavity up/down or deeply covered in the mucus layer. Data is presented as mean $\pm$ SD (n=4). Significant difference: \*\* p=0.0038.

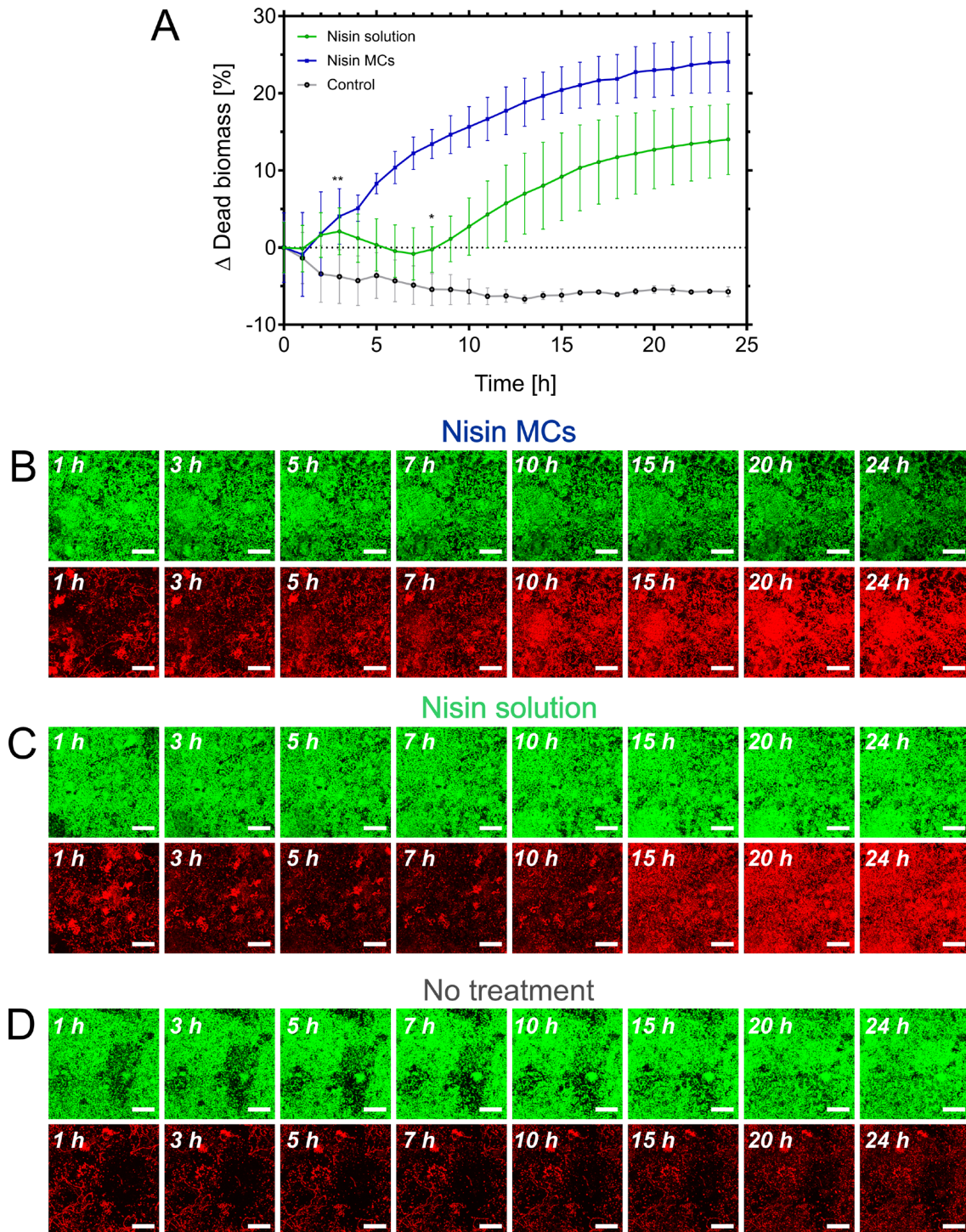


**Figure 4.** Confocal microscopy time-lapse on multi-species biofilm after treatment with nisin in microcontainers (MCs) coated with chitosan or nisin in solution. Percentage of dead biomass was calculated in relation to the total biomass at the specified time-point and normalized at  $t=0$  in order to compare the  $\Delta$ Dead biomass. Data presented as mean $\pm$ SD. Significant difference: \*  $p=0.017$ , \*\*  $p=0.0091$  (A). Confocal images of biofilm after treatment with nisin MCs (B), nisin solution (C) or no treatment (D). 2 biological replicates were performed acquiring 2-3 images (technical replicates) at random positions in the well. Scale bars: 20  $\mu$ m.

## ACKNOWLEDGEMENTS

This work was supported by the Danish National Research Foundation (DNRF122), Denmark and Villum Fonden (Grant No. 9301), Denmark for Intelligent Drug Delivery and Sensing Using Microcontainers and Nanomechanics (IDUN). Postdoc Signe Maria Nielsen, Interdisciplinary Nanoscience Center (iNANO), Aarhus University is thanked for her support in preparing the saliva-derived biofilm protocol. Additionally, the 3D Imaging Center at the Technical University of Denmark is acknowledge. Graphical abstract was created with figures adapted from Servier Medical Art by Servier and licensed under a Creative Commons Attribution 3.0.

## 4. REFERENCES

- [1] B.R. Da Silva, V.A.A. De Freitas, L.G. Nascimento-Neto, V.A. Carneiro, F.V.S. Arruda, A.S.W. De Aguiar, B.S. Cavada, E.H. Teixeira, Antimicrobial peptide control of pathogenic microorganisms of the oral cavity: A review of the literature, *Peptides*. 36 (2012) 315–321. <https://doi.org/10.1016/j.peptides.2012.05.015>.
- [2] P.I. Diaz, A.M. Valm, Microbial Interactions in Oral Communities Mediate Emergent Biofilm Properties, *J. Dent. Res.* 99 (2020) 18–25. <https://doi.org/10.1177/0022034519880157>.
- [3] P.D. Marsh, Controlling the oral biofilm with antimicrobials, *J. Dent.* 38 (2010) S11–S15. [https://doi.org/10.1016/S0300-5712\(10\)70005-1](https://doi.org/10.1016/S0300-5712(10)70005-1).
- [4] L. Dreyer, C. Smith, S.M. Deane, L.M.T. Dicks, A.D. van Staden, Migration of Bacteriocins Across Gastrointestinal Epithelial and Vascular Endothelial Cells, as Determined Using In Vitro Simulations, *Sci. Rep.* 9 (2019) 1–11. <https://doi.org/10.1038/s41598-019-47843-9>.
- [5] K.I. Okuda, T. Zendo, S. Sugimoto, T. Iwase, A. Tajima, S. Yamada, K. Sonomoto, Y. Mizunoe, Effects of bacteriocins on methicillin-resistant *Staphylococcus aureus* biofilm, *Antimicrob. Agents Chemother.* 57 (2013) 5572–5579. <https://doi.org/10.1128/AAC.00888-13>.
- [6] J.M. Shin, I. Ateia, J.R. Paulus, H. Liu, J.C. Fenno, A.H. Rickard, Y.L. Kapila, Antimicrobial nisin acts against saliva derived multi-species biofilms without cytotoxicity to human oral cells, *Front. Microbiol.* 6 (2015) 1–14. <https://doi.org/10.3389/fmicb.2015.00617>.
- [7] S.E. Birk, J.A.J. Haagensen, H.K. Johansen, S. Molin, L.H. Nielsen, A. Boisen, Microcontainer Delivery of Antibiotic Improves Treatment of *Pseudomonas aeruginosa* Biofilms, *Adv. Healthc. Mater.* 9 (2020) 1901779. <https://doi.org/10.1002/adhm.201901779>.
- [8] M.D. Mosgaard, S. Strindberg, Z. Abid, R.S. Petersen, L.H.E. Thamdrup, A.J. Andersen, S.S. Keller, A. Müllertz, L.H. Nielsen, A. Boisen, Ex vivo intestinal perfusion model for investigating mucoadhesion of microcontainers, *Int. J. Pharm.* 570 (2019) 118658. <https://doi.org/10.1016/j.ijpharm.2019.118658>.
- [9] K.D. Madsen, C. Sander, S. Baldursdottir, A.M.L. Pedersen, J. Jacobsen, Development of an ex vivo retention model simulating bioadhesion in the oral cavity using human saliva and physiologically relevant irrigation media, *Int. J. Pharm.* 448 (2013) 373–381. <https://doi.org/10.1016/j.ijpharm.2013.03.031>.
- [10] L. Vaut, E. Scarano, G. Tosello, A. Boisen, Fully replicable and automated retention measurement setup for characterization of bio-adhesion, The Authors, 2019. <https://doi.org/10.1016/j.ohx.2019.e00071>.
- [11] L.M.C. Collins, C. Dawes, The Surface Area of the Adult Human Mouth and Thickness of the Salivary Film Covering the Teeth and Oral Mucosa, *J. Dent. Res.* 66 (1987) 1300–1302. <https://doi.org/10.1177/00220345870660080201>.